

**THE ROLE OF THE ENDOTHELIAL CELL  
ENDOTHELIN B RECEPTOR IN  
CARDIOVASCULAR FUNCTION**

**Dr Nicholas Kelland**

**Presented for the degree of Doctor of Philosophy  
University of Edinburgh  
March 2007**

## **Declaration**

This thesis and the data presented within it are entirely the results of my own efforts, except where stated otherwise. This work contains no material that has been accepted for the award of any other degree or diploma in any university or tertiary institution and, to the best of my knowledge, contains no material previously published or written by another person, except where stated in the text.

.....2007

Dr Nicholas Francis Kelland

# Table of contents

|   |              |
|---|--------------|
| <b>DECLARATION .....</b>  | <b>I</b>     |
| <b>TABLE OF CONTENTS.....</b>   | <b>II</b>    |
| <b>FIGURES .....</b>  | <b>VII</b>   |
| <b>TABLES .....</b>   | <b>IX</b>    |
| <b>PRESENTATIONS, PRIZES AND PUBLICATIONS .....</b>   | <b>X</b>     |
| Presentations .....   | x            |
| Prizes .....  | xii          |
| Publications .....  | xiii         |
| <b>ACKNOWLEDGEMENTS .....</b>   | <b>XIV</b>   |
| <b>ABBREVIATIONS.....</b>   | <b>XVI</b>   |
| <b>ABSTRACT.....</b>  | <b>XVIII</b> |
| <b>1   CHAPTER 1: GENERAL INTRODUCTION.....</b>   | <b>1</b>     |
| <b>1.1    Pharmacology of Endothelin.....</b>   | <b>1</b>     |
| 1.1.1    Structure of ET-1 .....  | 1            |
| 1.1.2    Production of ET-1 .....   | 2            |
| 1.1.3    Endothelin Converting Enzyme .....   | 6            |
| 1.1.4    Endothelin receptors.....  | 7            |
| 1.1.5    Internalisation of receptors.....  | 10           |
| 1.1.6    Clearance of ET-1 .....  | 11           |
| <b>1.2    Physiological roles of Endothelin.....</b>  | <b>12</b>    |
| 1.2.1    Role of Endothelins in development.....  | 12           |
| 1.2.2    Role of Endothelins in vessels .....   | 14           |
| 1.2.3    Role of Endothelin in the kidney .....   | 20           |
| 1.2.4    Role of endothelin in the lungs .....  | 24           |
| <b>1.3    Generation of EC-specific ET<sub>B</sub> receptor Down-regulated mice .....</b>               | <b>37</b>    |
| 1.3.1    Gene targeting: The classical approach .....   | 37           |
| 1.3.2    Refining classical gene targeting by the Cre- <i>loxP</i> recombination system .....           | 37           |
| 1.3.3    Conditional gene targeting: Tissue specific knockout/downregulation .....                      | 39           |
| 1.3.4    Endothelial cell specific downregulation .....   | 41           |
| 1.3.5    Generation of EC-specific ET <sub>B</sub> receptor down-regulated mice .....                   | 42           |
| 1.3.6    Initial characterisation of the EC-specific ET <sub>B</sub> receptor down-regulated mice ..... | 43           |
| <b>1.4    Aims of the project .....</b>   | <b>46</b>    |

|             |  |           |
|-------------|--|-----------|
| <b>2</b>    | <b>CHAPTER 2: MATERIALS AND METHODS .....</b>  | <b>48</b> |
| <b>2.1</b>  | <b>Animals .....</b>   | <b>48</b> |
| <b>2.2</b>  | <b>Breeding.....</b>   | <b>48</b> |
| 2.2.1       | Breeding strategy to generate ET <sub>B</sub> null animals.....                                      | 48        |
| 2.2.2       | Analytical breeding crosses to assess sex linkage of recombination events .....                      | 48        |
| 2.2.3       | Breeding strategy to generate experimental animals .....   | 50        |
| <b>2.3</b>  | <b>Genotyping .....</b>  | <b>50</b> |
| 2.3.1       | Preparation of genomic DNA from tail/ ear biopsy .....   | 50        |
| 2.3.2       | Polymerase Chain Reaction of genomic DNA.....  | 51        |
| 2.3.3       | Quantitation of nucleic acids.....   | 53        |
| 2.3.4       | Agarose gel electrophoresis .....  | 53        |
| <b>2.4</b>  | <b>Genotyping approaches .....</b>   | <b>54</b> |
| 2.4.1       | ‘Comparative’ PCR of tail biopsies .....   | 54        |
| 2.4.2       | PCR of ‘EC free’ tissue .....  | 54        |
| 2.4.3       | Southern blot.....   | 55        |
| <b>2.5</b>  | <b>EC specific Cre expression in Tie2-Cre mice.....</b>  | <b>58</b> |
| 2.5.1       | LacZ staining and histology .....  | 58        |
| 2.5.2       | Staining for β-galactosidase activity.....   | 58        |
| 2.5.3       | Immunohistological staining of ECs.....  | 59        |
| 2.5.4       | GFP reporter mice .....  | 60        |
| <b>2.6</b>  | <b>Expression studies in EC ET<sub>B</sub> down-regulated mice .....</b>                             | <b>60</b> |
| 2.6.1       | Quantitative autoradiography.....  | 60        |
| 2.6.2       | Image analysis .....   | 61        |
| 2.6.3       | Semi quantitative RT-PCR of the ET system .....  | 61        |
| 2.6.4       | RT-PCR .....   | 63        |
| 2.6.5       | Agarose gel electrophoresis and densitometry .....   | 64        |
| <b>2.7</b>  | <b>BP measurement in unconscious animals.....</b>  | <b>65</b> |
| <b>2.8</b>  | <b>BP measurement in conscious animals .....</b>   | <b>66</b> |
| 2.8.1       | Salt diet .....  | 66        |
| 2.8.2       | Indwelling carotid artery catheters.....   | 67        |
| 2.8.3       | Surgical implantation of telemetry devices .....   | 69        |
| 2.8.4       | Haematocrit measurements .....   | 70        |
| <b>2.9</b>  | <b>ET-1 clearance studies .....</b>  | <b>71</b> |
| 2.9.1       | Measurement of plasma ET-1 and big ET-1 concentrations .....   | 71        |
| 2.9.2       | Clearance studies .....  | 71        |
| <b>2.10</b> | <b>Pulmonary Arterial Hypertension Study .....</b>   | <b>72</b> |
| 2.10.1      | Hypobaric chamber .....  | 72        |
| 2.10.2      | Haemodynamic studies .....   | 73        |
| 2.10.3      | Measurement of RV hypertrophy .....  | 74        |
| 2.10.4      | Wire myography .....   | 74        |
| 2.10.5      | Lung histology .....   | 77        |
| <b>2.11</b> | <b>Statistical Analysis of Results .....</b>   | <b>78</b> |
| <b>3</b>    | <b>CHAPTER 3: CHARACTERISATION OF THE MURINE MODEL OF<br/>EC-ET<sub>B</sub> DOWN-REGULATION.....</b> | <b>79</b> |



|            |  |            |
|------------|--|------------|
| <b>3.1</b> | <b>Introduction.....</b>   | <b>79</b>  |
| 3.1.1      | Deletion of exons 3 and 4 prevents ET <sub>B</sub> expression .....                                | 79         |
| 3.1.2      | Tie2-Cre restricts expression of Cre recombinase to the endothelium.....                           | 80         |
| 3.1.3      | EC-specific ET <sub>B</sub> down-regulation in FF/Tie2 mice .....                                  | 81         |
| <b>3.2</b> | <b>Results .....</b>   | <b>84</b>  |
| 3.2.1      | Genotyping of experimental animals .....   | 84         |
| 3.2.2      | Generation of null ET <sub>B</sub> mice .....  | 85         |
| 3.2.3      | Analytical crosses .....   | 88         |
| 3.2.4      | Genotyping strategies .....  | 88         |
| 3.2.5      | Tie2-Cre restricts Cre expression to ECs .....   | 94         |
| 3.2.6      | Autoradiography to demonstrate ET receptor expression.....   | 97         |
| 3.2.7      | RT-PCR to demonstrate renal ET system expression .....   | 105        |
| <b>3.3</b> | <b>Discussion .....</b>  | <b>112</b> |
| 3.3.1      | Knockout of exons 3 and 4 is sufficient to prevent expression of ET <sub>B</sub> .....             | 112        |
| 3.3.2      | Sex linked germ line recombination .....   | 112        |
| 3.3.3      | Genotyping strategies .....  | 115        |
| 3.3.4      | Endothelial cell specific Cre expression.....  | 117        |
| 3.3.5      | EC specific ET <sub>B</sub> down-regulation in FF/Tie2 mice.....                                   | 118        |
| 3.3.6      | Expression of other components of the ET system in the FF/Tie2 mouse.....                          | 119        |
| <b>4</b>   | <b>CHAPTER 4: ROLE OF THE EC-ET<sub>B</sub> RECEPTOR IN THE CONTROL OF SYSTEMIC BP .....</b>       | <b>123</b> |
| <b>4.1</b> | <b>Introduction.....</b>   | <b>123</b> |
| <b>4.2</b> | <b>Methods/Protocols .....</b>   | <b>125</b> |
| 4.2.1      | Measurement of BP under anaesthesia .....  | 125        |
| 4.2.2      | Measurement of BP under conscious unrestrained conditions using fluid filled catheters<br>125      |            |
| 4.2.3      | Continuous measurement of BP under conscious unrestrained conditions using<br>radiotelemetry ..... | 125        |
| <b>4.3</b> | <b>Results .....</b>   | <b>129</b> |
| 4.3.1      | Measurement of BP under anaesthesia .....  | 129        |
| 4.3.2      | Continuous measurement of BP under conscious unrestrained conditions using<br>radiotelemetry ..... | 134        |
| 4.3.3      | Influence of age on heart/ body weight ratio.....  | 177        |
| <b>4.4</b> | <b>Discussion .....</b>  | <b>179</b> |
| 4.4.1      | Deletion of the EC ET <sub>B</sub> receptor does not alter the BP response to salt .....           | 179        |
| 4.4.2      | BP measurement in mice.....  | 182        |
| 4.4.3      | Why did the results from the radiotelemetry and direct catheter BP studies differ? .....           | 185        |
| <b>5</b>   | <b>CHAPTER 5: ROLE OF THE EC-ET<sub>B</sub> RECEPTOR IN THE PLASMA CLEARANCE OF ET-1 .....</b>     | <b>189</b> |
| <b>5.1</b> | <b>Introduction.....</b>   | <b>189</b> |
| <b>5.2</b> | <b>Methods/Protocols .....</b>   | <b>190</b> |
| 5.2.1      | Plasma ET-1 and big ET-1 concentrations .....  | 190        |
| 5.2.2      | Clearance studies .....  | 190        |
| <b>5.3</b> | <b>Results .....</b>   | <b>191</b> |

|                                      |   |            |
|--------------------------------------|---|------------|
| 5.3.1                                | Plasma ET-1 concentrations.....   | 191        |
| 5.3.2                                | Plasma big ET-1 concentrations .....  | 192        |
| 5.3.3                                | Effect of genotype on clearance of ET-1 .....   | 193        |
| 5.3.4                                | Effect of pharmacological ET <sub>B</sub> blockade on clearance of ET-1 .....   | 195        |
| <b>5.4</b>                           | <b>Discussion .....</b>   | <b>200</b> |
| 5.4.1                                | Plasma ET-1 and big ET-1 concentrations .....   | 200        |
| 5.4.2                                | Plasma clearance studies .....  | 202        |
| 5.4.3                                | Non ET <sub>B</sub> receptor mediated ET-1 clearance.....   | 203        |
| 5.4.4                                | Technical considerations in plasma clearance studies .....  | 203        |
| <b>6</b>                             | <b>CHAPTER 6: ROLE OF THE EC-ET<sub>B</sub> RECEPTOR IN THE CONTROL OF PULMONARY VASCULAR TONE AND THE DEVELOPMENT OF PULMONARY ARTERIAL HYPERTENSION .....</b> | <b>206</b> |
| <b>6.1</b>                           | <b>Introduction.....</b>  | <b>206</b> |
| <b>6.2</b>                           | <b>Methods/Protocols .....</b>  | <b>208</b> |
| 6.2.1                                | Myography protocol .....  | 208        |
| <b>6.3</b>                           | <b>Results .....</b>  | <b>209</b> |
| 6.3.1                                | Weights .....   | 209        |
| 6.3.2                                | Haemodynamic studies .....  | 209        |
| 6.3.3                                | Right ventricular hypertrophy .....   | 211        |
| 6.3.4                                | Myography .....   | 212        |
| 6.3.5                                | Vascular remodeling.....  | 221        |
| <b>6.4</b>                           | <b>Discussion .....</b>   | <b>223</b> |
| 6.4.1                                | Mechanisms responsible for PAH .....  | 224        |
| 6.4.2                                | Influence of vascular remodeling and vasoconstriction in chronic hypoxic PAH.....   | 225        |
| 6.4.3                                | Study limitations.....  | 227        |
| <b>7</b>                             | <b>CHAPTER 7: CONCLUSIONS AND FUTURE WORK.....</b>  | <b>230</b> |
| <b>7.1</b>                           | <b>Introduction.....</b>  | <b>230</b> |
| <b>7.2</b>                           | <b>Limitations of the project as a whole .....</b>  | <b>230</b> |
| 7.2.1                                | Genetic background.....   | 230        |
| 7.2.2                                | Possible compensatory mechanisms .....  | 231        |
| <b>7.3</b>                           | <b>Body Weight of EC ET<sub>B</sub> down-regulated mice.....</b>  | <b>231</b> |
| <b>7.4</b>                           | <b>Expression of ET receptors in EC ET<sub>B</sub> down-regulated mice.....</b>   | <b>233</b> |
| <b>7.5</b>                           | <b>Role of EC ET<sub>B</sub> in control of systemic vascular tone and response to salt .....</b>  | <b>234</b> |
| <b>7.6</b>                           | <b>Contribution of EC ET<sub>B</sub> receptor to the clearance of plasma ET-1 .....</b>   | <b>235</b> |
| <b>7.7</b>                           | <b>The EC ET<sub>B</sub> receptor in the control of pulmonary vascular tone.....</b>  | <b>236</b> |
| <b>7.8</b>                           | <b>Summary.....</b>   | <b>237</b> |
| <b>CHAPTER 8: BIBLIOGRAPHY .....</b> | <b>238</b>  |            |



## Figures

|  |     |
|--|-----|
| Figure 1-1: Structure of ET-1, ET-2, ET-3 and S6c.....   | 2   |
| Figure 1-2: Factors affecting the synthesis of ET-1.....   | 4   |
| Figure 1-3: ET receptor intracellular signalling.....  | 8   |
| Figure 1-4: Autocrine versus paracrine control of ET <sub>B</sub> mediated natriuresis .....   | 22  |
| Figure 1-5: Pathogenesis of PAH .....  | 30  |
| Figure 1-6: Endothelial dysfunction in PAH.....  | 33  |
| Figure 1-7: Generation of mice with loxP-flanked target genes (flox). .....  | 39  |
| Figure 1-8: Gene targeting of the ET <sub>B</sub> gene .....   | 42  |
| Figure 1-9: Reduced ET-1 binding in pulmonary ECs from FF/Tie2 mice.....   | 44  |
| Figure 1-10: Functional evidence of EC ET <sub>B</sub> down-regulation in FF/Tie2 mice .....   | 45  |
| Figure 2-1: Breeding strategy to generate piebalds and analytical crosses.....   | 49  |
| Figure 2-2: Breeding strategy for experimental animals .....   | 50  |
| Figure 2-3: PCR genotyping strategy .....  | 52  |
| Figure 2-4: Southern blot strategy .....   | 56  |
| Figure 2-5: Procedure for mounting of pulmonary artery rings onto the wire myograph.....   | 75  |
| Figure 3-1: Cre mediated recombination.....  | 81  |
| Figure 3-2: Flox PCR .....   | 84  |
| Figure 3-3: Tie2 PCR .....   | 85  |
| Figure 3-4: Piebald mice .....   | 87  |
| Figure 3-5: Semi-quantitative PCR.....   | 89  |
| Figure 3-6: Hair DNA PCR.....  | 91  |
| Figure 3-7: Testes DNA PCR .....   | 92  |
| Figure 3-8: Cardiomyocyte DNA PCR.....   | 93  |
| Figure 3-9: Southern blot genotyping.....  | 94  |
| Figure 3-10: LacZ and CD31 antibody staining in kidneys from WW/Tie2-Cre and WW/Tie2-Cre/R26R mice. ....   | 95  |
| Figure 3-11: GFP autofluorescence in day 11 FF/Tie2-Cre/GFP embryos.....   | 96  |
| Figure 3-12: Total ET <sub>B</sub> binding in FF/Tie2 and control mice .....   | 99  |
| Figure 3-13 ET <sub>B</sub> binding in lung and kidney.....  | 100 |
| Figure 3-14: Specific ET <sub>B</sub> binding in lung, kidney and liver.....   | 101 |
| Figure 3-15: Autoradiographs of total binding of the radiolabelled ET <sub>A</sub> selective ligand [ <sup>125</sup> I]-PD151242 in WW/-- (A) FF/-- (B) and FF/Tie2 (C) mice. ....           | 103 |
| Figure 3-16: Specific ET <sub>A</sub> binding in kidney, lung and liver. ....  | 104 |
| Figure 3-17: Denaturing gel.....   | 105 |
| Figure 3-18: Optimisation of PCR temperature .....   | 106 |
| Figure 3-19: Optimisation of PCR cycle number.....   | 107 |
| Figure 3-20: Serial dilution of cDNA.....  | 109 |
| Figure 3-21: Effect of genotype on the relative expression of the renal ET system.....   | 110 |
| Figure 3-22 Effect of age and sex on the relative expression of the renal ET system.....   | 111 |
| Figure 4-1: Study protocol for the first phase of the telemetry BP study.....  | 126 |
| Figure 4-2: Study protocol for the second phase of the telemetry BP study.....   | 127 |
| Figure 4-3 Representative BP trace of an anaesthetised WW/-- mouse.....  | 129 |
| Figure 4-4 Representative BP trace of an anaesthetised FF/Tie2 mouse. ....   | 130 |
| Figure 4-5: MABP of anaesthetized animals.....   | 130 |
| Figure 4-6 Representative BP traces of conscious unrestrained mice. ....   | 132 |
| Figure 4-7: MABP of unrestrained conscious mice.....   | 133 |
| Figure 4-8: HR of unrestrained conscious mice.....   | 134 |
| Figure 4-9: 12 hourly SBP .....  | 135 |
| Figure 4-10: SBP of telemetered mice during the 7 days of normal salt (0.76% NaCl) diet (week 1) [A] and during the 7 days of low salt (0.076% NaCl) diet (week 2) [B]. ....                 | 136 |
| Figure 4-11: SBP of telemetered mice during the 7 days of high salt (7.6% NaCl) diet (week 3) [A] and during the 7 days of high salt + A627 (5 mg.kg <sup>-1</sup> ) diet (week 4) [B]. .... | 137 |

|   |     |
|---|-----|
| Figure 4-12: Comparison of: the averaged SBP of FF/-- (n=12) and FF/Tie2 (n=10) mice during the last 72 hours of each week-long dietary period [A]; the averaged minimal SBP values during the day [B]; and the averaged maximal SBP values during the night [C]. | 139 |
| Figure 4-13: 12 hourly DBP.   | 139 |
| Figure 4-14: DBP of telemetered mice during the 7 days of normal salt (0.76% NaCl) diet (week 1) [A] and during the 7 days of low salt (0.076% NaCl) diet (week 2) [B].   | 140 |
| Figure 4-15: DBP of telemetered mice during the 7 days of high salt (7.6% NaCl) diet (week 3) [A] and during the 7 days of high salt + A627 (5 mg.kg <sup>-1</sup> ) diet (week 4) [B].   | 141 |
| Figure 4-16: Comparison of: the averaged DBP of FF/-- (n=12) and FF/Tie2 (n=10) mice during the last 72 hours of each dietary period [A]; the averaged minimal DBP values during the day [B]; and the averaged minimal DBP values during the night [C].           | 143 |
| Figure 4-17: 12 hourly MBP  | 143 |
| Figure 4-18: MBP of telemetered mice during the 7 days of normal salt (0.76% NaCl) diet (week 1) [A] and during the 7 days of low salt (0.076% NaCl) diet (week 2)[B].  | 144 |
| Figure 4-19: MBP of telemetered mice during the 7 days of high salt (7.6% NaCl) diet (week 3) [A] and during the 7 days of high salt + A627 (5 mg.kg <sup>-1</sup> ) diet (week 4) [B].   | 145 |
| Figure 4-20: Comparison of: the averaged MBP of FF/-- (n=12) and FF/Tie2 (n=10) mice during the last 72 hours of each week-long dietary period [A]; the averaged minimal MBP values during the day [B]; and the averaged minimal MBP values during the night [C]. | 147 |
| Figure 4-21: 12 hourly heart rate.  | 147 |
| Figure 4-22: Heart rate of telemetered mice during the 7 days of normal salt (0.76% NaCl) diet (week 1) [A] and during the 7 days of low salt (0.076% NaCl) diet (week 2) [B].  | 148 |
| Figure 4-23: Heart rate of telemetered mice during the 7 days of high salt (7.6% NaCl) diet (week 3) [A] and during the 7 days of high salt + A627 (5 mg.kg <sup>-1</sup> ) diet (week 4) [B].  | 149 |
| Figure 4-24: Comparison of: the averaged HR of FF/-- (n=12) and FF/Tie2 (n=10) mice during the last 72 hours of each week-long dietary period [A]; the averaged minimal HR during the day [B]; and the averaged maximal HR values during night [C].               | 151 |
| Figure 4-25: Average daily water consumption  | 151 |
| Figure 4-26: Average daily gel intake   | 152 |
| Figure 4-27: Average body weight  | 153 |
| Figure 4-28: Weight change versus the previous day  | 154 |
| Figure 4-29: 12 hourly SBP  | 155 |
| Figure 4-30: SBP of telemetered mice during the second week of normal salt (0.76% NaCl) diet (week 5) [A], during the 7-days of high salt (7.6% NaCl) + A192621 (week 6) [B] and during the 7 days of 2.5% NaCl diet (week 7) [C].                                | 157 |
| Figure 4-31: Comparison of: the averaged SBP of FF/-- (n=7) and FF/Tie2 (n=6) mice during the last 72 hours of each week-long dietary period [A]; the averaged minimal SBP values during the day [B]; and the averaged maximal SBP values during the night [C].   | 159 |
| Figure 4-32: 12 hourly DBP.   | 160 |
| Figure 4-33: DBP of telemetered mice during the second week of normal salt (0.76% NaCl) diet (week 5) [A], during the 7-days of high salt (7.6% NaCl) + A192621 (week 6) [B] and during the 7 days of 2.5% NaCl diet (week 7) [C].                                | 162 |
| Figure 4-34: Comparison of: the averaged DBP of FF/-- (n=7) and FF/Tie2 (n=6) mice during the last 72 hours of each week-long dietary period [A]; the averaged minimal DBP values during the day [B]; and the averaged maximal DBP values during the night [C].   | 164 |
| Figure 4-35: 12 hourly MBP  | 165 |
| Figure 4-36: MBP of telemetered mice during the second week of normal salt (0.76% NaCl) diet (week 5) [A], during the 7-days of high salt (7.6% NaCl) + A192621 (week 6) [B] and during the 7 days of 2.5% NaCl diet (week 7) [C].                                | 167 |
| Figure 4-37: Comparison of: the averaged MBP of FF/-- (n=7) and FF/Tie2 (n=6) mice during the last 72 hours of each week-long dietary period [A]; the averaged minimal MBP values during the day [B]; and the averaged maximal MBP values during the night [C].   | 169 |
| Figure 4-38: 12 hourly HR   | 170 |
| Figure 4-39: HR of telemetered mice during the second week of normal salt (0.76% NaCl) diet (week 5) [A], during the 7-days of high salt (7.6% NaCl) + A192621 (week 6) [B] and during the 7 days of 2.5% NaCl diet (week 7) [C].                                 | 172 |

|  |     |
|--|-----|
| Figure 4-40: Comparison of: the averaged HR of FF/-- (n=7) and FF/Tie2 (n=6) mice during the last 72 hours of each week-long dietary period [A]; the averaged minimal HR values during the day [B]; and the averaged maximal HR values during the night [C]. | 174 |
| Figure 4-41: Average daily water consumption (second extended study only).   | 174 |
| Figure 4-42: Average daily gel intake (second extended study only).  | 175 |
| Figure 4-43: Average daily body weight (second extended study only).   | 176 |
| Figure 4-44: Packed cell volume of mice in second study  | 176 |
| Figure 4-45: Heart to body weight ratio for young and old mice   | 177 |
| Figure 5-1: Plasma concentrations of ET-1 were elevated in FF/Tie2 mice.   | 191 |
| Figure 5-2: Plasma concentration of big ET-1 was only marginally elevated in FF/Tie2 mice.   | 192 |
| Figure 5-3: Concentration – time graph showing that elimination of a bolus of radiolabelled ET-1 was impaired in FF/Tie2 compared to WW/-- mice.   | 193 |
| Figure 5-4: Clearance of ET-1 was similar in WW/-- and FF/-- mice.   | 194 |
| Figure 5-5: ET <sub>B</sub> blockade with A192621 impaired ET-1 clearance in WW/-- mice to a similar extent to that of untreated FF/Tie2 mice.   | 196 |
| Figure 5-6: Both low and high dose A192621 had similar effects on ET-1 clearance in WW/-- mice.  | 197 |
| Figure 5-7: Logarithmic plot of concentration against time was not different between genotypes   | 198 |
| Figure 5-8: Clearance of ET-1 was impaired in FF/Tie2 mice, and in mice of both genotypes treated with ET <sub>B</sub> blockade.   | 200 |
| Figure 6-1: Systemic haemodynamics did not differ between genotypes under both normoxic and hypoxic conditions.  | 209 |
| Figure 6-2: The systolic RVP of FF/Tie2 mice was significantly elevated under hypoxic conditions   | 210 |
| Figure 6-3: Hypoxia results in right ventricular hypertrophy in hypoxic mice FF/Tie2 mice  | 212 |
| Figure 6-4: (previous 2 pages). Representative tracing of a wire myography study of a 3 <sup>rd</sup> order PA ring from FF/-- mouse, housed under normoxic conditions, not exposed to L-NAME.   | 215 |
| Figure 6-5: Length (internal circumference) – tension relationship for all PA rings  | 216 |
| Figure 6-6: CRC of PAs to ET-1 under normoxia and hypoxia  | 217 |
| Figure 6-7: CRC of normoxic PA rings to ET-1 in the presence and absence of L-NAME   | 219 |
| Figure 6-8: CRC of hypoxic PA rings to ET-1 in the presence and absence of L-NAME  | 220 |
| Figure 6-9: Micrograph showing hypoxic remodeling  | 222 |
| Figure 6-10: The percentage of remodeled pulmonary vessels was increased in hypoxic FF/Tie2 mice   | 223 |
| Figure 7-1: Summary bar chart showing trend of EC ET <sub>B</sub> down-regulated mice to reduced body weights  | 232 |

## Tables

|  |     |
|--|-----|
| Table 1-1 Classification of pulmonary hypertension                                       | 27  |
| Table 2-1: PCR conditions  | 53  |
| Table 3-1: Results of analytical breeding pairs  | 88  |
| Table 3-2: Optimum conditions for semi-quantitative PCR of ET system                     | 108 |
| Table 4-1: Pre-surgery weights   | 132 |
| Table 4-2: Heart and body weights for young (2 month old) and old (4 month) mice         | 178 |
| Table 5-1: Body weights on day of clearance study  | 195 |
| Table 5-2: Pharmacokinetic data for elimination of a bolus of [ <sup>125</sup> I]-ET-1   | 199 |
| Table 6-1: Weights of mice   | 209 |
| Table 6-2: Indices of right ventricular hypertrophy                                      | 211 |
| Table 6-3: Potency and maximum effect of ET-1 in PA rings from FF/Tie2 and FF/-- animals | 221 |

## **Presentations, Prizes and Publications**

The following presentations, prizes awarded and publications have arisen from the work described in this thesis:

### **PRESENTATIONS**

**Kelland NF**, Bagnall AJ, Gray GA, Gulliver-Sloan FH, Kotelevtsev YV, Webb DJ. Endothelial cell endothelin B receptors mediate a tonic hypotensive effect that is insensitive to salt. *Proceedings of the British Pharmacological Society*. 2003; <http://www.pa2online.org/Vol1Issue4abst070P>, [Poster presentation at the Winter BPS Meeting, London UK]

**Kelland NF**, Bagnall AJ, Gulliver-Sloan FH, Gray GA, Kotelevtsev YV, Webb DJ. Endothelial cell-specific knockout of the endothelin B receptor results in hypertension that is resistant to salt. *Journal of Hypertension*. 2004;22:S9. [Oral presentation at the European Society of Hypertension, Paris, France]

**Kelland NF**, Bagnall AJ, Gulliver-Sloan FH, Gray GA, Kotelevtsev YV, Webb DJ. The endothelial cell endothelin B receptor plays an important role in the clearance of ET-1. *Journal of Hypertension*. 2004;22:S49. [Poster presentation at the European Society of Hypertension, Paris, France]

**Kelland NF**, Bagnall AJ, Gulliver-Sloan FH, Kuc RE, Davenport AP, Gray GA, Kotelevtsev YV and Webb DJ. Investigation of the clearance of endothelin-1 from plasma using a murine endothelial cell specific endothelin B receptor knockout model. *Heart* 2004; 90:e68. <http://www.heartjnl.com/cgi/content/full/90/12/e68>. [Poster presentation at the British Society for Cardiovascular Research Autumn Meeting, London]

**Kelland NF**, Bagnall AJ, Gulliver-Sloan F, Gray GA, Kotelevtsev Y, Webb DJ. The endothelial cell ETBR exerts a hypotensive effect and is responsible for the clearance

of endothelin-1. *Hypertension* 2004; 44(4):51. [Oral presentation at the AHA Council for High BP research, Chicago, USA]

Armour DL, **Kelland NF**, Bagnall AB, Gulliver-Sloan FH, Kotelevtsev YV and Webb DJ. The effect of targeted disruption of the endothelial cell endothelin B receptor on gene expression of the renal endothelin system. [Poster presentation at the Ninth International Conference on Endothelin. Salt Lake City, Utah, USA]

Bagnall AB, **Kelland NF**, Gulliver-Sloan FH, Davenport AP, Gray GA, Yanagisawa M, Kotelevtsev YV and Webb DJ. Targeted Disruption of the Endothelial Cell Endothelin B Receptor does not affect the BP Response to Salt. Ninth International Conference on Endothelin. Salt Lake City, Utah, USA.

**Kelland NF**, Bagnall AJ, Gulliver-Sloan F, Kuc RE, Maguire JJ, Davenport AP, Gray GA, Kotelevtsev Y and Webb DJ. Scavenging of plasma endothelin-1 is mediated by the endothelial cell endothelin B receptors. [Oral presentation at the Ninth International Conference on Endothelin. Salt Lake City, Utah, USA]

**Kelland NF**, Bagnall AJ, Morecroft I, Gulliver-Sloan F, Dempsie FH, Nilson M, MacLean MR, Kotelevtsev Y and Webb DJ. Endothelial cell-specific knockout of the ET<sub>B</sub> receptor exaggerates hypoxia induced pulmonary arterial hypertension. [Oral presentation at the Winter BPS Meeting, London UK].



## **PRIZES**

Young Investigator Award, Centre for Cardiovascular Science Day, Edinburgh University, July 2004

Pfizer Academic Travel Award, Aug 2004

New Investigator Award for European Fellows, AHA Council for High Blood Pressure Research, Chicago, USA, Oct 2004

Sir Stanley Davidson Travel Award, University of Edinburgh, April 2005

Young Investigator Award, Ninth International Conference on Endothelin, Utah, USA, Sept 2005

## PUBLICATIONS

Bagnall AB and **Kelland NF**, Gulliver-Sloan FH, Davenport AP, Gray GA, Yanagisawa M, Webb DJ and Kotelevtsev YV. (2006). Deletion of endothelial cell endothelin B receptors does not affect blood pressure or sensitivity to salt. *Hypertension*: **48**; 286-93.

**Kelland NF**, Webb, DJ. (2006). Clinical Trials of Endothelin Antagonists in Heart Failure: A Question of Dose? *Experimental Biology and Medicine*: **231**; 696-699.

Battistini B, Berthiaume N, **Kelland NF**, Webb DJ and Kohan DE. (2006). Profile of Past and Current Clinical Trials Involving Endothelin Receptor Antagonists: The Novel "-Sentan" Class of Drug. *Experimental Biology and Medicine*: **231**; 653-695.

**Kelland NF** and Webb DJ. (2007). Clinical trials of endothelin antagonists in heart failure: publication is good for the public health. *Heart*: **93**; 2-4.

**Kelland NF**, Kuc RE, Armour DL, Bagnall AJ, Gulliver-Sloan F, Maguire JJ, Davenport AP, Gray GA, Kotelevtsev Y and Webb DJ. Endothelial Cell Specific Knockout of the Endothelin B Receptor Demonstrates Its Crucial Role In The Clearance Of Endothelin-1. (Manuscript in preparation).

**Kelland NF**, Bagnall AJ, Morecroft I, Gulliver-Sloan F, Dempsie Y, Nilsen M, Kotelevtsev Y and Webb DJ. Endothelial cell ET<sub>B</sub> receptors limit vascular remodeling and the development of pulmonary hypertension during hypoxia. (Manuscript in preparation).

## Acknowledgements

I would like to thank my supervisors Drs Yuri Kotelevtsev, Gillian Gray and Professor David Webb. Yuri supervised Alan Bagnall during his PhD, resulting in the generation of the mouse model, and has continued to lead the project, giving me limitless advice and guidance, allowing me to characterise the cardiovascular phenotype of the animal. Gillian's direction and support, not only during the writing of my BHF Junior Research Fellowship, but in overcoming the many difficulties and obstacles posed by physiological experiments in small rodents, has been crucial to the success of this project. David provided support whilst the pilot experiments necessary for my BHF Fellowship were performed, and greatly assisted me in writing the resulting successful application. Without his overview of the project, objective assessment of experimental design and critical review of the data, the work would not have been possible.

Alan Bagnall's commitment to the project and enthusiasm to extend the possible applications of the mouse he generated with Yuri has resulted in many useful discussions and new approaches being followed. Without Fiona Gulliver-Sloan's ceaseless efforts, contributing significantly to the genotyping and management of the colony as well as her great experience of physiological and pharmacological experiments, much of this project would have stumbled and faltered.

I am also indebted to my wife Cathy, whose support throughout this project has been crucial to its success.

I would also like to thank:

Neil Johnson, Amie Bowler and Nicola Brewster for carrying out the plasma ET-1 radioimmunoassay;

Danielle Armour who worked tirelessly with the renal ET system RT-PCR for her Pharmacology BSc Honours project, and more latterly with the LacZ studies and endothelial cell microscopy;

Ian Megson for countless discussions about the most suitable method of data analysis;

Animal house staff: Carole, Pat, Vince, Keith and Julie for their husbandry of the colony;

Masashi Yanagisawa for the generous donation of the Tie2-Cre mice;

Alexander Medvinsky for the donation of EGFP reporter mice and for carrying out the EGFP expression studies;

Nathalie Berthiaume and Pedro d'Orlean-Juste for helpful advice concerning the radiolabelled [<sup>125</sup>I]-ET-1 clearance experiments;

Hans van Wyk (Quintiles), Gillian Brooker, Isam Sharif and Veterinary Surgeons Jane Conole and Eleanor Weir for surgical advice and assistance;

Abbott Pharmaceuticals, IL, USA for donation of A192621 and ABT627 and David Pollock for advice about how best to administer them to mice;

Ruth Andrew for discussions about the ET-1 clearance data, and for her help in analysing the results;

Don Kohan for advice about salt feeding;

Chris Kenyon and Janice Paterson for useful discussions concerning telemetry data analysis;

John Mullins, Head of the Centre for Cardiovascular Science, for cooperation to use the BHF telemetry facilities;

Pete Hodgson for surgical insertion of telemetry devices;

all in Cambridge who worked with me on the autoradiography experiments - Anthony Davenport, Rhoda Kuc and Janet Maguire;

Mandy MacLean, Ian Morecroft, Yvonne, and Margaret Nelson (University of Glasgow) for their collaboration and assistance with the PAH study;

the other students in our lab for making the place a great place to work: Adele, Kat, Mike, Katie, Markus, Mark, Helen, Sarah and Katsuaki;

and the British Heart Foundation for funding me during my PhD.

## Abbreviations

|                  |   |
|------------------|---|
| ACE              | Angiotensin Converting Enzyme   |
| ANF              | Atrial Natriuretic Factor   |
| ANOVA            | Analysis of Variance  |
| AQ2-Cre          | Aquaporin2 Promoter/ enhancer Cre transgene (Inner medullary collecting duct cell specific) |
| AUC              | Area Under the Curve  |
| $\beta$ -gal     | $\beta$ -galactosidase  |
| BMPR2            | Bone Morphogenetic Protein Receptor II  |
| bp               | Base Pair   |
| BP               | Blood Pressure  |
| bpm              | Beats per minute (Heart rate)   |
| BSA              | Bovine serum albumin  |
| BW               | Body Weight   |
| $C_L$            | Clearance   |
| CRC              | Concentration Response Curve  |
| Cre              | Cre recombinase   |
| dATP             | 2'-deoxyadenosine 5'-triphosphate   |
| DBP              | Diastolic BP  |
| dCTP             | 2'-deoxycytidine 5'-triphosphate  |
| dGTP             | 2'-deoxyguanosine 5'-triphosphate   |
| DNA              | Deoxyribonucleic Acid   |
| dTTP             | 2'-deoxythymidine 5'-triphosphate   |
| EC               | Endothelial Cell  |
| ECE              | Endothelin Converting Enzyme  |
| EDTA             | Ethylenediaminetetraacetic acid   |
| EGFP             | Enhanced Green Fluorescent Peptide  |
| $E_{max}$        | Maximal observed response   |
| ENaC             | Epithelial Sodium Channel   |
| eNOS             | Endothelial Nitric Oxide Synthase   |
| ES Cells         | Embryonic Stem Cells  |
| ET               | Endothelin  |
| ET <sub>A</sub>  | Endothelin A Receptor   |
| ET <sub>B</sub>  | Endothelin B Receptor   |
| EVG              | Elastica–van Gieson stain   |
| FiO <sub>2</sub> | Percentage of oxygen in inhaled air   |
| Flox             | Floxed ET <sub>B</sub> Receptor Allele  |
| G                | Gravity   |
| GAPDH            | Glyceraldehyde-3-phosphate dehydrogenase  |
| GFP              | Green Fluorescent Peptide   |
| GPCR             | G-protein Coupled Receptor  |
| IC               | Internal Circumference  |
| I.D.             | Internal Diameter   |
| IMCD             | Inner Medullary Collecting Duct   |
| IP               | Intra-Peritoneal  |

|                     |   |
|---------------------|---|
| IV                  | Intra-Venous  |
| $K_{el}$            | Elimination constant  |
| KO                  | Knockout  |
| Lac Z               | Galactosidase Gene  |
| L-NAME              | N <sup>o</sup> -Nitro-L-Arginine Methyl Ester Hydrochloride   |
| LV                  | Left Ventricle  |
| LV + S              | Left Ventricle + Septum   |
| MABP                | Mean Arterial Blood Pressure  |
| MMPs                | Metalloproteinases  |
| mRNA                | Messenger Ribonucleic Acid  |
| NAD(P)H             | Nicotinamide adenine dinucleotide phoshate  |
| NO                  | Nitric Oxide  |
| NOS                 | Nitric Oxide Synthase   |
| O.D.                | Outside Diameter  |
| OD                  | Optical Density   |
| PA                  | Pulmonary Artery  |
| PAH                 | Pulmonary Arterial Hypertension   |
| PBS                 | Phosphate Buffered Saline   |
| PCR                 | Polymerase Chain Reaction   |
| PCV                 | Packed Cell Volume (Haematocrit)  |
| pEC <sub>50</sub>   | Negative Logarithm of EC <sub>50</sub> (Concentration required to cause 50% of maximal observed response) |
| PGI <sub>2</sub>    | Prostacyclin  |
| PGI <sub>2</sub> -S | Prostacyclin Synthase   |
| PVR                 | Pulmonary Vascular Resistance   |
| R26R                | Rosa 26 reporter mouse strain   |
| RIA                 | Radioimmunoassay  |
| RT-PCR              | Reverse Transcriptase – Polymerase Chain Reaction   |
| RV                  | Right Ventricle   |
| RVP                 | Right Ventricular Pressure  |
| S6c                 | Sarafotoxin 6c  |
| SBP                 | Systolic BP   |
| SDS                 | Sodium Duodecyl Sulphate Buffer   |
| Smads               | Stimulatory mothers against decapentaplegic proteins  |
| SMS                 | Smooth Muscle Cell  |
| SSC                 | Sodium Sodium Citrate Buffer  |
| Tie2                | Tie2 Promoter/ enhancer of Cre transgene (endothelial cell specific)                                      |
| TV                  | Total Ventricles  |
| v/v                 | Volume per Volume   |
| V <sub>d</sub>      | Volume of distribution  |
| VSMC                | Vascular Smooth Muscle Cell   |
| vWF                 | von Willibrand factor   |
| W                   | Wild type ET <sub>B</sub> Receptor Allele   |
| w/v                 | Weight per Volume   |

## Abstract

Endothelin-1 (ET-1) binds to endothelin A (ET<sub>A</sub>) and B (ET<sub>B</sub>) receptors on vascular smooth muscle cells, resulting in profound vasoconstriction and cellular proliferation. In contrast, activation of endothelial cell (EC) ET<sub>B</sub> receptors releases nitric oxide (NO) and prostacyclin (PGI<sub>2</sub>), which are anti-mitotic and mediate vasodilatation. ET<sub>B</sub> receptors are also responsible for the clearance of ET-1 from the circulation and renal ET<sub>B</sub> receptors contribute to sodium and water balance. Pharmacological blockade and genetic models featuring total ET<sub>B</sub> ablation, demonstrate salt sensitive hypertension. However, these do not allow the role of the EC ET<sub>B</sub> in cardiovascular homeostasis to be determined. Mice featuring loxP sites flanking exons 3 and 4 of the ET<sub>B</sub> gene (floxed ET<sub>B</sub> mice: FF/--) were crossed with Tie2-Cre mice (WW/Tie2-Cre), in which the expression of a Cre recombinase cDNA transgene is limited to EC, to generate EC-specific ET<sub>B</sub> down-regulated mice (FF/Tie2-Cre). Having demonstrated EC-specific down-regulation of ET<sub>B</sub> receptors using autoradiography, the role and relative contribution of the EC ET<sub>B</sub> to the regulation of systemic BP, to the clearance of ET-1 from the plasma, as well as to the development of pulmonary arterial hypertension were investigated.

Autoradiography revealed significant down-regulation of ET<sub>B</sub> in EC-rich tissues such as lung of FF/Tie2-Cre animals ( $8 \pm 3$  amol.mm<sup>-2</sup>) compared to controls ( $80 \pm 21$  amol.mm<sup>-2</sup>) (n=4;  $p < 0.05$ ). Levels of ET<sub>A</sub> expression were preserved despite higher concentrations of plasma ET-1 in the FF/Tie2-Cre samples ( $12.4 \pm 3.0$  pg.ml<sup>-1</sup>) compared to controls ( $3.0 \pm 0.8$  pg.ml<sup>-1</sup>) (n=6;  $p < 0.001$ ). Using radiotelemetry, mean arterial blood pressure of FF/Tie2 mice was not significantly different to that of FF/- controls on low salt (FF/Tie2-Cre:  $122.7 \pm 1.52$  mmHg, n=10; FF/--:  $125.7 \pm 0.58$  mmHg, n=12), normal salt (FF/Tie2-Cre:  $133.8 \pm 4.0$  mmHg, n=10; FF/--:  $131.5 \pm 3.33$  mmHg, n=12) or high salt diet (FF/Tie2-Cre:  $149.2 \pm 2.71$  mmHg, n=10; FF/--:  $143.9 \pm 2.97$  mmHg, n=12). Similarly no differences in SBP, DBP or HR were seen between genotypes. The clearance of an intravenous bolus of radiolabelled ET-1 was significantly impaired in FF/Tie2-Cre mice ( $0.054 \pm 0.006$  ml.sec<sup>-1</sup>) compared to control mice ( $0.175 \pm 0.032$  ml.sec<sup>-1</sup>) (n=5;  $p < 0.01$ ). ET<sub>B</sub> blockade of control mice

reduced ET-1 clearance to that of untreated FF/Tie2-Cre animals (n=4). Two weeks of hypobaric hypoxia induced an exaggerated increase in systolic right ventricular pressure in FF/Tie2-Cre mice ( $34.4 \pm 1.2$  mmHg, n=10) compared with FF/-- mice ( $24.6 \pm 1.4$  mmHg, n=10;  $p < 0.05$ ), associated with an increased right ventricular/ left ventricular + septum ratio in FF/Tie2-Cre mice (normoxia:  $0.224 \pm 0.009$ ; hypoxia:  $0.285 \pm 0.017$ ;  $p < 0.01$ ), but not in FF/-- mice. Hypoxia increased the percentage of remodeled vessels in FF/-- mice (normoxia:  $5.6 \pm 0.6\%$ ; hypoxia:  $11.4 \pm 0.6\%$ ; n=6;  $p < 0.001$ ), and this was augmented in FF/Tie2-Cre mice (normoxia:  $7.1 \pm 0.5\%$ ; hypoxia:  $18.5 \pm 1.2\%$ ; n=6;  $p < 0.001$ ).

The EC ET<sub>B</sub> receptor does not play a significant role in the BP response to salt, suggesting that ET<sub>B</sub> signalling on other cell types is responsible for ET<sub>B</sub> mediated natriuresis. However, the EC ET<sub>B</sub> receptor is crucial to the elimination of ET-1 from the circulation and is protective against the development of pulmonary arterial hypertension, most likely by preventing remodeling of small pulmonary arteries.



# **1 CHAPTER 1: GENERAL INTRODUCTION**

## **1.1 PHARMACOLOGY OF ENDOTHELIN**

### **1.1.1 Structure of ET-1**

Endothelin-1 (ET-1) was first isolated and characterised as a novel vasoconstrictor peptide derived from cultured porcine aortic ECs (Yanagisawa *et al.*, 1988). As well as controlling basal vascular tone, the ET system plays a pivotal role in embryonic development, fluid balance, cardiac and respiratory function. There are 2 other isoforms of the peptide: endothelin 2 and endothelin 3. All 3 share structural homology: a 21 amino acid peptide whose secondary structure is stabilised by 2 N-terminal disulphide bonds, with a highly preserved hydrophobic C terminal sequence (see Figure 1-1). ET-1 is the only isoform constitutively expressed in EC (Inoue *et al.*, 1989; Levin, 1995).

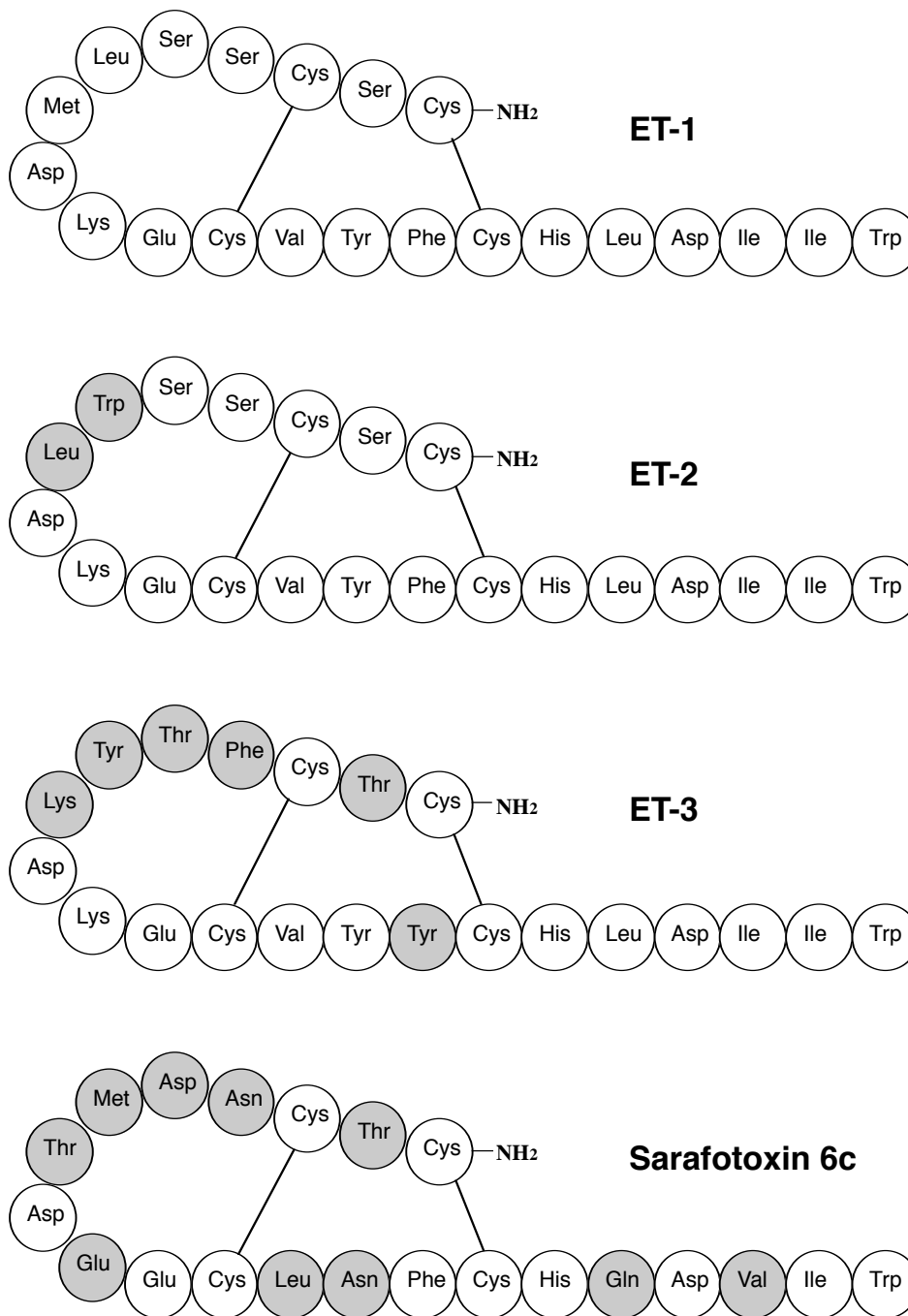


**Figure 1-1: Structure of ET-1, ET-2, ET-3 and S6c**

### **1.1.2 Production of ET-1**

The human genes for ET-1, ET-2 and ET-3 are located on chromosomes 6, 1, and 20 respectively. These peptides are synthesised as large ~200-residue precursors before being processed by 2 proteases to create the mature active forms. Regulation of

peptides such as endothelin can occur at the level of synthesis, storage and release. Much of the control of ET-1 production occurs at the level of transcription. Transcription of ET-1 mRNA is upregulated by cytokines (transforming growth factor  $\beta$ , tumor necrosis factor  $\alpha$ , interleukins and endotoxin), hormones (insulin, catecholamines, angiotensin II, vasopressin, cortisol, and endothelin) and thrombin (Emori *et al.*, 1992; Kurihara *et al.*, 1989; Yanagisawa *et al.*, 1988). In ECs, ET-1 transcription is increased by hypoxia and low shear stress, but inhibited by higher stretch forces (Malek *et al.*, 1999). Inhibition of ET-1 transcription is caused by atrial natriuretic factor (ANF) and endothelial derived relaxing factors such as prostacyclin ( $\text{PGI}_2$ ) and nitric oxide (NO) (Boulanger *et al.*, 1990; Kohno *et al.*, 1992; Prins *et al.*, 1994) (see Figure 1-2).

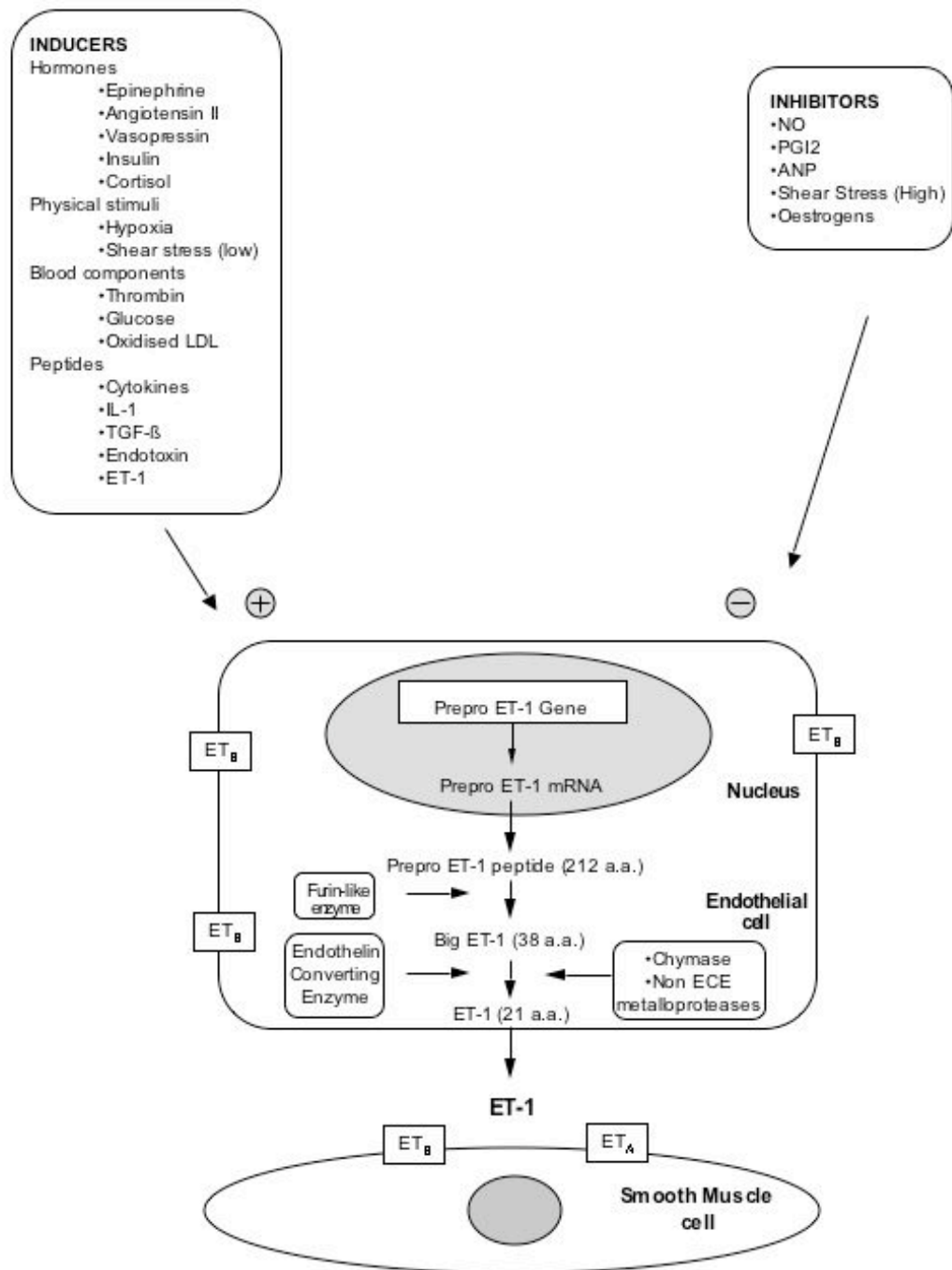


**Figure 1-2: Factors affecting the synthesis of ET-1.**  
(For references see text)

The ~200 - amino acid preproendothelins are cleaved at dibasic sites by furin-like endopeptidases to form biologically inactive intermediates: 37 to 41 amino acid peptides termed big endothelins (big ETs). Next, cleavage at Trp<sup>21</sup>-Val<sup>22</sup> of ET-1 and

ET-2, and Trp<sup>21</sup>-Ile<sup>22</sup> of ET-3, catalysed by the metalloprotease endothelin-converting enzymes (ECEs), generates mature ET-1, ET-2 and ET-3 respectively.

The release of ET-1 may occur by both constitutive and regulated pathways. Using immuno-electron microscopy, ET-1 immunoreactivity has been identified in both secretory granules (involved in the constitutive pathway) as well as EC-specific storage granules known as Weibel-Palade bodies (likely to be involved in the regulated pathway) (Russell *et al.*, 1998a). It is thought that these Weibel-Palade bodies degranulate after chemical or mechanical stimuli that result in cytosolic calcium influx (Russell *et al.*, 1998b). ECE-1 has also been identified within these Weibel-Palade bodies, allowing the release of mature ET-1 when intracellular calcium rises.

ET-1 is synthesised by a range of different cell types. As well as ECs (Yanagisawa *et al.*, 1988), the predominant source of the peptide *in vivo*, ET-1 is produced by airway epithelial cells (Giaid *et al.*, 1991; MacCumber *et al.*, 1989), macrophages (Rubanyi *et al.*, 1991), fibroblasts (Rubanyi *et al.*, 1991), cardiomyocytes (Sakai *et al.*, 1996), renal epithelial cells (Karet *et al.*, 1996; Kohan, 1991), various brain neurons (Lee *et al.*, 1990) and other cells (Rubanyi *et al.*, 1991).

The plasma concentration of ET-1 in many species is  $\sim 1$  pM (3 pg.ml<sup>-1</sup>) (Battistini *et al.*, 1993), more than 100 fold lower than the pharmacological threshold. Originally this was taken as evidence that endogenously produced ET-1 had little or no effect on basal vascular tone. However administration of ET antagonists has a marked haemodynamic effect both locally (Haynes *et al.*, 1994) and systemically (Spratt *et al.*, 2001; Strachan *et al.*, 1999), clearly demonstrating that ET-1 has endogenous activity.

Therefore, under normal physiological conditions, ET-1 is not a circulating hormone, rather acting as a local autocrine or paracrine mediator at multiple sites throughout the body.

### 1.1.3 Endothelin Converting Enzyme

Three isoforms of ECE have been identified in animals (ECE-1, ECE-2 and ECE-3) but only ECE-1 and ECE-2 have been identified in humans (Russell *et al.*, 1999). ECE-1 has an optimum pH of 6.8, suggesting that ECE-1 is involved in the constitutive production of ET-1 (Russell *et al.*, 1999) both intracellularly and at the cell surface (Xu *et al.*, 1994). In contrast, ECE-2 has a pH optimum of 5.5 and has been shown to be present in acidic secretory vesicles within ECs, suggesting that this enzyme has a pathogenic role in states where the intracellular pH is reduced (eg myocardial ischaemia) (Russell *et al.*, 1999). As well as these 2 proteases, another unidentified enzyme is capable of processing big ETs, as mice lacking both ECE-1 and ECE-2 exhibit significant concentrations of mature ET peptides (Yanagisawa *et al.*, 2000).

The human ECE-1 gene is located on chromosome 1. Four splice variants exist named ECE-1a to ECE-1d in the human (Turner *et al.*, 1998). They share a common C terminus catalytic domain (from amino acid position 33) but differ in only a few amino acids at the N-terminus. This determines the exact cellular location of these isoforms (Valdenaire *et al.*, 1999). ECE-1c, the primary isoform in humans, is found in both the cell membrane as well as in the cytoplasm; ECE-1a is mainly found only in the cell membrane; and ECE-2b is exclusively intracellular.

To date there have only been 2 isoforms of ECE-1 identified in the rat (Shimada *et al.*, 1995). These have been rather confusingly named ECE-1 $\alpha$ , which is now known to be analogous to ECE-1a, and ECE-1 $\beta$ , which was originally thought to be the equivalent of ECE-1a but has now been shown to be the counterpart of ECE-1c.

ECEs are characterised by their sensitivity to phosphoramidon, a dual ECE and neutral endopeptidase (NEP) inhibitor, but are resistant to the action of the NEP selective inhibitor thiorphan.

#### 1.1.4 Endothelin receptors

In mammals, two ET receptors (ET<sub>A</sub> and ET<sub>B</sub>) have been identified (Arai *et al.*, 1990; Sakurai *et al.*, 1990). These are both G protein coupled receptors (GPCRs) and contain 7 transmembrane domains of 22-26 hydrophobic amino acids in their 400-residue sequences. Each receptor activates an overlapping set of G proteins (G<sub>s</sub>, G<sub>i</sub>, or G<sub>q</sub>) each composed of three subunits ( $\alpha$ ,  $\beta$  and  $\gamma$ ), leading to activation of a range of intracellular second messengers. Evidence from G-protein inhibitors, such as *Bordatella pertussis* toxin and subunit specific antisera, indicates that ET receptors can interact with at least 3 different G <sub>$\alpha$</sub> -subunits to activate the various downstream second messenger pathways (Douglas *et al.*, 1997). For example, ET<sub>A</sub> and ET<sub>B</sub> receptors, located on vascular smooth muscle, are coupled to phospholipase C (PLC) via G $\alpha_q$ . Activation of this pathway results in elevated intracellular levels of inositol triphosphate, diacylglycerol and calcium causing, amongst other effects, a long lasting vasoconstriction (Pollock *et al.*, 1995). VSMC ET<sub>A</sub> receptors are also coupled to adenylate cyclase (AC) by G $\alpha_s$ , whereas EC ET<sub>B</sub> receptors are linked to AC via G $\alpha_i$  (Rubanyi *et al.*, 1994). Thus the particular second messenger pathway activated is dependent on the cell type on which the ET receptors are expressed.

The precise signalling mechanisms utilised by ET<sub>A</sub> compared to ET<sub>B</sub> receptors, on cells types such as vascular smooth muscle cells (VSMCs), may exhibit certain differences but the exact nature of these has not been determined (Douglas *et al.*, 1997).

Activation of the EC ET<sub>B</sub> receptor, in contrast, results in increased endothelial nitric oxide synthase (eNOS) (Hirata *et al.*, 1993) and prostacyclin synthase (PGI<sub>2</sub>-S) (see Figure 1-3 below).

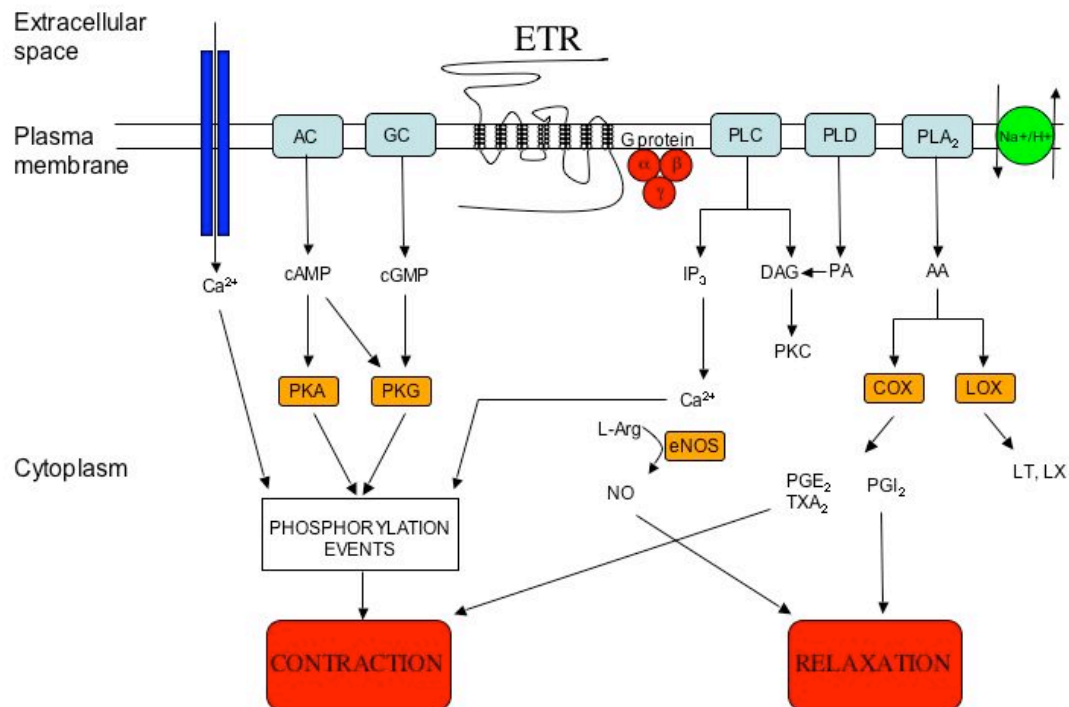


**Figure 1-3: ET receptor intracellular signalling**

Schematic illustration of the intracellular signalling pathways involved in the response of the cell to activation of the G protein linked ET receptor. AA, arachidonic acid; AC, adenylylase; COX, cyclo-oxygenase; DAG, diacylglycerol; eNOS, endothelial NO synthase; GC, guanylate cyclase; IP<sub>3</sub>, inositol 1,4,5-trisphosphate; LOX, lipoxygenase; LT, LX, leukotrienes; PA, phosphatidic acid; PGE<sub>2</sub>, prostaglandin E<sub>2</sub>; PGI<sub>2</sub>, prostaglandin I<sub>2</sub>; PKA, protein kinase A; PKC, protein kinase C; PKG, protein kinase G. (Adapted from (D'Orleans-Juste *et al.*, 2002)).

#### 1.1.4.1 ET<sub>A</sub> RECEPTOR

The ET<sub>A</sub> receptor has subnanomolar affinities for ET-1 and ET-2 but very much lower affinity for ET-3 (Arai *et al.*, 1990). ET<sub>A</sub> receptors are found on vessel and airway smooth muscle cells, cardiomyocytes, liver stellate cells and hepatocytes, brain neurons, osteoblasts, melanocytes and keratocytes, adipocytes and various cells of the reproductive tract (Kedzierski *et al.*, 2001).



#### 1.1.4.2 ET<sub>B</sub> RECEPTOR

##### 1.1.4.2.1 Molecular structure of ET<sub>B</sub> receptor

The ET<sub>B</sub> receptor has a relative molecular mass of 50 kDa and exhibits remarkable structural homology across species although the chromosomal location and number of amino acids are species specific (D'Orleans-Juste *et al.*, 2002). Mutations of the gene have been identified in patients with Hirschsprung's disease (Berthiaume *et al.*, 2000; Chakravarti, 1996; Edery *et al.*, 1996; Gariepy, 2001). A mutation in the first transmembrane domain of the human ET<sub>B</sub> receptor (Cys<sup>109</sup> replaced by L-Arg) impedes the translocation of the receptor to the membrane (Tanaka *et al.*, 1998). Furthermore, substitution in the fifth transmembrane domain of the highly conserved Try<sup>276</sup> by Cys does not affect the binding of the ligand to the receptor, but markedly reduces calcium entry and mobilization of the ligand receptor complex (Puffenberger *et al.*, 1994). In addition, substitution of Ser<sup>390</sup> by L-Arg in the last intracellular C-terminal loop of the GPCR does not affect binding, but markedly reduces the capacity of the complex to increase intracellular calcium (Tanaka *et al.*, 1998).

##### 1.1.4.2.2 Pharmacology of ET<sub>B</sub> receptor

In contrast to the ET<sub>A</sub> receptors, the ET<sub>B</sub> receptor binds all ETs with equal affinity (Sakurai *et al.*, 1990). During the 1990s, a subdivision of ET<sub>B</sub> receptors into ET<sub>B1</sub> and ET<sub>B2</sub> was proposed based on the much lower observed affinity of VSMC ET<sub>B</sub> receptors compared to those of ECs. Functional studies had suggested that PD142893, a dual ET<sub>A/B</sub> antagonist, could block the vasodilator actions of ET-1 at EC ET<sub>B</sub> receptors, but not constrictor responses mediated by VSMC ET<sub>B</sub> (Douglas *et al.*, 1995; Warner *et al.*, 1993). However, in the ET<sub>B</sub> receptor gene knockout (KO) mouse, both the PD142893-sensitive vasodilator response and the PD142893-resistant contractile response to the ET<sub>B</sub> agonist sarafotoxin S6c were completely absent (Mizuguchi *et al.*, 1997). These results indicate that the pharmacologically heterogeneous responses to S6c are mediated by ET<sub>B</sub> receptors derived from the same gene, providing strong evidence against a molecular basis for the sub-classification of the ET<sub>B</sub>. Furthermore, in human tissue, both ET<sub>A</sub>- and ET<sub>B</sub>- selective radiolabeled ligands bound with a single affinity, and Hill slopes close to unity (Davenport *et al.*, 1998; Davenport *et al.*, 1994; Molenaar *et al.*, 1992). Similarly,

competition studies using unlabeled ligands provided no evidence to suggest any sub-classification of the ET<sub>B</sub> receptor (Peter *et al.*, 1996; Russell *et al.*, 1996).

#### 1.1.4.2.3 Expression of ET<sub>B</sub> receptor

ET<sub>B</sub> receptors are found on a wide range of tissues: vessel ECs as well as smooth muscle cells, liver hepatocytes and Ito cells, renal collecting duct epithelial cells, airway smooth muscle cells, osteoblasts, neurons of the CNS and PNS (Kedzierski *et al.*, 2001). Here they play fundamental roles in the regulation of several physiological functions, such as modulation of vascular resistance (Strachan *et al.*, 1999), natriuresis (Clavell *et al.*, 1995), hepatic function (Rockey *et al.*, 1996), and neuronal activities (Lysko *et al.*, 1995).

### 1.1.5 Internalisation of receptors

Elegant studies have used fluorescence microscopy to track the movement of fluorescein-conjugated ET-1 when bound to ET<sub>B</sub> receptors labeled with green fluorescent peptide (GFP). Chinese hamster ovary cells expressing the ET<sub>B</sub>/GFP fusion protein demonstrate strong signals at the plasma membrane. On addition of fluorescein-conjugated ET-1, internalisation of ligand and receptor occurs within 5 minutes, via a sucrose-sensitive (i.e. clathrin-mediated) pathway (Oksche *et al.*, 2000). In contrast, ET<sub>A</sub> receptors are internalised via caveolae (Chun *et al.*, 1995), where they remain intact for up to 2 hours, until the ET-1/ ET<sub>A</sub> receptor complex separates, most likely within acidic lysosomes. If such prolonged binding of ET-1 to ET<sub>A</sub> receptors results in the continued activation of signal-transducing G proteins, then this might account for the prolonged period of ET-1 induced VSMC contraction. Whilst ET<sub>A</sub> receptors are eventually recycled back to the cell surface (Marsault *et al.*, 1993), ET-1 remains bound to ET<sub>B</sub> (see below) (Oksche *et al.*, 2000). Reappearance of ET<sub>B</sub> at the cell surface is therefore dependent on *de novo* synthesis of receptors. The lack of trafficking of ET<sub>B</sub> back to the cell membrane helps provide an explanation for the rapid tachyphylaxis of ET<sub>B</sub> modulated vasodilatation seen in response to repeated boluses of ET-1, whilst ET<sub>A</sub>-mediated vasoconstriction is preserved (Le Monnier de Gouville *et al.*, 1990).

### 1.1.6 Clearance of ET-1

ET-1 is removed from the plasma largely by binding to ET<sub>B</sub> receptors although it is also degraded by neutral endopeptidases (Deng *et al.*, 1992). Inhibition of neprilysin (neutral endopeptidase EC 3.4.24.11) increases both urinary and plasma ET-1 concentrations, implying it plays a role in controlling ET-1 removal from the circulation (Abassi *et al.*, 1992). The sites of this non ET<sub>B</sub> mediated clearance are likely to be in the kidney and liver (Burkhardt *et al.*, 2000).

As outlined above, fluorescence microscopy has shown that ET<sub>B</sub> receptors bind ET-1 and internalise it, thereby removing the peptide from the plasma (Oksche *et al.*, 2000). Early work in rats has shown that exogenous radiolabelled ET-1 is rapidly removed from the plasma and trapped mostly in the lungs, but also in the liver and kidneys (Fukuroda *et al.*, 1994). The lungs contain ~50% of the endothelium of the entire vascular tree, and so unsurprisingly are extremely efficient at scavenging ET-1 from the plasma: they retain >60% of the circulating ET-1 at each pulmonary pass (de Nucci *et al.*, 1988; Dupuis *et al.*, 1996b). This clearance is significantly inhibited by the ET<sub>B</sub> antagonist BQ-788, whilst ET<sub>A</sub> blockade with BQ-123 has no such effect (Fukuroda *et al.*, 1994). Similar studies in isolated rat hearts showed that ET<sub>B</sub> blockade increases plasma ET-1 concentration (Brunner *et al.*, 1996).

ECs in culture swiftly scavenge exogenous ET-1 in an ET<sub>B</sub> dependent, ET<sub>A</sub> independent manner (Ozaki *et al.*, 1995). Furthermore, transgenic rats, featuring a homozygous mutation in the ET<sub>B</sub> gene, have an increased circulating concentration of ET-1 (Garipey *et al.*, 2000). Both wild type rats treated with ET<sub>B</sub> antagonists (Burkhardt *et al.*, 2000) as well as heterozygote ET<sub>B</sub> knockout (KO) mice (Berthiaume *et al.*, 2000) demonstrate impaired ET-1 scavenging whereas wild type rats given ET<sub>A</sub> antagonists and heterozygote ET<sub>A</sub> KO mice have normal ET-1 clearance.

Studies in humans have shown that the lungs are a major site of ET-1 extraction from the plasma (Dupuis *et al.*, 1996b) and that agents that block the ET<sub>B</sub> receptor cause increases in plasma ET-1 concentrations (Cowburn *et al.*, 2005; Dingemanse *et al.*, 2002; Goddard *et al.*, 2004b; Haynes *et al.*, 1996; Strachan *et al.*, 1999; Sutsch *et al.*, 1998; Weber *et al.*, 1996). In contrast there was no significant increase in ET-1 plasma concentration at a range of ET<sub>A</sub> selective doses of BQ-123 (Cowburn *et al.*, 2005; Goddard *et al.*, 2004b; Spratt *et al.*, 2001).

In summary, whilst there is limited evidence for degradation of ET-1 by peptidases, most of the removal of ET-1 from the circulation is via binding to the ET<sub>B</sub> receptor followed by internalisation.

## **1.2 PHYSIOLOGICAL ROLES OF ENDOTHELIN**

The ET system is involved in a wide spectrum of different physiological processes throughout the body. Here, the role of ET in embryological development, the control of vascular tone, renal function as well as in the pulmonary vascular tone and remodelling will be discussed.

### **1.2.1 Role of Endothelins in development**

The discovery that the ET system is important in development was serendipitous. Initial efforts to generate transgenic animal models featuring gene KO of different components of the ET system were complicated by embryonic lethality. Study of the phenotype of these models has revealed the importance of the ET system in correct pattern formation during embryonic development.

ET-1, ET<sub>A</sub>, or ECE-1 deficient animals have craniofacial malformations including cleft palate, small mandible, hypoplastic tongue, and abnormal fusion of the hyoid bone to the base of the skull (Clouthier *et al.*, 1998; Clouthier *et al.*, 2004; Kurihara *et al.*, 1994; Yanagisawa *et al.*, 1998) and so die at birth due to airway obstruction. For normal development of the cephalic neural crest cells, ET-1 produced by the

epithelium of the pharyngeal arches must activate ET<sub>A</sub> receptors on these neural crest cells (Clouthier *et al.*, 2000). Similarly, activation of ET<sub>A</sub> receptors on cardiac neural crest cells, by ET-1 produced from overlying ECs, is required for normal development of the great vessels and ventricular outflow tract. ET-1, ET<sub>A</sub>, or ECE-1 KO mice also feature cardiac abnormalities including interruption of the aorta, presence of a right-sided aortic arch and ventricular septal defects (Clouthier *et al.*, 1998; Kurihara *et al.*, 1995; Yanagisawa *et al.*, 1998). ECE-2 KO mice are healthy into adulthood, are fertile in both sexes, and live a normal life span. However, when they are bred onto an ECE-1-null background, defects in cardiac outflow structures become more severe than those in ECE-1 single KO embryos (Yanagisawa *et al.*, 2000).

ET-3 and ET<sub>B</sub> KO mice are viable until weaned at ~3 weeks of age. ECE-1 KO mice display the additive phenotype of animals lacking ET-1/ET<sub>A</sub> and ET-3/ET<sub>B</sub> pathways. ET-3, ET<sub>B</sub> or ECE-1 deficient mice have white spotted hair and skin colour, but normal black eyes. They die at weaning due to intestinal obstruction caused by aganglionic megacolon (Baynash *et al.*, 1994; Hosoda *et al.*, 1994; Yanagisawa *et al.*, 1998). Correct development of the myenteric plexus depends on ET-3 released by mesenchymal tissue activating ET<sub>B</sub> receptors on neural crest cells (Xie *et al.*, 1997). It has been shown that these neural crest cells develop into melanocytes (Shin *et al.*, 1999). The phenotype of spotted white coat colour and intestinal aganglionosis is also seen in naturally occurring mutations of the ET-3 (lethal spotted mice) (Baynash *et al.*, 1994) and ET<sub>B</sub> receptor (piebald-lethal) (Hosoda *et al.*, 1994) genes. Furthermore ET<sub>B</sub> receptor and ET-3 mutations have been identified in patients with Hirschsprung's disease (Chakravarti, 1996; Edery *et al.*, 1996; Garipey, 2001).

Thus ET-3, ET<sub>B</sub> and ECE-1 are necessary for normal development of neural crest derived epidermal melanocytes and enteric neurons, whilst ET-1, ET<sub>A</sub> and ECE-1 are necessary for the successful development of cephalic and cardiac neural crest derived craniofacial and cardiac outflow structures.

### 1.2.2 Role of Endothelins in vessels

When identified in 1988, ET-1 was first characterised as a highly potent vasoconstrictor peptide (Yanagisawa *et al.*, 1988), and so, not surprisingly, much effort has been focussed on its role in the control of vascular tone and regulation of BP. ET-1 is the only isoform of the 3 ETs produced by ECs (Inoue *et al.*, 1989), and of the 3 has the most marked effects on the vessel wall (Levin, 1995). Its local concentration is ~100-fold that found in the plasma, as more than three quarters of ET-1 is secreted abluminally from the basolateral side of ECs (Wagner *et al.*, 1992). Both ET<sub>A</sub> and ET<sub>B</sub> receptors are expressed by VSMCs within the blood vessel wall (Arai *et al.*, 1990; Batra *et al.*, 1993), whereas only ET<sub>B</sub> receptors, are found on ECs (Saetrum Opgaard *et al.*, 1996). In a wide range of species, an intravenous bolus of ET-1 results in a biphasic response (Yanagisawa *et al.*, 1998): there is an initial fall in vascular resistance, lasting seconds to minutes (which is not seen in mice (Giller *et al.*, 1997)), before a longer lasting vasoconstriction (minutes to hours). Experiments, using selective antagonists in combination with inhibitors of NO and PGI<sub>2</sub> synthesis, have revealed that the initial hypotensive response is mediated by EC ET<sub>B</sub> derived NO or PGI<sub>2</sub> (Giardina *et al.*, 2001). The longer lasting vasoconstriction is dependent on VSMC ET<sub>A</sub> receptor activation (Bird *et al.*, 1993).

#### 1.2.2.1 CLINICAL STUDIES

Evidence of involvement of endogenous ET-1 the regulation of basal vascular tone regulation comes from studies using selective ET antagonists. Infusion of the selective ET<sub>A</sub> antagonist BQ123 results in vasodilatation of the forearm circulation of healthy human volunteers (Haynes *et al.*, 1994), demonstrating that ET<sub>A</sub> receptors are tonically activated. In contrast, ET<sub>B</sub> receptor blockade with BQ788 causes similar forearm vasoconstriction to NOS inhibition, suggesting that ET<sub>B</sub> receptors cause tonic vasodilatation mediated by NO (Verhaar *et al.*, 1998). Further work has confirmed that such selective ET receptor blockade has a similar effect on systemic haemodynamics (Spratt *et al.*, 2001; Strachan *et al.*, 1999).

### 1.2.2.2 GENETIC ANIMAL MODELS

Further evidence for the direct role of ET-1 in the regulation of vascular tone comes from experiments using rodents featuring genetic disruption of components of the ET system.

#### 1.2.2.2.1 *Animal models deficient in ET-1*

As outlined above in section 1.2.1, ET-1 null mice perish at birth, dying due to airway obstruction caused by craniofacial malformation. However, animals heterozygous for ET-1 KO are viable, and demonstrate mild hypertension compared to wild type controls, despite reduced plasma and lung ET-1 concentrations (Kurihara *et al.*, 1994). The ET-1 +/- mice demonstrated no difference in response to an intravenous bolus of ET-1 or nitric oxide synthase inhibitor, N-nitro-L-arginine-methyl ester (L-NAME), compared to controls. Thus the authors conclude that whilst ET-1 is clearly important in BP homeostasis, ET-1 +/- mice do not have significantly impaired NO production or different patterns of ET receptor expression.

Further work involving a number of different mutants, has shown that whilst ET-1 +/- mice and ET<sub>B</sub>-/- mice (with only 1/8<sup>th</sup> of normal level of ET<sub>B</sub> expression – see 1.2.2.2.4) demonstrate hypertension, ECE +/-, ET<sub>A</sub>+/- mice are normotensive (Kuwaki *et al.*, 1999). Attenuation of reflex increases in respiration frequency and minute volume, in response to hypoxia and hypercapnia, were apparent in ET-1 -/- and ET<sub>A</sub> receptor-null mutated tracheotomised newborn mice, but not in ET<sub>B</sub> receptor-null mutated newborn mice, strongly suggesting that the ET-1/ET<sub>A</sub> receptor signaling system is critically involved in the reflex control of respiration. In a further set of experiments ET-1 +/- mice demonstrate augmented renal sympathetic nerve activity and blunted phrenic nerve activity in response to hypercapnia and hypoxia, relative to controls (Kuwaki *et al.*, 1999). ET<sub>B</sub>-/- animals display no such differences. The authors conclude that endogenous ET-1 plays an important role in the central neural control of circulation and respiration, most likely mediated by ET<sub>A</sub> receptors.

In addition to problems of embryonic lethality, such experiments illustrate a further drawback with using transgenic models featuring germline genetic modification of components of the ET system in an effort to determine the role of ET in cardiovascular homeostasis. Interpretation of the resulting phenotype can be complicated by unexpected effects in different tissues throughout the body. By generating conditional knockouts, where gene deletion or overexpression is limited to a certain cell type, the role of different components of the ET system expressed by particular tissues can be more easily determined.

The advantage of tissue specific KO mouse models, is illustrated by the generation of an EC specific ET-1 KO mouse (Kisanuki *et al.*, 1999). Although these mice display similar responses to inhibitors of the angiotensin and sympathetic systems in comparison to controls, they are hypotensive. Thus it would appear that ET-1, generated by ECs, has a tonic effect at neighbouring VSMCs, acting to increase vascular tone.

#### *1.2.2.2.2 Animal models overexpressing ET-1*

Adenoviral gene transfer of the prepro-ET-1 gene, whilst not resulting in a germline mutation, caused a transient increase in hepatic ET-1 synthesis and raised plasma ET-1 concentrations in treated rats (Niranjan *et al.*, 1996) over a limited period. These animals displayed significant hypertension that was reversed by treatment with an ET<sub>A</sub> antagonist, implying that the raised BP was due to increased activation of vasoconstrictive ET<sub>A</sub> receptors.

Somewhat surprisingly however, mice featuring germline over expression of ET-1 do not exhibit hypertension (Hochoer *et al.*, 1997) unless exposed to high salt diet (Shindo *et al.*, 2002). When ET-1 overexpression is restricted to the endothelium using the Tie2 promoter to target expression of human preproET-1 to ECs, the transgenic mice exhibit 3-fold increased vascular wall ET-1 mRNA, a 7-fold raised ET-1 plasma concentration, but no elevation in BP (Amiri *et al.*, 2004). The authors used radiotelemetry to measure BP over an extended period in conscious undisturbed



mice, resulting in data of increased reliability compared to other studies that involved anaesthetised preparations measured over only a limited duration, or tail cuff sphygmomanometry (Pickering *et al.*, 2005). These EC ET-1 overexpressing mice exhibited marked hypertrophic remodeling and endothelial dysfunction of resistance vessels, altered ET-1 and ET-3 vascular responses, and significant increases in ET<sub>B</sub> expression compared with WT littermates. The authors conclude that ET-1 has a direct non-haemodynamic effect on vessels to cause remodelling, endothelial dysfunction perhaps through activation of NADPH oxidase.

#### *1.2.2.2.3 Animal models deficient in ET<sub>A</sub> receptors*

As described above (section 1.2.1), KO of the ET<sub>A</sub> receptor results in death due to airway obstruction. However, by delivering ET<sub>A</sub> <sup>-/-</sup> mice by caesarean section on the expected day of delivery and performing tracheotomies, this technical obstacle has been overcome, allowing the survival of the mice for a limited period (Kuwaki *et al.*, 2002). BP, recorded under anaesthesia, was not different from that of age-matched, similarly treated wild-type mice, demonstrating that, at least during very early life, ET<sub>A</sub> receptors are not involved in cardiovascular regulation. There is no known hypomorphic allele of the ET<sub>A</sub> gene, unlike that for the ET<sub>B</sub> gene (see below).

Heterozygote ET<sub>A</sub> receptor KO mice develop normally into adulthood and are normotensive (Berthiaume *et al.*, 2000). A VSMC ET<sub>A</sub> receptor specific KO animal, ideally with temporal as well as spatial control of ET<sub>A</sub> receptor expression, would allow the role of the ET<sub>A</sub> receptor in BP regulation to be fully addressed.

#### *1.2.2.2.4 Animal models deficient in ET<sub>B</sub> receptors*

As with other components of the ET system, KO of the ET<sub>B</sub> receptor results in a lethal phenotype (Gariépy *et al.*, 1998; Hosoda *et al.*, 1994). The ET<sub>B</sub> receptor on neural crest cells is required for normal epidermal melanocyte and enteric neuron development as discussed in section 1.2.1. A naturally occurring recessive mutation, known as piebald lethal (sl), is caused by complete deletion of the ET<sub>B</sub> receptor gene.

A milder allele, piebald (s), which produces spotted coat colour only, expresses around one quarter of the levels of structurally intact ET<sub>B</sub> receptor mRNA and protein found in wild type mice (Hosoda *et al.*, 1994). Ohuchi and colleagues crossed such mice with heterozygote ET<sub>B</sub> KO (ET<sub>B</sub><sup>+/-</sup>) animals, resulting in animals with one eighth the level of normal ET<sub>B</sub> receptor expression (Ohuchi *et al.*, 1999). Although these mice all had a spotted coat colour, only a minority developed aganglionic megacolon (7/37) and data from such animals were excluded. The BP of ET<sub>B</sub><sup>-/s</sup> mice was significantly higher than that in ET<sub>B</sub><sup>+s</sup> or ET<sub>B</sub><sup>+/+</sup> mice. Interestingly the plasma concentration of ET-1 was not different between ET<sub>B</sub><sup>-/s</sup> and ET<sub>B</sub><sup>+s</sup> mice (both ~15 pg.ml<sup>-1</sup>), although the paper does not reveal the plasma concentration of ET-1 found in ET<sub>B</sub><sup>+/+</sup> mice, which one would expect to be around the normal concentration ~4 pg.ml<sup>-1</sup> (see section 5.3.1; (Amiri *et al.*, 2004; Shindo *et al.*, 2002). Acute blockade with the selective ET<sub>B</sub> antagonist, BQ-788, increased BP in ET<sub>B</sub><sup>+s</sup> and ET<sub>B</sub><sup>+/+</sup> but not in ET<sub>B</sub><sup>-/s</sup> mice. This was attenuated by pretreatment with indomethacin (a PGI<sub>2</sub>-S inhibitor), but not with L-NAME. Thus it seems that endogenous ET<sub>B</sub> activation elicits a depressor effect, in part through tonic production of prostaglandins, and not by means of unimpaired clearance of circulating ET-1.

Others have also found ET<sub>B</sub> deficient mice to be hypertensive compared to controls, but they have identified different mechanisms responsible for the raised BP (Berthiaume *et al.*, 2000). In this study, hypertensive ET<sub>B</sub><sup>+/-</sup> mice demonstrated impaired clearance of ET-1. The hypertension was normalised by treatment with the ET<sub>A</sub> antagonist BQ-123, suggesting that the raised BP was secondary to raised plasma ET-1 concentrations causing increased stimulation of vasoconstrictive ET<sub>A</sub> receptors.

Similar to piebald lethal mice, the spotting lethal rat, a naturally occurring rodent model of Hirschsprung's disease, carries a deletion in the ET<sub>B</sub> receptor gene that abrogates expression of functional ET<sub>B</sub> receptors. Rats homozygous for this mutation (sl) exhibit coat color spotting and congenital intestinal aganglionosis (Garipey *et al.*, 1996). An elegant approach to investigate the role of the ET<sub>B</sub> receptor in the control of BP has involved the 'genetic rescue' of such sl rats that would otherwise die at

weaning from intestinal obstruction. The human dopamine- $\beta$ -hydroxylase (D $\beta$ H) promoter was used to direct transgenic expression of ET<sub>B</sub> to colonising enteric neuronal precursors in the sl/sl rat. The D $\beta$ H-ET<sub>B</sub> transgene compensates for deficient endogenous ET<sub>B</sub> in these rats and prevents the intestinal agangliosis (Gariépy *et al.*, 1998). On a normal diet, these rescued ET<sub>B</sub> deficient rats demonstrate mild hypertension, which is markedly accentuated by increasing the salt in the chow. Intravenous L-NAME and indomethacin had a similar effect in both rescued and control animals, suggesting that there is no difference in NO or PGI<sub>2</sub> availability in the vessels of these rescued ET<sub>B</sub> deficient rats compared with controls. As will be discussed in the renal section (1.2.3.2) below, the authors conclude that the salt sensitive hypertension is due to impaired ET<sub>B</sub> mediated natriuresis.

A similarly ‘rescued’ ET<sub>B</sub> deficient mouse has been found to demonstrate mild hypertension on a normal sodium diet by one group (Murakoshi *et al.*, 2002), whilst others, have shown this same model to exhibit raised BP only when fed high salt diet (Quaschnig *et al.*, 2005). Interestingly the ET<sub>B</sub> deficient mice exhibits endothelial dysfunction, even when not hypertensive on a normal salt diet (Quaschnig *et al.*, 2005).

From the studies described above, there are a number of possible mechanisms that would explain the observed hypertension in ET<sub>B</sub> deficient animals. Firstly, reduced NO availability caused by loss of EC ET<sub>B</sub> receptors could result in increased vascular tone; second, elevated plasma ET-1 concentrations, due to impaired ET<sub>B</sub> mediated clearance of ET-1, is likely to enhance vasoconstrictive ET<sub>A</sub> activity; and third, the raised BP could be a result of the lack of ET<sub>B</sub> mediated natriuresis. The development and phenotyping of tissue specific ET<sub>B</sub> receptor down-regulated mice will greatly assist in the understanding of the important roles played by ET<sub>B</sub> receptors expressed on different cell types.

### 1.2.3 Role of Endothelin in the kidney

In addition to being synthesised by ECs within the kidney, ET-1, as well as, ET-3 are produced by a number of different cells throughout the nephron including inner medullary and cortical collecting duct epithelial cells (Karet *et al.*, 1996; Kohan, 1991). The highest concentration of ET-1 has been localised to the renal medulla (Kitamura *et al.*, 1989). ET receptors are expressed on renal blood vessels, as well as on tubular epithelial cells, where the ET<sub>B</sub> receptor is the predominant receptor subtype, particularly in the inner medulla (Chow *et al.*, 1995; Terada *et al.*, 1992). As well as influencing renal blood flow, the renal endothelin system controls water and sodium balance, and is very important in acid-base homeostasis.

#### 1.2.3.1 ROLE OF ET<sub>A</sub> AND ET<sub>B</sub> RECEPTORS IN CONTROL OF ACID –BASE HOMEOSTASIS

The ET system, through the ET<sub>B</sub> receptor, plays a role in renal acid-base balance. Wild type mice respond to an acid diet by increasing their acid excretion, by means of a range of different mechanisms, including elevating the expression of the Na<sup>+</sup>/H<sup>+</sup> (NHE3) cation exchanger in the luminal membrane of the proximal convoluted tubule and thick ascending limb of the loop of Henle (Ambuhl *et al.*, 1996). In cells expressing NHE3, ET<sub>B</sub> activation results in increased proton excretion (Chu *et al.*, 1996). When ET<sub>B</sub> deficient mice are challenged with increased dietary acid, they develop more severe metabolic acidosis than wild type controls (Laghmani *et al.*, 2001). Further work, using ET<sub>A</sub>/ ET<sub>B</sub> receptor chimeras and site-directed mutagenesis, has identified the ET receptor domain(s) involved in ET-1 regulation of NHE3 activity in isolated kidney cells. ET<sub>A</sub> receptor activation inhibits NHE3 activity, an effect for which the COOH-terminal tail is necessary and sufficient. Activation of NHE3 by ET-1 requires the COOH-terminal tail as well as the second intracellular loop of the ET<sub>B</sub> receptor (Laghmani *et al.*, 2005).

### 1.2.3.2 ROLE OF ET<sub>A</sub> AND ET<sub>B</sub> RECEPTORS IN CONTROL OF SODIUM BALANCE

Intra-arterial ET-1, infused into rabbits, reduces renal blood flow, cortical perfusion, glomerular filtration rate, urinary flow and sodium excretion (Evans *et al.*, 1998), most probably secondary to ET<sub>A</sub> mediated vasoconstriction (Pollock *et al.*, 1994). When big ET-1 is infused into the femoral artery of rats, an increase in sodium and water excretion is observed, that cannot be blocked by the ET<sub>A</sub> antagonist BQ123 (Pollock *et al.*, 1994), suggesting that ET<sub>B</sub> activation within the medulla causes natriuresis and diuresis. In cultured inner medullary collecting duct (IMCD) cells, ET<sub>B</sub> activation reduces the water permeability 6-fold in vasopressin stimulated cells (Edwards *et al.*, 1993), suggesting that *in vivo*, ET-1 acts at ET<sub>B</sub> receptors to lower water reuptake from the nephron and increase urinary water loss.

The role of ET<sub>B</sub> in the control of water and sodium balance by the kidney has been further investigated using genetically modified animals. As outlined in the previous section (1.2.2.2.4), ET<sub>B</sub> deficient rodents were found to be hypertensive by several different groups (Berthiaume *et al.*, 2000; Gariepy *et al.*, 2000; Murakoshi *et al.*, 2002; Ohuchi *et al.*, 1999; Quaschnig *et al.*, 2005). Early studies suggested that the raised BP was secondary to loss of ET<sub>B</sub> mediated tonic vasodilatation (Ohuchi *et al.*, 1999), or due to increased ET<sub>A</sub> receptor activation caused by raised plasma ET-1 concentrations (Berthiaume *et al.*, 2000). The animals in these studies were all fed diet of a 'normal' NaCl composition (usually 0.76% NaCl). The hypertension of 'rescued' ET<sub>B</sub> deficient rodents was found to markedly salt sensitive (Gariepy *et al.*, 2000; Murakoshi *et al.*, 2002; Quaschnig *et al.*, 2005). Whilst the ET<sub>B</sub> deficient rats exhibited elevated plasma ET-1 concentrations, an intravenous bolus of ET<sub>A</sub> receptor antagonist failed to normalise the hypertension (although it did result in a greater depressor response than seen in controls) (Gariepy *et al.*, 2000). Acute inhibition of NO and PG synthesis had a similar hypertensive effect in both controls and rescued ET<sub>B</sub> deficient rats, and there was no difference in either the aldosterone concentration, plasma renin activity or in response to the ACE inhibitor captopril. Thus it seems that the salt sensitive hypertension is secondary to loss of ET<sub>B</sub> mediated natriuresis. As the hypertension is normalised by amiloride, which inhibits

the epithelial sodium channel ENaC, the authors propose that tonic activation of ET<sub>B</sub> limits ENaC sodium reabsorption in the renal collecting duct.

Within the renal medulla ET<sub>B</sub> receptors are expressed on several different cell types including ECs, IMCDs (Kohan *et al.*, 1992) and renal interstitial cells (Wilkes *et al.*, 1991). Each of these is capable of generating NO (Hughes *et al.*, 1995; Wu *et al.*, 1999; Zhuo, 2000). It is generally accepted that NO acts to inhibit sodium reabsorption in the nephron (Wilcox, 2000) as well as antagonising the action of vasopressin (Stoos *et al.*, 1995). Both the NO synthase inhibitor, L-NAME, and the specific ET<sub>B</sub> antagonist, A192621, independently abolish the diuretic and natriuretic effects of big ET-1 in the kidneys of anaesthetised rats (Hoffman *et al.*, 2000). From the experiments using rescued ET<sub>B</sub> deficient rats (Gariépy *et al.*, 2000), described above, it is unclear whether IMCD-derived ET-1 targets ET<sub>B</sub> receptors on IMCD cells (in an autocrine fashion) or neighbouring ECs/ interstitial cells (paracrine mechanism), to release NO that inhibits sodium reabsorption (see Figure 1-4).

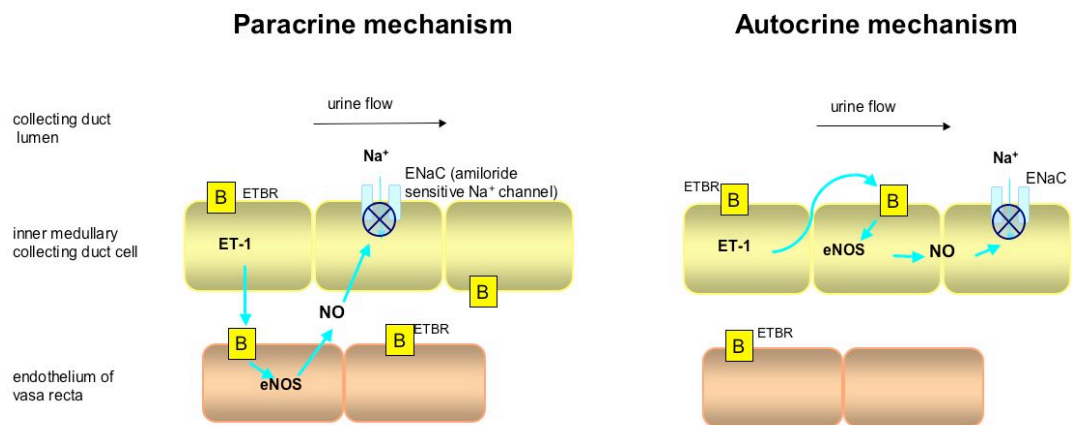


**Figure 1-4: Autocrine versus paracrine control of ET<sub>B</sub> mediated natriuresis** adapted from (Kotelevtsev *et al.*, 2001).

By determining whether any of a panel of cell specific ET<sub>B</sub> receptor down-regulated mice demonstrate salt sensitive hypertension, the identity of this unknown cell type can be determined, allowing fuller understanding of the renal ET system.

#### 1.2.3.3 ANIMAL MODELS FEATURING ALTERED EXPRESSION OF ET-1: EFFECT ON RENAL SODIUM HANDLING/RENAL FUNCTION

Animals deficient in ET-1 are hypertensive (Kurihara *et al.*, 1994), most likely secondary to altered central sympathetic outflow (Kuwaki *et al.*, 1999), rather than due to abnormal sodium handling by the kidney, as heterozygote ET-/+ mice do not demonstrate salt sensitivity (Morita *et al.*, 1999).

Despite a reduced glomerular filtration rate, mice overexpressing human ET-1 are not hypertensive on a normal salt diet, but develop glomerulosclerosis, interstitial fibrosis and renal cysts (Hoher *et al.*, 1997). A second transgenic strain of ET-1 overexpressing mice, generated by another group (Shindo *et al.*, 2002), had normal BP and no histological abnormalities in the visceral organs of young (8 weeks old) animals. However, in old transgenic mice (12 months of age), renal manifestations, including prominent interstitial fibrosis, renal cysts, glomerulosclerosis as well as narrowing of the arterioles, were detected. These pathological changes were accompanied by decreased creatinine clearance, elevated urinary protein excretion and salt-dependent hypertension. It thus appears that mild, chronic overproduction of ET-1 does not primarily cause hypertension but triggers damaging changes in the kidney which lead to the susceptibility to salt-induced hypertension.

EC ET-1 overexpressing mice are normotensive at 10 weeks of age (Amiri *et al.*, 2004), and preliminary results in 10 month old mice show only a minimal elevation of systolic BP with salt loading (Amiri *et al.*, 2005).

By using the Cre/lox system Ahn and colleagues have investigated the role played by IMCD derived ET-1 (Ahn *et al.*, 2004). They developed an IMCD specific ET-1 KO mouse and demonstrated that it too exhibited salt sensitive hypertension. This supports the hypothesis that IMCD-derived ET-1 acts at local ET<sub>B</sub> receptors, to stimulate the generation of NO that, in turn, reduces tubular sodium reabsorption. An autocrine action for this IMCD-derived ET-1 was demonstrated by the finding that

IMCD specific ET<sub>B</sub> down-regulated mice demonstrated salt sensitive hypertension (Ge *et al.*, 2006). However, this was more modest than that seen in IMCD ET-1 KO animals, suggesting that IMCD-derived ET-1 also acts in a paracrine manner on ET<sub>B</sub> on neighboring cells.

However, EC and renal interstitial cell specific ET<sub>B</sub> receptor down-regulated mice are required before the location of these ET<sub>B</sub> receptors can be identified.

#### **1.2.4 Role of endothelin in the lungs**

The highest level of ET-1 has been identified in the healthy rat lung, where concentrations are more than five-fold greater than in any other organ (Firth *et al.*, 1992). ET-1 is produced by pulmonary ECs, airway epithelial cells, and macrophages (Ehrenreich *et al.*, 1990; MacCumber *et al.*, 1989). As well as being found on blood vessels within the lung, ET receptors are present on the smooth muscle cells of bronchioles. The ratio of ET<sub>A</sub> to ET<sub>B</sub> receptors expressed on airways smooth muscle varies across species: in man there are ~10 times the number of ET<sub>B</sub> receptors as ET<sub>A</sub> receptors (Goldie *et al.*, 1995), whereas the opposite is true in sheep (Ergul *et al.*, 1995; Goldie *et al.*, 1994). In rodents airways, there are approximately equal proportions of ET<sub>A</sub> and ET<sub>B</sub> receptors (Henry, 1993). As well as being expressed in blood vessels, ET<sub>B</sub> receptors are also found on the neurones of the intramural autonomic nervous system (Takimoto *et al.*, 1993).

##### **1.2.4.1 ROLE OF ET-1 IN CONTROL OF AIRWAY RESISTANCE**

###### **1.2.4.1.1 Interstitial lung disease**

In the lung, the ET system is involved in the control of both airway and vascular tone. Intravenous administration of ET-1 increases airway resistance in a dose dependent manner (Adamicza *et al.*, 1999). This airway constricting effect of ET-1, along with its proliferative effects, is likely to contribute to the pathogenesis of interstitial lung disease and asthma. Mice overexpressing human preproET-1 have progressive pulmonary fibrosis and accumulation of inflammatory cells in the absence of pulmonary hypertension (Hochoer *et al.*, 2000). A model using gene



transfer to increase ET-1 expression in alveolar macrophages and lung epithelial cells, showed oedematous alveolar septa and hyperplastic connective tissue plaques in a manner characteristic of that seen in human bronchiolitis obliterans (Takeda *et al.*, 1997).

#### 1.2.4.1.2 Asthma

Asthma is an inflammatory obstructive lung disease involving elevated airway tone, hypersecretion of mucus, airway smooth muscle and fibroblast proliferation as well as inflammatory cell recruitment and activation. ET-1 is an airway smooth muscle spasmogen and mitogen, mucus secretagogue and inflammatory cell activator (Goldie *et al.*, 1996). ET-1 also greatly enhances cholinergic neuronal activity in human (Fernandes *et al.*, 1996) and animal (Henry *et al.*, 1995) airways. This is important, because cholinergic nerves provide the dominant constrictor innervation in the respiratory tract and this system is overactive in some asthmatics. In a guinea pig model of asthma, the ET<sub>B</sub> antagonist BQ788 suppressed the immediate constrictive phase of the asthmatic response, whereas the late phase was blocked by ET<sub>A</sub> blockade with BQ123 (Uchida *et al.*, 1996). Asthmatic patients have increased ET-1 concentrations in their bronchoalveolar lavage fluid (Sofia *et al.*, 1993), and when challenged with aerosolised ET-1 they demonstrate bronchoconstriction not seen in healthy volunteers (Chalmers *et al.*, 1997).

#### 1.2.4.2 ROLE OF ET-1 IN PULMONARY CIRCULATION

In the pulmonary vasculature, the expression of ET<sub>B</sub> relative to ET<sub>A</sub> receptors increases as one moves distally down the vascular tree (Davie *et al.*, 2002). ET-1 induces a biphasic response: initial vasodilatation followed by vasoconstriction (Hasunuma *et al.*, 1990). However, blockade of VSMC ET<sub>A</sub> and ET<sub>B</sub> receptors with mixed ET antagonists is required to inhibit this ET-1 mediated vasoconstriction (Sato *et al.*, 1995). Activation of both subtypes of ET receptor also results in proliferation of vascular smooth muscle (Davie *et al.*, 2002). Indeed, mice overexpressing ET-1 display pulmonary fibrosis (Hoche *et al.*, 2000).

The role of the EC ET<sub>B</sub> receptor in the control of pulmonary vascular tone is less straightforward to define. As well as clearing ET-1 from the circulation (Dupuis *et al.*, 1994; Dupuis *et al.*, 1996b) as outlined in section 1.1.6, pulmonary EC ET<sub>B</sub> activation causes release of antiproliferative vasodilators NO and PGI<sub>2</sub>, which in turn inhibit the synthesis of ET-1 (de Nucci *et al.*, 1988; Lal *et al.*, 1996). However, part of the ET-1 induced vasoconstriction in PAs is dependent on thromboxane A<sub>2</sub> (TXA<sub>2</sub>) (Curzen *et al.*, 1995; Horgan *et al.*, 1991) with studies suggesting that this is mediated by the ET<sub>B</sub> receptor (Curzen *et al.*, 1995; D'Orleans-Juste *et al.*, 1994; Noguchi *et al.*, 1996) on the endothelium (Curzen *et al.*, 1995). Although the production of TXA<sub>2</sub> within the lungs varies across species (Westcott *et al.*, 1988), the EC ET<sub>B</sub> receptor may have a dual role in the pulmonary vasculature, modulating both vasoconstriction and vasodilatation.

#### 1.2.4.3 PULMONARY ARTERIAL HYPERTENSION

Before detailing the important role of the ET system in the pathogenesis of pulmonary arterial hypertension (PAH), the classification, pathology, genetic and molecular basis for this debilitating condition will be discussed. PAH is a rare disease affecting ~1-2 individuals per million per year (Morrell *et al.*, 2001a). It is a progressive condition, characterised by a persistent increase in pulmonary vascular resistance that ultimately leads to right heart failure and death (median survival 2.8 years following diagnosis (Rubin, 1997)). Idiopathic PAH can be either familial or occur as an isolated phenomenon. PAH can also develop secondary to a number of diseases: collagen vascular diseases (such as systemic sclerosis or systemic lupus erythematosus); congenital left to right shunts; sarcoidosis; chronic thromboembolic disease and chronic lung disease (Braun-Moscovici *et al.*, 2004; Galie *et al.*, 2004) (Table 1-1).

### **Table 1-1 Classification of pulmonary hypertension**

The 2003 Venice Classification (Rubin, 2004).

1. Pulmonary arterial hypertension (PAH)
  - Sporadic (IPAH)
  - Familial (FPAH)
  - Associated with:
    - Collagen vascular disease
    - Congenital systemic-to-pulmonary shunts
    - Portal hypertension
    - HIV infection
    - Drugs and toxins
    - Other: HHT, haemoglobinopathies, etc.
  - PAH with significant venous or capillary involvement
    - Pulmonary veno-occlusive disease
    - Pulmonary capillary haemangiomatosis
  - Persistent pulmonary hypertension of the newborn
2. Pulmonary hypertension with left heart disease
3. Pulmonary hypertension associated with lung disease and/or hypoxaemia
  - Chronic obstructive pulmonary disease
  - Interstitial lung disease
  - Sleep-disordered breathing
  - Alveolar hypoventilation disorders
  - Chronic exposure to high altitudes
  - Developmental abnormalities
4. Pulmonary hypertension due to chronic thrombotic and/or embolic disease
5. Miscellaneous: Sarcoidosis, histiocytosis X, etc.

#### *1.2.4.3.1 Pathology*

In both idiopathic and secondary PAH obstruction of small PAs, plexiform lesions, medial hypertrophy, concentric laminar intimal fibrosis, fibrinoid degeneration, and thrombotic lesions are seen in severe cases (Bjornsson *et al.*, 1985; Palevsky *et al.*, 1989; Pietra *et al.*, 1989; Wagenvoort, 1980). The term plexogenic arteriopathy is used because of the existence of plexiform lesions (200–400µm diameter) which are a tangle of capillary-like channels adjacent to a small pulmonary artery (PA) (Cool *et al.*, 1999). The ECs comprising plexiform lesions in idiopathic PAH appear to be due to a monoclonal proliferation of cells, whereas lesions in secondary PAH are of polyclonal origin (Lee *et al.*, 1998). Discussion remains as to the relative contribution of vasoconstriction versus the structural changes associated with remodeling to the phenotype of PAH (Stenmark *et al.*, 2005).

#### 1.2.4.3.2 Genetics of PAH

The low incidence of the disease, combined with the observation that the majority of cases appeared to be ‘sporadic’, have hampered the generation of detailed pedigrees of patients suffering from PAH. However, following the establishment of a US National Institutes of Health central registry of all those diagnosed with the condition, it was determined that the condition is most likely autosomal dominant with incomplete penetrance (Loyd *et al.*, 1984). A genome screen using polymorphic microsatellite markers, established linkage between idiopathic PAH and a region on the long arm of chromosome 2 (2q33) (Morse *et al.*, 1998; Nichols *et al.*, 1997). Sequencing of positional candidate genes revealed heterozygous mutations involving the gene encoding the bone morphogenetic protein receptor type 2 (BMPR2), a member of the transforming growth factor- $\beta$  (TGF $\beta$ ) superfamily of receptors (Deng *et al.*, 2000; Lane *et al.*, 2000). The heterogeneous mutations include frameshift, nonsense and missense. The frameshift and nonsense mutations predict premature truncation of the 1038 amino acid protein. Missense mutations occur at highly conserved and functionally important sites that are predicted to perturb ligand binding or disrupt the kinase domain of the receptor. Interestingly, the same mutations underlie 26% of apparently sporadic cases of idiopathic PAH, some of which are in fact familial, the remainder arising *de novo* (Thomson *et al.*, 2000).

#### 1.2.4.3.3 Cellular mechanisms in the pathogenesis of PAH

Originally discovered in association with bone growth, bone morphogenetic proteins (BMPs), the major ligands for bone-morphogenetic-protein receptors, are also important in embryogenesis, development, apoptosis, cell differentiation, and proliferation. BMPR2s forms a heterodimer complex with BMPR1s to bind these ligands on the cell surface. This complex then propagates signal via intra cellular proteins known as Smad (mothers against decapentaplegic proteins) molecules (Blobe *et al.*, 2000; Heldin *et al.*, 1997) eventually resulting in altered expression of various proteins required for arresting cell growth and inducing apoptosis.

Reduced expression of BMPR2 has been proposed as a mechanism for the development of PAH in subjects with BMPR2 mutations (Machado *et al.*, 2001). Furthermore VSMC specific BMPR2 KO mice develop raised PA pressures and display pulmonary vascular remodeling (West *et al.*, 2004). Immunohistochemistry demonstrates that ECs from the lungs of idiopathic PAH patients have reduced BMPR2 expression compared to ECs from healthy controls (Atkinson *et al.*, 2002), the lowest expression being seen in patients with known BMPR2 mutations. It remains unclear how different mutations in the BMPR2 gene can lead to the development of the same PAH phenotype. Interestingly, plexiform lesions, from BMPR2 heterozygote individuals with PAH, do not exhibit a further somatic mutation in the second BMPR2 allele, suggesting that somatic loss of the remaining wild type BMPR2 allele does not play a significant role in modulating the onset and progression of PAH (Machado *et al.*, 2005).

As the superfamily of TGF $\beta$  receptors are involved in the control of cell proliferation and apoptosis, it is highly likely that a reduction or alteration in BMPR2 signaling could lead to loss of antiproliferative or apoptotic mechanisms in the pulmonary circulation. The normal growth of aortic and pulmonary VSMCs, in response to growth factors, is suppressed by BMPs (Dorai *et al.*, 2000; Morrell *et al.*, 2001b). In contrast, in lungs from patients with PAH, BMPs have a proliferative effect on pulmonary VSMCs and exert a proapoptotic effect on ECs (Morrell *et al.*, 2001b). TGF $\beta$  receptors mutations have been detected in atherosclerotic lesions (McCaffrey *et al.*, 1997) and in cell populations isolated from patients with hereditary polyposis colon cancer (Akiyama *et al.*, 1997).

However, as phenotypic disease occurs in only 10-20% of individuals with BMPR2 mutations, other factors, such as modifier genes and environmental factors, must be necessary for the development of PAH. Such a 'multi-hit' theory has been proposed whereby an individual with a BMPR2 mutation (or an alternative mutation) would require additional insults before developing clinical PAH (Rudarakanchana *et al.*, 2001; Runo *et al.*, 2003) (see Figure 1-5).

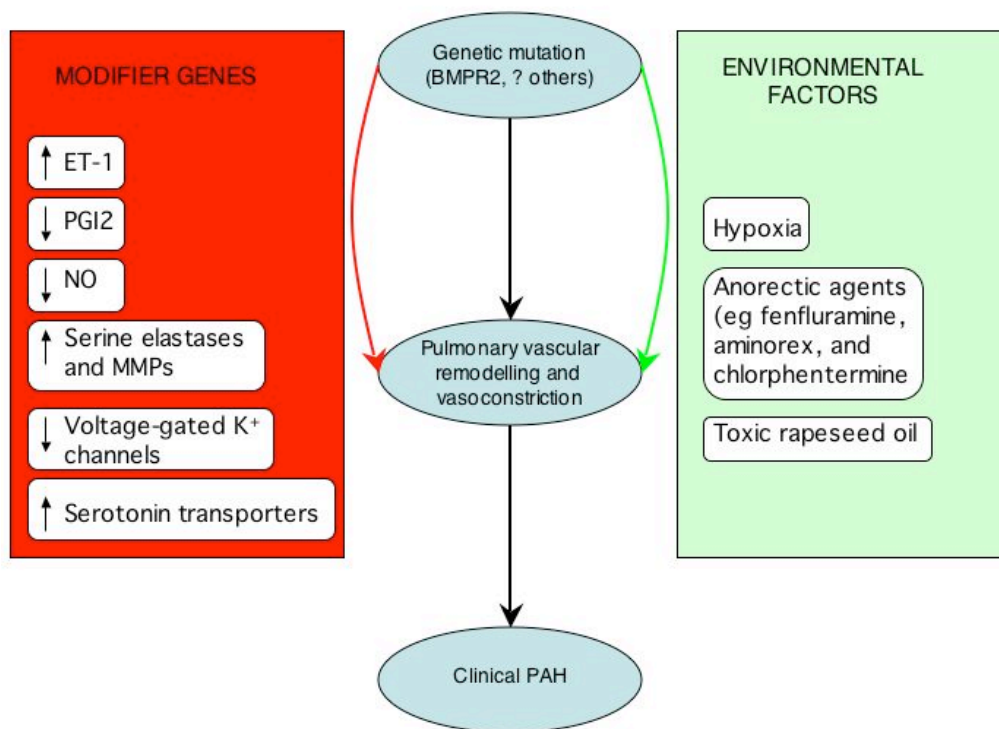


**Figure 1-5: Pathogenesis of PAH**

Proposed pathogenesis for the development of PAH. Pulmonary vascular remodelling results from the effects of genetics, modifying genes, and environment.

#### 1.2.4.3.4 Serotonin

Serotonin is associated with pulmonary vasoconstriction and VSMC proliferation (Lee *et al.*, 1991; MacLean *et al.*, 2000; McGoan *et al.*, 1984). Hypoxia stimulates pulmonary neuroendocrine cells to release serotonin (MacLean *et al.*, 2000) resulting in the elevated plasma concentrations found in patients with idiopathic PAH (Herve *et al.*, 1990; Herve *et al.*, 1995). Transgenic mice lacking the serotonin transporter are protected against developing hypoxia induced PAH (Eddahibi *et al.*, 2000) whereas the opposite is seen in mice over expressing this transporter (MacLean *et al.*, 2004).

Appetite suppressing drugs can act as a substrate for serotonin transporters and so are transported into pulmonary VSMCs (Rothman *et al.*, 1999). The vasoconstrictive effects of these agents are partially blocked by serotonin antagonists, indicating that

their effects are at least partially mediated via serotonin receptors (Belohlavkova *et al.*, 2001). Such actions could serve as links between anorectic agents and the development of PAH.

#### *1.2.4.3.5 Extra cellular matrix*

By breaking down the extracellular matrix, vascular serine elastases and matrix metalloproteinases (MMPs) release matrix bound mitogens and induce tenascin C, resulting in VSMC proliferation (Cowan *et al.*, 2000b). In rats with experimental PAH, pharmacological inhibition of these enzymes reduces the concentration of tenascin C, increases VSMC apoptosis and lowers PA pressures (Cowan *et al.*, 2000a; Cowan *et al.*, 2000b). NO has also been shown to limit serine elastase activity, a further mechanism through which this mediator inhibits vascular remodeling (Mitani *et al.*, 2000).

#### *1.2.4.3.6 Voltage-gated potassium channels*

Increased intracellular calcium concentrations results in contraction and proliferation of PA VSMCs (Yuan *et al.*, 1998a). Voltage-gated potassium channels control cell membrane potential and the release of calcium from intracellular stores within the sarcoplasmic reticulum (Yuan *et al.*, 1998a). PA VSMCs from patients with idiopathic PAH, express less mRNA coding for voltage-gated potassium channels, have a reduced channel current and increased intracellular calcium concentrations compared with control PA VSMCs (Yuan *et al.*, 1998a; Yuan *et al.*, 1998b). Such elevated intracellular calcium concentrations could be one factor responsible for the development of clinically significant PAH. Appetite suppressant drugs may result in PAH by blocking voltage-gated potassium channels (Belohlavkova *et al.*, 2001; Weir *et al.*, 1996).

#### *1.2.4.3.7 Other possible modifiers*

Patients with idiopathic PAH exhibit both increased fibrinogen plasma levels and a diminished fibrinolytic response compared with healthy subjects. Such a prothrombotic state could predispose to the development of PAH (Huber *et al.*, 1994).

The renin-angiotensin-aldosterone system may also be implicated in the pathogenesis of PAH. Increased expression of angiotensin converting enzyme (ACE) is found in intimal and plexiform PAH lesions (Orte *et al.*, 2000; Schuster *et al.*, 1996). Hypoxia causes increased PA VSMC angiotensin receptor expression (Chassagne *et al.*, 2000). Angiotensin II stimulates the growth of human PA VSMCs and may contribute to vascular remodeling in distal PAs (Morrell *et al.*, 1999). Administration of ACE inhibitors to rats with monocrotaline induced PAH, results in restoration of their endothelial function (Kanno *et al.*, 2001), and when given to hypoxic rats prevented medial thickening of PAs (Clozel *et al.*, 1991; van Suylen *et al.*, 1998).

#### *1.2.4.3.8 Endothelial dysfunction and the ET system in PAH*

The vascular endothelium and activation of various mediators and growth factors such as the ET system are thought to play a crucial role in the development of PAH. In the healthy lung a balance exists between vasodilators/ anti-mitogens (such as NO and PGI<sub>2</sub>) and vasoconstrictors/ mitogens (such as TXA<sub>2</sub> and ET-1). In PAH this balance is shifted towards the factors causing vasoconstriction and vascular remodeling, leading to endothelial dysfunction and widespread pulmonary vascular obstruction (Figure 1-6).



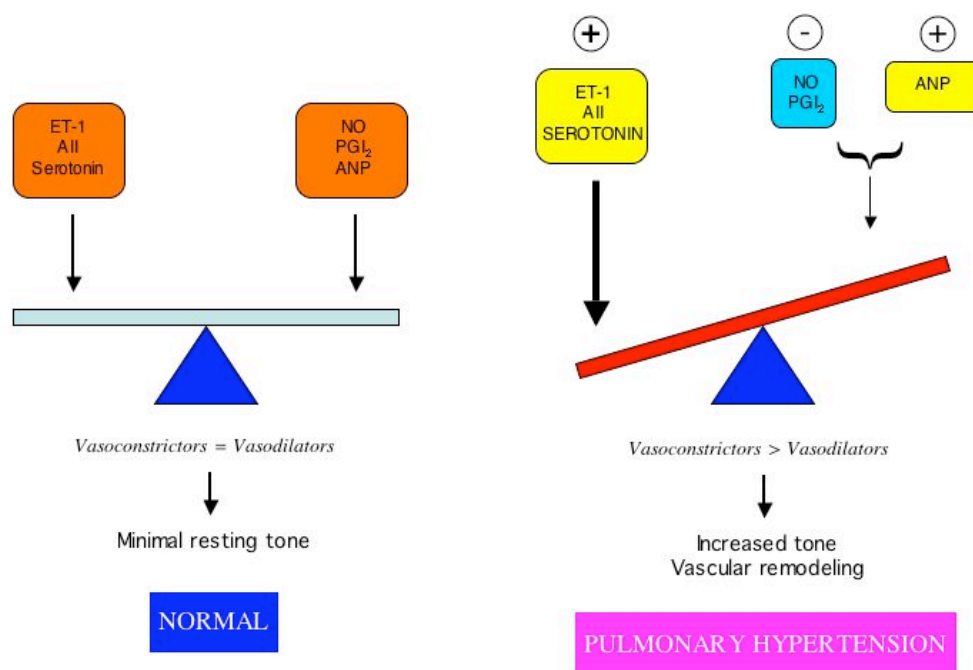


**Figure 1-6: Endothelial dysfunction in PAH**

Vasoconstriction and vasodilatation in the pulmonary circulation. In the normal pulmonary circulation, there is a balance between the mediators of vasoconstriction and vasodilatation, maintaining minimal resting tone. In the hypertensive pulmonary circulation there is upregulation of vasoconstrictor pathways and reduced production of NO and PGI<sub>2</sub>. Although there are increased circulating levels of vasodilators, such as atrial natriuretic peptide (ANP), these are insufficient to counteract the effect of vasoconstrictors, the net result being increased pulmonary vascular tone and vascular remodeling.

Early work has shown that patients with idiopathic PAH demonstrate increased production of TXA<sub>2</sub> and reduced concentrations of PGI<sub>2</sub> (Christman *et al.*, 1992) likely secondary to lowered expression of PGI<sub>2</sub>-S (Tuder *et al.*, 1999). Immunohistochemical staining has revealed minimal levels of NOS expression in idiopathic PAH patients compared to healthy controls (Giaid *et al.*, 1995). When mice lacking key factors such as eNOS (Fagan *et al.*, 1999) or atrial natriuretic peptide (ANP) or its receptor, NPR-A (Zhao *et al.*, 1999), are exposed to a hypoxic environment for prolonged periods (>1 week) they develop more severe pulmonary hypertension, vascular remodeling and right ventricular hypertrophy than wild type mice. Transgenic mice that overexpress prostacyclin synthase are protected against

developing hypoxia induced PAH (Geraci *et al.*, 1999). Thus alterations in the level of expression of these mediators (Figure 1-6), perhaps due to underlying genetic polymorphisms, could conceivably alter susceptibility to hypoxia-induced pulmonary hypertension in man.

A number of animal models have been used to investigate PAH: chronic hypoxia; the treatment with the endothelial toxin monocrotaline; bleomycin lung injury; left to right shunts. Such experimental models of PAH all exhibit increased plasma concentrations of ET-1 (Frasch *et al.*, 1999; Li *et al.*, 1994a). The ratio of systemic arterial to venous ET-1 concentrations is significantly increased in patients with PAH. Whether this represents increased local ET-1 production within the lung, with spilling over into the circulation, perhaps combined with a reduced ET<sub>B</sub> mediated clearance, remains to be fully established (Dupuis *et al.*, 1998; Stewart *et al.*, 1991). These raised ET-1 concentrations are more likely to be a marker of disease severity rather than directly mediating the development of PAH, as neither rats chronically infused with ET-1 (Migneault *et al.*, 2005) nor 12 month old transgenic ET-1 overexpressing mice (Hoche *et al.*, 2000) display PAH. Activation of the ET system in isolation is not sufficient to cause PAH: this must be combined with an imbalance of other endothelial factors (such as NO, PGI<sub>2</sub>, or TXA<sub>2</sub>) as well as modifications of VSMC properties (eg voltage gated potassium channels (Archer *et al.*, 1989) and the BMPR2 (Lane *et al.*, 2000)). However the most compelling evidence of activation of the ET system in PAH, is that increased ET-1 expression is not only found in patients suffering from the condition, but also correlates with the severity of the disease (Giaid *et al.*, 1993). Patients with PAH display a two-fold increase in [<sup>125</sup>I]-ET-1 binding in the media of distal PAs (Davie *et al.*, 2002), due to increased ET<sub>B</sub> receptor expression (Bauer *et al.*, 2002).

#### 1.2.4.3.9 ET antagonists in PAH

Both mixed ET<sub>A/B</sub> and ET<sub>A</sub> selective antagonists have demonstrated efficacy in the prevention and treatment of PAH in a wide range of experimental models (Okada *et al.*, 1995; Oparil *et al.*, 1995; Park *et al.*, 1997; Prie *et al.*, 1997; Rondelet *et al.*,

2003). Reduction in pulmonary vascular tone, decreased medial hypertrophy relative to luminal diameter and improved endothelial function are all possible mechanisms of the beneficial effects of ET blockade (Prie et al., 1998). In addition to ET<sub>A</sub> receptor inhibition, antagonism of the pulmonary VSMC ET<sub>B</sub> receptor, if significantly expressed, would offer more complete blockade of the vasoconstrictive, proliferative, and profibrotic effects of ET-1. However, blockade of the EC ET<sub>B</sub> receptor would inhibit the beneficial effects of NO and prostacyclin release. Thus the net effect of ET<sub>B</sub> receptor blockade is not clear.

There has been only one direct comparison of mixed ET<sub>A/B</sub> and ET<sub>A</sub> selective antagonists in a model of PAH (Jasmin *et al.*, 2001). Using monocrotaline induced PAH, both agents improved survival, but this only reached statistical significance for the mixed ET<sub>A/B</sub> antagonist. However, similar falls in right ventricular (RV) systolic pressure were seen with both agents. Indirect evidence in support of the use of selective ET<sub>A</sub> receptor blockade comes from studies involving genetic disruption of the ET<sub>B</sub> receptor. ‘Rescued’ ET<sub>B</sub> deficient rats exhibit an exaggerated pulmonary hypertensive response to hypoxia (Ivy *et al.*, 2001; Ivy *et al.*, 2002), suggesting that, at least in a rodent model of PAH, the net effect of ET<sub>B</sub> blockade is beneficial.

#### *1.2.4.3.10 Clinical trials of ET antagonists in PAH*

Clinical therapy for PAH includes anticoagulation, digoxin, diuretics and calcium channel blockers (in the small proportion of those patients that responded favourably to acute vasoreactivity testing) (Runo *et al.*, 2003). Further treatment strategies include PGI<sub>2</sub>, either as a continuous intravenous infusion or as inhaled therapy (Iloprost) (Humbert *et al.*, 2004). The beneficial effects of ET antagonists in animal models provided a sound rationale for testing this form of treatment in humans. The BREATHE-1 (Bosentan: Randomized Trial of Endothelin Receptor Antagonist Therapy) study randomised 213 NYHA Class III/IV patients to either placebo or bosentan 62.5 mg for 4 weeks, followed by either 125 mg or 250 mg, twice daily, for a further 12 weeks (Rubin *et al.*, 2002). Both doses improved NYHA class, distance walked in 6 minutes and reduced time to clinical worsening. A dose dependent

reversible disturbance in hepatic transaminases was observed, resulting in the lower dose of 125 mg, twice daily, receiving approval for the treatment of Class III/IV PAH in the US and Europe.

The clinical efficacy of selective ET<sub>A</sub> antagonists was evaluated in the STRIDE-1 (Sitaxsentan to Relieve Impaired Exercise) study (Barst *et al.*, 2004). This trial randomised 178 patients with NYHA II/III/IV PAH to placebo, sitaxsentan 100 mg or sitaxsentan 300 mg given once daily for 12 weeks. Whilst the primary endpoint of increased VO<sub>2 max</sub> (the maximum amount of O<sub>2</sub> that can be catabolised per unit body weight) was not reached, significant improvements in 6 minute walk distance (6MW) and pulmonary haemodynamics were seen.

In STRIDE-2, 247 patients with PAH were randomised to placebo, sitaxsentan 50 mg, sitaxsentan 100 mg or bosentan (125 mg twice daily) for 18 weeks and their 6MW compared (Barst *et al.*, 2006). Due to problems of cooperation with its suppliers, the bosentan arm was 'open label' and included for observation purposes only. Those patients treated with 100mg sitaxsentan had the most improved 6MW, and had a lower incidence of hepatic toxicity than the open label bosentan group.

Following STRIDE-2, a truly blinded, fully randomised head-to-head trial between mixed ET and selective ET<sub>A</sub> antagonism in the treatment of PAH is unlikely to be performed, but such a study is needed to allow a direct comparison between these 2 classes of drugs.

### **1.3 GENERATION OF EC-SPECIFIC ET<sub>B</sub> RECEPTOR DOWN-REGULATED MICE**

#### **1.3.1 Gene targeting: The classical approach**

Prior to the development of gene targeting techniques, the understanding of the *in vivo* function of genes was dependent on their analysis by inactivation or modification due to mutation, and the study of the consequences of this mutation in the mutant organism. In mammals, this approach was limited to the rare spontaneous mutations reflected in obvious phenotypes, as in the case of inheritable diseases in man. The targeted mutagenesis of the mouse germline was thus a fundamental breakthrough in this area of research. In its original form, gene targeting involves the inactivation of a given gene in the genome of embryonic stem (ES) cells by homologous recombination (Koller *et al.*, 1992; Thomas *et al.*, 1987). ES cells derive from an early stage of mouse development (the inner cell mass of 4.5-day old blastocyst) and so retain their totipotency. Thus they can participate in the generation of all cell lineages of the mouse (including germ cells) if transferred into an early mouse embryo. Transfer of mutant ES cells into mouse embryos thus allows the transmission of the mutation in question into the mouse germline.

Gene inactivation is achieved by replacing a predetermined gene segment with a mutant version of this segment, through homologous recombination. Since the latter is infrequent in mammalian cells, the isolation of the mutant ES cells requires stringent selection. In the original experiments, this was achieved by placing a selectable gene (the neomycin resistance gene) into the targeted locus in a manner that allows its expression (and hence cellular selection) while inactivating the target gene (Thomas *et al.*, 1987).

#### **1.3.2 Refining classical gene targeting by the Cre-loxP recombination system**

A limitation of classical gene targeting comes from the presence of a selection marker gene in the targeted locus. Since this gene must be active in order to allow ES cell selection, it is possible that its expression might affect the mutant phenotype in

an unpredictable way. This potential problem can be avoided by the elimination of the selection marker genes from the targeted locus, using the Cre-*loxP* recombination system (Hoess *et al.*, 1982; Sternberg *et al.*, 1981). The bacteriophage enzyme, Cre recombinase, recognizes a sequence motif of 34 bp, called *loxP* (Hoess *et al.*, 1982). If a DNA segment is flanked by two *loxP*, Cre excises that segment from the DNA, leaving a single *loxP* site behind. Assuming this *loxP* site does not itself affect gene expression, ‘clean’ deletions can thus be produced. In a gene targeting experiment, if the selection marker gene (such as the neomycin resistance gene) on the targeting vector (subsequently inserted into the target locus by homologous recombination) is flanked by *loxP* sites, it can later be removed from the ES cell genome via transient transfection of a Cre-expression vector into these cells (see Figure 1-7). However, perhaps more importantly, Cre-*loxP*-mediated targeted mutagenesis, facilitates conditional (rather than general) gene targeting.

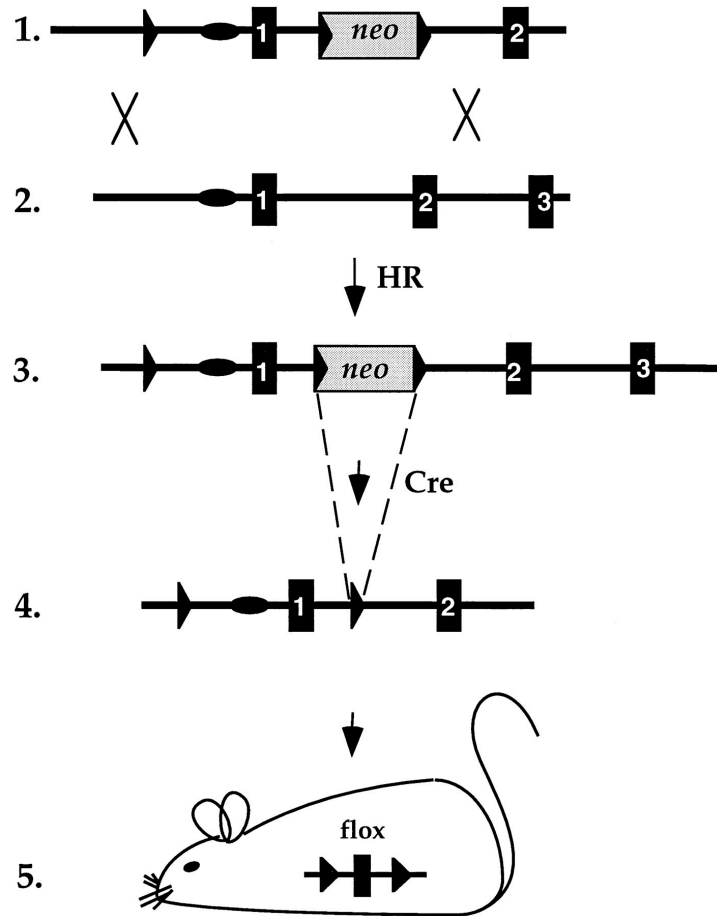


**Figure 1-7: Generation of mice with loxP-flanked target genes (flox).**

(1) Gene targeting vector containing three loxP sites (*filled triangles*), two of them flanking the Neomycin resistance (*neo*) gene. (2) Target gene in the genome of ES cells (exons drawn as filled boxes). (3) Genomic locus modified by homologous recombination (*HR*) between vector and target gene. (4) Deletion of the loxP-flanked *neo* gene by transient Cre expression in ES cells. Two loxP sites remain in the target gene. (5) Generation of a loxP-containing mouse line from modified ES cells. (Adapted from (Rajewsky *et al.*, 1996).

### 1.3.3 Conditional gene targeting: Tissue specific knockout/downregulation

Conditional (ie cell-type specific or inducible) gene targeting is useful for several reasons. Firstly, germline mutations may result in a lethal phenotype (as seen with ET<sub>B</sub> null animals) preventing the study of the function of that gene in the adult animal. Second, genes may code for proteins that exert different effects when expressed on different cell types. For example, ET<sub>B</sub> receptors on VSMCs exert the opposite effect (vasoconstriction) to EC ET<sub>B</sub> receptors (vasodilatation).

The strategy of conditional targeting of endogenous genes, that was used in the generation of our EC ET<sub>B</sub> down-regulated mice, consists of flanking a target gene or gene segment with *loxP* sites in ES cells by classical gene targeting and deleting the selection marker gene by transient transfection with a Cre-encoding plasmid. This process yields ES cell mutants in which the gene segment of interest is either flanked by *loxP* sites or deleted. Either mutation can be transmitted into the germline. In the former case, the mutant mice carry a functional, but *loxP*-flanked gene in their genome (Figure 1-7). In the latter the gene is deleted in all cells of the body, generating the situation of a classical knockout experiment, except that no selection marker gene remains in the mutant locus.

Conditional targeting of *loxP*-flanked genes or gene segments can be achieved by crossing the mutant animal with a second strain of mouse (in our case the EC specific Tie2-Cre) in which Cre recombinase is expressed in a cell-type-specific manner. Although all cells in the progeny contain floxed alleles, expression of Cre recombinase only occurs in cells in which the tissue-specific promoter is active, thereby limiting recombination exclusively to these cells. The success of such tissue specific conditional gene targeting is entirely dependent on the precise restriction of Cre expression to the desired target cell type. ‘Leaky’ expression of Cre will result in recombination in other cell types, whilst a ‘patchy’ expression of Cre in target cells will result in reduced rate of recombination and a mosaic pattern of gene knockout. Either of these events would complicate the interpretation of any observed phenotype.

Many other groups have established that, in principle, cell-type-specific gene targeting can be successfully performed in this manner (Ahn *et al.*, 2004; Gu *et al.*, 1994; Hirota *et al.*, 1999; Kedzierski *et al.*, 2003; Shohet *et al.*, 2004). If Cre expression could be induced specifically in any given cell type, then the gene in question can be specifically knocked out/ knocked down in that particular cell type. By crossing the floxed mouse with a range of such tissue specific Cre lines a panel of tissue specific down-regulated mice can be generated.



### 1.3.4 Endothelial cell specific downregulation

The Tie2 gene encodes the vascular EC tyrosine kinase angiopoietin receptor (Loughna *et al.*, 2001). Promoter and enhancer elements from this Tie2 gene, are capable of directing  $\beta$ -galactosidase reporter gene expression specifically into ECs of transgenic mouse embryos (Schlaeger *et al.*, 1997). This is maintained throughout development and into adulthood. Tie2-Cre mice, in which the Cre recombinase gene is expressed under the control of the Tie2 promoter, have been generated (Kisanuki *et al.*, 2001). Accurate assessment of the expression pattern of Tie2-Cre transgenic mice is essential for predicting the pattern of recombination events in mice harbouring functional *loxP* sites. By crossing Tie2-Cre mice with a reporter mouse strain CAG-CAT-Z and Rosa 26 (R26R) (Kisanuki *et al.*, 2001), the distribution of Cre mediated recombination can be determined from the pattern of *lacZ* expression. *LacZ* was seen in ECs, but was also found in endocardial and mesenchymal cells of the atrioventricular canal and proximal cardiac outflow tract (Kisanuki *et al.*, 2001). Such work demonstrating the EC specificity of Cre expression have been repeated by others, using the same Tie2-Cre transgenic line (Liao *et al.*, 2001). This group, characterising an EC specific Connexin 48 knockout mouse, went on to investigate the efficiency of Tie2-Cre mediated gene deletion. Using tissue from their KO mice, they showed that cultured pulmonary ECs had ~80% of the Connexin 48 gene deleted compared to brain gray matter.

Other groups have now produced different strains of Tie2-Cre transgenic mice (Constien *et al.*, 2001; Theis *et al.*, 2001) and have observed small differences in expression pattern most likely secondary to variations in the insertion site of the transgene. The EC ET<sub>B</sub> down-regulated mice, generated in our laboratory, utilised the Tie2-Cre mice of Kisanuki and colleagues, a kind gift of Professor Masashi Yanagisawa (University of Texas, USA).

### 1.3.5 Generation of EC-specific ET<sub>B</sub> receptor down-regulated mice

The generation of the EC-specific ET<sub>B</sub> receptor down-regulated mouse (FF/Tie2) was carried out by Dr A Bagnall under the supervision of Dr Yuri Kotelevtsev (University of Edinburgh, UK) (Bagnall *et al.*, 2006). A fragment of the ET<sub>B</sub> receptor gene was replaced with a targeting vector, featuring *loxP* sites flanking exons 3 and 4 and a *loxP*-flanked selection marker (including a neomycin-resistance gene and thymidine kinase gene), by homologous recombination into ES cells from 129/01a embryos. Neomycin-resistant clones were selected and DNA extracted and analysed by PCR. Specific recombination was detected by polymerase chain reaction (PCR) and Southern analysis with a 3' external probe in 6/97 colonies of ES cells analysed (Figure 1-8).

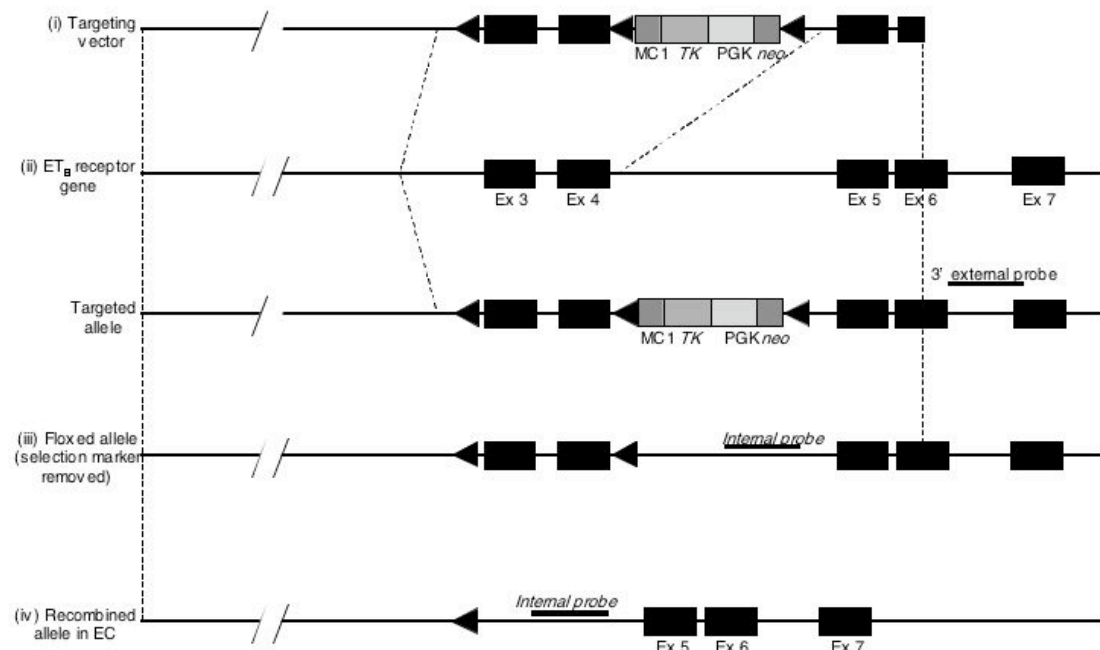


**Figure 1-8: Gene targeting of the ET<sub>B</sub> gene**

Structure of the targeting vector (i) and ET<sub>B</sub> receptor gene (ii): Black rectangles, exons; black triangles, *loxP* sites; MC1, Mario Cappecci-1 promoter; PGK, Phosphoglucokinase promoter; TK, Thymidine kinase gene; *Neo*, neomycin resistance gene. The positions of internal and external probes used for Southern analysis are illustrated. Following homologous recombination events in ES cells, the selection marker was removed by Cre recombinase-mediated excision. The structures

of the targeted ('floxed') allele (iii) and of the floxed allele following *in vivo* Cre-mediated recombination in ECs (iv) are illustrated.

Three ES cell clones underwent transfection with Cre-recombinase. Of the resulting daughter colonies, 294 were gancyclovir-resistant (hence lacked the selection cassette containing the thymidine kinase gene). By PCR genotyping, 11 of these were found to retain *loxP* sites flanking exons 3 and 4 but to lack the selection marker. Sequence analysis confirmed no mutations within either *loxP* sites or coding regions in these clones. Cells from 3 clones were injected into C57BL/6 blastocysts. Germline transmission was achieved in one male chimeric mouse, which was mated to BKW females. Around half of the offspring were heterozygous for the floxed ET<sub>B</sub> receptor gene allele. Genotype was confirmed by PCR and Southern analysis using an internal probe as detailed in section 2.3 below. Homozygous floxed mice were bred by intercross and backcross of BKW;129/01a heterozygotes. No abnormality of pigmentation, gut development or longevity was observed in homozygous floxed mice, and no deviation from Mendelian distribution of alleles was seen in intercross experiments.

Homozygous floxed ET<sub>B</sub> receptor mice (Flox/Flox; background 50% 129/01a, 50% BKW) were crossed with Tie2-Cre transgenic mice (Kisanuki *et al.*, 2001) (C57BL6/SJLF<sub>1</sub> background). Mice were genotyped by PCR and Southern as described in the section 2.3.

### **1.3.6 Initial characterisation of the EC-specific ET<sub>B</sub> receptor down-regulated mice**

Having generated the EC ET<sub>B</sub> down-regulated (FF/Tie2) mouse Dr Alan Bagnall carried out initial phenotyping experiments (Bagnall *et al.*, 2006).

### 1.3.6.1 ET<sub>B</sub> RECEPTOR-MEDIATED ET-1 BINDING IS DECREASED IN EC OF EC-SPECIFIC ET<sub>B</sub> RECEPTOR DOWN-REGULATED MICE

To quantitatively assess the extent of ET<sub>A</sub> and ET<sub>B</sub> receptor binding in ECs, competitive radioligand binding studies were performed. An EC-enriched cell population was isolated from pulmonary tissue using an EC-specific lectin, and binding of [<sup>125</sup>I]-ET-1 was measured, in the presence and absence of selective ET receptor antagonists.

ET<sub>B</sub>-mediated binding (ET-1 binding in the presence of an ET<sub>A</sub> selective antagonist) was significantly decreased by 82% in FF/Tie2 pulmonary ECs compared with wild type controls (Figure 1-9). ET<sub>A</sub> receptor-mediated binding (ET-1 binding in the presence of ET<sub>B</sub> blockade) did not differ between groups.

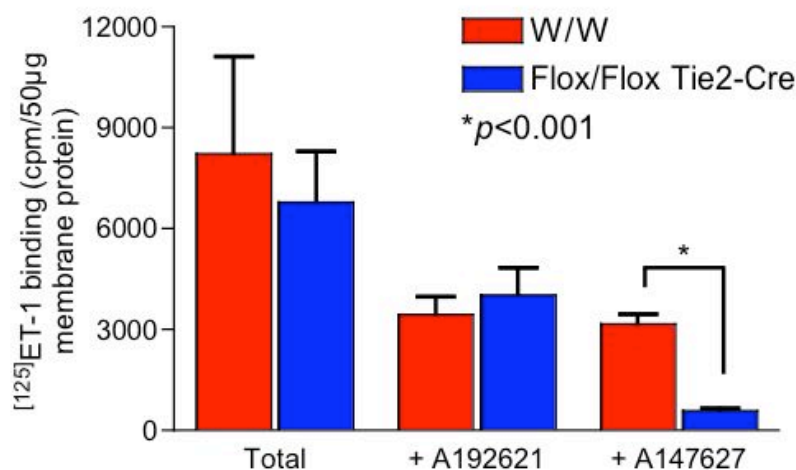


**Figure 1-9: Reduced ET-1 binding in pulmonary ECs from FF/Tie2 mice**

EC ET<sub>B</sub>-dependent binding of [<sup>125</sup>I]-ET-1 was significantly decreased in EC-enriched pulmonary cells from FF/Tie2 mice ( $p < 0.001$ ). Total and ET<sub>A</sub> mediated binding did not differ between groups ( $n=3$  in each group).

### 1.3.6.2 ET<sub>B</sub> RECEPTOR-MEDIATED VASODILATATION IS IMPAIRED IN EC-SPECIFIC ET<sub>B</sub> RECEPTOR DOWN-REGULATED MICE.

Functional EC ET<sub>B</sub> receptor-mediated responses were assessed in aortic rings using wire myography. The ET<sub>B</sub> receptor selective agonist S6c produced vasodilatation of aortic rings precontracted with norepinephrine in all genotypes (Figure 1-10A). The vasodilator response was significantly attenuated in FF/Tie2 mice compared to WW/-- controls.

Thus although not abolished, EC ET<sub>B</sub> receptor mediated vasodilation is significantly reduced in the FF/Tie2 mice.

### 1.3.6.3 ET<sub>B</sub> RECEPTOR-MEDIATED RESPONSES IN NON-EC ARE MAINTAINED IN EC-SPECIFIC ET<sub>B</sub> RECEPTOR DOWN-REGULATED MICE.

FF/Tie2 mice displayed normal gut development and pigmentation, consistent with functional expression of ET<sub>B</sub> receptors on neuroblasts and melanoblasts, and produced healthy offspring. S6c-induced tracheal smooth muscle cell constriction (Figure 1-10B) was unaltered in FF/Tie2 mice, compared to controls, demonstrating that non-EC ET<sub>B</sub> mediated responses are preserved.

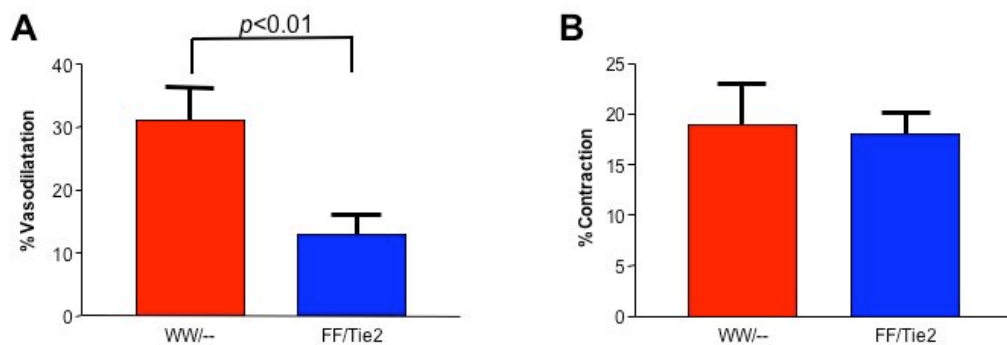


**Figure 1-10: Functional evidence of EC ET<sub>B</sub> down-regulation in FF/Tie2 mice**

A: Endothelium-dependent relaxation in response to the ET<sub>B</sub> selective agonist S6c ( $10^{-7}$ M) was significantly decreased in aortic rings from FF/Tie2 compared to WW/-- mice ( $p < 0.01$ ;  $n=10$ ); B Smooth muscle constriction in response to S6c ( $10^{-8}$ M) in tracheal rings was unaltered in FF/Tie2 compared to WW/-- mice ( $n=16$ ).

## 1.4 AIMS OF THE PROJECT

The ET<sub>B</sub> receptor mediates a wide range of effects when expressed on different cell types. As outlined in the sections above, ET<sub>B</sub> activation plays a fundamental role in the control of vascular tone, in both the systemic and pulmonary circulation, as well as controlling sodium and water balance in the kidney, and scavenging ET-1 from the plasma. The role played by the EC ET<sub>B</sub> receptor in mediating the effect of ET-1 cannot be determined using currently available pharmacological antagonists, as these are unable to selectively block ET<sub>B</sub> receptors in one particular cell type, without also blocking ET<sub>B</sub> receptors expressed throughout all tissues. Such difficulties might be overcome by utilising drug delivery mechanisms that selectively release locally active or cell type targeted concentrations of antagonists. However, in many tissues the different ET<sub>B</sub> expressing effector cells lie in close proximity, and so selective targeting of a single cell type is not straightforward. Alternatively, the effects of antagonists might be studied *in vitro* and the results extrapolated to an *in vivo* model. Such an approach has provided the majority of the data on which the current understanding of the physiology of the ET system is based.

Genetic manipulation of receptors provides a further mechanism whereby loss of function effects may be studied *in vivo*. However, as outlined previously, complete knockout of ET<sub>B</sub> receptor function produces a lethal phenotype that precludes study of *in vivo* adult physiology. Studies on young mice prior to the onset of intestinal obstruction are possible, but the quality of the data recorded is likely to be compromised. A great deal of insight has been gained from the study of rescued ET<sub>B</sub> receptor-deficient animals. However, the concurrent knockout of ET<sub>B</sub> from multiple tissues, whilst elegant, adds little advantage over experiments using pharmacological antagonists in terms of data interpretation. The advent of technologies that permit the spatial and temporal regulation of gene expression provides a powerful mechanism by which the understanding of the physiological role of the ET<sub>B</sub> receptor in an individual cell type may be more fully characterised. Cell-specific regulation of ET<sub>B</sub> receptor expression allows the contribution of these receptors to cardiovascular physiology to be determined without the confounding effects of receptor down-regulation or blockade in other tissues. By characterising the phenotype of a line of

transgenic mice in which the ET<sub>B</sub> receptor is selectively and specifically down-regulated in ECs, the role played by EC ET<sub>B</sub> in cardiovascular homeostasis can be determined, without the confounding effects of receptor down-regulation or blockade of the ET<sub>B</sub> receptor in all other tissues. This work complements other studies, using similar conditional transgenic approaches (Ahn *et al.*, 2004; Amiri *et al.*, 2004; Ge *et al.*, 2005; Ge *et al.*, 2006; Kedzierski *et al.*, 2003; Shohet *et al.*, 2004), which taken together, will allow a more complete understanding of ET-1 signalling, and thus better inform clinical research in this area.

I have used this EC ET<sub>B</sub> receptor specific down-regulated mouse to test the following hypotheses:

- The EC ET<sub>B</sub> receptor plays an important role in the control of gene and protein expression of the ET system in the mouse.
- The EC ET<sub>B</sub> receptor influences the control of BP through its influence on vascular tone.
- The EC ET<sub>B</sub> receptor influences the control of BP through its role in sodium excretion.
- The EC ET<sub>B</sub> receptor is responsible for clearing ET-1 from the plasma.
- The EC ET<sub>B</sub> receptor is protective against the development of hypoxia-induced pulmonary hypertension.

The following chapters detail how I have characterised the phenotype of this EC specific ET<sub>B</sub> receptor down-regulated mouse, generated in our laboratory. Having established a successful breeding strategy and demonstrated that the mouse exhibits tissue specific ET<sub>B</sub> down-regulation, I have carried out a range of experiments to test the hypotheses detailed above.

## **2 CHAPTER 2: MATERIALS AND METHODS**

### **2.1 Animals**

All experiments were performed on male mice aged 2 – 4 months, weighing 25 - 40g unless otherwise stated. Mice were given free access to tap water and standard (0.76% NaCl) mouse chow until 21 days prior to experiments. Mice were housed according to UK Home Office recommendations at 22°C with 12-hour diurnal light/dark cycles. All procedures were performed under the provisions of the Animals in Scientific Procedures Act (1986) (<http://www.archive.official-documents.co.uk/document/hoc/321/321-xa.htm>).

### **2.2 Breeding**

#### **2.2.1 Breeding strategy to generate ET<sub>B</sub> null animals**

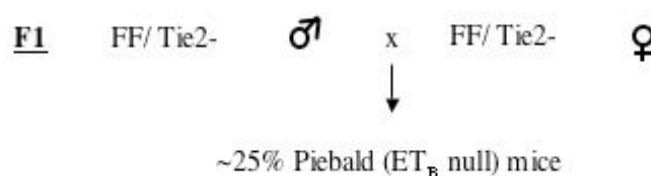
Male and female offspring from a single breeding pair, in which a high rate of germ cell recombination had been identified, were deliberately intercrossed to assess whether a recombination event within the ET<sub>B</sub> gene was sufficient to prevent expression of functional ET<sub>B</sub> receptors (and generate piebald ET<sub>B</sub> receptor null mice) (Figure 2-1A).

#### **2.2.2 Analytical breeding crosses to assess sex linkage of recombination events**

In order to accurately determine whether the rate of recombination varied with the sex of germline transmission, analytical crosses were established. Reciprocal crosses of FF/Tie2 animals paired with W0/-- (heterozygous ET<sub>B</sub> null) mice were set up. If recombination occurred in all gametes produced by the FF/Tie2 animal, then 50% of the progeny would be expected to be piebald (ET<sub>B</sub> receptor null mice). If recombination occurred in only 10% of the gametes produced by the FF/Tie2 animal, then 5% of the progeny would be expected to be piebald (Figure 2-1B).



### A: Breeding Strategy for piebald animals



### KEY

|          |   |
|----------|---|
| FF/Tie2- | Homozygous floxed/<br>heterozygous Tie2-Cre                                   |
| W0/--    | Heterozygous wild type<br>and null ET <sub>B</sub> /<br>homozygous no Cre     |
| FW/Tie2- | Heterozygous floxed and<br>wild type/ heterozygous<br>Tie2-Cre                |
| FW/--    | Heterozygous floxed and<br>wild type/ homozygous<br>no Cre                    |
| F0/Tie2- | Heterozygous floxed and<br>null ET <sub>B</sub> / heterozygous<br>Tie2-Cre    |
| 0W/Tie2- | Heterozygous wild type<br>and null ET <sub>B</sub> /<br>heterozygous Tie2-Cre |
| F0/--    | Heterozygous floxed and<br>null ET <sub>B</sub> / homozygous<br>no Cre        |

### B: Reciprocal analytical breeding crosses

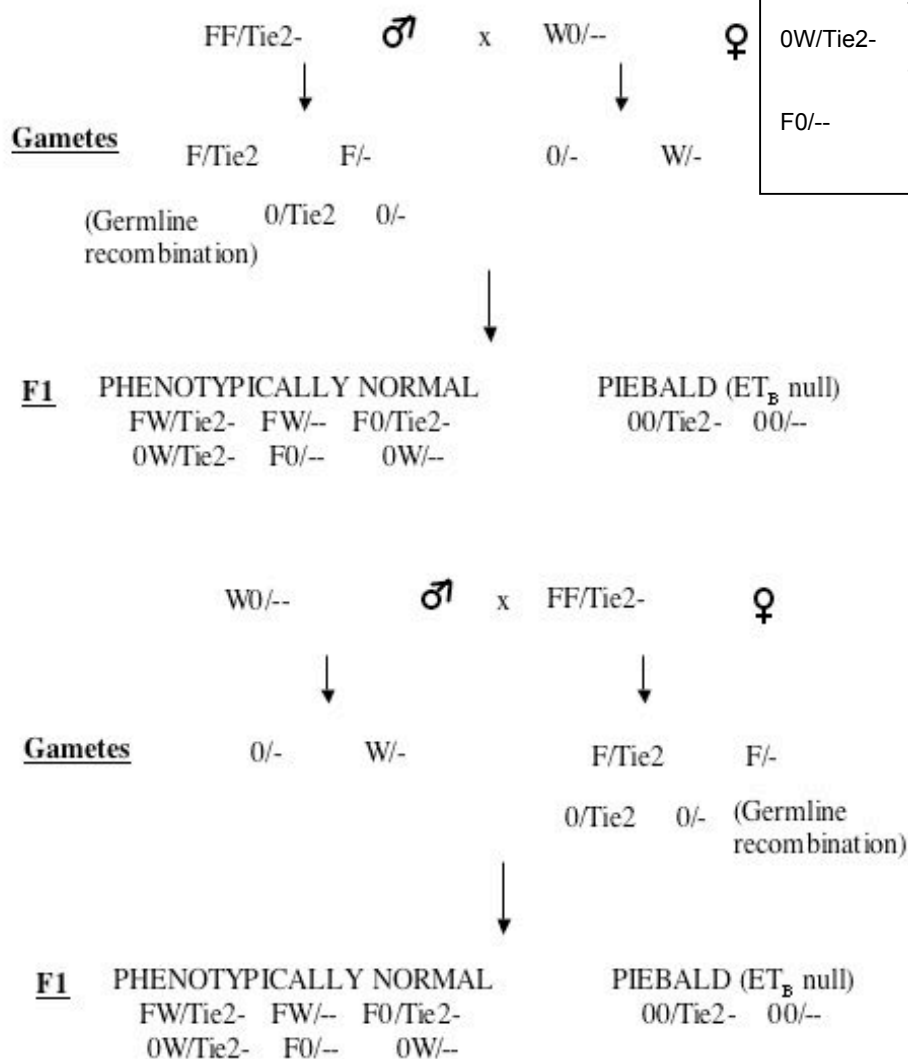


**Figure 2-1: Breeding strategy to generate piebalds and analytical crosses**

Schematic of breeding strategy used to produce (A) piebald null ET<sub>B</sub> receptor mice; and (B) reciprocal analytical breeding pairs to determine the effect of the sex of germline transmission on the rate of recombination.

### 2.2.3 Breeding strategy to generate experimental animals

Breeding was organised to minimise the likelihood of unrestricted recombination (see Figure 2-2). Harems were arranged consisting of 1 FF/Tie2 male mated with 2 FF/-- female mice in order to maximise the number of mice generated. Homozygous floxed ET<sub>B</sub> receptor mice (Flox/Flox; background 50% 129/01a, 50% BKW) were crossed with Tie2-Cre transgenic mice (Kisanuki *et al.*, 2001) (C57BL6/SJLF<sub>1</sub> background).

#### Breeding Strategy for experimental animals

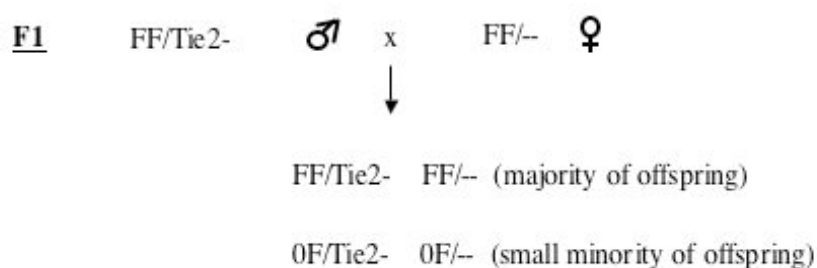


#### **Figure 2-2: Breeding strategy for experimental animals**

Schematic of breeding strategy used to produce EC-specific ET<sub>B</sub> receptor down-regulated mice (FF/Tie2-), and floxed (FF/-- controls). (For definition of genotypes see key in Figure 2-1.)

## 2.3 Genotyping

### 2.3.1 Preparation of genomic DNA from tail/ ear biopsy

In the initial stages of this work, genomic DNA was prepared from tail-tip biopsies and mice identified by numbered ear tagging. However, more recently, to reduce the severity of this procedure suffered by the animals, in accordance with the aims of the Animals in Scientific Procedure Act (1986) (<http://www.archive.official-documents.co.uk/document/hoc/321/321-xa.htm>) ear punching was used not only to sample DNA but as a method of animal identification. Tail biopsy was performed under general anaesthesia (Halothane-Vet, Merial Animal Health Ltd., Harlow, UK) in weaned pups up to 28 days old. A 0.5cm length of tail was biopsied. Ear biopsy

did not require anaesthesia as it is not a Home Office licenced procedure. All samples were stored at  $-20^{\circ}\text{C}$  until DNA extraction.

Biopsies were incubated at  $55^{\circ}\text{C}$  in  $600\mu\text{l}$  of tail buffer (200 mM Tris HCl, 400 mM EDTA pH 8.0, 4 M NaCl, and 10% (v/v) SDS) and  $35\mu\text{l}$  of  $10\text{ mg.ml}^{-1}$  Proteinase K and rotated continuously overnight in a Techne Hybridiser HB-1D oven (Techne, Cambridge Ltd, UK). The following day,  $20\mu\text{l}$  of  $20\mu\text{g.ml}^{-1}$  DNase free RNase (Sigma-Aldrich, Steinheim, Germany) was added and tails incubated for 1 hour at  $37^{\circ}\text{C}$ .

$600\mu\text{l}$  of Tris-saturated phenol and  $37.5\mu\text{l}$  of 2 M mercaptoethanol were added to each tube. Tubes were rotated for 15 minutes, followed by centrifugation at  $12\,000\text{ g}$  for 2 minutes. The aqueous phase and interphase were transferred to a fresh Eppendorff tube and extracted with 1 volume of phenol: chloroform: isoamyl alcohol (25:24:1), and centrifuged again at  $12\,000\text{ g}$  for 2 minutes. The process was repeated using 1 volume of chloroform: isoamyl alcohol (24:1). The DNA was precipitated from the aqueous phase with  $600\mu\text{l}$  of room temperature isopropanol by gentle rotation for 5 minutes. The stringy genomic DNA precipitate was pelleted by centrifugation ( $12\,000\text{ g}$ , 2 minutes) and washed in  $200\mu\text{l}$  of 70% ethanol. DNA was air dried for 10 minutes then dissolved in  $200\mu\text{l}$  of TE, pH 8.0. Samples were then left to dissolve completely for 30 minutes at  $37^{\circ}\text{C}$  before being mixed gently and stored at  $-20^{\circ}\text{C}$  until required.

### **2.3.2 Polymerase Chain Reaction of genomic DNA**

*Genotyping for Floxed  $ET_b$  mice:* Genotyping to identify floxed (F), wild type (W) and recombined (0) alleles was performed by PCR using forward primer 454F (5'-TCA GTT GTA ATG AGA CAC AGA C -3') and reverse primer 681R (5'-AGC CAT AAA GTC ACA GCC ATT C-3'). These PCR oligos flanked a  $\sim 1.1\text{ kb}$  sequence spanning both *loxP* sites in the targeted allele, and a  $2.2\text{ kb}$  sequence in the W allele (Figure 2-3).

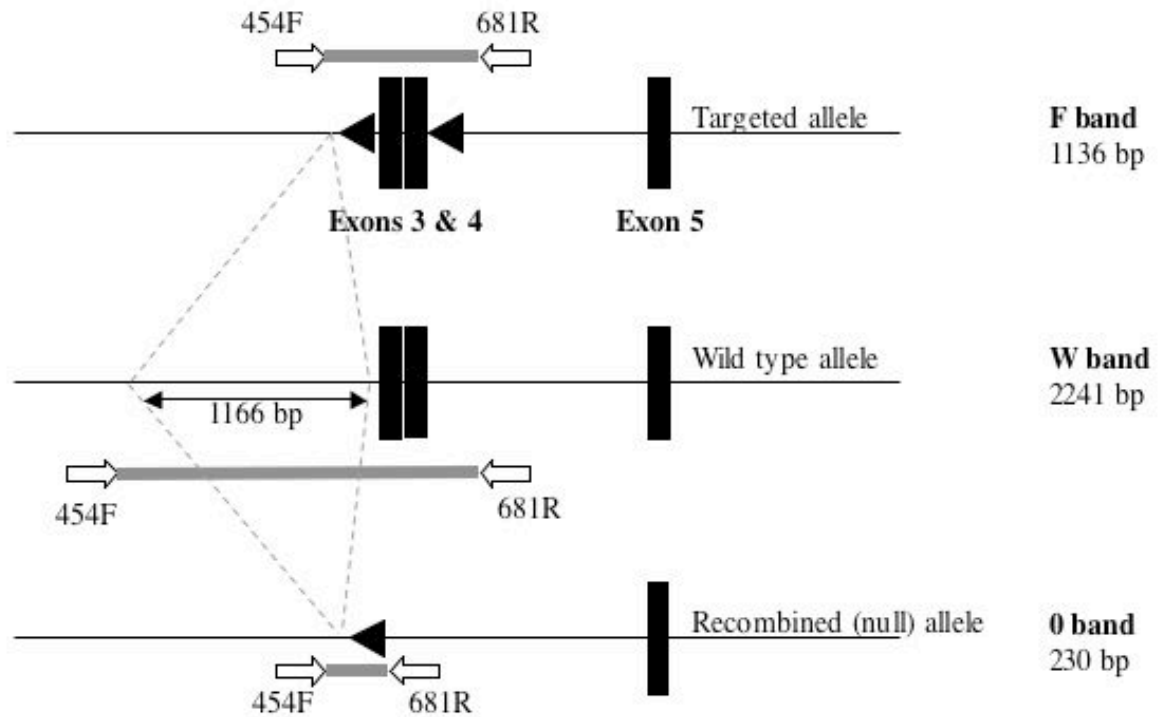


**Figure 2-3: PCR genotyping strategy**

The primers 454F and 681R were used to amplify PCR products of 1136 bp, 2241 bp, and 230 bp from the floxed, wild type and recombined alleles respectively.

*Genotyping for Tie2-Cre Transgene:* The presence of the Tie2-Cre transgene was detected by PCR using forward primer TIE2 98F: (5'-CGC ATA ACC AGT GAA ACA GCA TTG C-3') and reverse primer TIE2 101R: (5'- CCC TGT GCT CAG ACA GAA ATG AGA-3') (Kisanuki *et al.*, 2001).

Each of the PCRs were performed in a total of volume of 25  $\mu$ l containing 500  $\mu$ M of each deoxyribonucleotide (dATP; dTTP; dCTP; dGTP), 300 nM of each primer, 1  $\mu$ g of genomic DNA, 2.5  $\mu$ l of 10 x Bioline<sup>TM</sup> PCR buffer, 1.125  $\mu$ l of 50 mM MgCl<sub>2</sub> and 0.2 units of Bioline<sup>TM</sup> Taq polymerase. Samples were amplified using a MJ Research Peltier Thermal Cycler PT-200 with a heated lid with the following conditions:

**Table 2-1: PCR conditions**

|               | <b>Flox PCR</b>            | <b>Tie2 PCR</b>            |
|---------------|----------------------------|----------------------------|
| <b>Step 1</b> | 92°C for 2 minutes         | 92°C for 3 minutes         |
| <b>Step 2</b> | 92°C for 30 seconds        | 92°C for 30 seconds        |
| <b>Step 3</b> | 60°C for 30 seconds        | 55°C for 30 seconds        |
| <b>Step 4</b> | 68°C for 2 minutes         | 68°C for 2 minutes         |
| <b>Step 5</b> | Return to step 2, 30 times | Return to step 2, 29 times |
| <b>Step 6</b> | 68°C for 10 minutes        | 68°C for 10 minutes        |

### **2.3.3 Quantitation of nucleic acids**

Optical absorbance at 260 nm ( $OD_{260}$ ) of DNA-containing solutions was measured using a Bio-Rad SmartSpec 3000 Spectrophotometer (Bio-Rad, UK). DNA samples were diluted 1:50 to a final volume of 200  $\mu$ l. Dilutions of samples were adjusted if the spectrophotometric readings were outside the range 0.1 – 0.8 (optimal range of the spectrophotometer). The spectrophotometer calculated the concentration of DNA in each sample and values of total DNA yield ( $\mu$ g. $\mu$ l<sup>-1</sup>) in each sample were obtained by adjusting for the dilution factor.

### **2.3.4 Agarose gel electrophoresis**

DNA molecules were separated according to size using 1% agarose gel electrophoresis. All gels were prepared with SeaKem LE agarose (FMC Bioproducts, Rocklands, USA) using 1 x TAE (40 mM Tris-acetate, 1 mM EDTA) and were stained with 0.5  $\mu$ g.ml<sup>-1</sup> of ethidium bromide (Product code E-8752, Sigma-Aldrich, Gillingham, Dorset, UK). Samples were mixed with 6 x loading dye solution (0.09% bromophenol blue, 0.015% xylene cyanol FF and 10% glycerol) to a final concentration of 1 x before electrophoresis. All sizes were judged according to 100 bp ladder size markers run concurrently on the same gel (GeneRuler™: 1000, 900, 800, 700, 600, 500, 400, 300, 200, 100, 80 bp; MBI Fermentas, St Leon-Rot, Germany). DNA was visualised on the gel using a transilluminator and digital acquisition system (Ultra-Violet Products Ltd, Cambridge, UK).

## **2.4 GENOTYPING APPROACHES**

### **2.4.1 ‘Comparative’ PCR of tail biopsies**

This involved using identical quantities of tail derived DNA in each PCR, and then comparing band intensity on the resulting gels.

Tails were biopsied and DNA extracted as outlined above (see section 2.3.1). The concentration of DNA in each sample was determined using spectrometry to determine the OD<sub>260</sub> (see section 2.3.3). 50 ng of sample was used in each PCR mix, which was otherwise performed as outlined above (see section 2.3.2). 17 µl of the products of the PCR were loaded onto a 1% agarose gel. Attempts were then made to compare the intensity of the O band and F band amongst samples and with those of control of known genotype.

### **2.4.2 PCR of ‘EC free’ tissue**

**Hair:** Hair sampling offers a potential source of genomic DNA for genotyping involving minimal distress to the animals (Schmitteckert *et al.*, 1999). Hair was plucked from mice using forceps and the hair bulbs collected. The shaft of the hair filament was discarded. DNA was then extracted from the hair samples using the same protocol as for the tail/ ear biopsies (see section 2.3.1) and the PCR performed as described previously (see section 2.3.2).

**Testes:** Testes were removed post mortem from experimental animals and frozen in liquid nitrogen until DNA extraction. Using a fresh scalpel blade for each sample, approximately one third of the testis was cut up and minced before DNA was extracted using the same protocol as for the tail/ ear biopsies (see section 2.3.1) and the PCR performed as described previously (see section 2.3.2).

**Hearts:** Using collagenase digestion followed by centrifugation, we aimed to crudely separate the larger and heavier cardiomyocytes from other less dense cells such as ECs.

Hearts were removed from a selection of freshly culled experimental animals and rinsed in PBS, before being cut into halves. One portion of the whole heart was put on ice for later extraction. Crude isolation of cardiomyocytes was performed on the other half of the heart, using collagenase digestion followed by centrifugation. We intended to separate the larger and heavier cardiomyocytes from other less dense cells such as ECs. This involved mincing the cardiac tissue in a Petri dish using small scissors, in ~1 ml of phosphate buffered saline (PBS). After adding 1 ml of collagenase (10mg.ml<sup>-1</sup>; Sigma-Aldrich, Steinheim, Germany) the mixture was incubated for 60 minutes at 37°C. The mixture was then poured through a filter basket (VWR International Ltd., Poole, UK) into a 50 ml Falcon tube. The filter basket was then rinsed with 20 ml PBS. The Falcon tube and its contents were centrifuged for 5 min at 1000 rpm. The supernatant was discarded, and the pellet resuspended in 15 ml PBS. The mixture was centrifuged for 3 minutes at 800 rpm, the supernatant discarded, and the pellet resuspended in the minimum volume of PBS required.

DNA was then extracted from both the crude isolate of cardiomyocytes and the undigested half of heart tissue, using the same protocol as for the tail/ ear biopsies (see section 2.3.1) and the PCR performed as described previously (see section 2.3.2).

### **2.4.3 Southern blot**

Southern analysis involves digestion of genomic DNA using a restriction endonuclease, cutting it into sequences of certain lengths. Fragments of interest can be labelled using a radiolabelled [<sup>32</sup>P]-homologous internal probe.

### 2.4.3.1 PRODUCTION OF INTERNAL PROBE FOR SOUTHERN BLOT ANALYSIS

Dr Yuri Kotelevtsev (University of Edinburgh, UK) produced the internal probe. This involved locating *EcoR* I restriction sites in the gene sequence with the insertion cassette, allowing an internal probe to be identified.

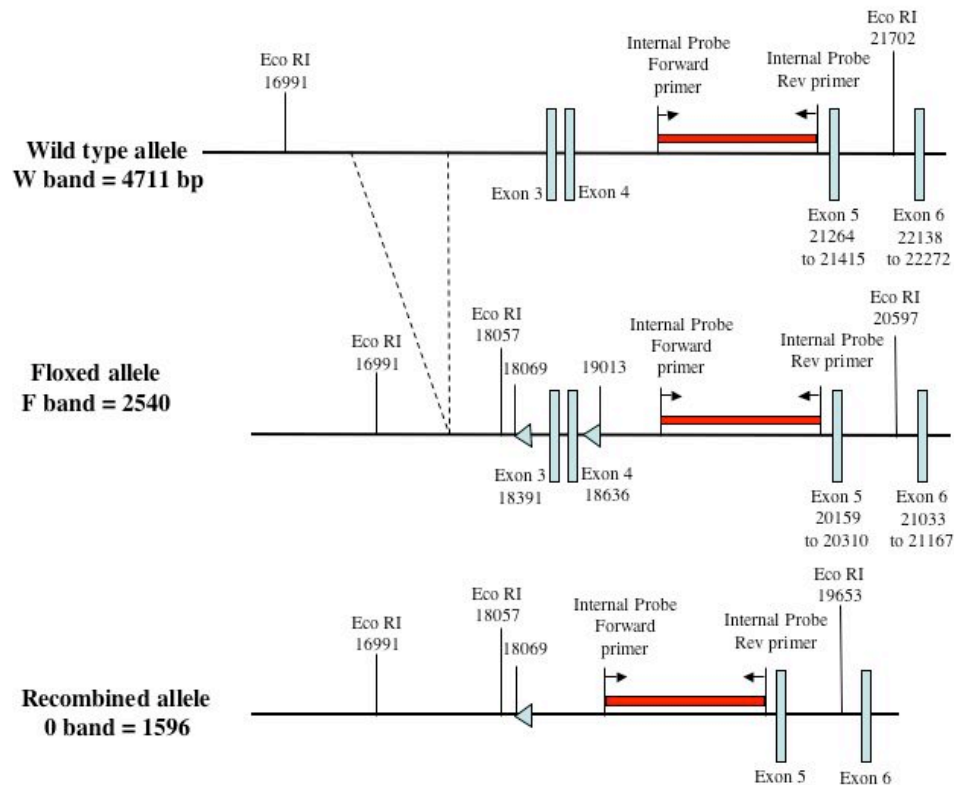


**Figure 2-4: Southern blot strategy**

The the probe, used in Southern Blot to genotype FF/Tie2 from F0/Tie2 mice, was located between exons 4 and 5.

The probe was amplified by PCR with primers homologous to either end of this sequence (forward primer: 5'-TAG ATA GAA GTT GCC TAA CCT TAG-3'; and reverse primer 5'CTT CTT CCA TTC TAC CTG CTT-3') using a fragment of the pλP ET<sub>B</sub> plasmid (kind gift by Dr A Bagnall, University of Edinburgh, UK) as the template. The probe was then purified by gel electrophoresis.



The probe was labeled using a modified protocol developed by Feinberg and colleagues (Feinberg *et al.*, 1983). This involved mixing 50 ng of template DNA, 2.5  $\mu$ l of 1 x hexanucleotide solution with sufficient dH<sub>2</sub>O to make a final volume of 14  $\mu$ l. The mixture was boiled for 5 minutes before immediate cooling to -20°C. After brief centrifuging 5  $\mu$ l of 5 x oligodeoxynucleotide labeling buffer (250 nM Tris-HCl pH 8.0; 25 mM MgCl<sub>2</sub>; 5 mM  $\beta$ -mercaptoethanol; 2.0 mM dCTP; 2.0 mM dATP; 2.0 mM dGTP; 2.0 mM dTTP; 1 M HEPES pH 6.6 and 1 mg.ml<sup>-1</sup> oligonucleotides), 5  $\mu$ l  $\alpha$ <sup>32</sup>P-dCTP(3000 Ci.mmol<sup>-1</sup>; 10 Ci. $\mu$ l<sup>-1</sup>) and 1  $\mu$ l of Klenow enzyme (2.0 units. $\mu$ l<sup>-1</sup>). The probe was labeled for 2 hours at 37°C before removal of incorporated nucleotides using a NAP-5 column (Pharmacia Biotech). The reaction mixture was diluted to a final volume of 400  $\mu$ l with TE (pH 8.0) and loaded onto an equilibrated column. The sample was eluted in 600  $\mu$ l of TE and denatured by boiling for 5 minutes.

#### 2.4.3.2 RESTRICTION OF GENOMIC DNA, SEPARATION OF DNA FRAGMENTS, SOUTHERN BLOTTING AND HYBRIDISATION

The Southern blot analysis was carried out both by myself and Dr Markus Schneider (University of Edinburgh, UK), under the close supervision of Dr Yuri Kotelevtsev (University of Edinburgh, UK). Approximately 10  $\mu$ g of genomic DNA were digested overnight at -20°C with 20 units of restriction enzyme (EcoRI). Reactions were terminated by heat inactivation of the enzyme at 65°C for 15 minutes. The entire sample was loaded on a 1% agarose gel and DNA fragments separated by electrophoresis. A photograph of the gel was taken alongside a transparent ruler. The DNA fragments were transferred by capillary action onto a positively charged nylon membrane (Boehringer Mannheim, Germany). Capillary transfer was performed by a rapid alkaline (0.4 M NaOH, 1 M NaCl) transfer procedure as described previously (Chomczynski *et al.*, 1984; Reed *et al.*, 1985). Nylon membranes were then neutralised with 2 x SSC (3 M NaCl, 0.3 M trisodium citrate, pH 7.4) for 15 minutes and DNA fixed to the membrane by ultra-violet cross-linking at 254 nm followed by baking at 80°C for 40 minutes. Membranes were washed in 25 ml of pre-hybridisation solution (0.25 M Na<sub>2</sub>HPO<sub>4</sub> [pH7.2], 7% [w/v] SDS, 1.0 mM EDTA and

50 – 200  $\mu\text{g}.\text{ml}^{-1}$  of sheared and denatured salmon sperm DNA) in a pre-warmed hybridisation bottle at 68°C for 1 hour. The bottle was continuously rotated using a Techne hybridisation oven (Techne (Cambridge) Ltd, Cambridge, UK). This first wash was discarded and replaced with a further 25 ml of pre-hybridisation solution pre-warmed to 68°C, containing the heat denatured radiolabelled probe ( $1 \times 10^6$  -  $2.5 \times 10^5$  cpm.ml<sup>-1</sup>).

Membranes were washed for 16 hours by continuous rotation at 68°C before the hybridisation solution was discarded. Membranes were then washed twice, each for 10 minutes, in 25 ml of washing solution A (20 mM Na<sub>2</sub>HPO<sub>4</sub> [pH7.2], 1.0 mM EDTA [pH 8.0], 5% (w/v) SDS) followed by a further 2 washes of 10 minutes in washing solution B (20 mM Na<sub>2</sub>HPO<sub>4</sub> [pH7.2], 1.0 mM EDTA [pH 8.0], 1% (w/v) SDS). When dry, the membranes were covered in Saran Wrap and placed in an autoradiography cassette with 2 enhancement screens and Kodak X-Omat film. Autoradiographs were exposed for a minimum of 16 hrs at -70°C prior to development.

## **2.5 EC specific Cre expression in Tie2-Cre mice**

### **2.5.1 LacZ staining and histology**

LacZ gene expression can be visualised by the formation of a blue precipitate resulting from the hydrolysis of substrate 5-bromo-4-chloro-indolyl-B-D-galactosidase (X-gal) (Pearson *et al.*, 1961). X-gal can therefore be utilised to analyse  $\beta$ -galactosidase activity in tissues from transgenic animals (Fire, 1992).

### **2.5.2 Staining for $\beta$ -galactosidase activity**

Mice were asphyxiated with CO<sub>2</sub> and organs perfused via the heart with 15 ml of PBS (phosphate buffered saline) (pH 7.4) followed by 15 ml of 0.2% glutaraldehyde solution (5 mM EGTA, 100 mM MgCl<sub>2</sub>, 0.1 M NaPO<sub>4</sub>, 0.2% glutaraldehyde in PBS). Kidneys were removed and fixed in glutaraldehyde solution for 2 hours at 4°C, equilibrated with 15% sucrose for 4 hours and then in 30% sucrose overnight. The tissue was then frozen in liquid nitrogen and stored at -70°C. Prior to sectioning, the

kidneys were left for at least 30 minutes in the cryostat (Model OFT, Bright Instrument Company Ltd., Huntingdon, Cambridgeshire, UK) to allow the specimens to reach the chamber temperature of  $-20^{\circ}\text{C}$ . After mounting onto a sectioning chuck with 'cryo-M-bed' embedding compound (Bright Instrument Company Ltd., Huntingdon, Cambridgeshire, UK),  $10\text{ }\mu\text{m}$  sections were cut in the sagittal plane. The sections were thaw-mounted onto Superfrost Plus slides (VWR International).

For staining, the sections were briefly rinsed in PBS (pH 7.4) before being transferred to X-gal solution ( $1\text{ mg.ml}^{-1}$  X-gal [from stock solution of  $25\text{ mg.ml}^{-1}$  in DMSO];  $4\text{ mM}$  potassium ferricyanide ( $\text{K}_6[\text{CN}]_{12}\text{Fe}$ );  $4\text{ mM}$  potassium ferrocyanide ( $\text{K}_4\text{Fe}[\text{CN}]_6 \cdot 3\text{H}_2\text{O}$ );  $2\text{ mM}$   $\text{MgCl}_2$ ;  $0.02\%$  (v/v) Igepal Ca-630 prepared in PBS pH 7.4). Tissues were stained overnight at  $37^{\circ}\text{C}$ . Following a final rinse in PBS for 20 minutes, the sections were counterstained with eosin to allow visualisation of the individual cells. This involved immersion of the slides in eosin for 3 minutes followed by washing in tap water for 20 – 60 seconds.

### **2.5.3 Immunohistological staining of ECs**

Following quenching of endogenous peroxidase activity, sections were blocked with  $1\%$  BSA and avidin/biotin blocking reagents (Vector Labs, UK). Sections were then exposed to biotinylated rabbit-anti-mouse CD31 primary antibodies (BD Pharmingen; 553371, 1:100) at  $4^{\circ}\text{C}$  overnight. Bound primary antibodies were conjugated to streptavidin-biotin peroxidase (Vector Labs, UK) (1:200 dilution) and stained with DAB (Vector Labs, UK). In control sections the primary antibody was substituted for  $1\%$  BSA. Following my unsuccessful initial attempts at satisfactory LacZ and EC immunohistological staining, the results presented here were produced in further studies performed in our laboratory by Danielle Armour (University of Edinburgh).

#### **2.5.4 GFP reporter mice**

WW/Tie2 mice were mated with enhanced green fluorescent peptide (EGFP) reporter mice (kind gift of Dr Alexander Medvinsky, University of Edinburgh, UK) (Gilchrist *et al.*, 2003).

The embryos were harvested at day 11, fixed in 4% paraformaldehyde (PFA)/PBS for 60 min at 4°C. They were then washed several times in PBS. The embryos were analysed on day of isolation. Whole embryos were screened for expression of EGFP under an MZ FLIII fluorescent dissecting microscope (Leica).

### **2.6 Expression studies in EC ET<sub>B</sub> down-regulated mice**

#### **2.6.1 Quantitative autoradiography**

Following euthanasia by CO<sub>2</sub> asphyxiation, mice were rapidly frozen at -70°C. The torsos were mounted in a cryostat and consecutive 30 µm thick longitudinal sections were cut at a plane to encompass the heart. Sections were then thaw mounting onto gelatin-coated slides. These were prepared by washing the slides in a detergent solution, rinsing them in deionised water, before dipping them into a gelatin solution (5 g gelatin, 0.25 g chromium potassium sulphate, dissolved by heating to 45°C in 500 ml deionised water) air drying and then storing at room temperature (Davenport *et al.*, 2002). Ligand binding assays were carried out by incubating consecutive sections with 0.25 nmol of the ET<sub>B</sub> selective ligand, [<sup>125</sup>I]-BQ-3020 (K<sub>D</sub> ~ 0.1nM (Molenaar *et al.*, 1992)) or with 0.25 nmol of the ET<sub>A</sub>-selective ligand [<sup>125</sup>I]-PD-151242 (K<sub>D</sub> ~ 0.1nM (Davenport *et al.*, 1994)) (Amersham Bioscience, GE Healthcare, UK) for 2 hours at room temperature. Non-specific binding was determined by co-incubating adjacent sections in the presence of the ligand and an excess of corresponding unlabelled peptide. Slides with calibrated standards were exposed to Kodak MR-1 autoradiography film for four days before being developed.

### **2.6.2 Image analysis**

Autoradiograms were analysed by measuring the diffuse integrated OD using a computer-assisted image analysis system (Quantimet 970, Leica, Milton Keynes, U.K.) equipped with a shading corrector (with the correction performed in real time before each scan) compensating for any variation in illumination. The white level (100% transmission) was set and the scanner dark current (the current flowing in the scanner in the absence of a signal), which would otherwise contribute to the grey image, is eliminated.

The density of ET<sub>A</sub> or ET<sub>B</sub> receptors was measured by digitising each autoradiographical image of the mouse torsos into an array of 630 000 image points each with a grey value in the range 0-255. A measuring box was used to measure the integrated OD within discrete anatomical regions. Within individual organs, regions rich in ECs, such as lung parenchyma, renal medulla and liver sinusoids, were compared with more EC deplete anatomical regions such as lung briochioles and liver sinusoids. When all measurements had been made for a particular section, the threshold for detecting the autoradiogram was increased to produce a template that was used to align the autoradiographical image of an adjacent section used to define the non-specific binding. The second image was digitally subtracted from the first to measure the amount of specific binding. The resulting ODs were converted to the amount of specifically bound radioligand in amol.mm<sup>-2</sup> by interpolation from the <sup>125</sup>I standards curve. Corrections were made for decay of the radioligand from the time at which these measurements were made to the midpoint between apposing and developing the film. The inter-assay coefficients of variation was <3%.

### **2.6.3 Semi quantitative RT-PCR of the ET system**

#### **2.6.3.1 GENERAL LABORATORY PRACTICE**

All work was performed using RNase-free techniques to prevent contamination of environmental RNases. Gloves were worn at all times and work surfaces and equipment were regularly and thoroughly cleaned with RNaseZap solution (Ambion, Huntingdon, Cambridgeshire, UK). All solutions were made using 0.1%

DEPC distilled water (0.1% w/v diethyl diethylpyrocarbonate, shaken vigorously, left to stand overnight, before autoclaving to destroy the DEPC; Sigma-Aldrich, Poole, Dorset, UK). At all times, samples were kept on ice to minimise any degradation.

#### 2.6.3.2 RNA EXTRACTION

Following CO<sub>2</sub> euthanasia, kidneys were harvested from mice and frozen at -70°C. Total mRNA was isolated from mouse kidneys using a modified version of the acid guanidinium thiocyanate-phenol-chloroform method previously described (Chomczynski *et al.*, 1987). Each sample (~150 mg) was removed from the freezer (-80 °C), weighed and cut into halves, and immersed in 3 ml of denaturing solution (4 M guanidinium thiocyanate; 25 mM sodium citrate; 0.5% sarcosyl; 0.1 M β-mercaptoethanol; all dissolved in DEPC H<sub>2</sub>O) where it was homogenised at room temperature (Ultra-Turrax T8 Rotor-Stator homogeniser) before being disrupted by being drawn through a green (21 Gauge) then an orange needle (25 Gauge). An equal volume of water-saturated phenol (Fisher Scientific, Loughborough, UK) was then added, followed by 50 µl per ml of RNA solution (150 µl total) of 2 M sodium acetate (pH 4). The homogenate was then mixed thoroughly by inversion and the addition of 100 µl per ml (300 µl total) of chloroform: isoamyl alcohol (24:1) produced the final suspension which was shaken vigorously for 15 seconds and left on ice for 15 minutes. Subsequently, the samples were centrifuged at 10 000 G for 15 minutes and the upper aqueous phase, containing the RNA, was pipetted off into a fresh microfuge tube. Care was taken not to disturb the interphase and phenol phase, containing the DNA and protein residue. An equal volume of isopropanol (500 µl) was added to the lysate and the contents were mixed by inversion before being placed at -20 °C for at least 1 hour to precipitate the RNA. The samples were then centrifuged (micromax RF, IEC) at 10 000 G at 4 °C for 10 minutes to pellet the RNA. The supernatant was removed and the pellet washed twice with 1 ml of 75% ethanol. The pellets were then air dried at room temperature, before being dissolved in 30 µl of DEPC H<sub>2</sub>O at 60 °C and stored at -20 °C.

#### 2.6.3.3 RNA QUANTIFICATION AND INTEGRITY

The concentration of total RNA was determined by measuring OD<sub>260</sub> (Bio-Rad SmartSpec 3000 Spectrophotometer, Bio-Rad UK) (see section 2.3.3). RNA samples were diluted 100-fold with DEPC H<sub>2</sub>O and placed in an RNase-free quartz cuvette (200 µl, UV transparent cuvette, Bio-Rad UK). The spectrophotometer calculated the concentration of RNA in each sample and values of total RNA yield (µg.µl<sup>-1</sup>) were obtained by adjusting for the dilution factor. The purity of the RNA in each sample was determined by measuring the ratio between the absorbance values at 260 and 280 nm.

A denaturing agarose gel (1.2%) was used to verify the integrity of the RNA extracted. This was made using 0.6g of agarose, 5ml of 10x FA gel buffer (200 mM 3-[N-morpholino]propanesulfonic acid (MOPS) (free acid), 50 mM sodium acetate, 10 mM EDTA [pH to 7.0]) and 45 ml of DEPC H<sub>2</sub>O. Subsequently, 0.9ml of 37% formaldehyde (Sigma) and 0.5 µl of ethidium bromide were mixed to the melted agarose solution. The gel was allowed to equilibrate in 1x FA gel running buffer (100 ml of 10x FA gel buffer, 20 ml formaldehyde (37%) and 880 ml DEPC H<sub>2</sub>O) for 30 minutes prior to running the gel. Three µl of 5x loading buffer (16 µl saturated aqueous bromophenol blue solution, 80 µl 0.5 M EDTA [pH 8.0], 720 µl formaldehyde [37%], 2 ml glycerol [100%], 3.08 ml formamide, 4 ml 10x FA gel buffer and DEPC H<sub>2</sub>O to 10 ml) was added to 12µl of RNA sample and this mixture was heated at 65°C for 3-5 minutes, chilled on ice, and then 10µl were loaded onto the gel. The gel was run (5-7 V/cm) and the integrity of the RNA assessed by the presence of well-defined bands corresponding to 28S (4.7 kbp) and 18S (1.9 kbp) ribosomal RNA.

#### 2.6.4 RT-PCR

The reverse transcription was performed using 6 µg of RNA, with 50 pM random hexanucleotides (Promega) and 200 U Moloney-murine leukaemia virus reverse transcriptase (M-MLV RT, Promega), 0.5 mM dNTPs and 5x RT buffer (final concentration; 50 mM Tris-HCl, pH 8.3; 75mM KCl; 3mM MgCl<sub>2</sub>) in 58 µl. The

reaction was performed at 37°C for 45 minutes, then at 95°C for 5 minutes to denature the reverse transcriptase (PTC-200 Peltier thermal cycler, MJ Research Inc, USA).

Specific primers for the PCR step were designed, using GeneJockey II software (Biosoft, Cambridge, UK), for ET<sub>A</sub>, ET<sub>B</sub> and ECE-1 and were synthesised by MWG-Biotech (<http://www.mwg-biotech.com>). These primers were designed to span introns of the genes concerned to avoid false positive results arising from amplification of any contaminating genomic DNA. Primer optimisation was carried out for each gene by empirical adjustment of annealing temperature, magnesium concentration, dNTP concentration and cycle number. Once the optimal conditions had been determined, a control sample of cDNA was serially diluted, and the PCR for each component of the ET system performed. By plotting the OD of the PCR products against the dilution factor, the semiquantitative nature of the PCR was confirmed. The primer sequences, their sizes and their specific PCR conditions are summarised in Table 3-2.

PCR was then performed for each component of the ET system using cDNA prepared from mouse kidneys. Each PCR contained 1µl of cDNA, 5U Taq DNA polymerase (Promega), 200/300 µM dNTPs, 100 pM specific primers (MWG-Biotech), 10x PCR buffer (final concentration, 10 mM Tris-HCl, pH 9, 50 mM KCl and 0.1% triton, Promega) and MgCl<sub>2</sub> at a concentration specific to each primer (Table 3-2). Samples were placed in the thermocycler and the DNA was denatured for 4 minutes at 94°C. Subsequently, n cycles (Table 3-2) of amplification were performed, denaturation (1 min at 94°C), annealing (1 min at T<sub>A</sub> [specific temperature - Table 3-2) and elongation (2 mins at 72°C). After the last cycle, the 72°C elongation step was extended to 10 minutes.

#### **2.6.5 Agarose gel electrophoresis and densitometry**

The PCR products were run on a 2% agarose gel as described in section 2.3.4. Using a computer base image analysis system (SynGene software, GeneTools – File



version: 3.06.02, SynGene Laboratories), the OD of each band on the gel was measured, relative to the 500 bp marker of the 100 bp sizing ladder (Helena Biosciences Eurpoe, Sunderland, UK). Final expression values of gene of interest relative to that of glyceraldehyde-3-phosphate dehydrogenase (GAPDH) were calculated to control for the variable efficiency of the reverse transcriptase step.

## **2.7 BP measurement in unconscious animals**

Mean arterial blood pressure (MABP) was measured by direct cannulation of the left common carotid artery in adult male mice (8 – 12 weeks old; 25 - 35g) as previously described by Davisson and colleagues (Davisson *et al.*, 1998). Anaesthesia was induced with 5% isoflurane and maintained with 1.0 – 1.5% isoflurane (Merial Animal Health, Harlow, Essex) using a standard small animal Boyle's Machine anaesthetic apparatus with high flow oxygen. A small murine anaesthetic nose cone was used (VetTech Solutions Ltd, Congleton, Cheshire) to allow improved access to the cervical area of the mouse. The left common carotid artery was exposed and tied off distally, with care taken to prevent damage to the overlying submandibular salivary glands. The proximal end of the artery was briefly occluded to allow the vessel to be cannulated with a saline-filled Micro-Renathane® tubing catheter (MRE-040; 0.040 inches [= 1016  $\mu$ m] O.D. x 0.025 inches [= 635  $\mu$ m] I.D.; Braintree Laboratories Inc., MA, USA). Once inserted, the catheter was secured in place with sutures. Measurements were performed in a quiet procedure room of the MFAA (Medical Faculty Animal Area) Facility (University of Edinburgh, UK) where the temperature was 21 – 23°C. Anaesthesia was maintained at the lowest level possible (1-3 % isoflurane) so that the animal gave no response to painful stimuli (such as paw pinching) yet had a respiratory rate greater than 90 respirations/minute. Following cannulation of the carotid artery, the preparation was allowed to stabilise for 5 minutes before the MABP was recorded over a 10-minute period.

Some of the experimental protocols required venous access. For these experiments the right external jugular vein was exposed by careful dissection. The proximal end was occluded with a loose ligature, before the distal end was ligated. The vessel was

then cannulated with a saline filled catheter (MR-025; 0.025 inches [= 635  $\mu$ m] O.D. x 0.012 inches [= 305  $\mu$ m] I.D., Braintree Scientific, Inc, MA, USA), and secured with sutures, before the loose proximal ligature was released.

Catheters were produced in house by stretching the tip of a length of Micro-Renathane® tubing in hot sesame oil as recommended in the manufacturers' instructions (Sherer *et al.*, 1995). Catheters were filled with heparinised 0.9% saline (100 IU.ml<sup>-1</sup>) (Multiparin, CP Pharmaceuticals Ltd, Wrexham, UK), to minimise the risk of clot formation at the catheter tip. Catheter patency and position within the lumen of the artery was verified by observing pulsatile flow within the Micro-Renathane® tubing. BP measurements were performed after a period of stabilisation at a steady level of anaesthesia (respiratory rates maintained between 90 and 120 breaths.min<sup>-1</sup>). The catheter was connected via a MLT844 transducer (ADInstruments Ltd, Chalgrove, Oxfordshire, UK) to a PowerLab/4SP data acquisition system (Model No. ML750; ADInstruments Ltd) and displayed on a Powerbook G4 Laptop (Apple MacIntosh) using Chart 5.1 software (ADInstruments Ltd). The BP trace was recorded at 100 samples/ second. System damping, due to the long length of tubing required to connect to the transducer, resulted in a low pulse pressure, preventing the measurement of true systolic and diastolic BP. Thus MABP only was calculated from the traces obtained.

## **2.8 BP measurement in conscious animals**

### **2.8.1 Salt diet**

During initial studies, mice were fed either 0.8% NaCl or 8% NaCl powdered diet (Special Diet Service, Sussex, UK) offered in small glass hoppers. Mice were weighed weekly and given access to tap water *ad libitum*. However as the animals dispersed the powder both throughout the cage as well as all over themselves, it was impossible to determine their food consumption.

Therefore, for the telemetry studies, gel diet of varying salt content was made up following a similar method to that described by Ahn and colleagues (Ahn *et al.*,

2004). The mice did not disperse this gel diet around the cage. One hundred grams of diet consisted of 36 g of powder diet (Special Diet Service, Sussex, UK); 60.2 ml of distilled water; 3.8 g of beef gelatin (SuperCook, Sherburn-in-Elmet, Leeds, UK) and a varying amount of NaCl (Sigma-Aldrich, Gillingham, Dorset, UK) to give a final concentration of either 0.08%, 0.8%, 2.5% or 8% NaCl gel diet. The powder was mixed with NaCl, before boiling water was added and beef gelatin mixed in. The mixture was ladled into ice cube trays (J Sainsburys, Edinburgh, UK) and frozen at  $-20^{\circ}\text{C}$  until at least 45 minutes before use. Each cube weighed  $\sim 15$  g and therefore 1 cube/ day provided the mice (max weight 35 g) with adequate food intake (daily mouse powdered food requirements = 15g/ 100gms/ day (Baumans, 1999)). The animals were given access to either water or normal saline (0.9% NaCl) *ad libitum*. Mice, as well their water and gel consumption, were weighed daily whilst on the gel diet.

During certain phases of the experimental protocol selective ET antagonists were administered orally to the animals. Having determined the minimum daily gel consumption, and weight of each mouse, enough powdered ABT627 ( $\text{ET}_A$  antagonist) or A192621 ( $\text{ET}_B$  antagonist) was added to the food mix to ensure minimum doses of  $5 \text{ mg.kg}^{-1}$  and  $30 \text{ mg.kg}^{-1}$  respectively. These doses are known to exert maximum selective ET receptor blockade in rodents as discussed with Dr David Pollock (Medical College of Georgia, Alberta, USA) (Pollock *et al.*, 2001) and further demonstrated by my clearance studies (see section 5.3.4). The ABT627 and A192621 were kind donations from Abbott Pharmaceuticals (IL, USA).

### **2.8.2 Indwelling carotid artery catheters**

Aseptic techniques were used for all recovery surgical procedures. The procedure for cannulation of the left common carotid was followed as outlined above (section 2.7). Once the tapered tip of the catheter was located into the artery, it was secured in place with sutures and tissue glue (VetBond<sup>TM</sup> Tissue Adhesive, 3M<sup>TM</sup>, Bracknell, UK). The other end was tunnelled beneath the skin using a large bore trochar needle, to emerge in the inter-scapula area. Here it was secured, using VetBond tissue glue,

within a short (5 mm) section of more rigid supportive tubing, cut from a 4 French Portex<sup>TM</sup> catheter (Harvard Apparatus, Ltd, Edenbridge, UK), which was in turn fastened to the skin with glue. This stiffer tubing formed a “chimney” around the Micro-Renathane® tubing, making a firm attachment where the catheter left the skin. After flushing with heparinised hyperosmotic (10%) saline (see below) the catheter was sealed with a section of blunted dress-making pin (John-Lewis, UK).

Micro-Renathane® tubing has a small but finite permeability to water, which allows water to move across the wall of the tubing in the setting of a hydrostatic pressure gradient. Thus when a Micro-Renathane® catheter is inserted into the lumen of a high pressure vessel, such as a carotid artery, water will be lost from the catheter lumen, allowing a small amount of blood to enter the lumen. This is likely to clot and therefore block the catheter. To reduce the risk of this occurring, catheters were soaked in sterile saline for 24 hours prior to implantation and filled (between BP measurements) with hyper-osmotic solutions (10% saline - see above) to counteract hydrostatic gradients, as per the manufacturers’ instructions (Sherer *et al.*, 1995).

Post operatively the mice were given subcutaneous buprenorphine (0.3mg.ml<sup>-1</sup>) (Alstoe Animal Health, Melton Mowbray, Leicestershire, UK), 0.9% saline (0.5 – 1.0 ml/mouse) and warmed on a thermostatically controlled heat pad in singly housed cages until fully ambulant. Twenty-four hours post procedure, the mice were gently but firmly restrained, the dress-maker pin removed and the catheter flushed with heparinised saline. Forty-eight hours post-operation, the mice were again restrained, the dress-pin removed, and after flushing, the catheter was connected to the ADInstruments transducer (sample rate: 100/second) by means of a 20 cm length of saline-filled MicroRenathane® tubing to allow measurement of BP. The mice were returned to their cages, and after 30 minutes of acclimatisation, the BP was recorded for 30 minutes. Measurements were taken under unrestrained conscious conditions, in a quiet temperature controlled room (21 – 23°C) within the MFAA Facility (University of Edinburgh, UK). The heart rate was determined from analysis of the arterial BP trace. The mice were then culled by cervical dislocation.

### **2.8.3 Surgical implantation of telemetry devices**

In the 7 days prior to radiotelemetry device insertion, the mice were fed normal salt (0.76% NaCl) gel diet and housed in single cages to allow them to fully habituate to these changes in their environment before surgery. Each mouse was then anaesthetised with 6.7 ml.kg<sup>-1</sup> IP of a mixture of ketamine (100mg.ml<sup>-1</sup>) (Pfizer, Sandwich, UK) and metomidine (1mg.ml<sup>-1</sup>) (Pfizer, Sandwich, UK) to allow surgical implantation of BP telemetry transmitter devices (PA-C20; Data Science International Inc, St. Paul, MN, USA) using a similar protocol as that used for catheter insertion (section 2.7). In brief, the left common carotid artery was exposed and tied off distally. The proximal end of the artery was briefly occluded to allow the vessel to be cannulated with the transmitter catheter. Once inserted, the catheter was secured in place with sutures and VetBond<sup>TM</sup> tissue glue. The fidelity of the signal from the transmitter was checked with an FM radio – a fluctuating signal indicating pulsatile blood flow at the catheter tip. Once the catheter had been inserted a subcutaneous pocket was fashioned using blunt dissection down into the left hypochondrium of the mouse's abdomen. The body of the transmitter was carefully inserted into this pocket before the skin was closed with interrupted sutures. All telemetry surgery was performed by Mr Peter Hodgson (BHF Technician, University of Edinburgh, UK).

Post operatively the animals were treated with subcutaneous saline and buprenorphine (0.3mg.ml<sup>-1</sup>) (Alstoe Animal Health, Leicester) before being given atipamazole (25 mg.kg<sup>-1</sup>) (Pfizer, Sandwich, Kent) to reverse the effects of the anaesthetic. Until fully conscious and ambulant the mice were warmed at 35°C in a thermostatically controlled recovery chamber (VetTech Solutions Ltd, Congleton, Cheshire). The mice were housed singly in a specially adapted rack to allow signals from the telemetry devices to be recorded as required. The telemeter signals were processed using the following D.S.I. equipment: RLA1020 receiving pads, a 20 channel data exchange matrix, an APR-1 ambient pressure monitor and a DataQuest ART Silver 2.1 acquisition system. This arrangement allowed a carotid BP signal to

be recorded for 10 seconds on each hour for the duration of the study (200 samples/sec). BP data were excluded if the trace was clearly artefactual and not pulsatile. The undamped signal recorded with the radiotelemetry system allowed for SBP, DBP, MBP and HR to be determined. As in similar radiotelemetry work (Paterson *et al.*, 2004), the 6 hour rolling average was calculated for each of these parameters for each individual animal to reduce signal noise (e.g. value at 0900hr was the average of BP from 0600hr to 1100hr; the value at 1000hr was the average from 0700hr to 1200hr). Using these rolling averages, data was compared between genotypes in three different ways:

- i) **‘Last 72hrs’**: the average of all values for the last 3 days of each treatment period.
- ii) **‘Day’**: the average for values at 1100hr, 1200hr and 1300hr on the last 3 days of each treatment period. As mice are nocturnal this appeared to correspond to the period of minimal activity in their circadian rhythm.
- iii) **‘Night’**: the average for values at 2300hr, 2400hr and 0100hr on the last 3 days of each treatment period. This period appeared to correspond with maximal activity in the circadian rhythm.

The mice, their water bottles and diet were weighed daily.

At the completion of the study, the mice were culled by cervical dislocation, and blood was collected by direct cardiac puncture for haematocrit measurement.

#### **2.8.4 Haematocrit measurements**

Whole blood was transported as swiftly as possible on ice from the Animal Unit to the laboratory. Capillary tubes (Micro-Haematocrit Tubes, Hawksley and Sons Ltd., Sussex, England) were filled with blood before being spun for 5 minutes at 160G (Centurion Centrifuge, DJB Labcare, Buckinghamshire, UK). The haematocrit was determined by reading the percentage of erythrocyte sedimentation, within the plasma, using a Hawksley micro-haematocrit reader.

## **2.9 ET-1 clearance studies**

### **2.9.1 Measurement of plasma ET-1 and big ET-1 concentrations**

The low plasma concentration of ET-1 and big ET-1 prevents direct measurement by radioimmunoassay (RIA). Both peptides were therefore extracted from the plasma using the previously described acetic acid extraction (Rolinski *et al.*, 1994). Briefly, 1 ml of mouse plasma (pooled from 2 individual animals of identical genotype/experimental group) was mixed with 1 ml 20% acetic acid and applied to a Varian C18 Bond Elut column (Varian Inc., Lexington, USA). Columns were washed with 10% acetic acid and ethyl acetate. ET-1/ big ET-1 was eluted in 1.5 ml of elution buffer (1 volume 0.05 M  $\text{NH}_4\text{HCO}_3$ : 4 volumes methanol) and the sample concentrated by evaporating to dryness under nitrogen followed by resuspension in 100  $\mu\text{l}$  of RIA buffer (3.85 g  $\text{NaH}_2\text{PO}_4$ ; 18.1 g  $\text{Na}_2\text{HPO}_4$ ; 2.93g  $\text{NaCl}$ ; 1 g BSA; 1ml Triton X-100 and 100 mg sodium azide in 100 ml deionised  $\text{H}_2\text{O}$ ; pH 7.4). RIA was performed on the concentrated sample using a Peninsula Laboratory kit for determination of plasma ET-1/big ET-1 (Peninsula Europe Laboratories Ltd., St Helens, UK). Either 100  $\mu\text{l}$  of standard, sample or control was incubated for 4 hours with either rabbit anti-mouse ET-1 or rabbit anti-mouse big ET-1 antibody. A known concentration of either [ $^{125}\text{I}$ ]-ET-1 or big [ $^{125}\text{I}$ ]-ET-1 was then added and the tubes incubated for a further 16 hours. On day 2, the immune complexes were precipitated with Amerlex<sup>TM</sup> donkey anti-rabbit antibody. The precipitates were counted in a gamma counter, a standard curve constructed and the unknown values read from the curve. All measurements of plasma ET-1 and big ET-1 concentration were performed by Neil Johnston (Clinical Pharmacology Unit, University of Edinburgh, UK).

### **2.9.2 Clearance studies**

Mice were housed individually and fed either standard powdered chow (0.8%  $\text{NaCl}$ ) or chow mixed with the orally active  $\text{ET}_\text{B}$  antagonist A192621 (Abbott, IL, USA) (von Geldern *et al.*, 1999) to give a dose of either  $30\text{mg}\cdot\text{kg}^{-1}\cdot\text{day}^{-1}$  or  $100\text{mg}\cdot\text{kg}^{-1}\cdot\text{day}^{-1}$ , for the 7 days preceding surgery, as performed in previous studies

(Pollock *et al.*, 2001). Animals were weighed daily to ensure adequate nutrition. Under isoflurane anaesthesia, the right internal jugular and left common carotid artery were cannulated with Micro-Renathane® tubing (MR-025 ID, Braintree Scientific, Inc, MA, USA) as outlined above (see section 2.7). Following an intravenous bolus of radiolabelled [ $^{125}$ I]-ET-1 (0.37 pmol/mouse; 28 kBq/mouse [Amersham Bioscience, GE Healthcare]), drops ( $\sim 10 \mu\text{l}$ ) of arterial blood were collected over the subsequent 120 seconds as previously described (Berthiaume *et al.*, 2000). The length of the arterial line was minimised, to limit the dead-space of the system ( $\sim 10\text{-}15 \mu\text{l}$ ) as much as possible. The activity of these samples was measured using a gamma scintillation counter.

All carcasses of animals used in this study were disposed off in accordance with the University of Edinburgh Hazardous and Radioactive Substances Policy.

The results were analysed and processed with the assistance of Dr Ruth Andrew (University of Edinburgh) using the Kinetica (version 4.2) software program (Thermo Electron Corporation, <http://www.thermo.com/>).

## **2.10 Pulmonary Arterial Hypertension Study**

### **2.10.1 Hypobaric chamber**

Mice were exposed to hypoxic conditions, by housing them in a specially designed hypobaric chamber. This was depressurised over the course of 2 days to 550 mbar (55 kPa or 413 mmHg [equivalent to  $\text{FiO}_2$  (percentage oxygen in inspired air) = 10%]). Temperature was maintained at 21 to 22°C, and the chamber was ventilated with air at  $\sim 45 \text{ l}\cdot\text{min}^{-1}$ . At the end of each week, the chamber was repressurised back to atmospheric pressure over 1 hour. The bedding, diet and water were then changed and replenished, before the chamber was again depressurised over 1 hour back to 550 mbar. The duration of hypoxia was 14 days. Aged-matched control mice were maintained in room air under atmospheric pressure ( $\text{FiO}_2 = 21\%$ ) in the same room that contained the hypobaric chamber. Thus the controls were subjected to identical environmental conditions save for hypoxia.



### **2.10.2 Haemodynamic studies**

For the PAH haemodynamic studies, anaesthesia was induced with 2 - 4% halothane and maintained with 1.5% halothane using a standard small animal Boyle's Machine anaesthetic apparatus with a (1 part :3 parts) mix of NO<sub>2</sub> and high flow O<sub>2</sub>. The left carotid artery was cannulated in a similar method to that described above (section 2.7), using a stiffer catheter (Portex 0.75 mm O.D). The catheter was connected to an Elcomatic E751A and MP100 data acquisition system (BioPac Systems Inc, Santa Barbara, California, USA) to give systemic pressure readings (sample rate: 100/sec). Results were analysed off line using AcqKnowledge software package (version 3.5).

A 25-gauge needle, mounted in a stereotactic retort stand with micrometer gauge advance, was inserted into the RV using a transdiaphragmatic approach for measurement of RV pressure (RVP). The skin was removed from the thorax and upper abdomen of the mouse, and the needle orientated in the long axis of the animal, just to the right of the xiphisternum. The RVP needle was connected to a separate channel of the MP100 data acquisition system (sample rate: 100/sec). By comparing the trace from this needle with the systemic pressure trace (carotid catheter) it was possible to determine when the diaphragm had been crossed (negative pressure) before the RV was punctured (RVP systolic pressure < systemic systolic pressure; diastolic pressure ~ 0 – 4 mmHg). Systemic and RV pressures were recorded for ~10 minutes. The needle was then advanced further with the aim of recording a LV (left ventricular) trace (systolic LV pressure ~ systolic systemic carotid catheter pressure).

Once this had been achieved, the halothane anaesthesia was increased to maximum (5%) and the mouse euthanased.

The heart was removed, blotted dry of blood, and weighed. The right lung was taken for histology (fixed in formal saline (1 part of formaline 37%: 9 parts of saline 0.9% solution) and the left lung put on ice for later dissection to isolate the left PA used for wire myography.

### **2.10.3 Measurement of RV hypertrophy**

Having been rinsed in saline, hearts were dissected clean of all pericardial and thymus tissue. The atria and great vessels were removed to the plane of the atrioventricular valves. The RV free wall was dissected free from the LV together with the septum (LV + S), and blotted dry. These were weighed separately. The ratios of RV/LV + S; RV/Total Ventricles (TV); and RV/Body Weight (BW) were calculated.

### **2.10.4 Wire myography**

As the PA myography had to be performed swiftly following the euthanasia of each mouse (within 24 hours), these experiments were performed concurrently with the ongoing haemodynamic studies, by Dr Yvonne Dempsie (University of Glasgow UK). Following the culling of each mouse at the end of the haemodynamic study, the left lung was cut free from the heart and put on ice for transportation from the animal facility to the myography laboratory. Here, each PA was gently dissected from the neighbouring bronchiole and all adventitial tissue was carefully removed. Third order (first interlobar) PAs were cut to yield two 2mm long segments ( $\sim 300\ \mu\text{m}$  internal diameter). These segments were threaded onto  $40\ \mu\text{m}$  stainless steel wire and mounted on isometric wire-myographs. The mounting procedure is illustrated in Figure 2-5. Vessel rings were suspended between two intra-luminal mounting wires ( $40\ \mu\text{m}$  diameter,  $\sim 2.2\ \text{cm}$  in length) in a 10 ml myograph organ bath (Multi-myograph model 610M; JP Trading, Aarhus, Denmark). One wire was attached to the stationary support driven by a micrometer whilst the second wire was attached to an isometric force transducer. Care was taken not to damage the endothelium during the mounting procedure.

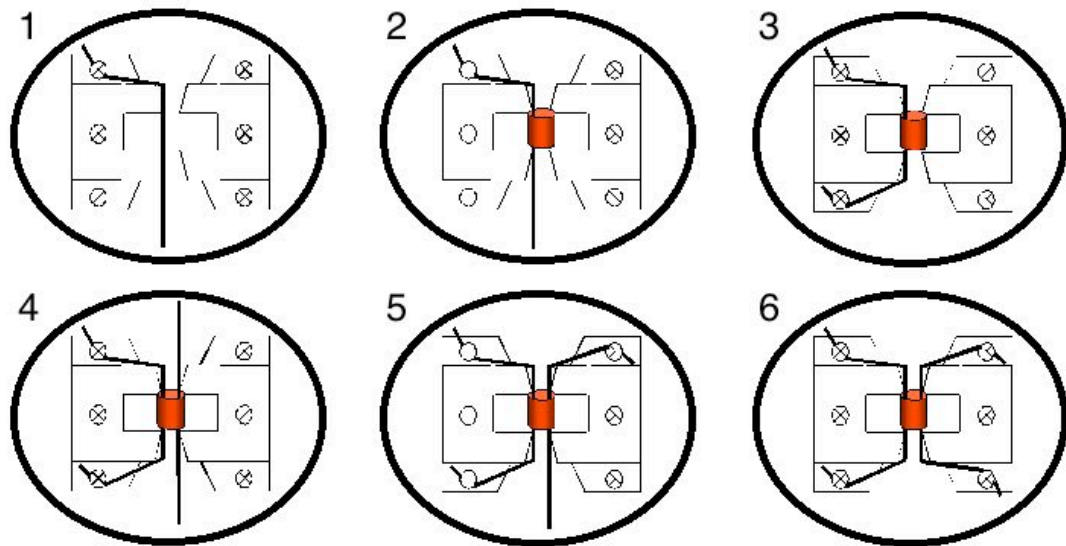


**Figure 2-5: Procedure for mounting of pulmonary artery rings onto the wire myograph**

Vessels were bathed in Krebs-buffer solution (118.4 mM NaCl; 25 mM NaHCO<sub>3</sub>; 4.7 mM KCl; 1.2 mM KH<sub>2</sub>PO<sub>4</sub>; 0.6 mM MgSO<sub>4</sub>; 2.5 mM CaCl<sub>2</sub>; 11 mM glucose; [pH 7.4]) at 37°C with a constant supply of 16% O<sub>2</sub>/5% CO<sub>2</sub>. During this normalisation period, tension was applied to give transmural pressures equivalent to those experienced by PAs *in vivo*, as originally described by Mulvany and Halpern (Mulvany *et al.*, 1977). This procedure allows vessels to be stretched to a required resting transmural pressure, based on the Laplace relationship for a cylindrical vessel:

$$P \text{ (transmural pressure)} = T \text{ (wall tension)} / R \text{ (radius of the vessel)}$$

where,

Wall tension is the force (**F**) divided by twice the vessel length (**L**):

$$\text{Wall tension} = F / 2L$$

the radius of the vessel can be calculated from the internal circumference (IC) of the PA ring. IC can be determined from the distance between the myography wires multiplied by 2 (see Figure 2-5 panel 6):

$$R = IC / 2\pi$$

therefore, rearranging substituting these values into the formula:

$$P = 2\pi \times F / 2 \times L(IC)$$

Thus by adjusting the tension on a given PA ring, and by measuring its length and internal circumference, the required transmural pressure can be generated.

PAs from normoxic mice were tensioned to an equivalent pressure of 12 to 14 mm Hg and PAs from hypoxic mice were tensioned to 30 to 33 mm Hg. These pressures are similar to those experienced by pulmonary vessels *in vivo* in rodents (Herget *et al.*, 1978; MacLean *et al.*, 2004). This contrasts with studies using systemic arteries, where the tension is usually adjusted to be equivalent to *in vivo* pressures of more than 60 mmHg (Mickleby *et al.*, 1997). As the pulmonary circulation has a high flow but a low resistance, it is more suitable for PAs to be set up under equivalent conditions to those experienced by the vessels *in vivo* (MacLean *et al.*, 1998; McCulloch *et al.*, 1996). Periodic adjustments were made to maintain this tension over the subsequent equilibration period. This tension was defined as zero for all following measurements. Signals from the myograph were processed by a MacLab/4e analogue-digital converter and displayed through Chart™ software (ADInstruments; Chalgrove, Oxfordshire, UK).

#### 2.10.4.1 PULMONARY ARTERY WAKE UP PROTOCOL

Following a 20 minute equilibration period, PA rings were contracted twice to obtain the maximum contraction to 50 mM KCl solution. KCl was washed out 5 times with Krebs-buffer solution and rings were allowed to return to baseline tension prior to further experiments. For details of the full myography protocol see section 6.2.1.

### 2.10.5 Lung histology

Right lungs, harvested at the end of the *in vivo* haemodynamic study, were dehydrated in 100% ethanol for between 5-7 days. The tissue was then embedded in paraffin wax and cut into 10  $\mu\text{m}$  sections. These were stained for collagen with Miller's Elastin Stain (Miller, 1971) and for collagen with Picro-Sirius Red (Junqueira *et al.*, 1979) according to the following protocol (all solutions and chemicals were sourced from Sigma-Aldrich, Steinheim, Germany unless otherwise stated). The sections were de-waxed by immersing in '*Tissue Clear*' (Bayer Plc, Newbury, Berkshire, UK) for 30 min, before being washed in a range of decreasingly concentrated ethanol baths (100% ethanol for 2 mins; 90% ethanol for 2 mins; 70% ethanol for 2 mins). Next, the sections were washed in running tap water for 10 mins, and then immersed in 0.5% (w/v) potassium permanganate for 5 mins. After rinsing in water the sections were put into 1% (w/v) oxalic acid for 2 – 3 minutes to decolourise them. The sections were rinsed in water, then 95% ethanol, before being immersed in Miller's Elastin stain for 3 hours.

The Miller's Elastin stain was made up prior to the staining: 1 g Victoria Blue 4R, 1 g New Fuschin, 1 g Crystal Violet were all dissolved in warmed 200 ml distilled water. Resoucin (4 g), then 1 g dextrin, then freshly prepared 30% ferric chloride was added to the mixture. After boiling for 5 minutes, the mixture was filtered whilst still hot. The precipitate plus filter paper was redissolved in 200 ml of 95% ethanol, boiled for 20 mins, the filtered and made up to 200 ml with 95% ethanol. Finally 2 ml of concentrated hydrochloric acid was added.

After washing in 95% ethanol, to remove excess stain, the sections were washed in running water and immersed in Picro-Sirius Red stain (0.5 g Sirius Red F3B in 500 ml saturated picric acid) for 1 hour. Following staining the sections were washed in 2 changes of acidified water (0.5% v/v acetic acid), and then dehydrated in 3 changes of 100% ethanol and mounted.

The sections were microscopically assessed for muscularisation of small PAs (25 to 100  $\mu\text{m}$  external diameter), associated with an airway distal to the respiratory

bronchiole. The arteries were considered muscularised if they possessed a distinct double-elastic lamina visible for at least half the diameter in the vessel cross-section. The percentage of vessels containing double-elastic lamina was calculated as number of muscularised vessels/total number of vessels counted per section x 100. Three sections from each right lung of 6 mice per group were assessed in this way. These assessments were each performed by two investigators working independently.

## **2.11 STATISTICAL ANALYSIS OF RESULTS**

Where only two data sets were compared, unpaired student's *t* tests were performed. All other data were analysed using repeated measures ANOVA with Newman-Keuls multiple comparison post-test analysis. *P*-values quoted in the text were accepted as statistically significant when  $p < 0.05$

### **3 CHAPTER 3: CHARACTERISATION OF THE MURINE MODEL OF EC-ET<sub>B</sub> DOWN-REGULATION**

#### **3.1 INTRODUCTION**

With any conditional knockout/knockdown animal, the initial step in characterising its phenotype is to determine that the targeted allele has been significantly down-regulated from the cell type of interest. I have employed a 3-stage approach to this process.

##### **3.1.1 Deletion of exons 3 and 4 prevents ET<sub>B</sub> expression**

Firstly, it was necessary to demonstrate that floxing exons 3 and 4 of the ET<sub>B</sub> gene was sufficient to knock it out in tissues expressing the bacteriophage enzyme Cre-recombinase. Other groups, using tissue specific Cre lines, have demonstrated that recombination events have been noted in the germ cells of female mice featuring a floxed allele and the Tie2-Cre transgene (Constien *et al.*, 2001; Koni *et al.*, 2001). We took advantage of this phenomenon, to organise a breeding strategy that generated mice exhibiting such germ line recombination. These mice had a piebald appearance and died at weaning from aganglionic megacolon. Genotyping later revealed them to be null ET<sub>B</sub> mice.

Analytical breeding crosses were then performed to empirically determine the rate of this germ line recombination in our colony, and to verify whether there was an increased incidence of germline recombination if the Cre transgene was expressed by the mother rather than the father.

Having demonstrated that male germline transmission resulted in substantially reduced rates of recombination, efforts were directed towards perfecting a swift and reliable method of identifying animals in which this germline recombination had occurred in one of its 2 alleles. Several different strategies were employed until a Southern Blot was successfully developed.

### 3.1.2 Tie2-Cre restricts expression of Cre recombinase to the endothelium

Second, having demonstrated that Cre mediated recombination can prevent the expression of a functional ET<sub>B</sub> receptor in floxed ET<sub>B</sub> mice, the next step was to demonstrate that, as long as the Tie2-Cre transgene is transmitted in the male germline, it restricts Cre expression to ECs. Ideally, Cre-mediated recombination occurs in both alleles of the gene of interest, resulting in complete knockout of target gene expression in the desired cell-type. Conversely, expression in all other cells should be unchanged from the wild-type pattern. Leaky or deregulated transcription of the Cre recombinase transgene will result in unwanted recombination events in other cell types. Either of these will complicate phenotype interpretation. Therefore it is necessary to determine the expression of Cre recombinase in the Tie2-Cre mice. At present, it is difficult to examine the distribution of the Cre protein directly, because no satisfactory Cre antibody has been produced which functions adequately in mouse tissues. Therefore other strategies to determine Cre expression were used. It has been shown that the expression of the indicator protein, enhanced green fluorescent protein (EGFP), under control of the Tie2 promoter, is restricted to the endothelium (Motoike *et al.*, 2000) and Tie2-*lacZ* mice demonstrate a panendothelial specific pattern of *lacZ* expression throughout embryogenesis and into adulthood (Schlaeger *et al.*, 1997). Furthermore, Tie2-Cre expression is limited to endothelial and endocardial tissue (Kisanuki *et al.*, 2001). To demonstrate that such EC-specific expression of Tie2-Cre was maintained in our colony, we crossed our Tie2-Cre mice with 2 different reporter strains: a *lacZ* Rosa26 reporter (R26R) mouse line and a GFP reporter strain.

#### 3.1.2.1 BREEDING WITH LACZ ROSA 26 REPORTER STRAIN

The tissues in which the bacteriophage enzyme Cre recombinase is expressed can be assessed using reporter mice that permit *in vivo* monitoring of Cre-mediated excision events in all tissues. Such a strain of mice was generated by the targeted insertion of a *lacZ* gene (which codes for the Escherichia coli enzyme  $\beta$ -galactosidase), preceded by a floxed strong transcriptional termination sequence (a STOP codon), into the ubiquitously expressed Rosa26 locus (R26R mice) (Mao *et al.*, 1999; Soriano, 1999).



The R26R allele terminates transcription of the *lacZ* gene prematurely, but when the mice are crossed with Cre-expressing transgenic mice, the Cre-mediated excision of the floxed termination sequence leads to constitutive *lacZ* expression. Thus, these doubly transgenic animals express *lacZ* only in the cells that express Cre. In tissues harvested from such animals, Cre expression is therefore mirrored by  $\beta$ -galactosidase activity.

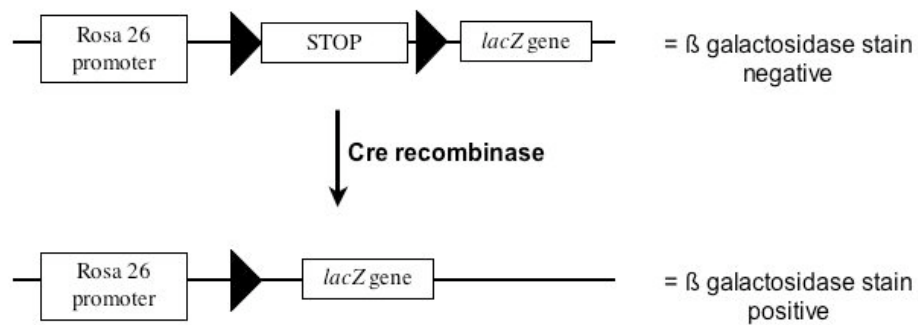


**Figure 3-1: Cre mediated recombination**

Cre mediated excision of the stop cassette results in expression of  $\beta$  galactosidase when R26R mice are crossed with mice expressing Cre in a tissue specific manner.

### 3.1.2.2 BREEDING WITH GFP REPORTER STRAIN

An alternative approach to using *lacZ* reporter mice to monitor the pattern of Cre expression within a particular mouse line, is to use a similar Cre reporter mouse that expresses EGFP in place of  $\beta$ -galactosidase. GFPs are autofluorescent proteins that can be visualised in living cells, and are therefore particularly useful for monitoring gene expression in whole embryos, animals or cultured cells and organs (Chalfie et al., 1994). The EGFP reporter mice generously supplied by Dr Alexander Medvinsky (University of Edinburgh, UK)(Gilchrist et al., 2003) contain the ubiquitously expressed phosphoglycerate kinase promoter, rather than the Rosa 26 promoter used in the *LacZ* mice.

### 3.1.3 EC-specific $ET_B$ down-regulation in FF/Tie2 mice

The third and final step was to demonstrate that in our FF/Tie2 mice, there was EC-specific  $ET_B$  down-regulation. Supporting evidence of EC specific knockdown was

provided by Dr Alan Bagnall's (University of Edinburgh, UK) work. He provided binding data in pulmonary ECs demonstrating ~82% reduction in ET<sub>B</sub> receptor mediated binding and functional wire myography studies in which aortic rings from FF/Tie2 mice demonstrated reduced endothelial dependent ET<sub>B</sub> mediated dilatation, but preserved non endothelial dependent tracheal ET<sub>B</sub> mediated constriction (Bagnall *et al.*, 2006) (see section 1.3.6).

We went on to use quantitative autoradiography to demonstrate reduced ET<sub>B</sub> expression in EC rich tissues such as the lung and renal medulla. We also used this technique to investigate the effect of EC-ET<sub>B</sub> receptor down-regulation on ET<sub>A</sub> receptor expression in different organs. Finally, semi quantitative RT-PCR was performed on kidneys from the FF/Tie2 mice to investigate the effect of EC-ET<sub>B</sub> receptor down-regulation on the gene expression of all components of the renal ET system.

#### 3.1.3.1 SEMI-QUANTITATIVE RT-PCR

Reverse transcription polymerase chain reaction (RT-PCR) is a highly sensitive method for the detection of low-abundance mRNA, obtained from small tissue samples. In RT-PCR, an RNA template is copied into a complementary DNA transcript (a cDNA) using a retroviral reverse transcriptase. The cDNA sequence of interest is then amplified exponentially using PCR. Real time PCR quantifies the amount of product at the end of each cycle, whereas end-point PCR requires optimisation of each PCR to ensure that the reaction is terminated during the exponential phase of amplification (since it is only during this phase that amplification is extremely reproducible). Such end-point RT-PCR can be used to measure changes in expression levels using either semi-quantitative, or fully quantitative competitive methods. Determination of the amount of PCR product is performed by agarose gel electrophoresis and by measuring the intensity of a fluorescent dye, such as ethidium bromide, that binds to it.

Semi-quantitative RT-PCR compares transcript abundance across multiple samples, using a co-amplified internal control, in order to normalize for differences in sample concentration and loading. Results are expressed as ratios of the gene-specific signal to the internal control signal. This yields a corrected relative value for the gene-specific product in each sample. These values may be compared between samples for an estimate of the relative expression of target RNA in the samples, eg sample 1 has 2.4-fold the ET<sub>B</sub> expression of sample 2. Ideally, the internal control should be a gene expressed at a constant level across the sample set. Commonly used internal samples are the 'housekeeping genes', glyceraldehyde-3-phosphate-dehydrogenase (GAPDH),  $\beta$ -actin mRNA, and 18S and 28S rRNAs. GAPDH was chosen for our study as it is commonly used (Carrell *et al.*, 2002; Haase *et al.*, 2002; Yalcintepe *et al.*, 2006) and the optimisation of the PCR conditions had already been established in our laboratory for RT-PCR of the ET system in the rat (Wallace, 2003; Wallace *et al.*, 2002). Although GAPDH expression has been shown to vary with age and across different organs (Oikarinen *et al.*, 1991), such effects were limited in our study as we compared gene expression in renal tissue from mice of the same age.

Fully quantitative RT-PCR, a competitive reaction, measures the absolute amount (e.g.  $5.3 \times 10^5$  copies) of a specific mRNA sequence in a sample. Dilutions of an external control, a synthetic RNA (identical in sequence, but slightly shorter than the endogenous target) are added to sample RNA replicates and are co-amplified with the endogenous target. The PCR product from the endogenous transcript is then compared to the concentration curve created by the external control, the synthetic 'competitor RNA'. The major disadvantage of this last method is that for each component of the ET system a different external control, a different synthetic RNA, must be generated. Semi-quantitative PCR, as we performed allows comparison of all ET components relative to the same internal control: GAPDH.

## 3.2 RESULTS

### 3.2.1 Genotyping of experimental animals

A representative agarose gel used to genotype mice for the floxed  $ET_B$  receptor allele is shown in Figure 3-2. Floxed/ Wild type heterozygous animals (FW/Tie2) demonstrated 3 bands: a 2241 bp band corresponding to the wild type (W) allele, a 1136 bp band amplified from the non-recombined floxed (F) allele, and a 230 bp band amplified from the recombined floxed (O) alleles present within the EC of the tail biopsy. FF/Tie2 mice exhibited bands of 1136 and 230 bp (F and O bands), whilst FF/-- mice exhibited only the 1136 bp band. A single 2241 bp band was amplified from the WW/-- and WW/Tie2 mice.

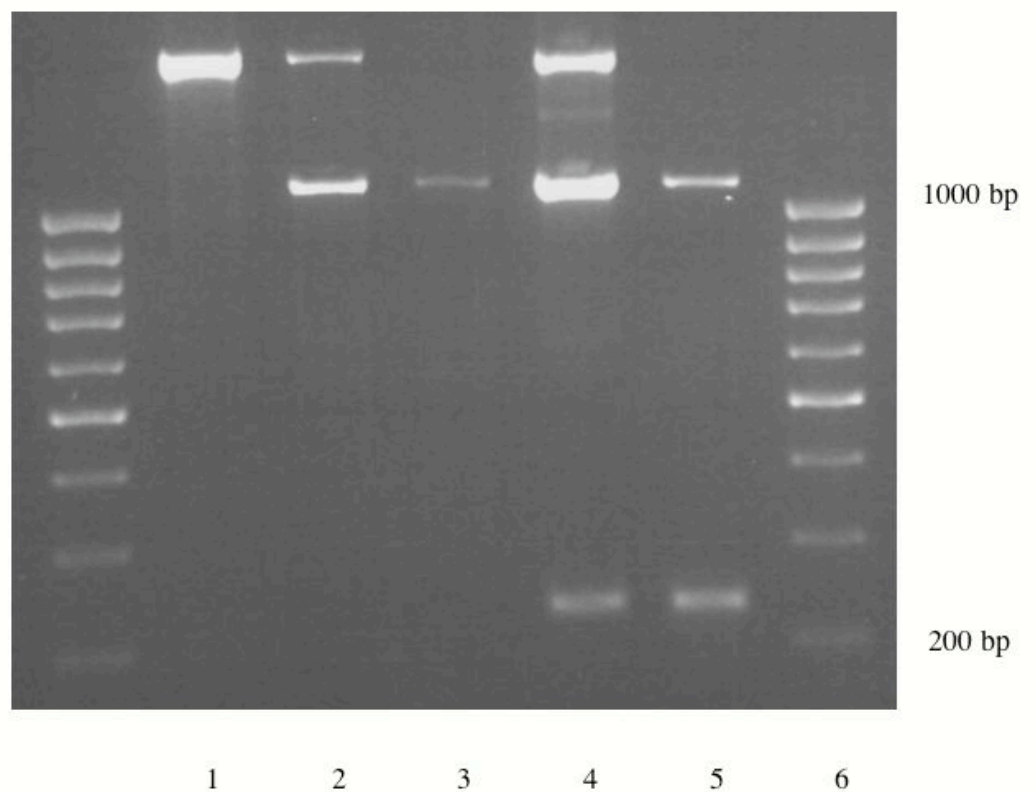


**Figure 3-2: Flox PCR**

An example of agarose gel used to genotype for the floxed  $ET_B$  receptor allele using primers 454F and 681R and tail/ ear punch biopsy DNA. Lane 1: WW/--; Lane 2: FW/Tie2; Lane 3: FF/--; Lane 4: FW/Tie2; Lane 5: FF/Tie2; Lane 6: 100 bp size marker ladder.

The presence of the Tie2-Cre transgene was detected by the amplification of a ~ 550 bp band in a separate PCR (see Figure 3-3).

Thus both the flox and the Tie2-Cre PCR were performed on all samples. As the exact insertion site Tie2-Cre transgene is not known (Kisanuki *et al.*, 2001), a conventional positive control for the Tie2-Cre PCR was not possible. Therefore, in the absence of a band amplified by the Tie2-Cre PCR, the integrity of the DNA sample was demonstrated by the presence of bands in the flox PCR. If no result was seen in either the Tie2-Cre or flox PCRs, then the sample was re-extracted and the PCRs repeated.

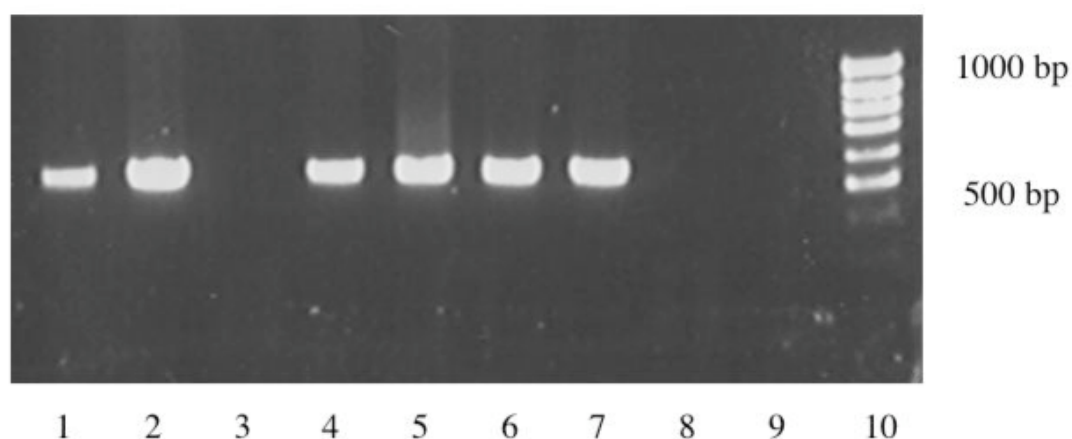


**Figure 3-3: Tie2 PCR**

An example of agarose gel used to genotype animals for the Tie2-Cre transgene. Lanes: 3, 8, and 9 transgene absent; Lanes: 1, 2, 4, 5, 6 and 7 transgene present. Lane 10: 100 bp size marker ladder.

### 3.2.2 Generation of null ET<sub>B</sub> mice

We took advantage of the higher frequency of recombination events in germ cells of female FW/Tie2 and FF/Tie2 mice to produce offspring homozygous for the recombined allele. These pups were of piebald appearance and died shortly after weaning from intestinal obstruction, consistent with functional ET<sub>B</sub> receptor

deficiency (Figure 3-4C, D). When genotyped by PCR, using the primers 454F and 681R, these piebald mice exhibited only the 230 bp recombined (0) allele, indicating that this recombined allele was unable to encode functional ET<sub>B</sub> receptor transcripts (Figure 3-4E).

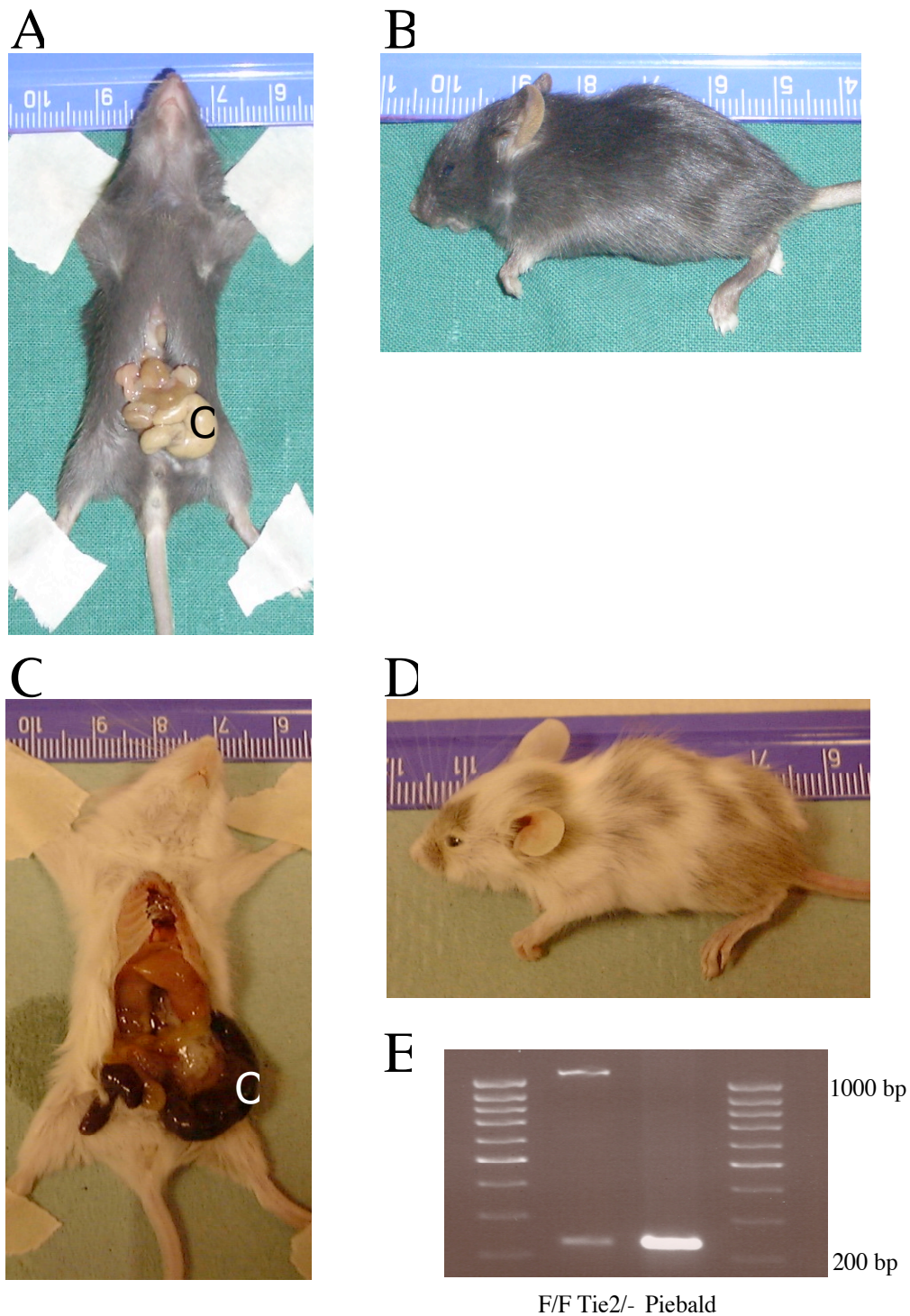


### Figure 3-4: Piebald mice

Intercross of FF/Tie2 mice results in progeny with the phenotype of  $ET_B$  receptor null mice: spotted or piebald coat appearance (D) and intestinal obstruction (C – obstructed colon labelled c). A male 3 week old FF/Tie2 mouse (A) with normal colon (B) shown for comparison. PCR genotyping indicates only the recombinant (0) allele in piebald mice, whereas FF/Tie2 PCR result exhibits both (F) and (0) bands (E).

### 3.2.3 Analytical crosses

Analytical breeding was performed over a period of ~4 months as outlined in the scheme above (see Figure 2-1). Only one W0/-- male could be mated with each FF/Tie2 female, whereas 2 W0/-- females could be established in a harem with each FF/Tie2 male. Thus many more pups were born to the analytical pairs in which FF/Tie2 males were tested compared with the pairs testing female FF/Tie2 mice. The total number of live births and piebald animals arising from each analytical cross is recorded in Table 3-1 below:

**Table 3-1: Results of analytical breeding pairs**

| Sex of FF/Tie2 animal  | Male    | Female  |
|--|---------|---------|
| Total number of analytical pairs                                 | 9       | 5       |
| Total number of live births                                      | 214     | 37      |
| Total number of piebalds born                                    | 16      | 6       |
| % Piebalds overall   | 7.48%   | 16.22%  |
| Range of % Piebald in each individual breeding pair              | 0 – 19% | 0 – 35% |
| Likely proportion of 'O' allele gametes generated by each parent | 0 – 38% | 0-70%   |

Piebald offspring were generated by pairings where the Tie2-Cre transgene was carried by either the male or the female parent, although the proportion of piebald mice was greater in the latter. As each FF/Tie2 animal was paired with a W0/-- mouse, the actual rate of germ line recombination during gametogenesis would have been double the proportion of observed piebald animals.

### 3.2.4 Genotyping strategies

As analytical breeding is costly and time consuming, different approaches were developed in order to identify the frequency of germline recombination with any individual breeding pair, swiftly and easily. Any such technique had to differentiate mice heterozygous for the recombined floxed  $ET_b$  allele and carrying the Tie2 transgene (F0/Tie2) from mice homozygous for the floxed allele and carrying the Tie2 transgene (FF/Tie2), in which recombination only occurs in ECs. With the



standard genotyping strategy of tail/ear biopsies (see section 2.3.2) both of these genotypes will exhibit a 'O' band of 230 bp as well as an 'F' band of 1136 bp.

A number of different approaches were attempted, before the Southern blot analysis was developed.

#### 3.2.4.1 'COMPARATIVE' PCR OF TAIL BIOPSIES

Initial attempts at solving this problem involved using identical quantities of tail derived DNA in each PCR, and then comparing band intensity on the resulting gels.

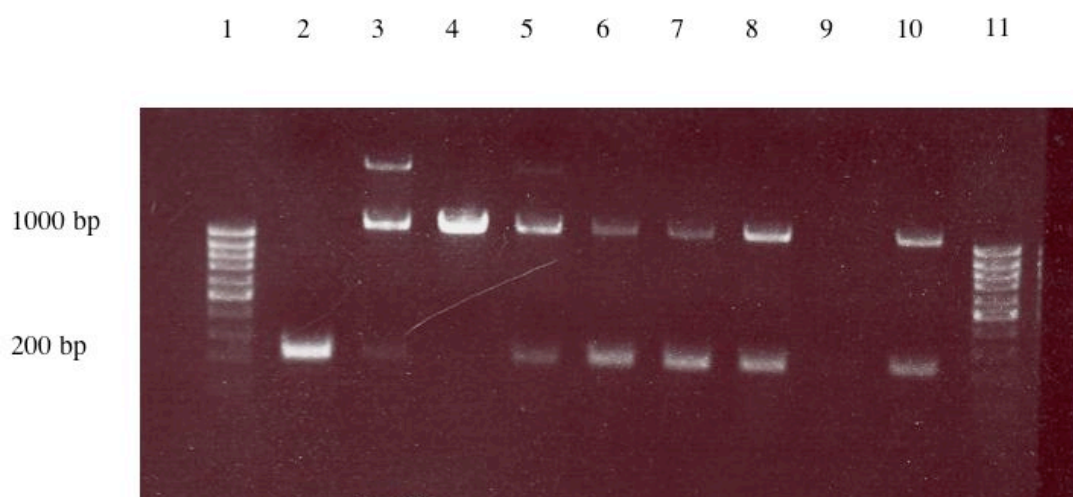


**Figure 3-5: Semi-quantitative PCR.**

An example of an agarose gel from 'semi-quantitative' PCR experiment. Lane 1: 100 bp size marker ladder; Lane 2: 00/-- (piebald animal); Lane 3: FW/Tie2; Lane 4: FF/--; Lane 5: FW/Tie2; Lane 6: F<sup>?</sup>/Tie2; Lane 7: F<sup>?</sup>/Tie2; Lane 8: FF/Tie2; Lane 9: FF/Tie2; Lane 10: FF/Tie2; Lane 11: 100 bp size marker ladder.

This did not give a reliable result – we were unable to differentiate the 'O' band from FF/Tie2 mice (identified as highly likely to be FF/Tie2 by analytical breeding [no PB after >50 pups]) from the 'O' band from F<sup>0</sup>/Tie2 mice.

#### 3.2.4.2 PCR OF 'EC FREE' TISSUE

An alternative approach was then used to differentiate FF/Tie2 from F0/Tie2 mice. If an 'EC free' tissue could be isolated, DNA could be extracted and PCR performed. Approximately 50% of cells from such F0/Tie2 'EC free' tissue should exhibit a '0' band of 230 bp. However, such tissue from FF/Tie2 mice should not exhibit a '0' band, as it would contain no cells in which recombination of the ET<sub>B</sub> gene had occurred. A number of potential 'EC free' tissues were tried:

**Hair:** DNA extracted from hair samples was analysed and compared with samples extracted from the tail biopsies of the same individual animals (see Figure 3-6). Even hair samples from animals identified as highly likely to be FF/Tie2 by analytical breeding (no PB after >50 pups) amplified a very bright 0 band. Further gels (not shown) revealed that hair DNA samples consistently exhibited faint 0 bands only, even when the mice involved were of FW/Tie2 genotype. Thus hair analysis was not a satisfactory method of genotyping our animals.

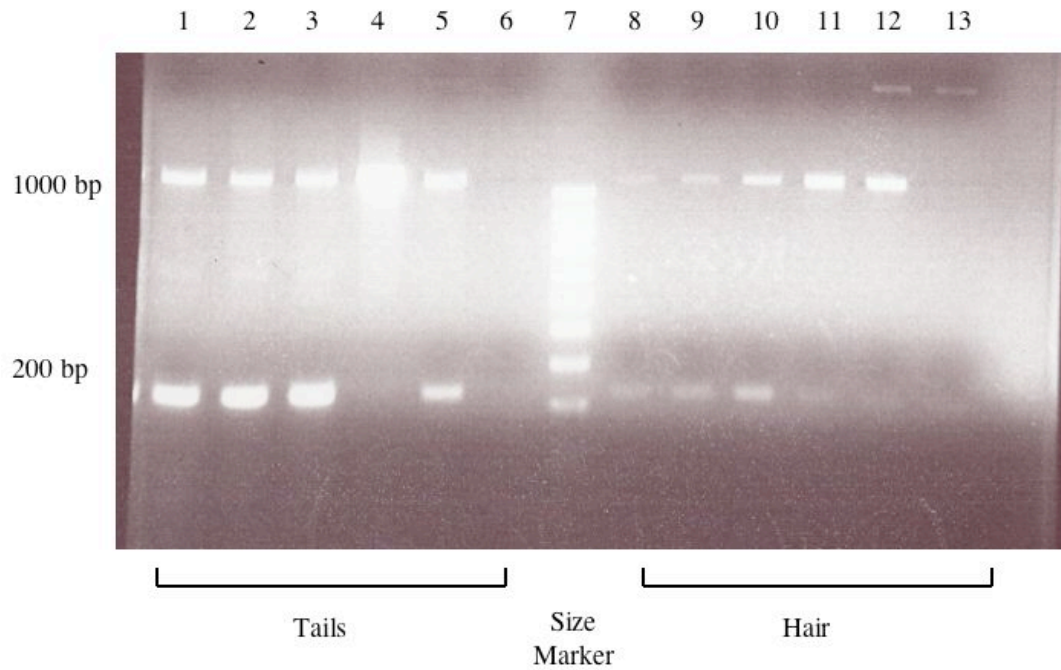


**Figure 3-6: Hair DNA PCR**

Lanes 1 - 6 DNA extracted from tail biopsies; Lane 7: 100 bp size marker ladder; Lanes 8 - 13 DNA extracted from hair. Lanes 1 and 8: FF/Tie2; Lanes 2 and 9: FF/Tie2; Lanes 3 and 10: FF/Tie2; Lanes 4 and 11: FF/--; Lanes 5 and 12: FW/Tie2; Lanes 6 and 13: WW/Tie2.

**Testes:** DNA was extracted from testes and tail biopsies of each individual mouse. Following PCR, the DNA from the testes of mice known to be FF/Tie2 or FW/Tie2, amplified a 0 band, often with no other bands being observed (Figure 3-7). No reliable pattern of results was seen and so the technique was abandoned as a method of distinguishing FF/Tie2 from F0/Tie2 mice.

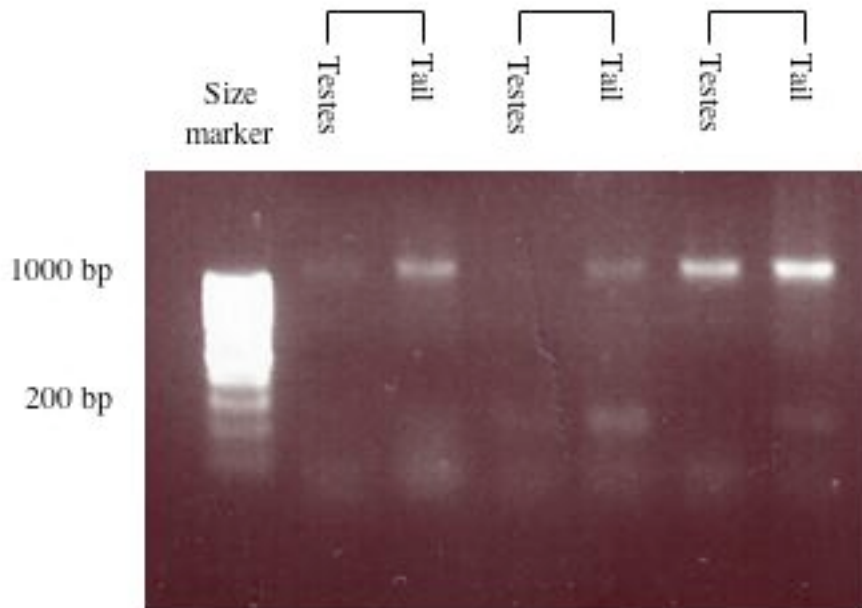


**Figure 3-7: Testes DNA PCR**

An example of a genotyping gel from 3 FF/Tie2 mice showing result of PCR of DNA extracted from both testes and tail tip biopsies.

**Heart:** Following genotyping PCR, DNA extracted from whole heart tissue was compared with DNA extracted from isolated cardiomyocytes. Although the amount of DNA was standardised according to OD<sub>260</sub>, the agarose gel for the isolated cardiomyocytes PCR are very faint (Figure 3-8). However, the ratio of O band/ F band appeared similar for the isolated cells and whole heart tissue. Therefore this method could not differentiate between F0 and FF/Tie2 mice.

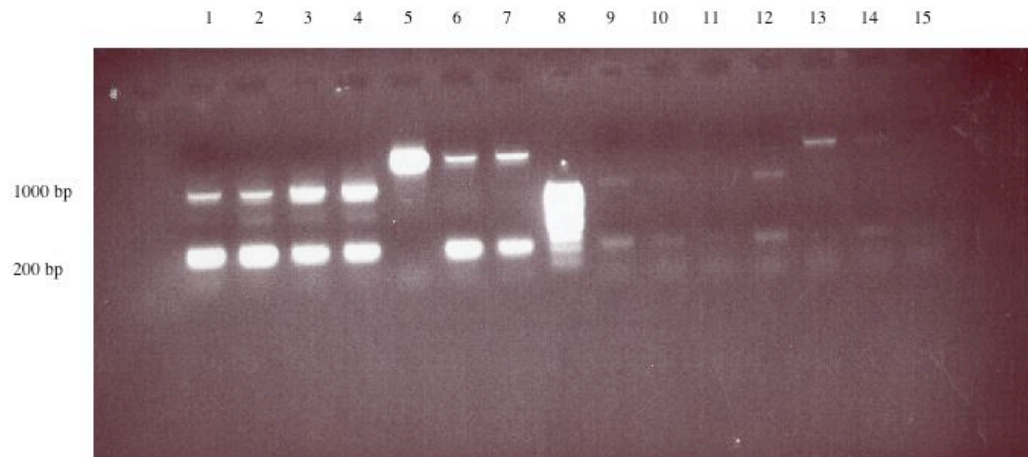


**Figure 3-8: Cardiomyocyte DNA PCR**

Lanes 1 - 7 DNA extracted from intact cardiac tissue; Lane 8: 100 bp size marker ladder; Lanes 9 – 15: DNA extracted from crudely isolated cardiomyocytes. Lanes 1 and 9: FF/Tie2; Lanes 2 and 10: FF/Tie2; Lanes 3 and 11: FF/Tie2; Lanes 4 and 12: FF/Tie2; Lanes 5 and 13: WW/--; Lanes 6 and 14: W0/Tie2; Lanes 7 and 15: W0/Tie2.

### 3.2.4.3 SOUTHERN ANALYSIS OF TAIL BIOPSY DNA

In contrast to FF/Tie2 mice, Southern analysis (as described in section 2.4.3) of F0/Tie2 tail tissue detected the presence of the recombined allele. Southern analysis detected only the recombined allele in piebalds, indicating that the recombined allele was unable to encode functional ET<sub>B</sub> receptor transcripts (see Figure 3-9).

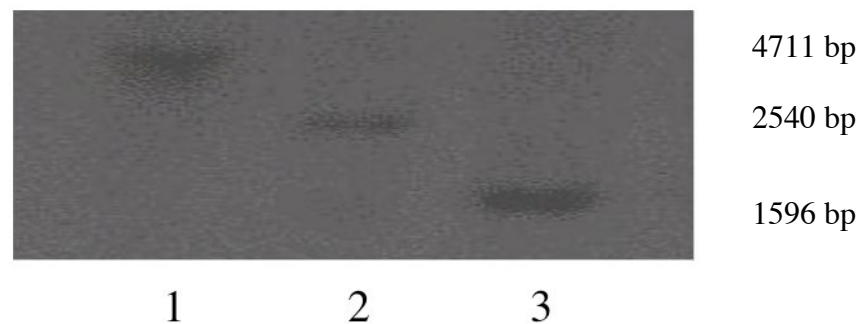


**Figure 3-9: Southern blot genotyping**

Southern blot hybridisation analysis of EcoR I-digested genomic DNA from WW/-- (Lane 1), FF/Tie2 (Lane 2) and piebald (Lane 3) mice. Southern analysis only detected the recombined allele in piebald mice (homozygous for the recombined allele).

### 3.2.5 Tie2-Cre restricts Cre expression to ECs

#### 3.2.5.1 LAC Z STAINING AND ENDOTHELIAL CELL STAINING

WW/Tie2 mice were mated in reciprocal crosses with R26R mice (kind gift of Dr Ian Simpson, University of Edinburgh). Mice (aged 8 weeks) were culled by CO<sub>2</sub> asphyxiation, their kidneys removed and stained for  $\beta$ -galactosidase. Immunohistochemistry was also performed to visualise EC using antibodies against CD31. Consistent with the results of previous studies (Kisanuki *et al.*, 2001), we observed EC-restricted LacZ staining in kidneys harvested from F1 offspring following Flox/Flox Tie2-Cre and R26R intercross. Intense staining for both LacZ and CD31 was seen in the glomeruli and adjoining capillaries and arterioles and in the medullary rays, but not in tubular epithelial cells (see



Figure 3-10). No LacZ staining was seen in control R26R mice lacking the Tie2-Cre transgene.

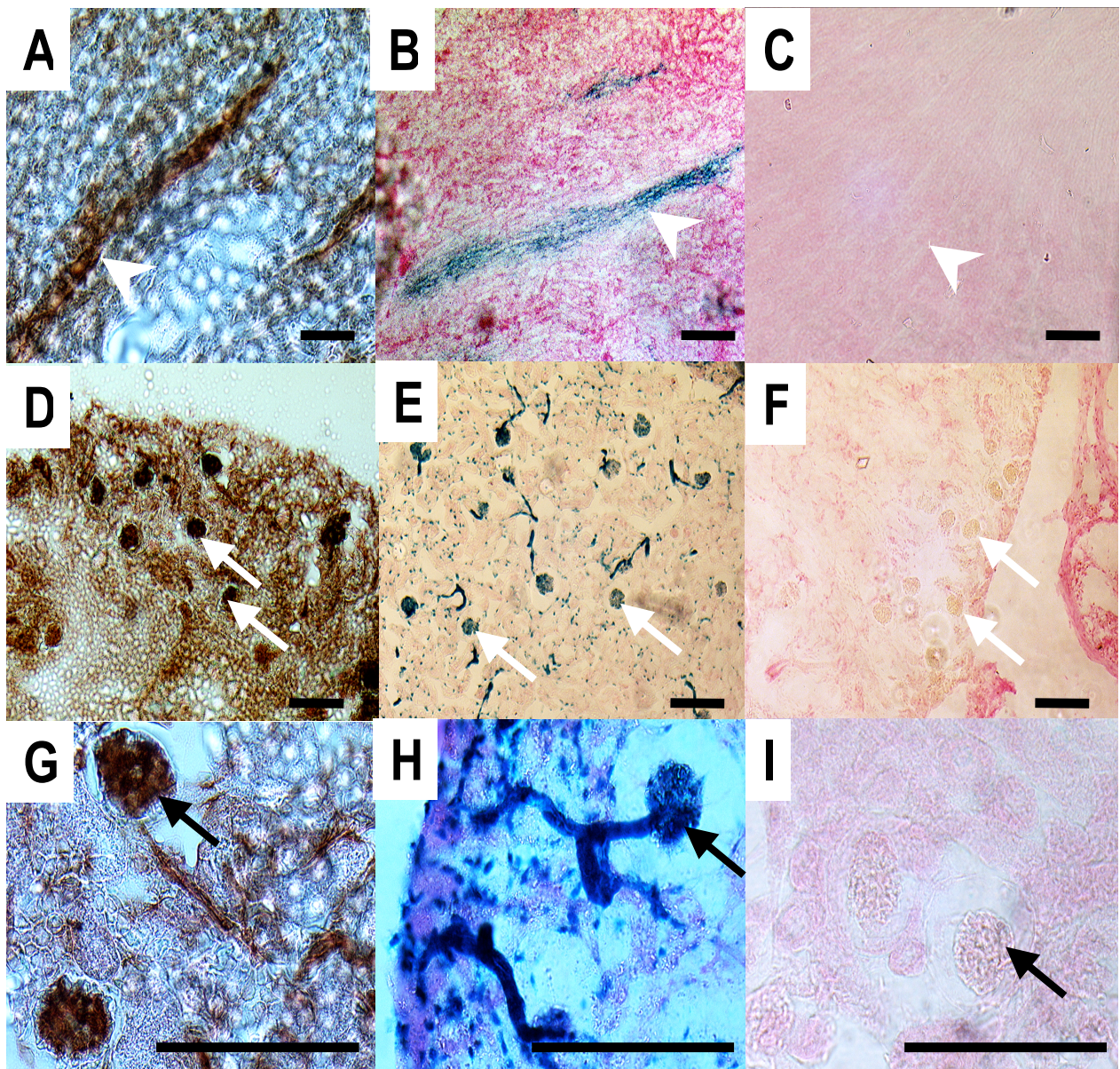


**Figure 3-10: LacZ and CD31 antibody staining in kidneys from WW/Tie2-Cre and WW/Tie2-Cre/R26R mice.**

EC stained brown using antibodies to CD31 in medullary rays (A), glomerular capillaries and arterioles (D and G). An identical pattern of LacZ staining (blue), indicating Tie2-Cre expression, is observed in F1 mice following intercross of FF/Tie2-Cre and R26R reporter mice (B, E and H), confirming EC-restricted transgene expression. Control R26R mice lacking the Tie2-Cre transgene demonstrated no blue LacZ staining (C, F and I). Arrows = glomerulus; Arrowheads

= medullary rays; Scale bar = 100  $\mu$ m. (Data from Danielle Armour, University of Edinburgh).

### 3.2.5.2 GFP STAINING

WW/Tie2 mice were also mated in reciprocal crosses with a second reporter strain (EGFP reporter mouse line – generous gift of Dr Alexander Medvinsky, University of Edinburgh, UK).

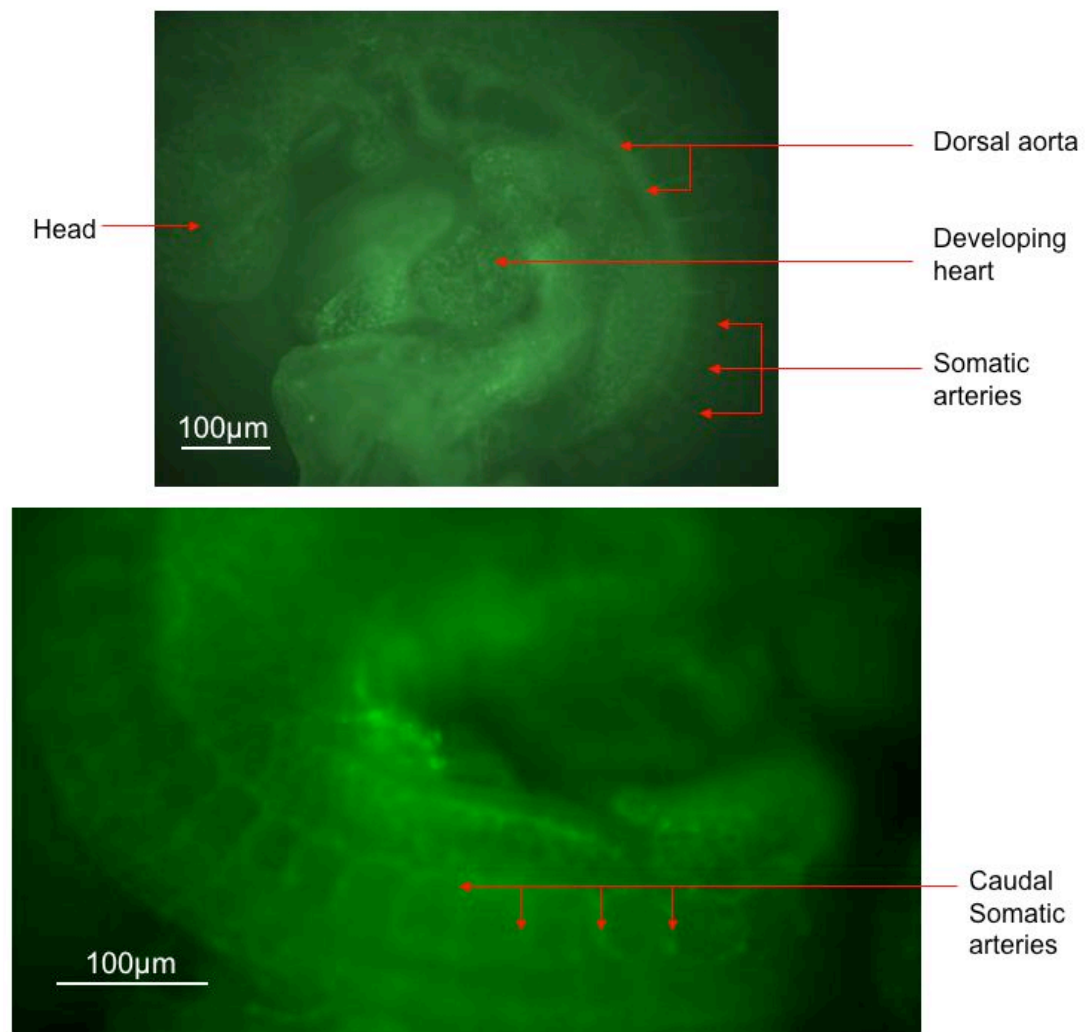


**Figure 3-11: GFP autofluorescence in day 11 FF/Tie2-Cre/GFP embryos**

Micrographs showing expression of GFP in F1 Tie2-Cre/GFP embryos, following intercross of FF/Tie2-Cre and EGFP reporter mice. Somatic arteries arising from the developing dorsal aorta are clearly seen, indicating EC specific distribution of Tie2-Cre.



In Tie2-Cre/GFP F1 offspring, the blood vessels autofluoresced markedly, in contrast to other epithelial surfaces such as the gut or bladder, offering further evidence of EC specific Tie2-Cre expression (see Figure 3-11). No autofluorescence was seen in the control NoCre/GFP sibling controls. These studies were all performed by members of Dr Alexander Medvinsky's laboratory.

### **3.2.6 Autoradiography to demonstrate ET receptor expression**

#### **3.2.6.1 WW/-- CONTROL MICE**

Autoradiographical images of longitudinal whole torso sections from control mice, cut at the level of the heart, revealed as expected, high densities of specific ET<sub>B</sub> binding to the liver, lungs, medulla of the kidney and gut epithelium with lower densities present in the heart and kidney cortex (Figure 3-12). Specific ET<sub>A</sub> binding was highest in the heart and smooth muscle of the gut with lower densities seen in the vasculature of organs including the kidney, liver and lungs.

#### **3.2.6.2 COMPARISON OF WW/-- AND FF/-- MICE**

I next tested whether FF/-- demonstrate altered ET<sub>B</sub> receptor expression. High levels of binding were found as expected in ET<sub>B</sub> rich organs including the kidney and lungs. The density of binding of ET<sub>B</sub> selective ligand to the longitudinal sections from WW/-- animals was not significantly different in the lungs, liver, renal cortex and medulla to those from FF/-- mice (Figure 3-12).

#### **3.2.6.3 FF/TIE2 MICE DEMONSTRATE REDUCED EC ET<sub>B</sub> EXPRESSION**

In autoradiographical images of longitudinal sections of FF/Tie2 mice, binding of ET<sub>B</sub> selective ligand in EC-rich tissue such as lung parenchyma (Figure 3-12C, Figure 3-13A) and renal cortex and medulla (Figure 3-12C, Figure 3-13C) was not distinguishable from the level of non-specific binding in these tissue regions. However, binding to other cell types known to express ET<sub>B</sub> receptors, such as epithelial cells of the lung and kidney, was preserved (Figure 3-13) compared with FF/-- controls.

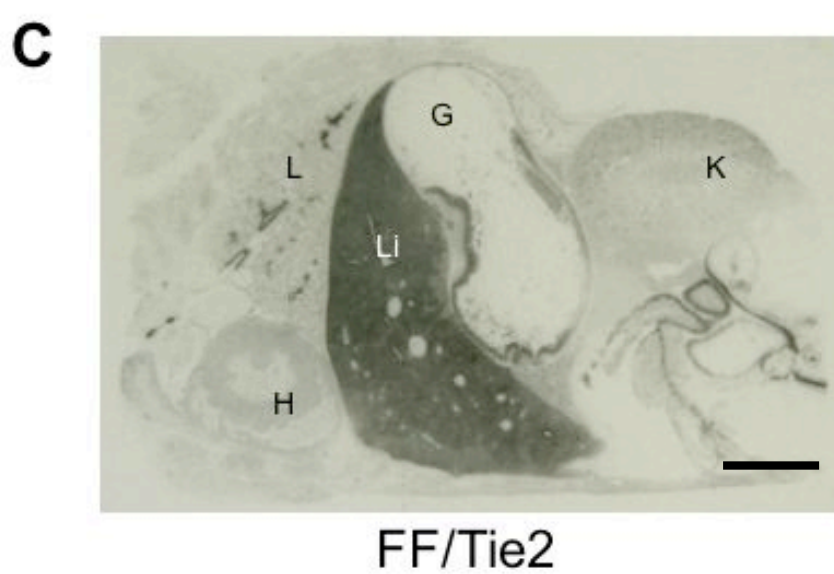
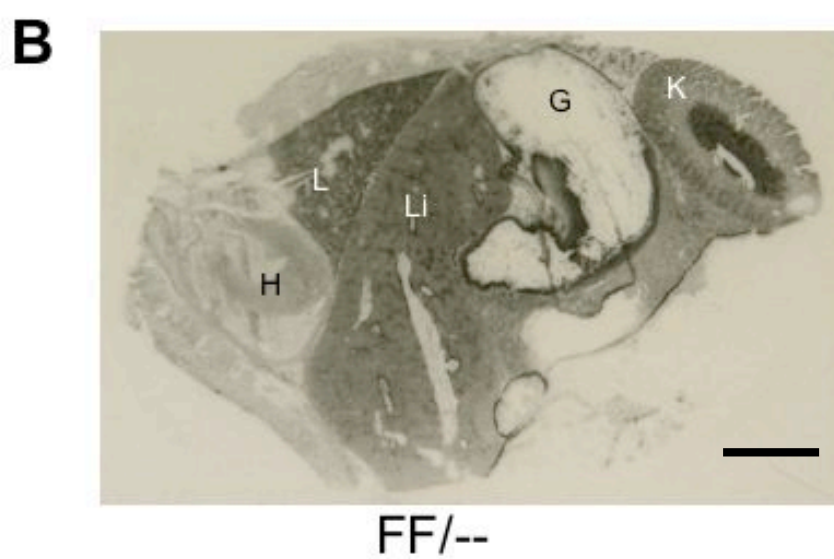
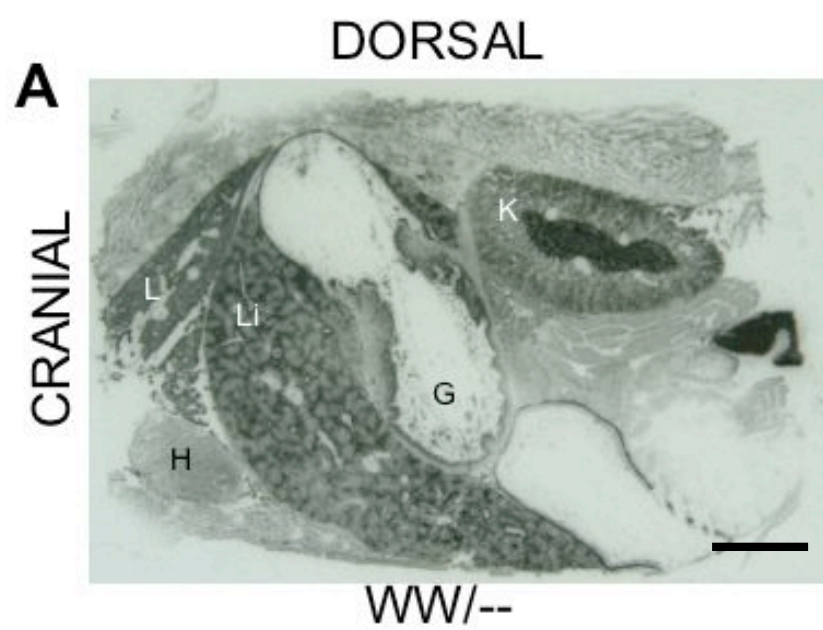


**Figure 3-12: Total ET<sub>B</sub> binding in FF/Tie2 and control mice**

(Previous page) Autoradiographs of total binding of the radiolabelled ET<sub>B</sub> selective ligand [<sup>125</sup>I]-BQ3020 in WW/-- (A) FF/-- (B) and FF/Tie2 (C) mice. FF/Tie2 mice demonstrate loss of ET<sub>B</sub> receptor-mediated binding in EC-rich organs such as lung and kidney but normal binding in less-EC rich tissue as such the liver. K = kidney, Li = liver, H = heart, G = gut, L = lung. Scale bar = 5 mm.

Quantitative autoradiographical analysis of representative areas known to contain high densities of EC (using this technique it is not possible to measure individual endothelial cells that are below the resolution of the image analyser) showed that specific binding was virtually abolished in discrete regions rich in EC including lung parenchyma (reduced to <6% of control, Figure 3-14A) and renal medulla (reduced to <5% of control, Figure 3-14C) and liver sinusoids (Figure 3-14E). In contrast, in epithelial tissue expressing non-EC ET<sub>B</sub> receptors such as those in the respiratory bronchi (Figure 3-14B) and liver parenchyma (Figure 3-14D) no significant difference was found compared with FF/-- controls, confirming the qualitative results.

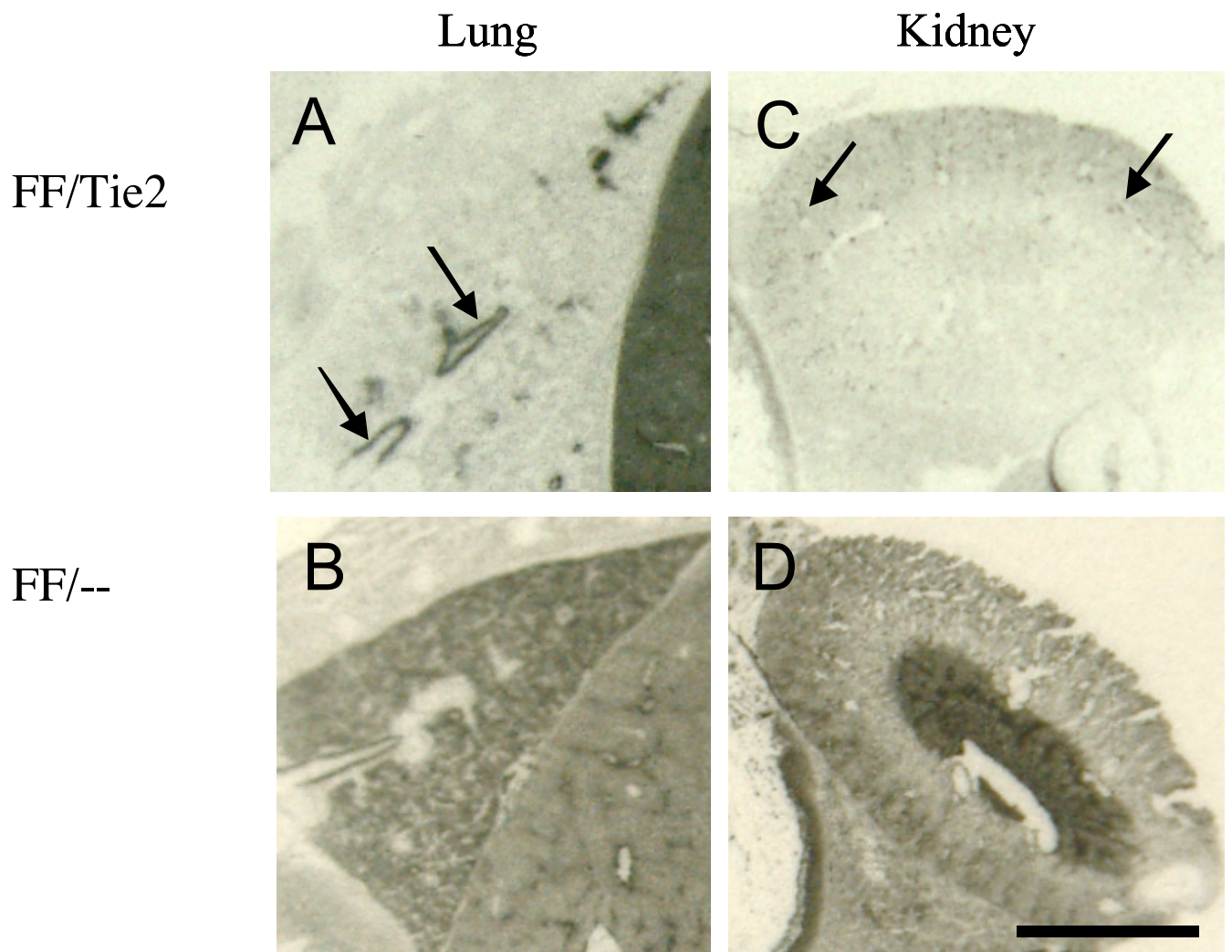


**Figure 3-13 ET<sub>B</sub> binding in lung and kidney**

High magnification images of autoradiograms, showing binding of [<sup>125</sup>I]-BQ3020 to ET<sub>B</sub> receptors in both FF/Tie2 (A and C) and FF/-- (B and D) mouse torsos. In the FF/-- as expected, high levels of specific ET<sub>B</sub> binding is seen throughout the lung (B) and kidney (D) however in the FF/Tie2 mouse only the non-endothelial ET<sub>B</sub> binding remains for example to the epithelial cells (indicated by arrows) of lung bronchi (A) and kidney (C). Scale bar = 5 mm.

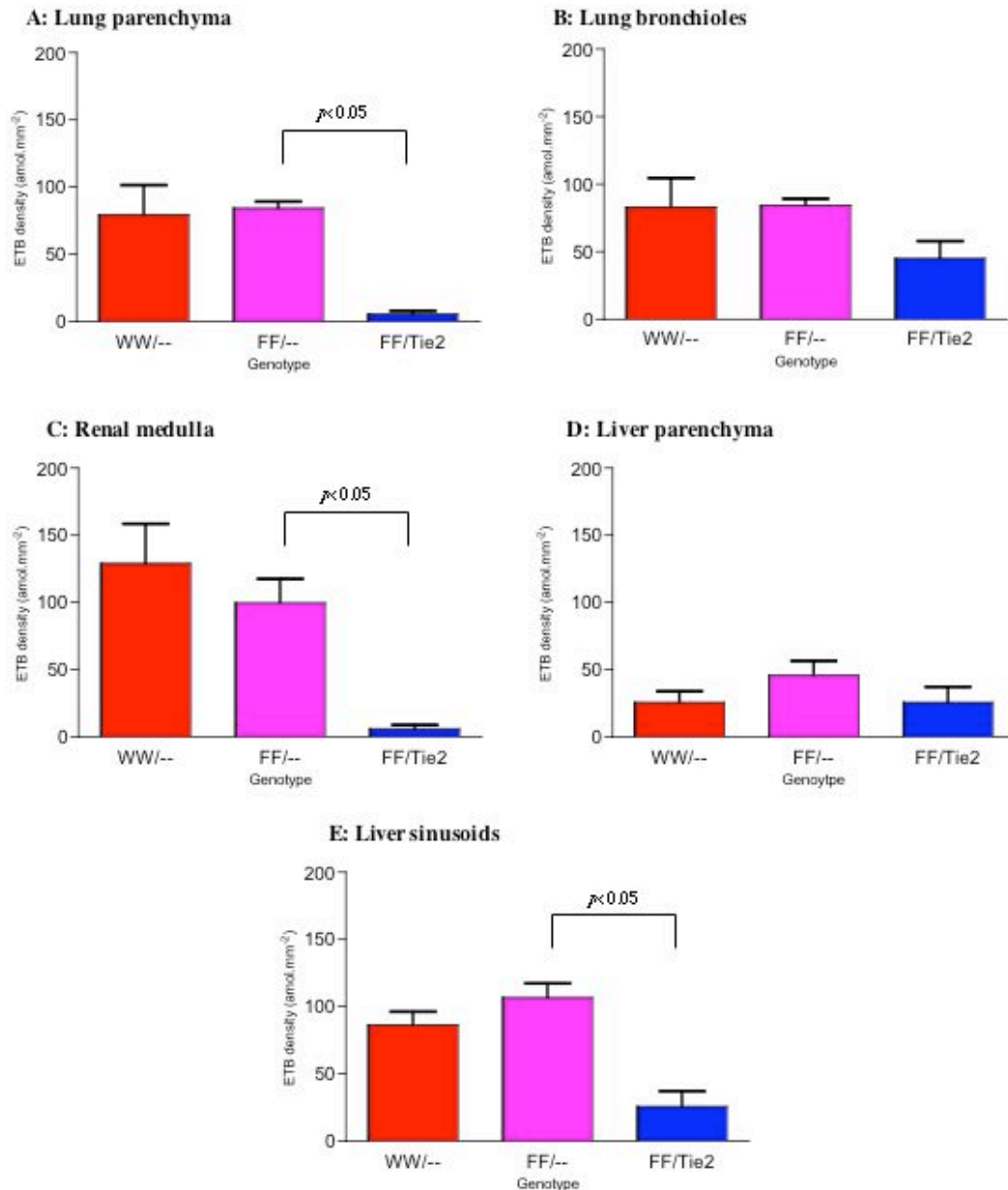


**Figure 3-14: Specific ET<sub>B</sub> binding in lung, kidney and liver**

Specific binding density of the radiolabelled ET<sub>B</sub> selective ligand [<sup>125</sup>I]-BQ3020 was significantly reduced in FF/Tie2 mice in EC-rich renal medulla (A) and lung parenchyma (B) and but relatively preserved in lung bronchioles (C). n = 4 for all groups.

#### 3.2.6.4 ET<sub>A</sub> EXPRESSION IN FF/TIE2 ANIMALS

Binding of the radiolabelled ET<sub>A</sub> selective ligand [<sup>125</sup>I]-PD151242 was not significantly different in FF/Tie2 animals compared to controls (Figure 3-15).

Quantification of the ET<sub>A</sub> selective autoradiography showed similar amounts of binding in specific tissues from FF/Tie2 mice (renal medulla, Figure 3-16A, renal cortex Figure 3-16B, lung, Figure 3-16C and liver, Figure 3-16D) compared to equivalent regions from FF/-- mice.

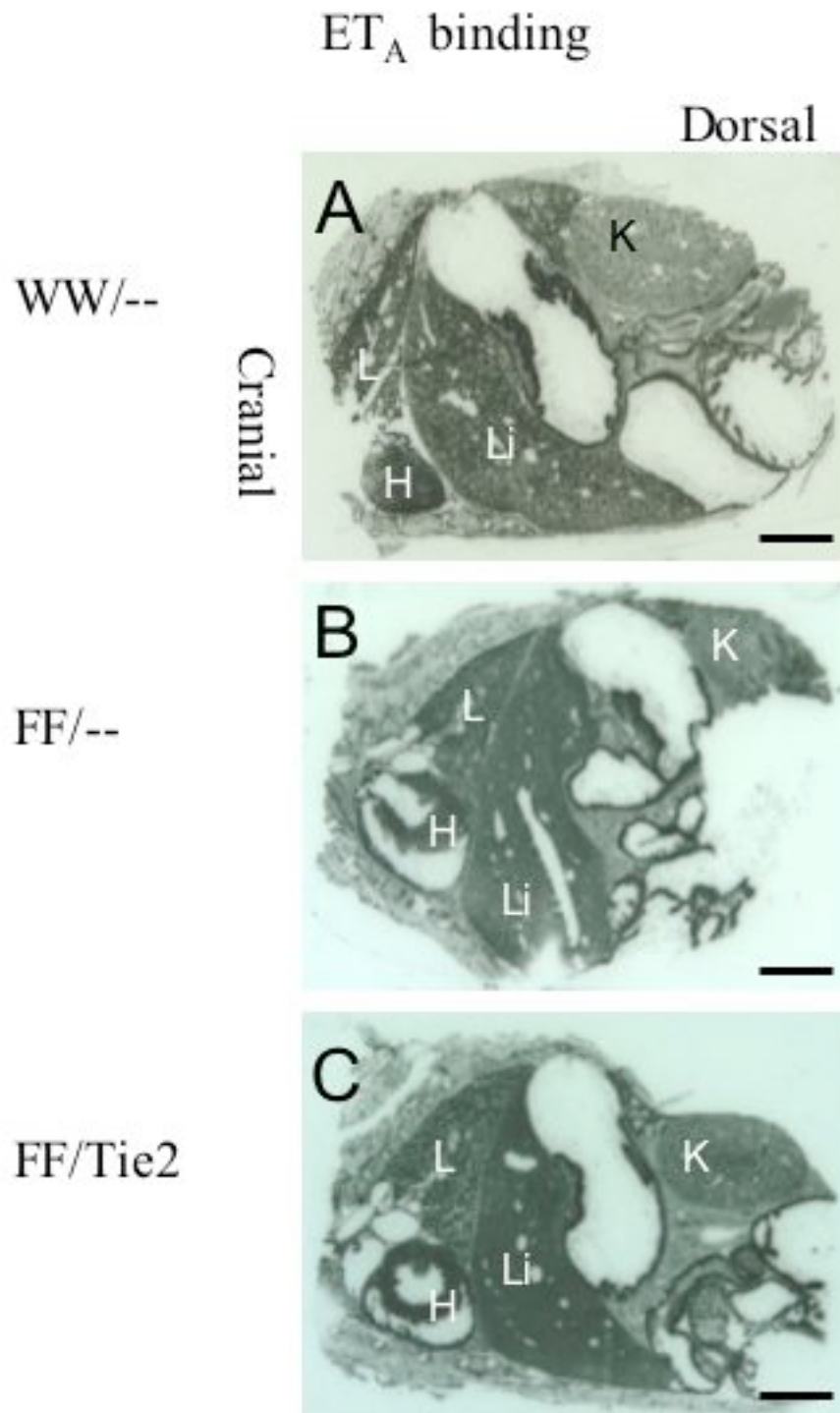


**Figure 3-15: Autoradiographs of total binding of the radiolabelled ET<sub>A</sub> selective ligand [<sup>125</sup>I]-PD151242 in WW/-- (A) FF/-- (B) and FF/Tie2 (C) mice.**

ET<sub>A</sub> receptor-mediated binding is greatest in the heart and smooth muscle of the gut with lower densities seen in the vasculature of the kidney, liver and lungs. ET<sub>A</sub> binding is similar in FF/Tie2 mice and controls, indicating that it is not altered by



EC-ET<sub>B</sub> down-regulation. K = kidney, Li = liver, H = heart, G = gut, L = lung. Scale bar = 5 mm.

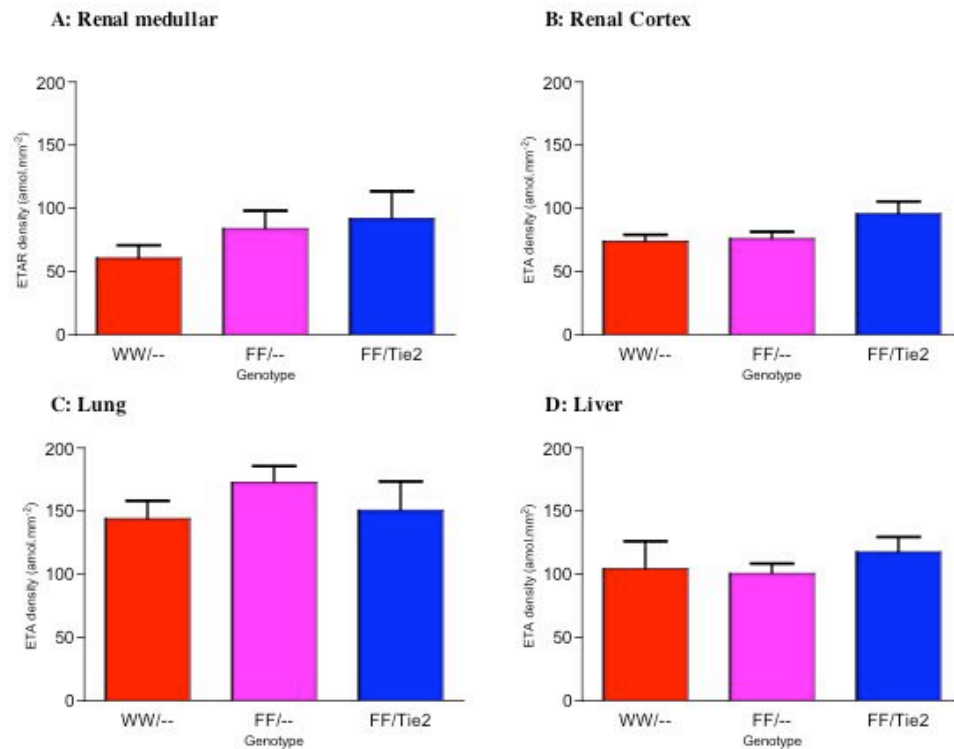


**Figure 3-16: Specific ET<sub>A</sub> binding in kidney, lung and liver.**

Specific binding of the ET<sub>A</sub> selective ligand [<sup>125</sup>I]-PD151242 in renal medulla (A), renal cortex (B), lung (C) and liver (D) was similar in WW/--, FF/-- and FF/Tie2 mice. (n=4).



### 3.2.7 RT-PCR to demonstrate renal ET system expression

#### 3.2.7.1 RNA INTEGRITY

Following extraction from the harvested mouse kidneys, the integrity of the RNA was assessed by running a RNA denaturing gel. A representative gel demonstrating well defined bands corresponding to 28S (4.7 kbp) and 18S (1.9 kbp) ribosomal RNA is shown below (Figure 3-17).

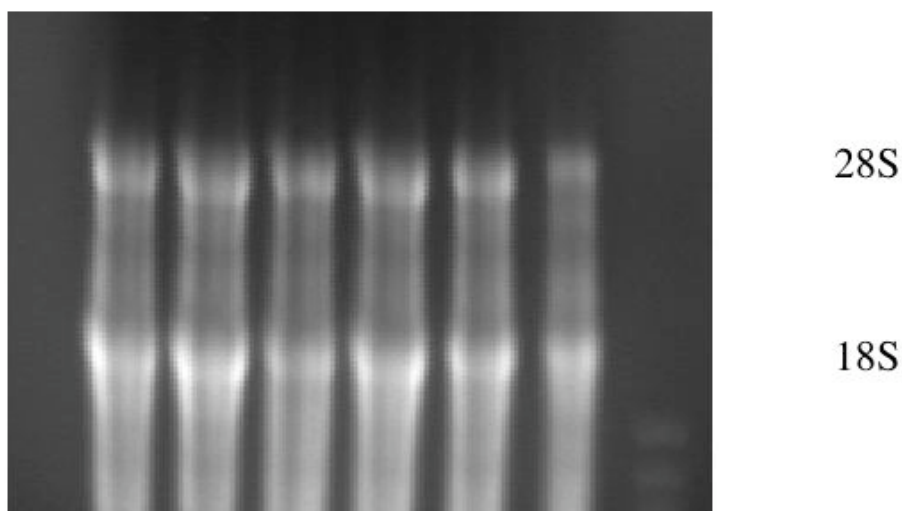


**Figure 3-17: Denaturing gel**

An example of a denaturing gel of RNA showing 18s and 28s ribosomal RNA.

#### 3.2.7.2 OPTIMISATION OF PCR CONDITIONS

Each endpoint PCR was optimised by varying the annealing temperature, magnesium concentration, dNTP concentration and cycle number. The optimum conditions were those producing the greatest yield of desired product relative to extraneous non-specific products (see Figure 3-18).

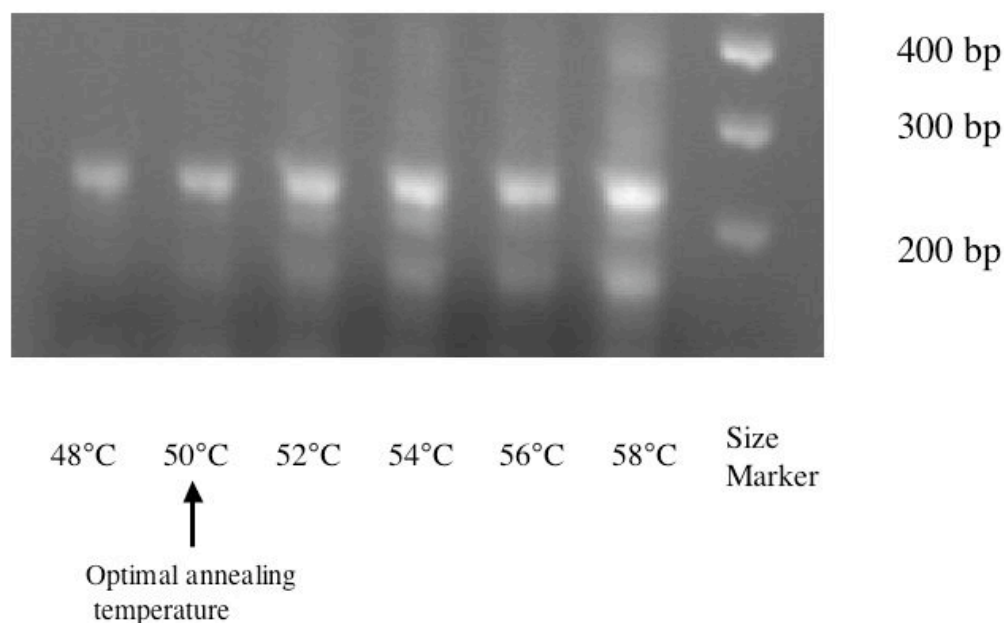


**Figure 3-18: Optimisation of PCR temperature**

Representative gel showing optimisation of ET<sub>A</sub> PCR annealing temperature. The lanes correspond to the ET<sub>A</sub> PCR carried out at a range of annealing temperatures (48 - 58°C). The right-hand lane corresponds to the 100 bp size marker. Under this particular magnesium concentration, 50°C was selected as the optimum temperature, as although it is not the brightest band, it has the least amount of non-specific product.

The cycle number that was chosen for each PCR was within the exponential range of amplification to ensure a linear relationship between the amount of input template and the amount of amplification product (see Figure 3-19).

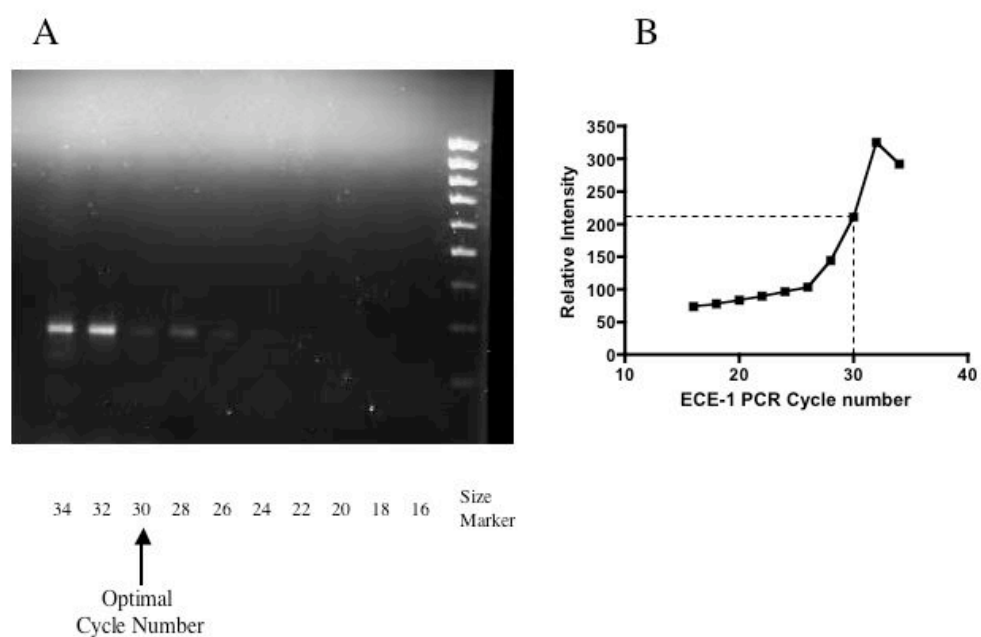


**Figure 3-19: Optimisation of PCR cycle number**

A: representative gel showing optimisation of ECE-1 PCR cycle number. B: Relationship of cycle number and relative band intensity. Thirty cycles were selected as this value lies on the linear portion of the graph.

**Table 3-2: Optimum conditions for semi-quantitative PCR of ET system**

These were determined empirically for each component of the ET system and GAPDH.

| Primer sequence   | Product size | Annealing temperature | Cycle number | [MgCl <sub>2</sub> ] (mM) | [dNTP] (μM) |
|---|--------------|-----------------------|--------------|---------------------------|-------------|
| GAPDH<br>5'-GCCATCAACGACCCCTTCATT-3'<br>5'-TGCCAGTGAGCTTCCCGTTC-3'        | 597          | 55.0°C                | 28           | 2.0                       | 200         |
| ET <sub>B</sub><br>5'-TGGTCTGTGGTTCTGG-3'<br>5'-TACAGAGCGATTGGATTGATGC-3' | 480          | 65.0°C                | 30           | 3.5                       | 300         |
| ET <sub>A</sub><br>5'-TGTCTGCTTCCGAGGAGC-3'<br>5'-GTGCCCAGAAAGTTGATC-3'   | 261          | 55.0°C                | 31           | 4.0                       | 200         |
| ECE-1<br>5'-CACCTGCCATCAACTGGTTACC-3'<br>5'-GGAATACAGGTCTTCTTCGTCC-3'     | 261          | 60.4°C                | 30           | 2.5                       | 200         |

Once the optimal conditions had been determined, the cDNA was serially diluted, and the PCR for each component of the ET system performed, to confirm the semiquantitative nature of each PCR (Figure 3-20).

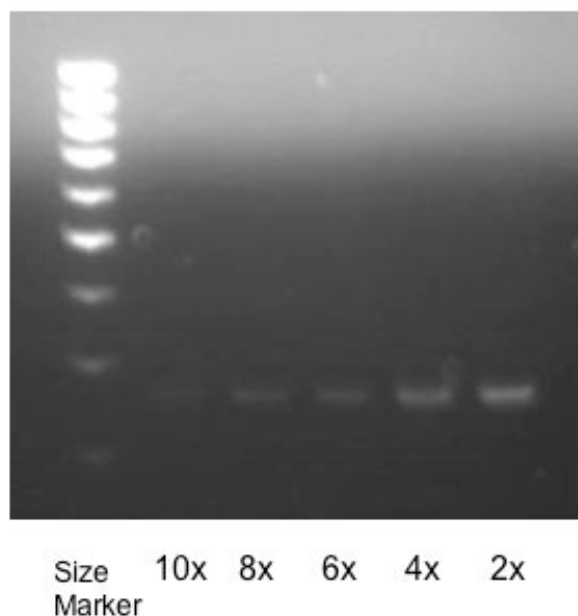


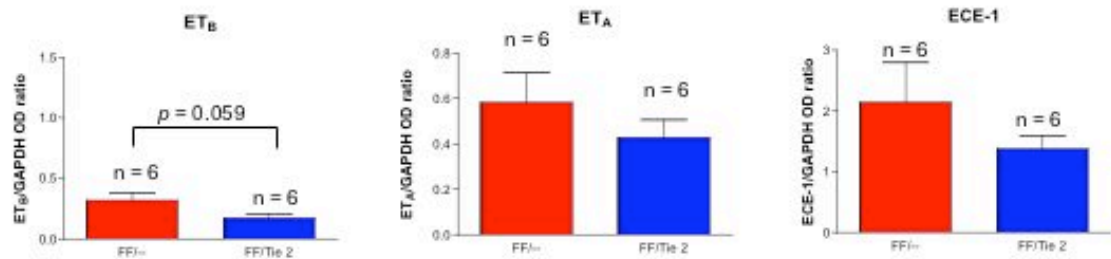
**Figure 3-20: Serial dilution of cDNA**

An example of a gel of the ECE-1 PCRs using serially diluted cDNA samples.

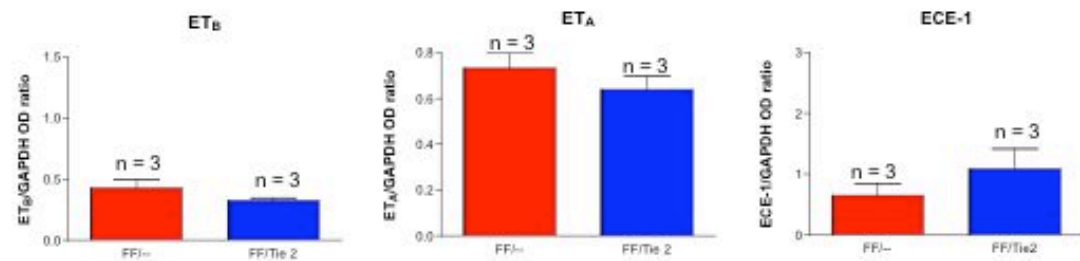
### 3.2.7.3 GENE EXPRESSION OF COMPONENTS OF THE ET SYSTEM

Semi-quantitative endpoint RT-PCR was then performed on kidneys from FF/-- and FF/Tie2 animals. Comparisons were made between the expression of the components of the ET system in kidneys from both genotypes of young (< 12 weeks old) male, young female and aged (> 52 weeks old) male mice.

### A: Young Males



### B: Aged Males



### C: Young Females

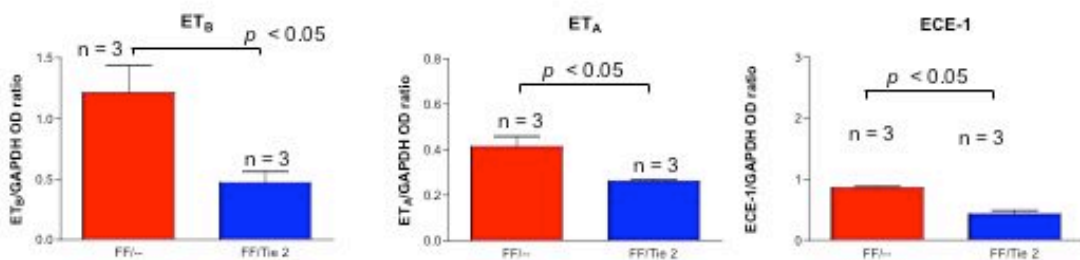
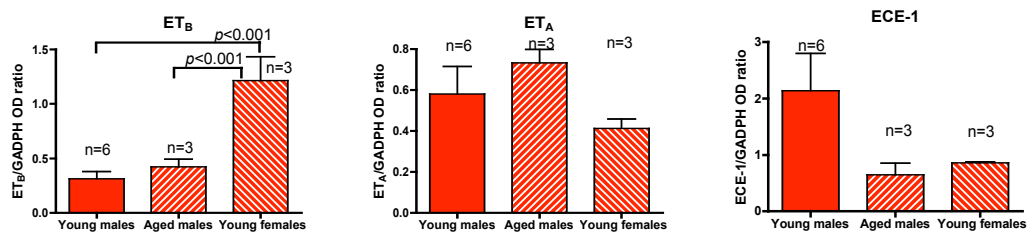


**Figure 3-21: Effect of genotype on the relative expression of the renal ET system** Relative expression of renal ET<sub>B</sub>, ET<sub>A</sub>, and ECE-1 mRNA in young male (A), old male (B) and young female (C) FF/Tie2 and FF/- mice.

Across all three groups, FF/Tie2 mice exhibited reduced  $ET_B$  gene expression compared to FF/-- controls. This difference was statistically significant in the young female mice and approaching significance in the young males. In both the young and aged males there was no alteration in  $ET_A$  or ECE-1 gene expression with genotype. In contrast, the young FF/Tie2 females demonstrated decreased gene expression of  $ET_A$  and ECE-1.

#### A: FF/-- mice



#### B: FF/Tie2 mice

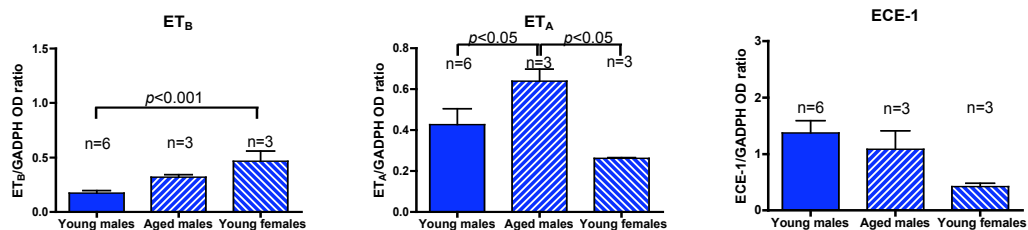


**Figure 3-22 Effect of age and sex on the relative expression of the renal ET system**  
Relative expression of renal  $ET_B$ ,  $ET_A$ , and ECE-1 mRNA in FF/-- (A) and FF/Tie2 (B) mice.

Comparing male and female mice, the FF/-- young females had almost 3-fold the  $ET_B$  expression of male FF/-- animals, both young and old. This pattern of increased expression in females was also seen with the residual (due to EC down-regulation)  $ET_B$  expression demonstrated by FF/Tie2 mice. Old male mice had similar  $ET_B$  gene expression compared to young males in both genotypes.

Both FF/-- and FF/Tie2 female mice exhibited a trend towards reduced  $ET_A$  gene expression, although this only reached statistical significance when comparing old male with young female FF/Tie2 mice. Both old and young male FF/-- mice

exhibited similar ET<sub>A</sub> expression, although FF/Tie2 old males had significantly increased ET<sub>A</sub> expression compared to young male FF/Tie2 mice.

Age and sex had no significant effect on ECE-1 expression in either genotype.

### **3.3 DISCUSSION**

#### **3.3.1 Knockout of exons 3 and 4 is sufficient to prevent expression of ET<sub>B</sub>**

In accordance with others (Constien *et al.*, 2001; Koni *et al.*, 2001), we have shown that intercrossing of FF/Tie2 mice results in a proportion of the progeny having a spotted coat or piebald appearance (see Figure 3-4). These animals had the phenotype of ET<sub>B</sub> receptor null animals (Gariépy *et al.*, 1996; Hosoda *et al.*, 1994): as well as the altered coat colour pattern (due to impaired neural crest-derived melanocyte migration) they do not survive beyond weaning due to obstructive aganglionic megacolon. This phenomenon of germ line recombination was used to deliberately generate mice homozygous for the recombined ET<sub>B</sub> receptor allele, to test the hypothesis that exons 3 and 4 of the ET<sub>B</sub> receptor gene are required for functional ET<sub>B</sub> receptor expression. In theory, truncated ET<sub>B</sub> receptors, lacking the protein sequences coded by exons 3 and 4, might still be functional. However, mice homozygous for the recombined allele displayed the lethal piebald phenotype of ET<sub>B</sub> null animals, confirming that deletion of exons 3 and 4 via Cre/loxP mediated recombination is sufficient to prevent normal ET<sub>B</sub> receptor function. These findings are reinforced by the publication of a strain of ET<sub>B</sub> receptor null mice in which a deletion of exons 3 and 4 has been demonstrated (Matsushima *et al.*, 2002).

#### **3.3.2 Sex linked germ line recombination**

Other groups (B.R. Duling, University of Virginia, USA, Personal Communication; (Koni *et al.*, 2001) have found that the rate of germline recombination of the Tie2-Cre transgene is sex linked – germline recombination occurs at a higher frequency when transmitted through the female parent. In order to determine whether a similar linkage of germline recombination with parental gender existed in our colony, a number of reciprocal analytical crosses were established. FF/Tie2 animals were bred



with wild type mice heterozygous for the recombined allele (W0/-- mice). The percentage of piebald mice in the progeny would be expected to be around half the proportion of gametes, produced by the FF/Tie2 parent, with the recombined (0) allele. Whilst the proportion of piebald mice were higher in the breeding pairs where the mother rather than the father carried the Tie2-Cre transgene, the total number of animals born to these litters was disappointingly small. The number of pups produced by these pairs was much lower than that produced by the matings where the male carried the Tie2-Cre transgene. This is because, although FF/Tie2 males were each tested by pairing them to 2 W0/-- females, female FF/Tie2 mice could only be paired with a single W0/-- male.

Furthermore, a much lower incidence of piebalds was observed in these analytical litters, than would be expected if the majority of gametes from female FF/Tie2 mice underwent germline recombination as reported by others (Koni *et al.*, 2001). If this was indeed the case then ~50% of the pups, from crosses where the mother carried the Tie2-Cre transgene, should have expressed the ET<sub>B</sub> receptor null phenotype. Some analytical crosses generated no piebalds whatsoever. There are a number of possible explanations for this.

Firstly, the low incidence of piebalds generated from the analytical breeding pairs could be due to reduced activity of the Tie2-Cre transgene. If this transgene had become inactivated during the breeding required for the establishment of our colony, then germline recombination would not occur and null ET<sub>B</sub> mice would not be produced. However, in the initial phenotyping experiments, FF/Tie2 mice demonstrated reduced ET<sub>B</sub> binding in enriched ECs and attenuated endothelial dependent ET<sub>B</sub> mediated vasodilatation of aortic rings (see section 1.3.6). These data, together with our *lacZ*/GFP reporter and radiolabelled quantitative autoradiography studies, demonstrate that the Tie2-Cre is active and effective, resulting in recombination in both the reporter and the floxed ET<sub>B</sub> mice.

Alternatively, germline recombination may well be a variable event: whereas one animal may be highly likely to produce many gametes with a recombined ET<sub>B</sub> allele, other animals may do this only infrequently. The mechanism and timing of germline recombination is poorly understood, but may result from demethylation events that occur during gametogenesis. We have observed offspring of FW/Tie2 females that are heterozygous for the recombined allele but do not possess the Tie2-Cre transgene. This suggests that recombination events occur during gametogenesis prior to segregation of the floxed allele and the Tie2-Cre transgene. The phenomenon of ubiquitous Cre-mediated recombination due to loss of normal spatial regulation of transgene expression does not appear to be limited only to the Tie2-Cre transgene. Progeny of male mice carrying both a floxed allele and the inner medullary collecting duct-specific Cre transgene, AQP2-Cre, demonstrate ubiquitous Cre-mediated recombination (Nelson *et al.*, 1998). However, studies with R26R-lacZ reporter animals have demonstrated that male AQP2-Cre transgenic mice express Cre recombinase in postmeiotic sperm (Nelson *et al.*, 1998; Stricklett *et al.*, 1998). Thus the sex linked ubiquitous Cre-mediated recombination may be due to the normal spatial pattern of AQP2-Cre expression, rather than dysregulation during gametogenesis. In contrast, offspring from female AQP2-Cre mice show collecting duct-specific and male reproductive tract-specific Cre-mediated recombination (Nelson *et al.*, 1998; Stricklett *et al.*, 1998).

Another possibility is that many of the null ET<sub>B</sub> progeny died *in utero* or in the early neonatal period from some currently unknown pathology. However, this is not supported by developmental studies that failed to identify a lethal phenotype of ET<sub>B</sub> null mice before weaning (Hosoda *et al.*, 1994). There would have been no way of accurately assessing these 2 possibilities in our experiment. Post mortem examination of the pregnant females to look for *in utero* deaths, as well as counting bodies of dead new-born mice, would not have been helpful as such young animals are bald and have not yet developed the characteristic piebald coat pigmentation. Also disturbing new-born suckling litters to look for dead young often with results in murine infanticide (C Mackenzie, BRR [Biomedical Research Resources], University of Edinburgh, Personal communication). Any dead pups could have been

genotyped using the Southern blot, but unfortunately, it had not yet been optimised by this stage of the project.

Although involving only small numbers of animals, these breeding experiments allow a number of limited conclusions to be drawn. The recombination event occurs with a low frequency in our colony overall, although this increases when the Tie2-Cre transgene is transmitted through the female parent. It soon became clear that to use analytical breeding as a method to reliably identify FF/Tie2 mice with a low rate of germline recombination, would involve a very large number of animals over an extended period. This would not only be expensive, but also be contrary to the principles of 'reduction, replacement and refinement' advocated by H.M. Home Office Guidelines ([www.homeoffice.gov.uk/comrace/animals/reference.html](http://www.homeoffice.gov.uk/comrace/animals/reference.html) - 3rs). Therefore other strategies were employed to identify animals heterozygous for germline recombination.

### **3.3.3 Genotyping strategies**

Rather than rely on Southern analysis for genotyping, which, as a multi-step process, takes a number of days to perform and involves radiolabelling of probes, attempts were made to develop a swift, reliable and less expensive method of genotyping the EC ET<sub>B</sub> receptor down-regulated mice.

#### **3.3.3.1 'COMPARITIVE' PCR**

PCR tends to preferentially amplify bands of smaller length (PCR product competition). Therefore, although many more cells in the tail/ ear biopsy from the F0/Tie2 animal contain the recombined (0) allele, it was not possible to directly compare the intensity of the 230 bp '0' band with that from FF/Tie2 mice. Both were preferentially amplified in the PCR process and appeared with equal intensity.

### 3.3.3.2 GENOTYPING OF NON-EC TISSUE: HAIR

The bulbs of hairs were harvested, in the expectation that such tissue would have a low EC content. However, in animals likely to be FF/Tie2, the 230 bp '0' band appeared more frequently in the PCR performed on DNA from hair bulbs than from tail DNA. This suggests that the hair bulb contains a very high proportion of ECs. Alternatively, in the smaller sample of DNA from the hair bulbs, PCR product competition is more likely to have occurred than in the larger sample of DNA from the tail sample. Thus a '0' band appeared more frequently in the hair sample than the tail sample PCR.

### 3.3.3.3 GENOTYPING OF NON-EC TISSUE: TESTES

Our initial assumption was that germline recombination of the floxed  $ET_B$  gene, seen in our piebald mice, occurred following fertilisation at some stage in the developing embryo. For this reason, testes from experimental animals were harvested, in the belief that they would yield a non-EC rich population. However, soon after this, we discovered that F0/-- mice arose from FW/Tie2 intercrosses, strongly suggesting that germline recombination occurred during gametogenesis. Thus it is likely that experimental animals that are FF/Tie2, might have had sperm in their testes in which recombination had taken place. Tissue from testes containing such sperm would amplify the 230 bp '0' band at PCR. Therefore this technique was also abandoned as a fundamentally flawed method of distinguishing FF/Tie2 from F0/Tie2 mice.

### 3.3.3.4 GENOTYPING OF NON-EC TISSUE: HEART

Cardiomyocytes were crudely isolated, aiming to produce a population of EC-free cells. Thus any 230 bp '0' band seen in the DNA extracted from this tissue would be due to germline recombination (ie F0/Tie2 mice) rather than due to recombination only within ECs (FF/Tie2 mice). Unfortunately '0' bands were seen both in samples extracted from these crudely isolated cardiomyocytes as well as in samples from whole heart tissue, even in mice identified as very likely FF/Tie2 by analytical breeding. It is likely that our population of crudely isolated cardiomyocytes

contained numerous endocardial cells as well as tissue arising from the mesenchymal ventricular outflow tract of the heart. Such tissue has been shown to express Tie2 (Kisanuki *et al.*, 2001) and so perhaps it is not surprising that using this method failed to distinguish FF/Tie2 animals from F0/Tie2 mice. We could have verified the homogeneity of our cardiomyocyte population, by sorting using cell-specific markers, but as we required a routine and convenient method of genotyping that could be applied to all experimental animals, this approach was not suitable.

#### 3.3.3.5 GENOTYPING BY SOUTHERN ANALYSIS

Due to the ubiquity of the vascular endothelium, finding a tissue that can be easily and routinely isolated, yet contains few ECs, is challenging. After unsuccessfully attempting this with a number of different tissues, attention was then focussed on development of the Southern blot to genotype the mice.

Unlike PCR, the Southern analysis does not involve an exponential amplification phase. Thus the density of bands produced in a Southern analysis more accurately reflects the amount of tissue expressing the recombined allele within a tail biopsy. In this way, PCR product competition is avoided. Southern analysis, in contrast to PCR, did not detect the recombined allele in FF/Tie2 animals, presumably because of the small proportion of tail DNA derived from ECs, whereas a band is observed in piebald mice (00/Tie2) as well as heterozygous mice (F0/Tie2).

### 3.3.4 Endothelial cell specific Cre expression

#### 3.3.4.1 BREEDING WITH LACZ R26R MICE

Renal tissue from adult F1 mice, arising from intercross of WW/Tie2-Cre and R26R animals, show a pattern of *lacZ* staining, in medullary rays, glomerular capillaries and arterioles, identical to that of EC staining using antibodies to CD31. This demonstrates that endothelial specific manner expression of the Tie2-Cre transgene is preserved in our colony, as in other colonies (Liao *et al.*, 2001) derived from the same original strain of Tie2-Cre mice (Kisanuki *et al.*, 2001).

#### 3.3.4.2 BREEDING WITH GFP REPORTER MICE

By crossing WW/Tie2-Cre mice with GFP reporter mice (Gilchrist *et al.*, 2003), we have shown that the distribution of Cre recombinase is restricted to the endothelium. This represents further good evidence that the Tie2-Cre mice generously provided by Dr Y. Kisanuki and Prof Misashi Yanagisawa do indeed exhibit EC specific Cre recombinase expression.

#### 3.3.5 EC specific ET<sub>B</sub> down-regulation in FF/Tie2 mice

Having shown that Tie2-Cre expression was specific to ECs, we went on to demonstrate that the Cre/*lox* based approach was effective in down-regulating the ET<sub>B</sub> gene from ECs. Work using the same Tie2-Cre line has shown ~80% deletion of the floxed allele in EC specific Connexin-43 knockout mice (Liao *et al.*, 2001). Previous studies in our laboratory have measured the ET<sub>B</sub> mediated binding of [<sup>125</sup>I]-ET-1 in a population of enriched pulmonary ECs. In ECs from FF/Tie2 tissue, such binding was reduced by ~80%, whereas ET<sub>A</sub> binding was preserved (see section 1.3.6.1) (Bagnall *et al.*, 2006). EC ET<sub>B</sub> receptor-mediated responses, assessed using aortic ring wire myography, were significantly impaired in tissue from FF/Tie2 mice (see section 1.3.6.2), whereas responses dependent upon non-EC ET<sub>B</sub> receptor activation were preserved (see section 1.3.6.3) (Bagnall *et al.*, 2006). These myography studies provide functional evidence of significant EC specific ET<sub>B</sub> down-regulation in FF/Tie2 mice. Using autoradiography, for the first time in the phenotyping of a cell type specific transgenic knockout/knockdown animal, we have further demonstrated EC specific down-regulation of the ET<sub>B</sub> in our FF/Tie2 mice. ET<sub>B</sub> binding was reduced in tissues with a high content of ECs (such as renal medulla, liver sinusoids and lung parenchyma) by >90% but relatively preserved in tissues with a reduced EC content (liver parenchyma and alveolar bronchioles). Furthermore, by showing similar ET<sub>B</sub> receptor expression in FF/-- and WW/-- animals, we have provided strong evidence that the insertion of *loxP* sites on either side of exons 3 and 4 of the ET<sub>B</sub> receptor gene, in the absence of the bacteriophage enzyme Cre recombinase, does not alter the physiological expression of the ET<sub>B</sub> receptor.

### 3.3.6 Expression of other components of the ET system in the FF/Tie2 mouse

Using  $ET_A$  specific radiolabelled ligands we have also used quantitative autoradiography to investigate how EC  $ET_B$  downregulation affects expression of  $ET_A$  receptors. The high plasma concentration of ET-1 in the FF/Tie2 mice (see section 5.3.1) might be expected to result in downregulation of  $ET_A$ , as found in the renal tissue of  $ET_B$  deficient rats (Taylor *et al.*, 2003b) and in vascular tissue in a hypertensive rat model of ET-1 overexpression (Telemaque-Potts *et al.*, 2002). However,  $ET_A$  binding in our FF/Tie2 mice was preserved. Similarly EC specific ET-1 overexpressing mice, which also feature raised plasma concentrations of ET-1, have recently been shown to have preserved levels of vascular  $ET_A$  gene expression (Amiri *et al.*, 2004). The authors argue that the lack of hypertension observed in these mice is due to a compensatory increase in expression of vascular vasodilatory  $ET_B$ . Different species may display different compensatory mechanisms to perturbations in the ET system, often with the result of stabilising BP. Raised ET-1 concentrations in the rat result in reduced  $ET_A$  expression, whereas mice exhibit increased  $ET_B$  expression. Binding studies in ET-1 overexpressing murine models (Hochoer *et al.*, 1997; Shindo *et al.*, 2002) have yet to be carried out.

We conclude that our model shows autoradiographical evidence of EC- $ET_B$  downregulation, which has no effect on the expression of the  $ET_A$  receptor.

To determine the expression of other components of the ET system, within the kidney, we have performed semi-quantitative end-point RT-PCR, which allows assessment of gene expression. Whilst this technique is straightforward and easily applicable to a wide range of different ligand systems, it only gives a measure of gene expression, which may not be directly related to the level of protein expression. Others have shown that the correlation between mRNA and protein levels is insufficient to predict protein expression levels from quantitative mRNA data (Gygi *et al.*, 1999). Indeed, for some genes, while the mRNA levels are of the same value,

the protein that is expressed varies by more than 20-fold. Conversely, invariant steady-state levels of certain proteins were observed with respective mRNA transcript levels that vary by as much as 30-fold (Gygi *et al.*, 1999). RT-PCR quantifies the amount of products of transcription of DNA into mRNA. It cannot give an indication of the rate of translation of mRNA into protein. Other techniques such as Western Blot analysis or quantitative autoradiography must be used to accurately determine protein expression. However, unlike semi-quantitative RT-PCR, these techniques require the generation of expensive radiolabelled probes or ligands, and are unable to detect very low levels of gene expression. Here we have used RT-PCR to determine expression of the ET system in the kidney of both control and FF/Tie2 mice of different ages and sex. As discussed above, we have used autoradiography to quantify ET<sub>A</sub> and ET<sub>B</sub> receptor expression in tissue from young male FF/-- and FF/Tie2 mice. These data were used to corroborate the RT-PCR results.

Across all groups ET<sub>B</sub> gene expression in the kidney, an organ with a high content of endothelium, was down-regulated in the FF/Tie2 compared to FF/-- mice. This was also demonstrated by the quantitative autoradiography experiments using the radiolabelled ET<sub>B</sub> ligand [<sup>125</sup>I]-BQ3020, and is consistent with significant EC-specific ET<sub>B</sub> receptor down-regulation. Furthermore, ET<sub>A</sub> and ECE-1 expression in male FF/Tie2 mice was not significantly different to that in control male animals. The former was also seen in the autoradiography experiments.

It is interesting that young female FF/-- mice demonstrate much greater ET<sub>B</sub> gene expression than male animals. The females also demonstrate a trend towards lower ET<sub>A</sub> expression. Whilst this may represent a true sex difference, the unexpected finding could be caused by experimental error and/ or variation due to oestrus cycle. Due to limitations of our breeding programme at the time these experiments were performed, some of these studies only involved a small number of animals (n = 3). Therefore this surprising result could merely be due to low numbers and a relatively large experimental error. However, as can be seen from Figure 3-21, the error bars are small. Another possibility is that the high ET<sub>B</sub> gene expression is caused by the



effect of the oestrus cycle. ET<sub>B</sub> receptor expression is regulated by 17- $\beta$  oestradiol in cardiac tissue (Nuedling *et al.*, 2003), and the expression of other GPCRs such as  $\beta_1$ -adrenoreceptors (Kam *et al.*, 2004) and AT1 receptors (Nickenig *et al.*, 1998) can alter with the administration of oestrogen. In our studies, we failed to control for the oestrus cycle when sampling kidneys from the female mice. Other studies have shown a sex difference in ET receptor expression. Female rats show a reduced haemodynamic response to exogenous ET-1 compared with male rats (Tatchum-Talom *et al.*, 2000). In human saphenous vein studies, increased ET<sub>B</sub> receptor expression has been demonstrated in women compared to men (Ergul *et al.*, 1998; Kellogg *et al.*, 2001). Expression of eNOS, which mediates the action of EC ET<sub>B</sub> receptor activation is also increased in female rats (Taylor *et al.*, 2003a). Increased nicotinamide-adenine dinucleotide phosphate (NAD(P)H) oxidase activity and superoxide production is associated with increased ET<sub>B</sub> gene expression, in a model of EC specific ET-1 overexpression (Amiri *et al.*, 2004). Thus a gender difference in oxidative stress (Baba *et al.*, 2005; Borrás *et al.*, 2003) may partly explain the observed increased ET<sub>B</sub>:ET<sub>A</sub> expression demonstrated by female mice in my study. The effect of gender on the gene expression of components of the ET-1 system supports our group's earlier decision to include young male mice only in our studies. If experimental and control groups were composed of different proportions of male and female mice, then measured variables might differ due to gender differences in ET-1 system expression rather than due to the effect of EC-specific ET<sub>B</sub> receptor down-regulation.

Age, in contrast to gender, was seen to have less of an effect on renal ET system expression. The kidneys of 12-month old male mice exhibit a broadly similar pattern of renal ET system expression in comparison to young males. This differs from rats where kidneys have been shown to demonstrate decreased ET<sub>A</sub> and increased ET<sub>B</sub> receptor expression with age (Hochoer *et al.*, 1995).

Down-regulation of EC ET<sub>B</sub> in both male and female mice had no significant effect on the expression of ECE-1 mRNA. In contrast, studies performed with cultured rat

ECs, have revealed that ET-1 acts in an ET<sub>B</sub> dependent manner to inhibit both the mRNA and protein levels of ECE-1 (Naomi *et al.*, 1998). As we did not find increased gene expression following down-regulation of EC ET<sub>B</sub>, our work suggests that ET-1 is acting via ET<sub>B</sub> receptors that are expressed on cells other than ECs.

Thus, by generating null ET<sub>B</sub> mice, we have demonstrated that recombination of the ET<sub>B</sub> gene, resulting in excision of exons 3 and 4 is sufficient to prevent expression of the ET<sub>B</sub> receptor. The Tie2 promoter restricts Cre expression to the endothelium, and so when floxed ET<sub>B</sub> mice are crossed with Tie2-Cre mice, mice featuring EC-specific ET<sub>B</sub> receptor down-regulation are produced. The autoradiography data provide evidence of EC specific ET<sub>B</sub> receptor down-regulation in the FF/Tie2 mice. Finally, we have shown that EC ET<sub>B</sub> receptor expression has minimal effect on either ET<sub>A</sub> or ECE-1 expression in young male mice.

## 4 CHAPTER 4: ROLE OF THE EC-ET<sub>B</sub> RECEPTOR IN THE CONTROL OF SYSTEMIC BP

### 4.1 INTRODUCTION

Defining the role played by the ET<sub>B</sub> receptor in the control of systemic BP is complicated due to the opposing action of ET<sub>B</sub> receptors expressed on neighbouring cell types. For example activation of ET<sub>B</sub> receptors on ECs promotes release of NO and PGI<sub>2</sub>, causing vasodilatation, whereas VSM ET<sub>B</sub> receptors act to increase intracellular calcium, resulting in vasoconstriction (Gray *et al.*, 1996). ET<sub>B</sub> receptors are also responsible for scavenging ET-1 from the plasma (Berthiaume *et al.*, 2000; Burkhardt *et al.*, 2000; Fukuroda *et al.*, 1994), preventing increased vasoconstrictive ET<sub>A</sub> receptor activation due to elevated plasma ET-1 concentrations. Furthermore ET<sub>B</sub> receptors are also central to the maintenance of sodium homeostasis (Clavell *et al.*, 1995; Kohan, 1997).

Studies with pharmacological antagonists have helped to reveal the action of ET<sub>B</sub> receptor activation on BP. ET<sub>B</sub> receptor blockade with BQ788 causes similar forearm vasoconstriction as that seen with NOS inhibition, suggesting that ET<sub>B</sub> receptors cause tonic vasodilatation mediated by NO (Verhaar *et al.*, 1998). Further work has confirmed that such selective ET receptor blockade has an equivalent effect on systemic haemodynamics (Spratt *et al.*, 2001; Strachan *et al.*, 1999).

Animal models featuring genetic disruption of the ET<sub>B</sub> receptor have also provided useful insights into the role of the ET<sub>B</sub> receptor in BP control. Several groups have shown ET<sub>B</sub> deficient rodents to demonstrate hypertension (Berthiaume *et al.*, 2000; Ohuchi *et al.*, 1999), which is sensitive to salt loading (Gariépy *et al.*, 2000; Murakoshi *et al.*, 2002; Quaschnig *et al.*, 2005). This salt sensitive hypertension is normalised by the sodium channel, ENaC, inhibitor amiloride (Gariépy *et al.*, 2000), suggesting that tonic ET<sub>B</sub> activation exerts its natriuretic effect by inhibiting ENaC. IMCD specific ET-1 KO mice have also been shown to demonstrate salt sensitive hypertension (Ahn *et al.*, 2004), suggesting that ET-1 from IMCD cells acts locally

at ET<sub>B</sub> receptors to regulate natriuresis. However, IMCD specific ET<sub>B</sub> down-regulated mice exhibit salt sensitive hypertension that is less marked than that observed in IMCD ET-1 KO mice (Ge *et al.*, 2006), suggesting that ET<sub>B</sub> located on cells other than IMCD (such as ECs) may be important in sodium excretion.

The aim of this study was to determine whether endogenous activation of the EC ET<sub>B</sub> receptor, through either its effect on natriuresis or on vascular tone, influences the control of systemic BP. Studies using pharmacological blockade or genetic disruption of the ET<sub>B</sub> receptor prevent ET<sub>B</sub> receptor activation on all cell types concurrently. The relative contribution of the EC ET<sub>B</sub> receptor to the control of systemic BP has not been assessed without the confounding influence of simultaneous loss of ET<sub>B</sub> receptor signalling on all other cell types, including the renal tubular cells and VSMCs. EC specific downregulation of ET<sub>B</sub> receptor expression therefore, provides an unique and powerful method by which to examine the relative contribution of ET<sub>B</sub> receptor signalling, in a single cell type, to the regulation of complex physiological systems, such as the control of systemic BP.

BP measurement was carried out in mice using a variety of different techniques. Initial data were acquired by measuring systemic BP under anaesthesia, before moving to chronic carotid artery cannulation, which allowed measurements to be taken under conscious non-restrained conditions. Data were compared on normal and high salt diet. Finally, in order to further improve the quality of our data, radiotelemetry devices were implanted in the mice which allowed for longitudinal studies to be performed on the animals investigating the effect low and high salt diet as well as ET receptor blockade on BP control.

## **4.2 METHODS/PROTOCOLS**

### **4.2.1 Measurement of BP under anaesthesia**

FF/Tie2 and control mice were anaesthetised with isoflurane and their BP measured by means of carotid cannulation as described in section 2.7.

### **4.2.2 Measurement of BP under conscious unrestrained conditions using fluid filled catheters**

Following 3 weeks of feeding with either normal or high salt powdered diet, carotid artery catheters were inserted into FF/Tie2 and control mice under anaesthesia, brought to the skin in the interscapular region, flushed and capped as described in section 2.8.2. The catheters were flushed at 24 hours, and used to measure BP 48 hours post operatively (see section 2.8.2).

### **4.2.3 Continuous measurement of BP under conscious unrestrained conditions using radiotelemetry**

In the 7 days prior to insertion of the radiotelemetry devices, the mice were housed singly and fed normal salt diet to allow them to habituate to their surroundings. The radiotelemetry devices were inserted as detailed in section 2.8.3. Due to limited numbers of receiving pads a maximum of 20 mice could be studied at any one period. Therefore the study was conducted in 2 phases, according to the protocols below (Figure 4-1 and Figure 4-2). Body weight, gel intake and water consumption were measured daily. Data was analysed and compared between genotypes and treatment periods as described in section 2.8.3.

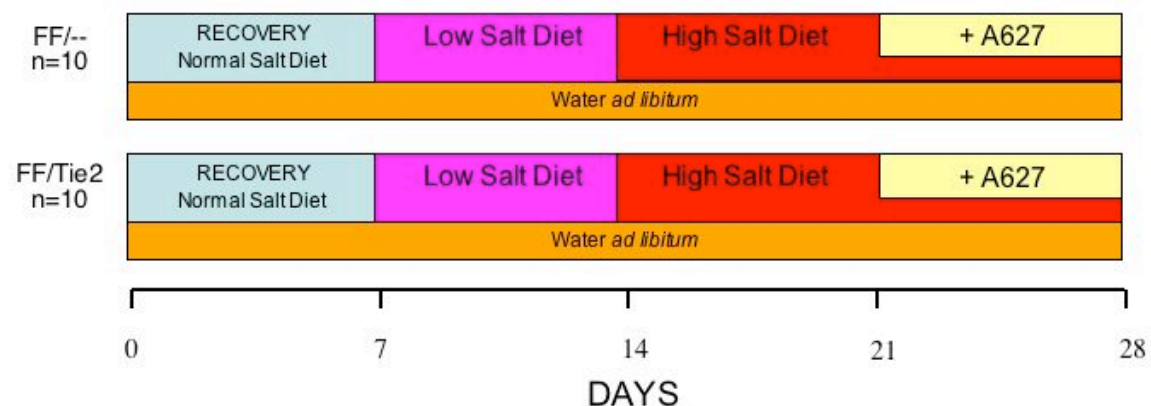


**Figure 4-1: Study protocol for the first phase of the telemetry BP study**

Radiotelemetry devices were inserted into equal numbers ( $n = 10$ ) of FF/Tie2 mice and FF/-- controls. In week 1 the mice were fed normal salt (0.76% NaCl) diet; in week 2 low salt (0.076% NaCl) diet; in week 3 high salt (7.6% NaCl) diet; and in the final week high salt diet plus the  $ET_A$  antagonist ABT627 ( $5 \text{ mg.kg}^{-1}.\text{day}^{-1}$ ). Mice were given access to drinking water *ad libitum* throughout the course of the study.

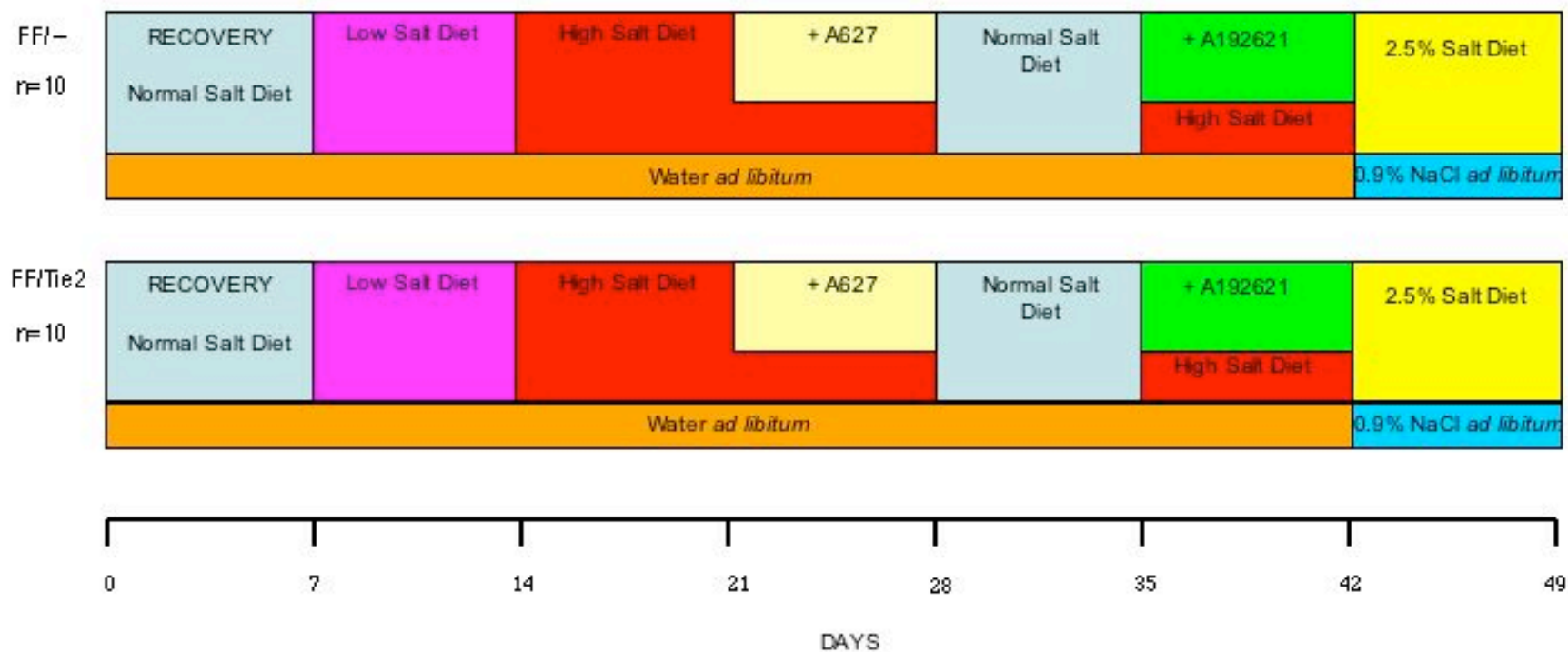


**Figure 4-2: Study protocol for the second phase of the telemetry BP study**

During the first four weeks, the mice were treated as in the first study. In week 5 the mice were fed normal salt (0.76% NaCl) diet; in week 6 high salt (7.6% NaCl) diet plus the  $ET_B$  antagonist A192621 ( $30 \text{ mg} \cdot \text{kg}^{-1} \cdot \text{day}^{-1}$ ); and in the final week 2.5% NaCl. For the first 6 weeks of the study mice were given *ad libitum* access to drinking water. In the final week, whilst fed 2.5% NaCl gel diet they were allowed access to 0.9% saline *ad libitum*.

At the end of the study, mice were culled by cervical dislocation, and blood collected by direct cardiac puncture for haemocrit determination. Hearts were harvested and the right ventricle (RV) and left ventricle plus septum (LV+S) weights were determined.

Hearts and chamber weights were also assessed for a separate cohort of aged (52-60 week old) male mice fed only normal salt (0.76% NaCl) diet.



## 4.3 RESULTS

### 4.3.1 Measurement of BP under anaesthesia

Using fluid filled catheters, inserted into the common carotid artery, to measure BP gave a rather damped trace. Sample traces for individual WW/-- and FF/Tie2 mice are shown (Figure 4-3 and Figure 4-4). Due to the low pulse pressure observed with these catheters, only mean arterial BP (MABP) was recorded.

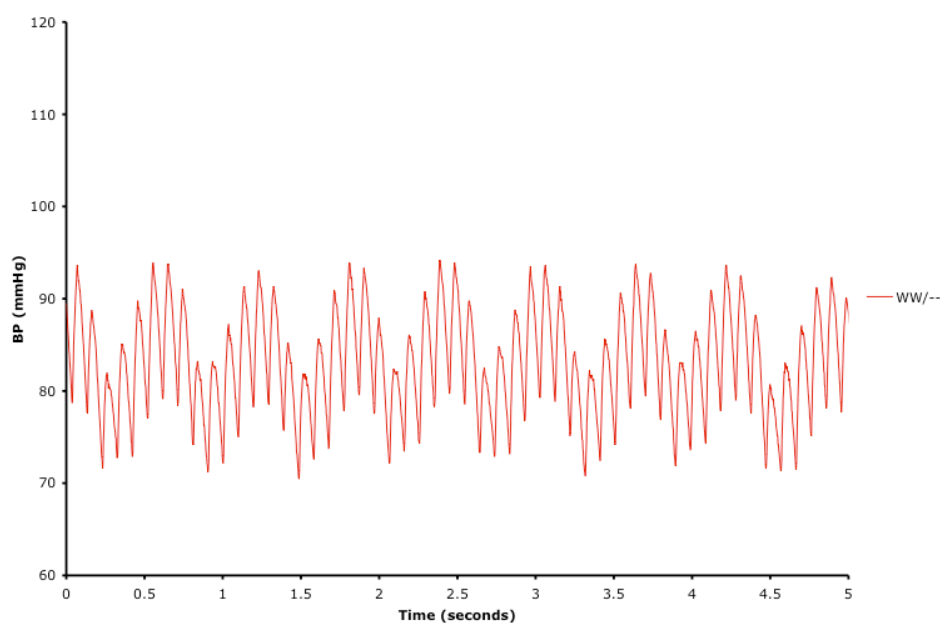


**Figure 4-3 Representative BP trace of an anaesthetised WW/-- mouse.**

Five-second sample from the arterial BP recording, performed using fluid filled carotid catheters in anaesthetised mice.

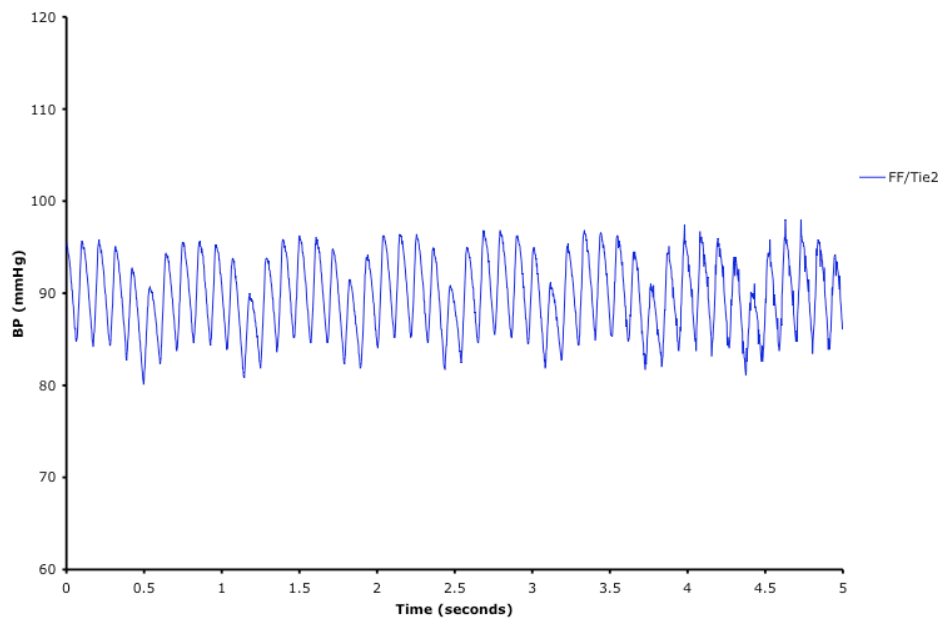


**Figure 4-4 Representative BP trace of an anaesthetised FF/Tie2 mouse.**

Five second sample from the arterial BP recording, performed using fluid filled carotid catheters in anaesthetised mice.

The MABP of the FF/Tie2 mice ( $97.0 \pm 3.59$  mmHg;  $n=6$ ) was significantly higher than that of controls ( $80.08 \pm 3.96$  mmHg;  $n=12$ ;  $p<0.05$ ) when measured under isoflurane anaesthesia. These results are illustrated in Figure 4-5 below.

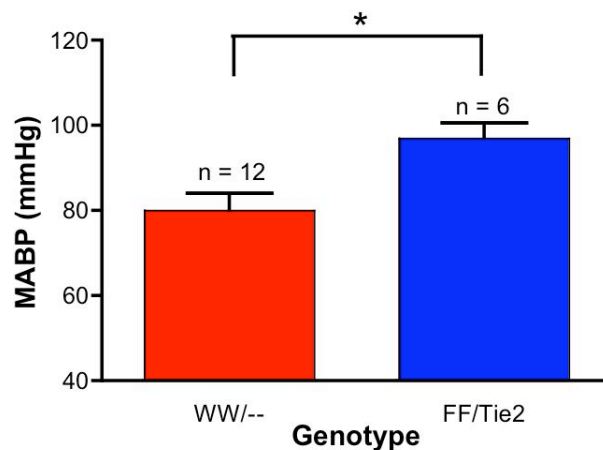


**Figure 4-5: MABP of anaesthetized animals**

Mean arterial BP of anaesthetised WW/-- and FF/Tie2 mice on normal salt diet (\* $p<0.05$ , student's T test).

There was no difference in heart rate between and the WW/-- (mean  $\pm$  SEM: 540  $\pm$  22.1 bpm) and FF/Tie2 animals (534  $\pm$  30 bpm).

#### *4.3.1.1.1 Measurement of BP under conscious unrestrained conditions using fluid filled catheters*

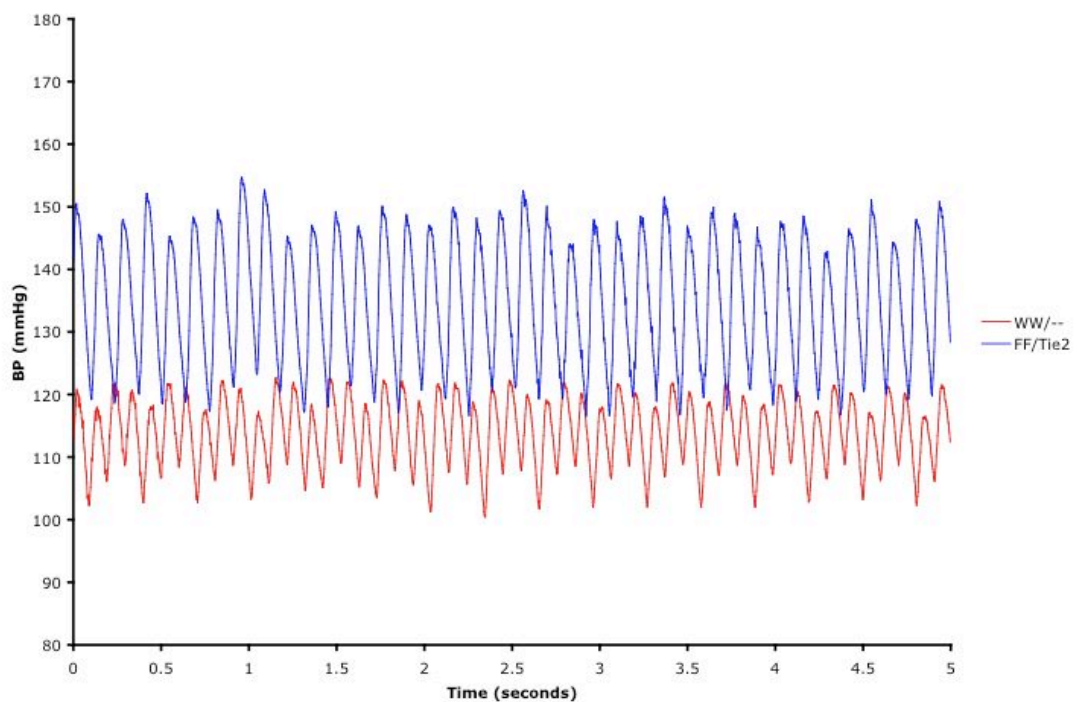
In the 21 days prior to carotid catheter surgery, the mean weights of all four groups of mice did not fall, indicating that normal and high salt diets were well tolerated (Table 4-1). The weight of the WW/-- mice fed normal salt diet was significantly greater than those in other groups.

**Table 4-1: Pre-surgery weights**

Mean body weight (BW) ( $\pm$  SEM) of WW/-- and FF/Tie2 mice fed either normal (0.76% NaCl) or high salt (7.6% NaCl) diet for 3 weeks prior to carotid cannulation surgery (\*  $p < 0.05$ ).

| Genotype                    | WW/--<br>(n = 6)   | FF/Tie2<br>(n = 5) | WW/--<br>(n = 4) | FF/Tie2<br>(n = 5) |
|-----------------------------|--------------------|--------------------|------------------|--------------------|
| Diet                        | 0.76% NaCl         | 0.76% NaCl         | 7.6% NaCl        | 7.6% NaCl          |
| BW 21 days prior to surgery | 36.20 $\pm$ 1.77 * | 26.03 $\pm$ 0.99   | 20.00 $\pm$ 1.50 | 26.82 $\pm$ 1.77   |
| BW at surgery               | 36.20 $\pm$ 1.90 * | 27.38 $\pm$ 1.05   | 25.35 $\pm$ 2.38 | 27.58 $\pm$ 1.35   |

As with the studies performed on anaesthetised animals, the BP traces obtained using the fluid filled intra-carotid catheters 48 hours after the carotid artery cannulation surgery gave artefactually small pulse pressures (Figure 4-6).

**Figure 4-6 Representative BP traces of conscious unrestrained mice.**

Five second sample from the 30 minute recording period in 2 individual conscious unrestrained mice (one of each genotype), performed 48 hours following carotid artery catheter insertion.

The MABP of FF/Tie2 mice ( $137.2 \pm 6.4$  mmHg) was significantly elevated compared to controls ( $113.7 \pm 4.7$  mmHg;  $p < 0.05$ ). High salt diet did not significantly alter the MABP of either genotype (FF/Tie2:  $141.0 \pm 6.7$  mmHg; WW/-:  $118.3 \pm 5.0$  mmHg;  $p < 0.05$ ) (Figure 4-7).

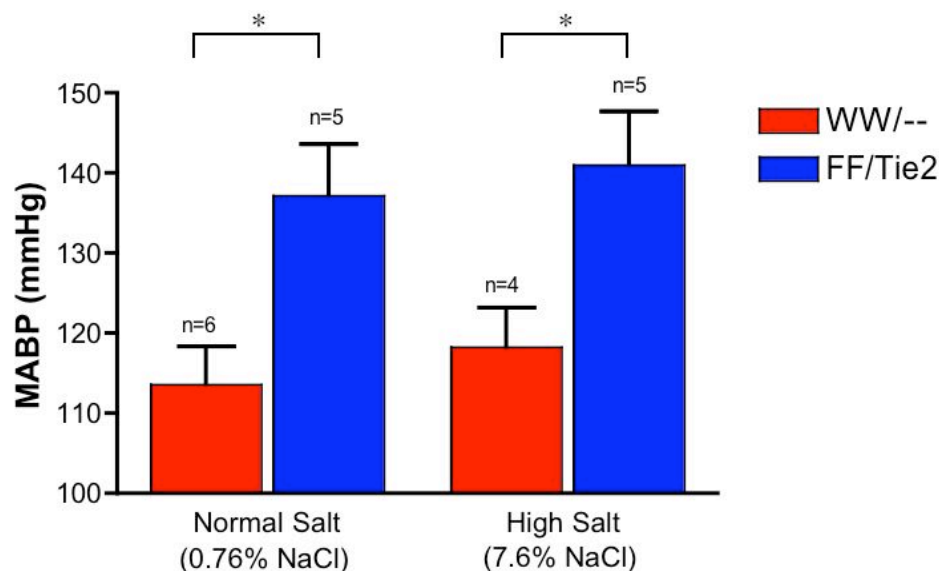


**Figure 4-7: MABP of unrestrained conscious mice**

MABP of WW/-- and FF/Tie2 fed on either normal or high salt chow, measured under conscious unrestrained conditions via carotid cannulation. (\*  $p < 0.05$ ).

The heart rate of FF/Tie2 mice ( $543 \pm 51$  bpm) was not statistically different to that of control animals ( $473 \pm 18$  bpm) on normal salt diet, under conscious unrestrained conditions. Heart rates were unaffected by high salt diet (FF/Tie2:  $454 \pm 50$  bpm; WW/-:  $578 \pm 28$  bpm) (Figure 4-8).

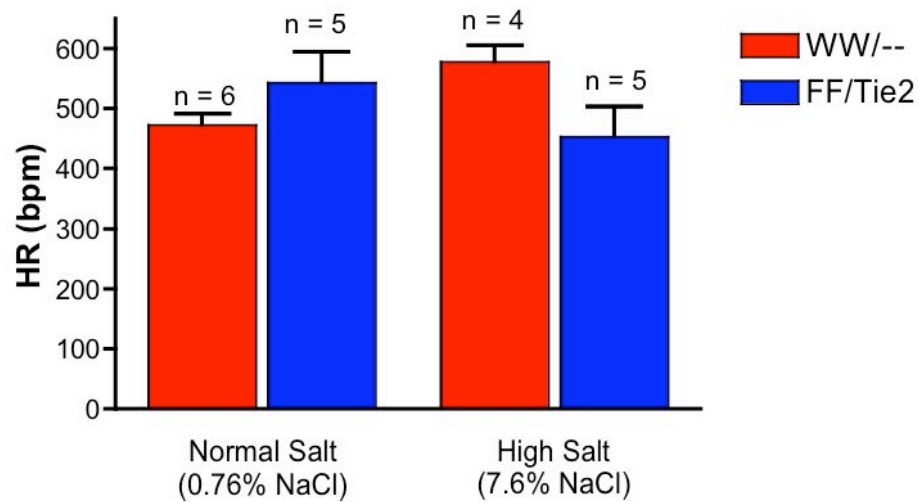


**Figure 4-8: HR of unrestrained conscious mice**

Heart rate of WW/-- and FF/Tie2 fed on either normal or high salt chow, measured under conscious unrestrained conditions via chronic carotid cannulation. No differences were seen.

#### **4.3.2 Continuous measurement of BP under conscious unrestrained conditions using radiotelemetry**

Data from the 2 telemetry studies are presented below. The results from the first study and the initial four weeks of the second study, which both followed the same sequence of diet/ drug treatments, have been combined to improve statistical power. The further data from the second study is detailed in the following section.

The ‘6 hour rolling averaged’ data for each of the parameters measured (SBP, DBP, MABP, and HR) is presented as a series of figures (as described in section 2.8.3):

- a summary trend of 12 hourly values throughout the 4 weeks of the study;
- hourly values during each separate week of the study;
- bar charts comparing the averaged values over the last 72 hours of each treatment period; the averaged minimal day-time values during the last 3 days of the treatment period; and the averaged maximal night-time values during the last 3 days of the treatment period.
- bar charts showing the difference in BP between genotypes (ie FF/Tie2 – FF/--) during the different treatment periods.

4.3.2.1 BOTH STUDIES SYSTOLIC BP

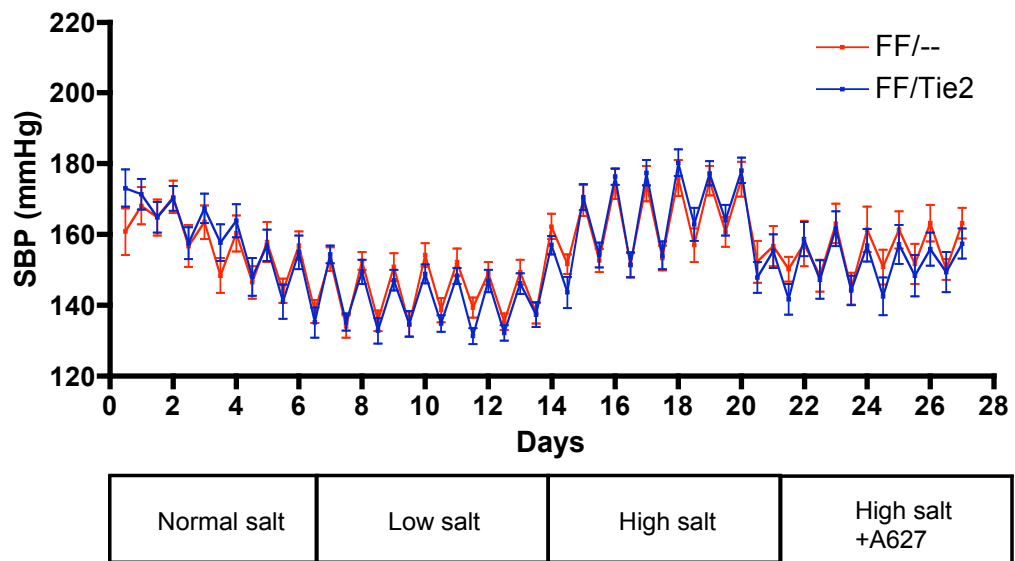


**Figure 4-9: 12 hourly SBP**  
SBP of FF/-- (n=12) and FF/Tie2 (n=10) mice recorded 12 hourly over the first four weeks of both studies.

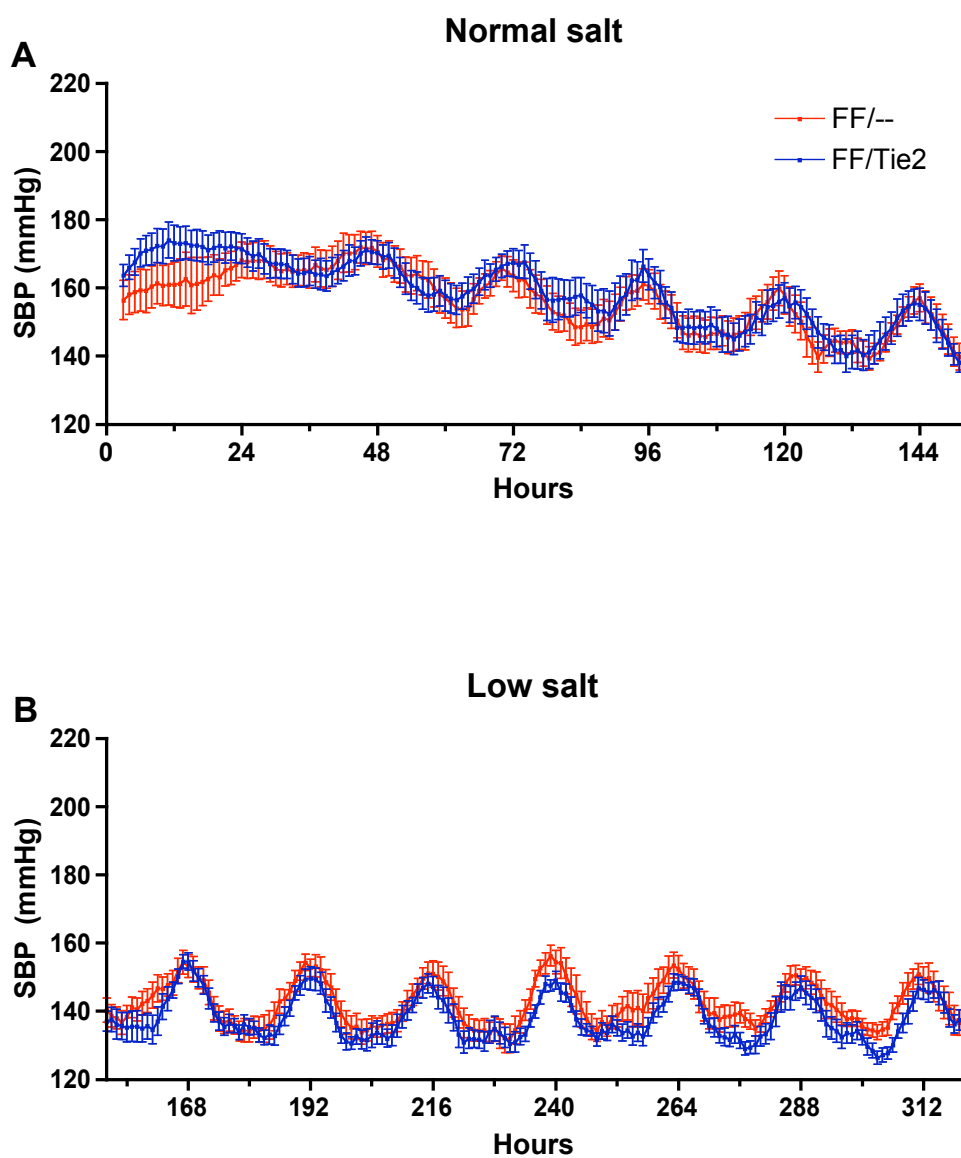


**Figure 4-10: SBP of telemetered mice during the 7 days of normal salt (0.76% NaCl) diet (week 1) [A] and during the 7 days of low salt (0.076% NaCl) diet (week 2) [B].**

Data shown are hourly rolling averages of the FF/-- (n=12) and FF/Tie2 (n=10) mice.



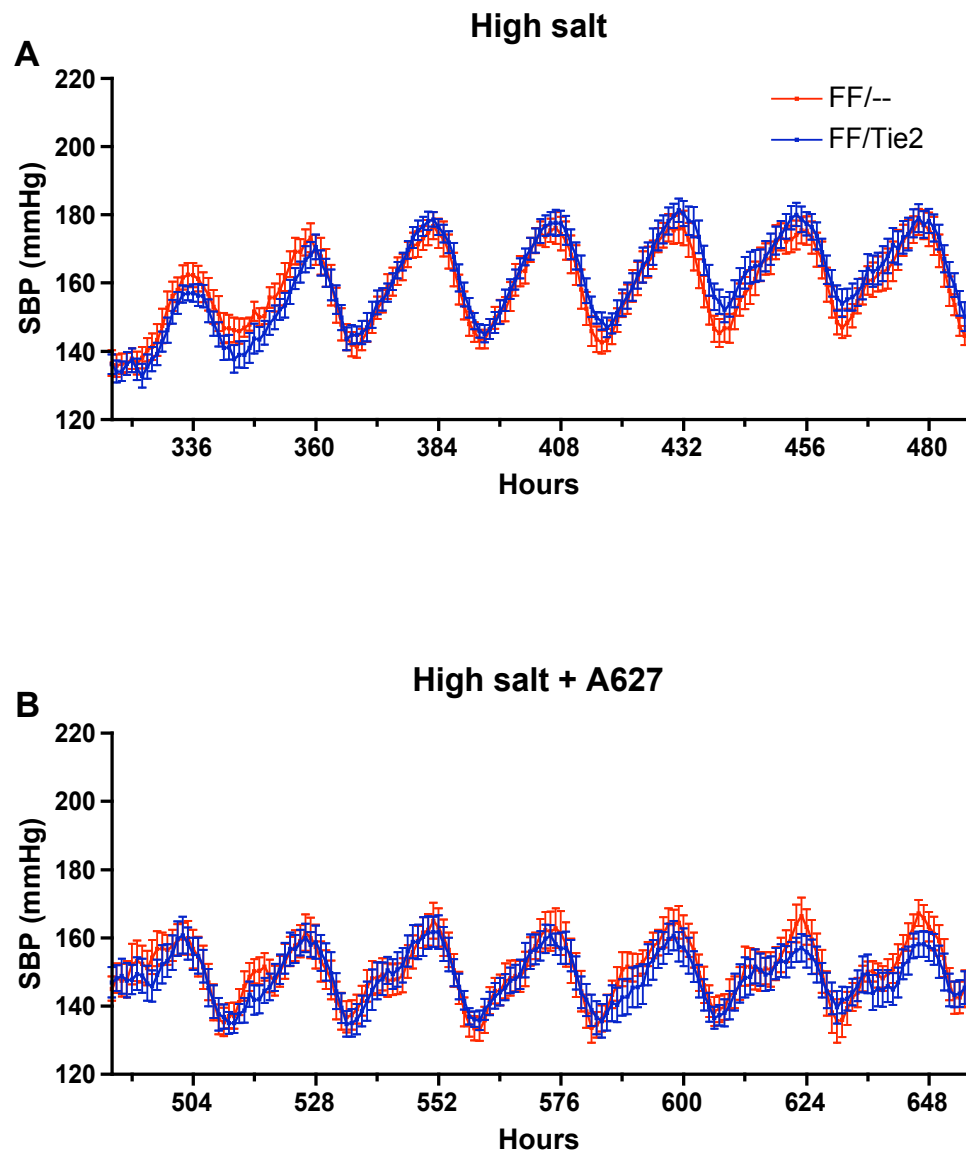


**Figure 4-11: SBP of telemetered mice during the 7 days of high salt (7.6% NaCl) diet (week 3) [A] and during the 7 days of high salt + A627 (5 mg.kg<sup>-1</sup>) diet (week 4) [B].**

Data shown are hourly rolling averages of the FF/-- (n=12) and FF/Tie2 (n=10) mice.



**Figure 4-12: Comparison of: the averaged SBP of FF/-- (n=12) and FF/Tie2 (n=10) mice during the last 72 hours of each week-long dietary period [A]; the averaged minimal SBP values during the day [B]; and the averaged maximal SBP values during the night [C].**

During the last 3 days of each treatment period, no differences were seen between genotypes when the mice were fed low salt (FF/Tie2:  $137.4 \pm 0.72$  mmHg; FF/--:  $142.1 \pm 2.50$  mmHg), normal salt (FF/Tie2:  $151.0 \pm 4.27$  mmHg; FF/--:  $149.5 \pm 4.02$  mmHg) or high salt diet (FF/Tie2:  $166.0 \pm 2.99$  mmHg; FF/--:  $162.2 \pm 3.81$  mmHg) (Figure 4-12A). The SBP of both FF/Tie2 and control mice rose with increased salt in the diet (Figure 4-12A) – an effect that was reversed by administration of the ET<sub>A</sub> antagonist ABT627 (Figure 4-12A).

Similarly, no differences were seen between genotypes at the extremes of circadian rhythm – neither around midday (when the mice are most likely to be sleeping) nor during the middle of the night (when the mice are most likely to be active) (Figure 4-12B and C).

#### 4.3.2.2 BOTH STUDIES – DIASTOLIC BP

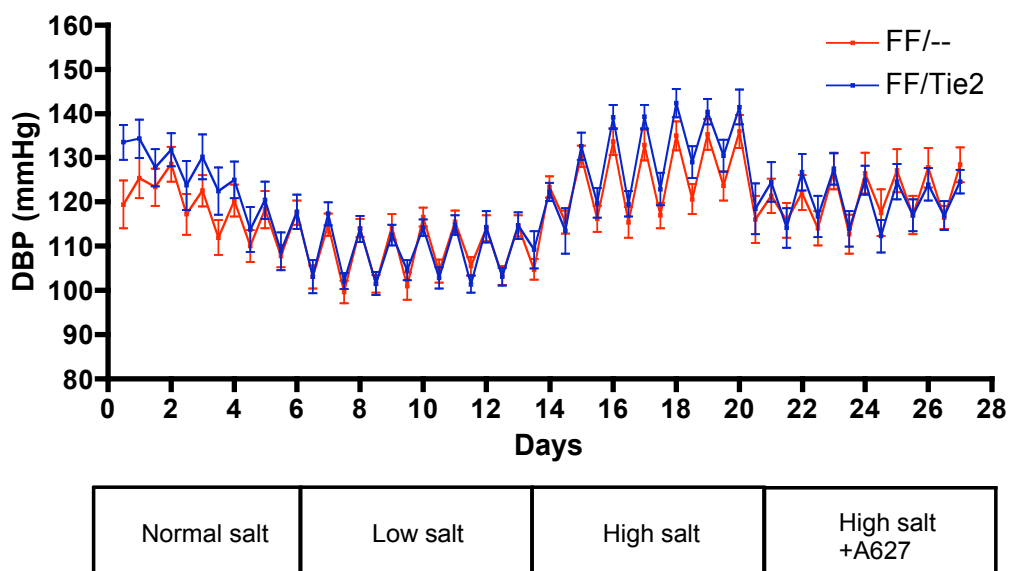


**Figure 4-13: 12 hourly DBP**

DBP of FF/-- (n=12) and FF/Tie2 (n=10) mice recorded 12 hourly over the first four weeks of both studies.

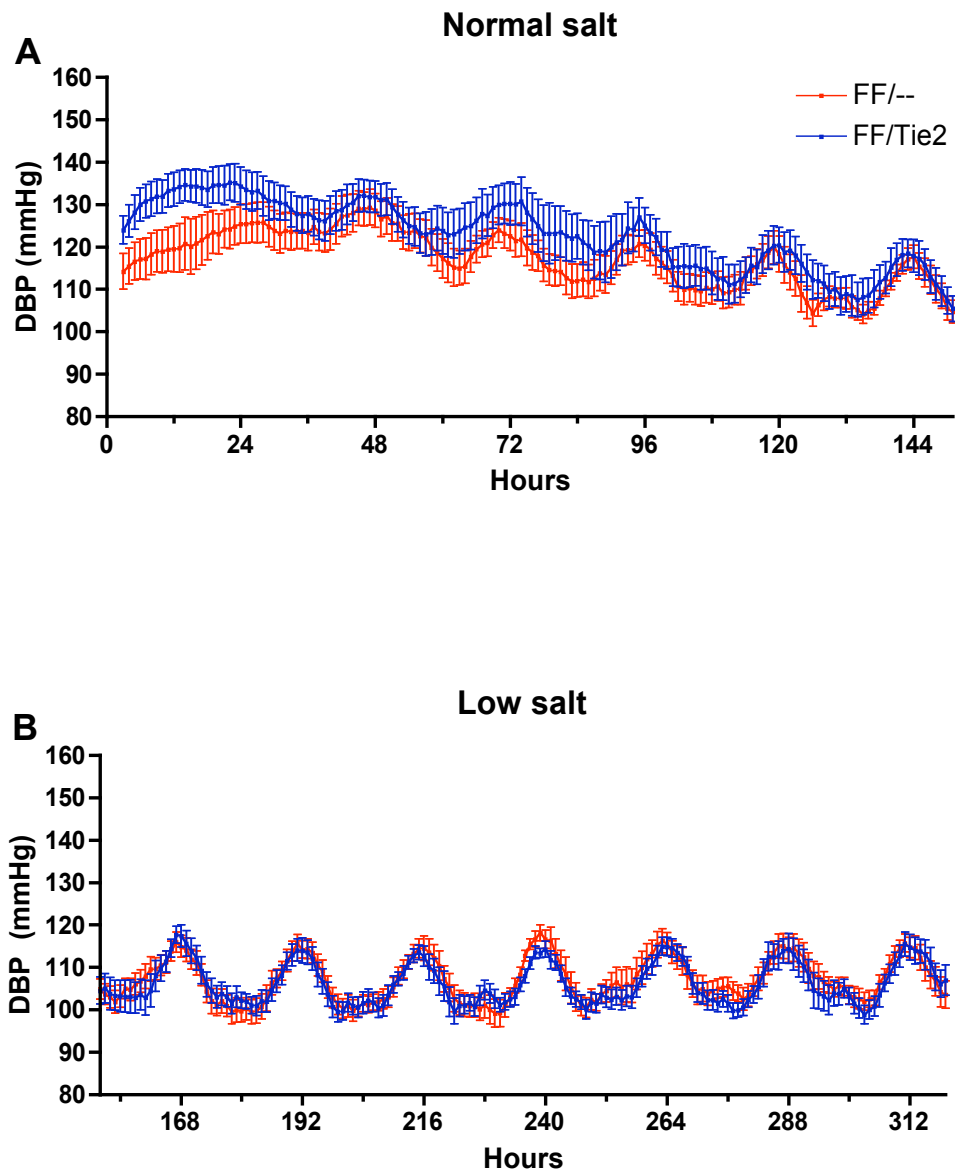


**Figure 4-14: DBP of telemetered mice during the 7 days of normal salt (0.76% NaCl) diet (week 1) [A] and during the 7 days of low salt (0.076% NaCl) diet (week 2) [B].**

Data shown are hourly rolling averages of the FF/-- (n=12) and FF/Tie2 (n=10) mice.

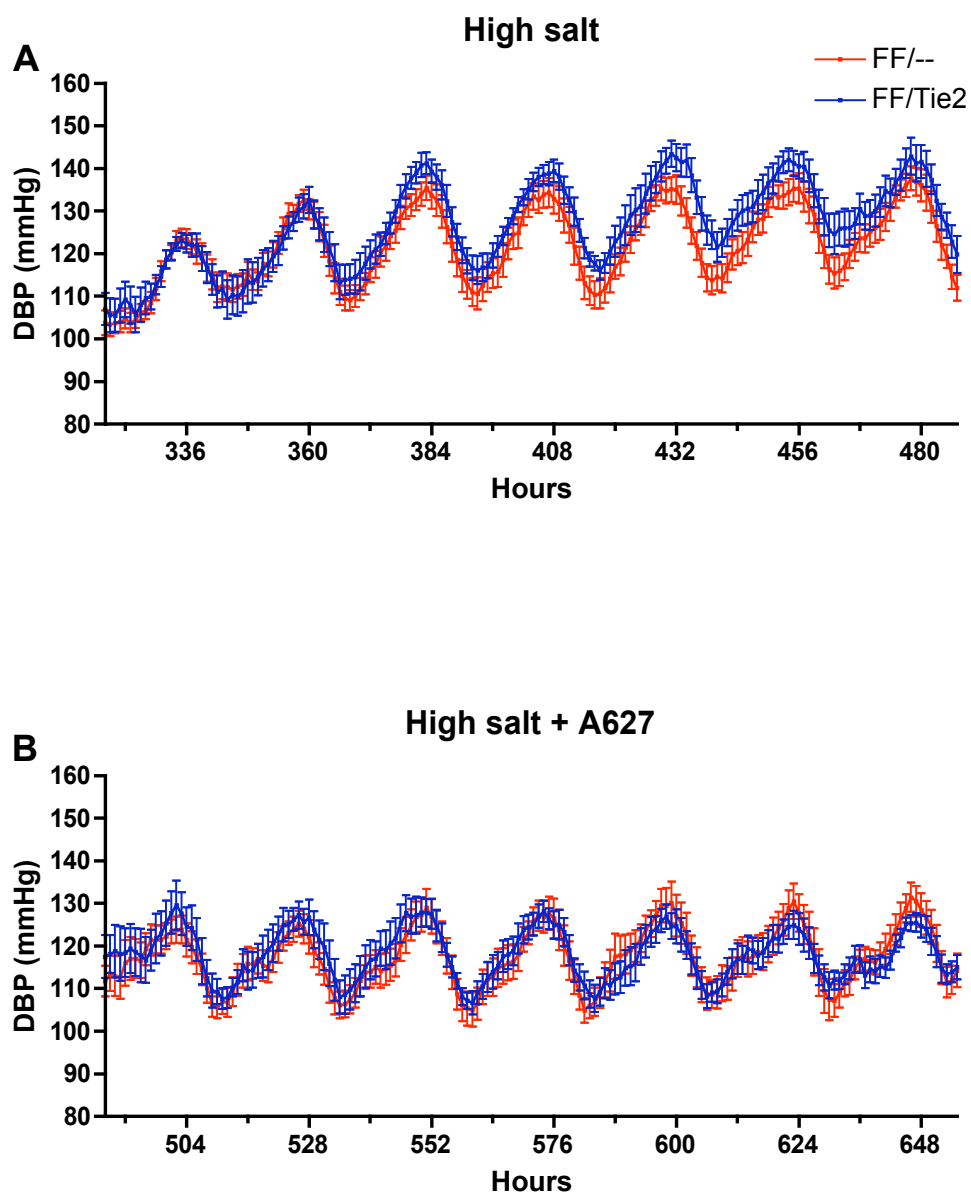


**Figure 4-15: DBP of telemetered mice during the 7 days of high salt (7.6% NaCl) diet (week 3) [A] and during the 7 days of high salt + A627 (5 mg.kg<sup>-1</sup>) diet (week 4) [B].**

Data shown are hourly rolling averages of FF/-- (n=12) and FF/-- (n=10) mice.

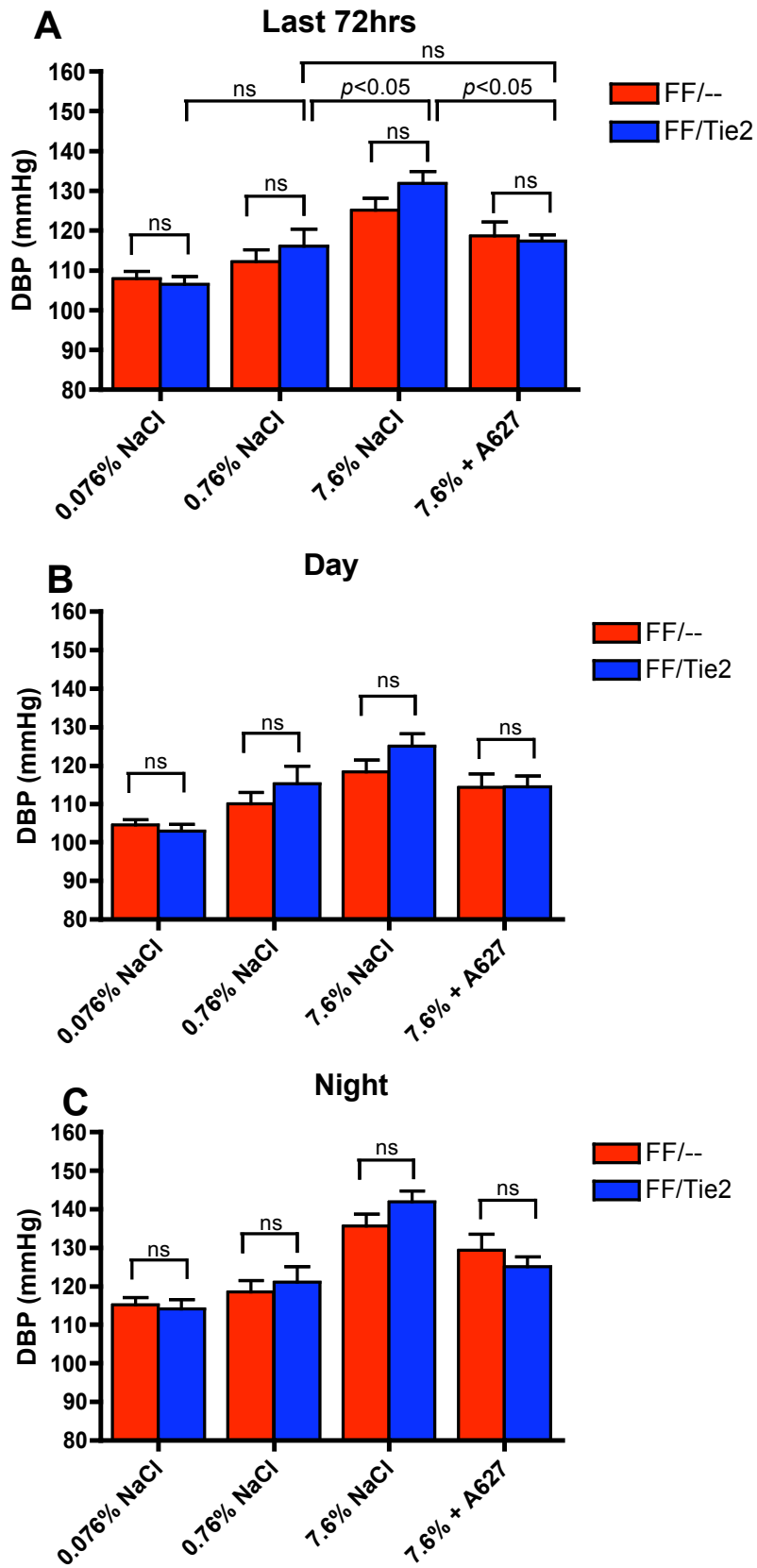


**Figure 4-16: Comparison of: the averaged DBP of FF/-- (n=12) and FF/Tie2 (n=10) mice during the last 72 hours of each dietary period [A]; the averaged minimal DBP values during the day [B]; and the averaged minimal DBP values during the night [C].**

During the last 3 days of each treatment period, no difference was seen between genotypes on low salt (FF/Tie2:  $106.6 \pm 1.91$  mmHg; FF/--:  $107.9 \pm 1.79$  mmHg), normal salt (FF/Tie2:  $116.1 \pm 4.29$  mmHg; FF/--:  $112.2 \pm 2.89$  mmHg) or high salt diet (FF/Tie2:  $131.9 \pm 2.86$  mmHg; FF/--:  $125.2 \pm 2.90$  mmHg) (Figure 4-16A).

Increased salt in the diet caused the DBP to rise in both genotypes, an effect that was reversed by the co-administration of  $ET_A$  blockade (Figure 4-16A).

During the middle of the day and the middle of the night no differences were seen between the DBP of FF/Tie2 and control mice (Figure 4-16B and C).

#### 4.3.2.3 BOTH STUDIES – MEAN BP

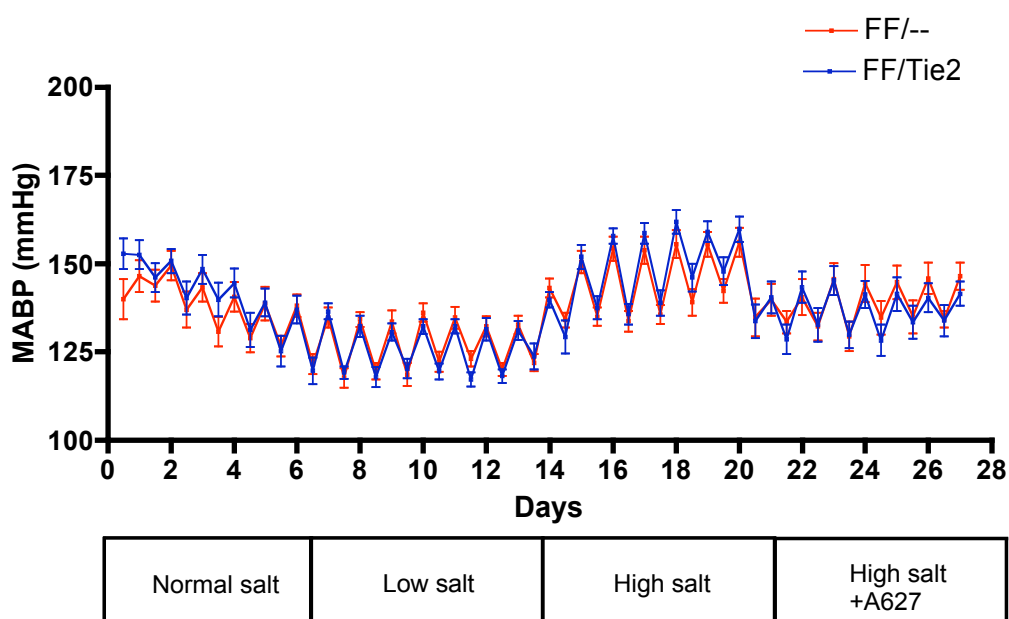


**Figure 4-17: 12 hourly MBP**

MBP of FF/-- (n=12) and FF/Tie2 (n=10) mice recorded 12 hourly over the first four weeks of both studies.

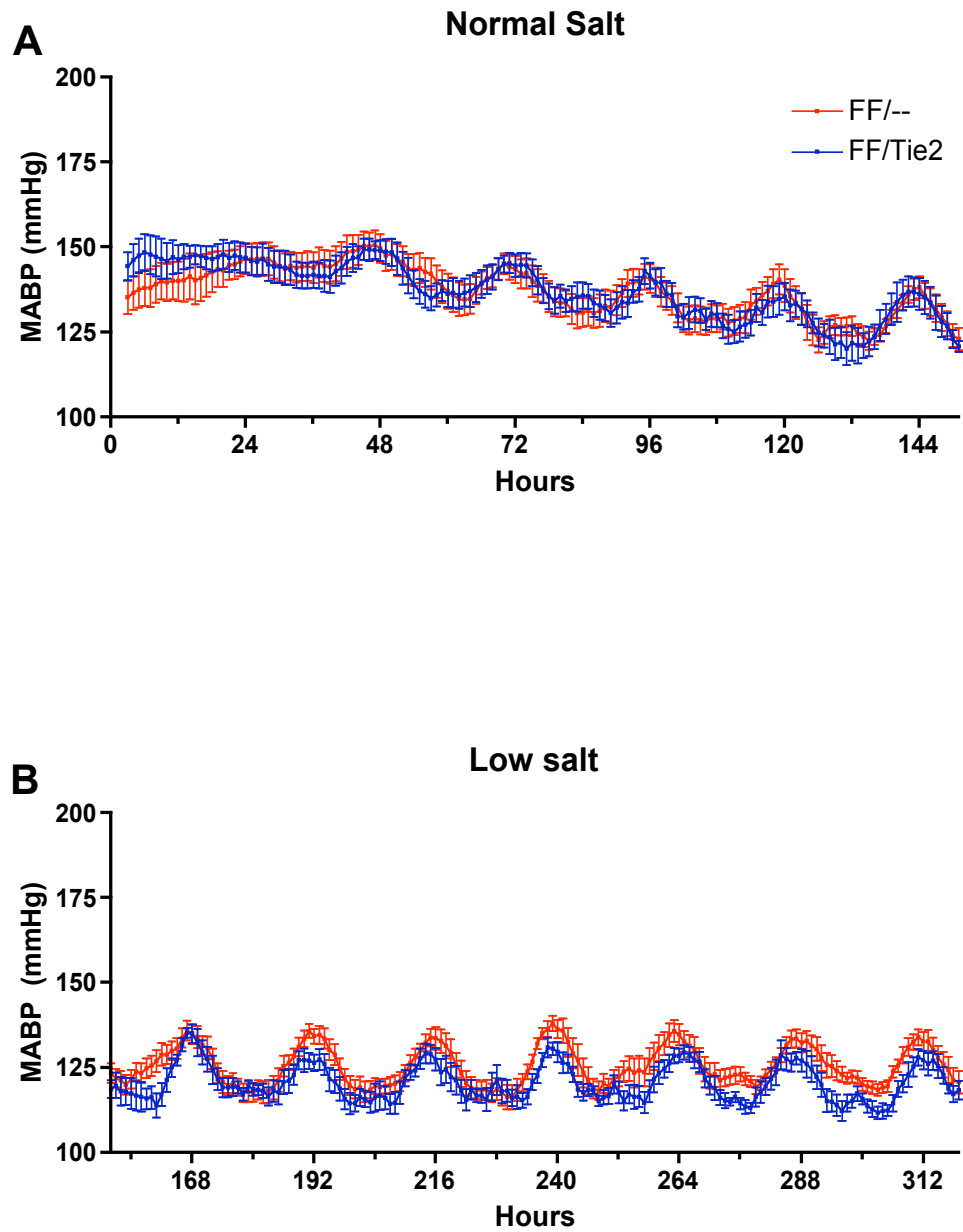


**Figure 4-18: MBP of telemetered mice during the 7 days of normal salt (0.76% NaCl) diet (week 1) [A] and during the 7 days of low salt (0.076% NaCl) diet (week 2)[B].**

Data shown are hourly rolling averages of FF/-- (n=12) and FF/Tie2 (n=10) mice.



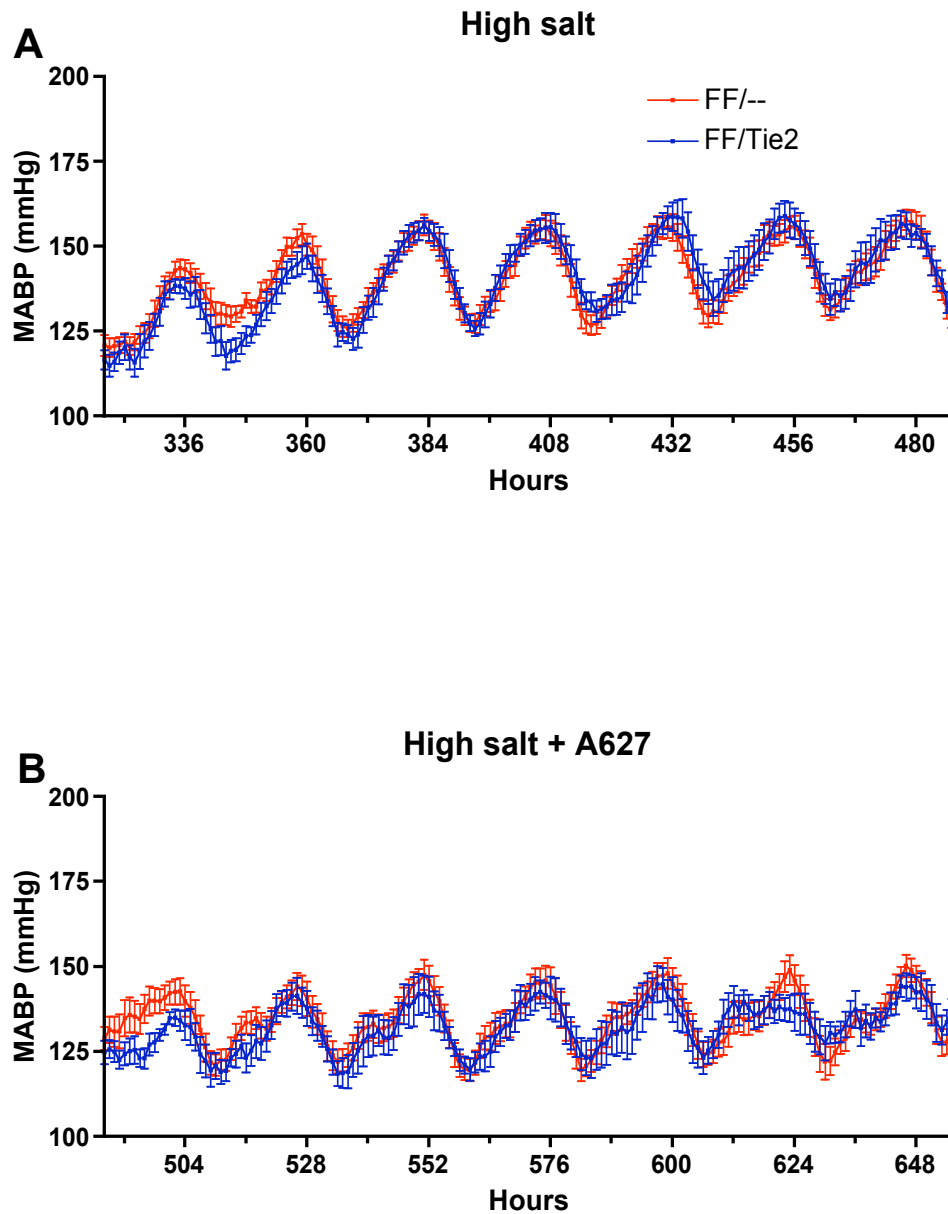


**Figure 4-19: MBP of telemetered mice during the 7 days of high salt (7.6% NaCl) diet (week 3) [A] and during the 7 days of high salt + A627 (5 mg.kg<sup>-1</sup>) diet (week 4) [B].**

Data shown are hourly rolling averages of the FF/-- (n=12) and FF/Tie2 (n=10) mice.



**Figure 4-20: Comparison of: the averaged MBP of FF/-- (n=12) and FF/Tie2 (n=10) mice during the last 72 hours of each week-long dietary period [A]; the averaged minimal MBP values during the day [B]; and the averaged minimal MBP values during the night [C].**

No significant difference was seen between genotypes on low (FF/Tie2:  $122.7 \pm 1.52$  mmHg; FF/--:  $125.7 \pm 1.85$  mmHg), normal (FF/Tie2:  $133.8 \pm 4.0$  mmHg; FF/--:  $131.5 \pm 3.33$  mmHg), or high salt diet (FF/Tie2:  $149.2 \pm 2.71$  mmHg; FF/--:  $143.9 \pm 2.97$  mmHg) during the last 3 days of each treatment period (Figure 4-20A). Salt had a hypertensive effect on the MBP of both genotypes that was reversed by addition of ABT627 (Figure 4-20A).

Even at the extremes of circadian rhythm – during the middle of the day and around midnight – FF/Tie2 mice were not shown to be hypertensive compared to FF/-- controls (Figure 4-20B and C).

#### 4.3.2.4 BOTH STUDIES – HEART RATE

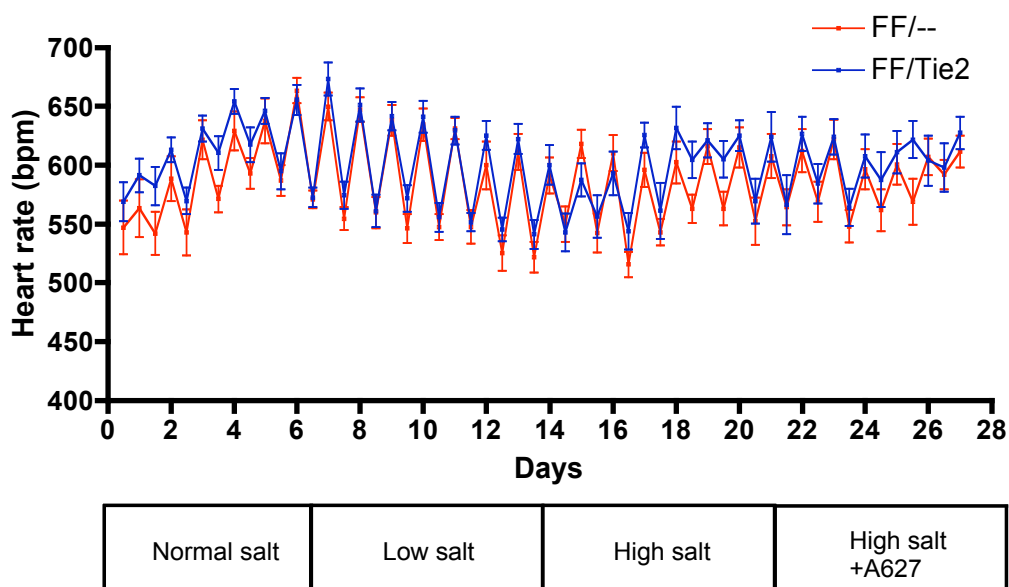


**Figure 4-21: 12 hourly heart rate.**

Heart rate of FF/-- (n=12) and FF/Tie2 (n=10) mice recorded 12 hourly over a 4-week period (both studies combined).

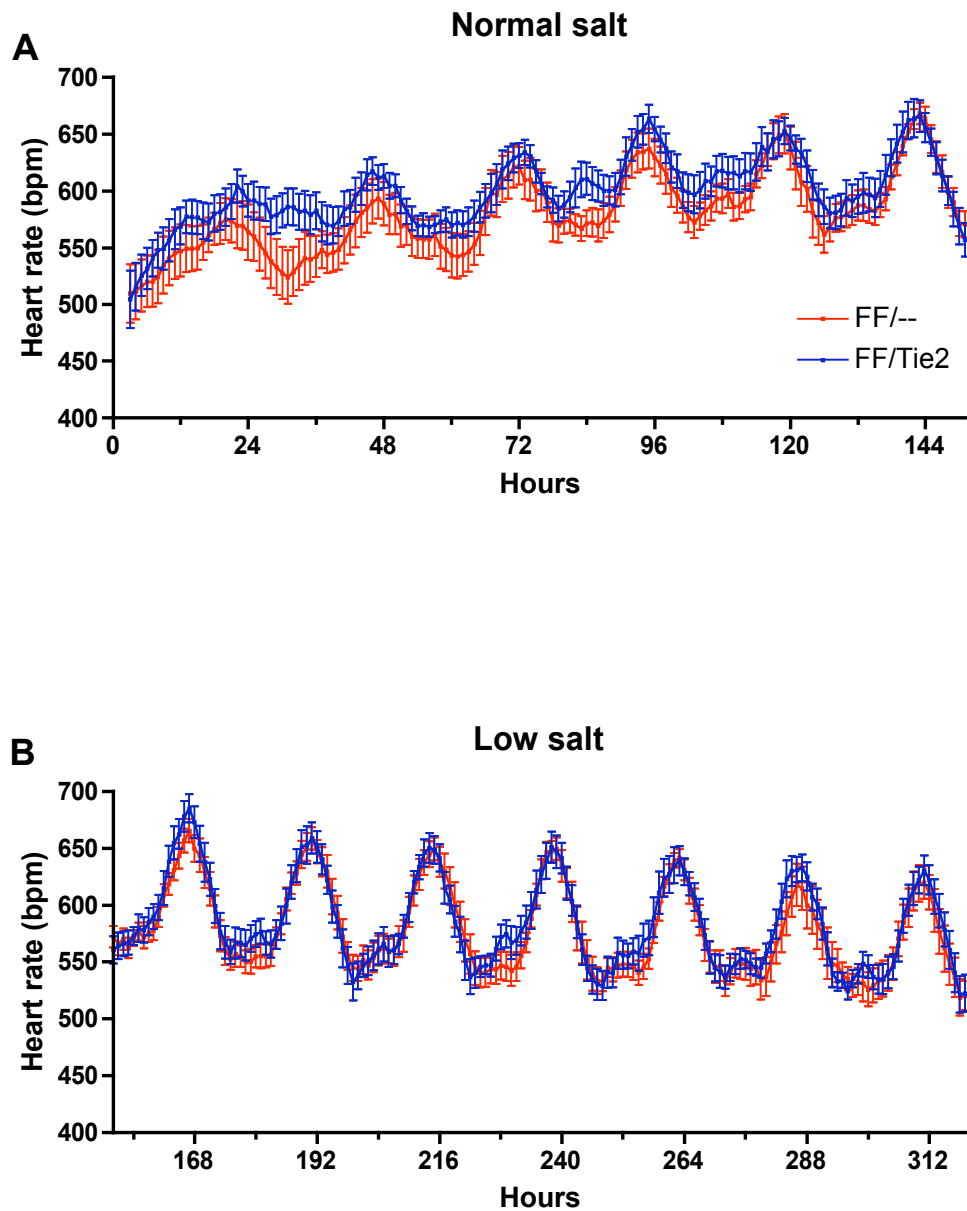


**Figure 4-22: Heart rate of telemetered mice during the 7 days of normal salt (0.76% NaCl) diet (week 1) [A] and during the 7 days of low salt (0.076% NaCl) diet (week 2) [B].**

Data shown are hourly rolling averages of the FF/-- (n=12) and FF/Tie2 (n=10) mice.

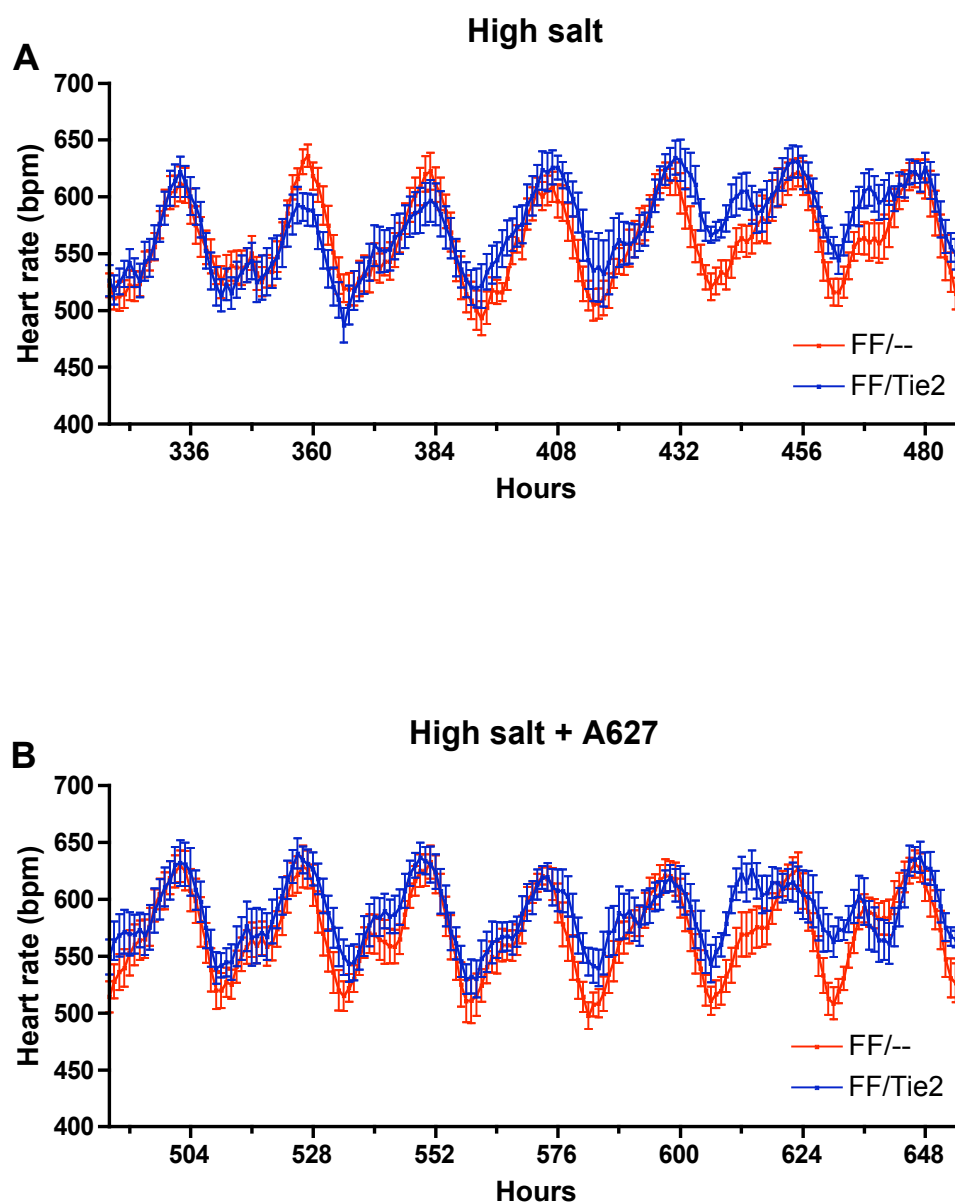


**Figure 4-23: Heart rate of telemetered mice during the 7 days of high salt (7.6% NaCl) diet (week 3) [A] and during the 7 days of high salt + A627 (5 mg.kg<sup>-1</sup>) diet (week 4) [B].**

Data shown are hourly rolling averages for FF/-- (n=12) and FF/Tie2 (n=10) mice.

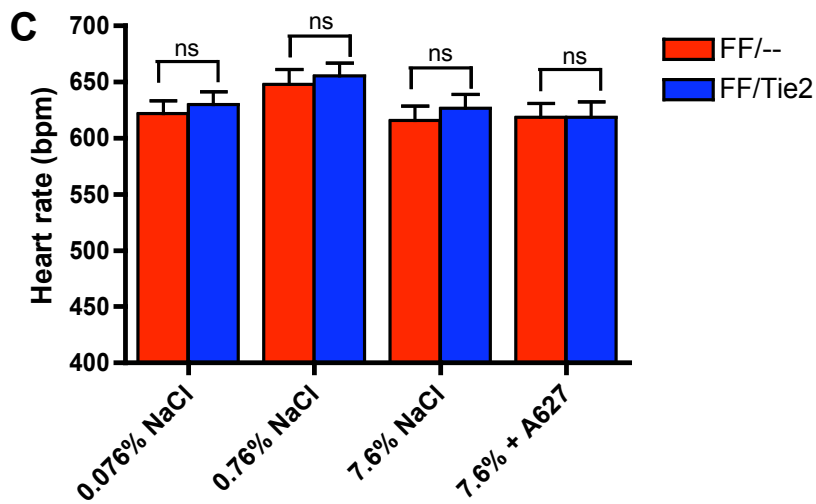
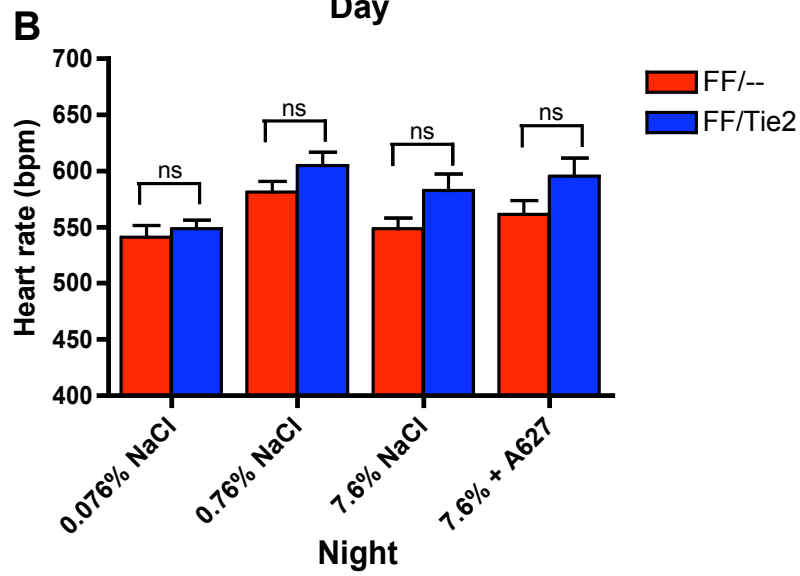
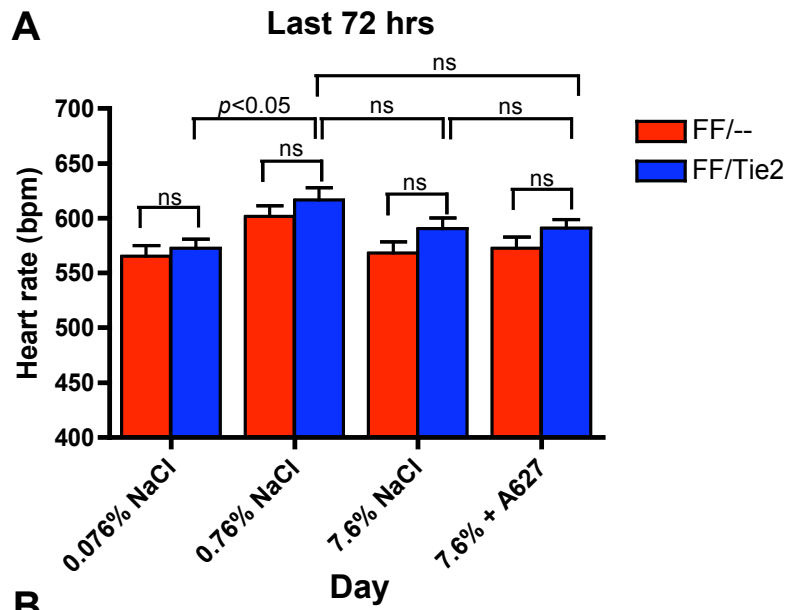


**Figure 4-24: Comparison of: the averaged HR of FF/-- (n=12) and FF/Tie2 (n=10) mice during the last 72 hours of each week-long dietary period [A]; the averaged minimal HR during the day [B]; and the averaged maximal HR values during night [C].**

No difference in HR was seen between genotypes in the last 72 hours of each treatment period. As expected, the mice were most tachycardic in the week following surgery (normal salt diet). After this, in contrast to BP, there was no clear relationship between dietary salt and HR (Figure 4-24A). ET<sub>A</sub> blockade with ABT627 had no influence on HR.

No significant difference in HR was seen between genotypes either in the middle of the day or night (Figure 4-24B and C).

#### 4.3.2.5 BOTH STUDIES – WATER, GEL CONSUMPTION AND BODY WEIGHT

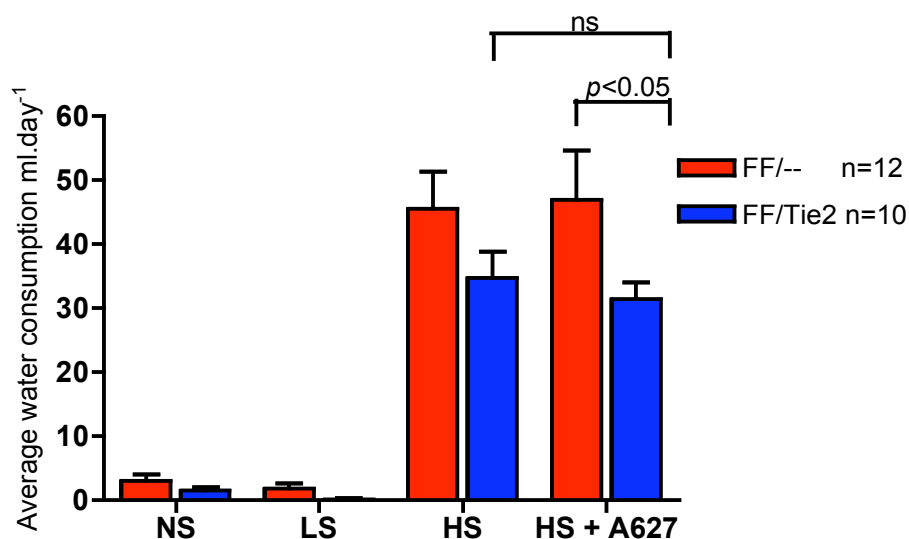


**Figure 4-25: Average daily water consumption**

Water consumed by FF/-- and FF/Tie2 mice when fed normal salt diet (NS), low salt diet (LS), high salt diet (HS) and high salt diet plus the ET<sub>A</sub> antagonist ABT627 (5mg.kg<sup>-1</sup>.day<sup>-1</sup>).

Water intake increased dramatically with the introduction of high salt diet. Although FF/Tie2 mice demonstrated a trend toward reduced drinking when fed high salt diet,

no significant difference in daily water consumption was observed between genotypes when the mice were fed normal, low or high salt diet (Figure 4-25). When fed ABT627 as well as high salt diet, FF/Tie2 mice drank significantly less than controls. However, despite lowering BP in both genotypes compared to the period when they were fed high salt diet alone, introduction of ABT627 to the high salt diet had little effect on the water consumption of each genotype.

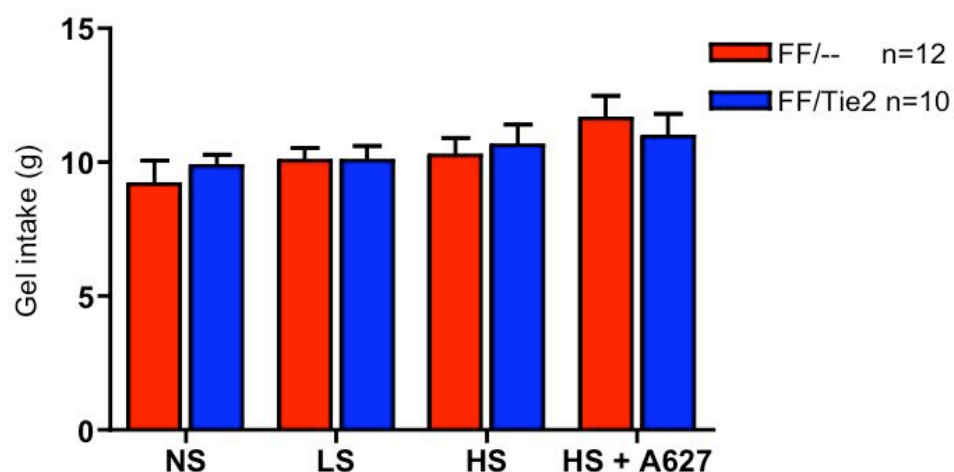


**Figure 4-26: Average daily gel intake**

Gel diet consumed by FF/-- and FF/Tie2 mice when fed normal salt diet (NS), low salt diet (LS), high salt diet (HS) and high salt diet plus the  $ET_A$  antagonist ABT627 ( $5\text{mg}\cdot\text{kg}^{-1}\cdot\text{day}^{-1}$ ).

No significant difference in gel intake between genotypes was observed (Figure 4-26).



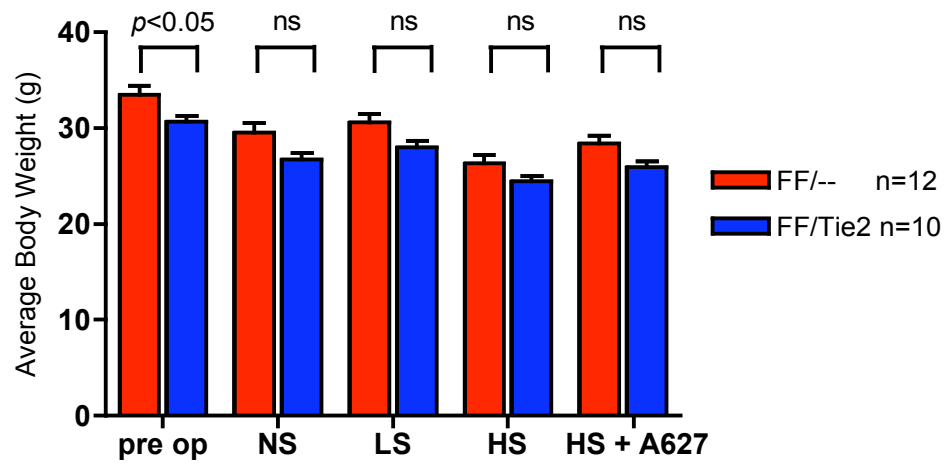


**Figure 4-27: Average body weight**

Body weight of FF/-- and FF/Tie2 mice when fed normal salt diet (NS), low salt diet (LS), high salt diet (HS) and high salt diet plus the  $ET_A$  antagonist ABT627 ( $5\text{mg}\cdot\text{kg}^{-1}\cdot\text{day}^{-1}$ ).

Although the FF/-- controls were heavier than FF/Tie2 mice immediately prior to surgery, in the post-operatively this difference disappeared (Figure 4-27).

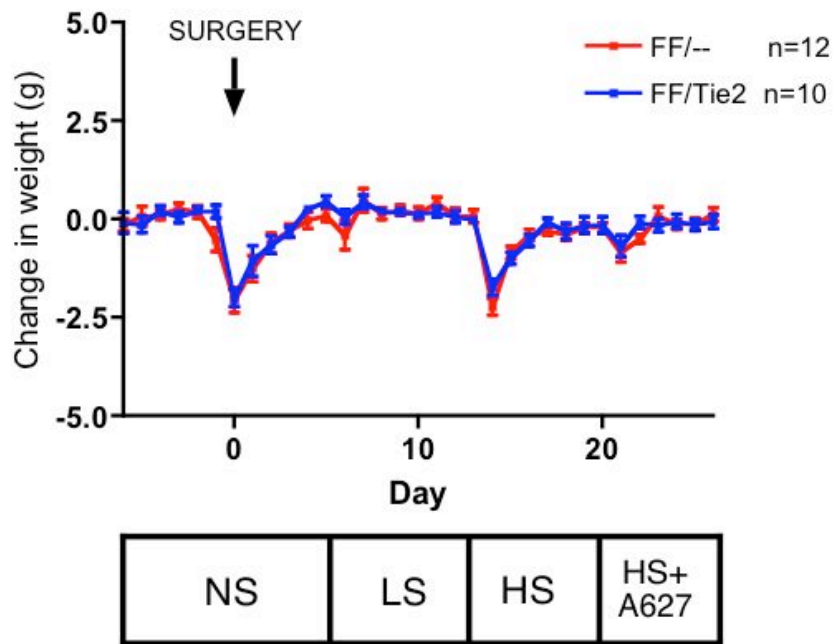


**Figure 4-28: Weight change versus the previous day**

Daily change in weight of FF/-- and FF/Tie2 mice when fed normal salt diet (NS), low salt diet (LS), high salt diet (HS) and high salt diet plus the  $ET_A$  antagonist ABT627 ( $5\text{mg}\cdot\text{kg}^{-1}\cdot\text{day}^{-1}$ ).

Body weight and gel intake decreased in the days immediately following surgery, but by the end of the first 7-day treatment period, the mice were eating and drinking normally, showing no further weight loss (Figure 4-28). As in other studies (Ahn *et al.*, 2004), mice ate most of what gel was offered to them, although intake and body weight fell slightly with the introduction of high salt diet in both genotypes.

#### 4.3.2.6 SECOND STUDY – SYSTOLIC BP

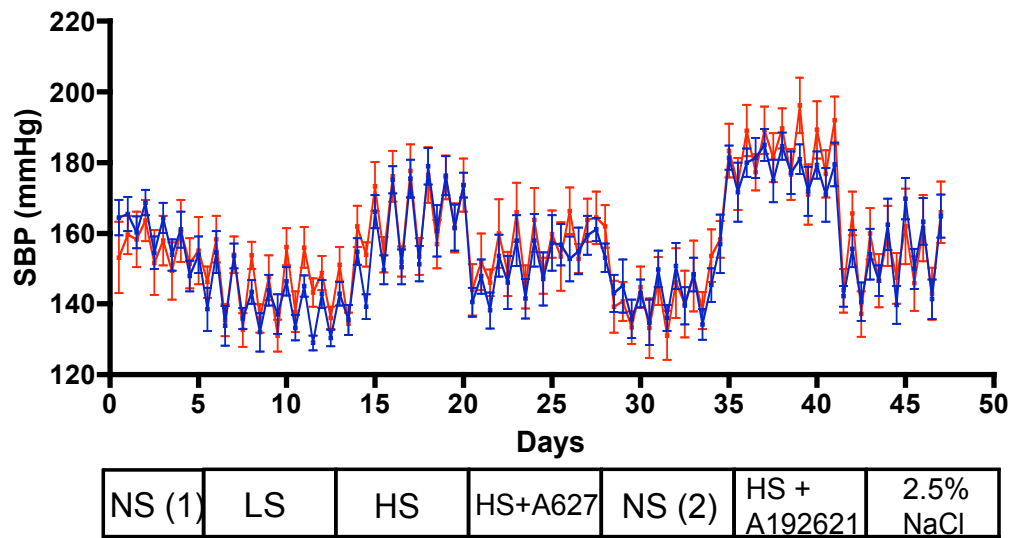


**Figure 4-29: 12 hourly SBP**

SBP of FF/-- (n=7) and FF/Tie2 (n=6) mice recorded 12 hourly over the 7-week of the second study (second study data only).

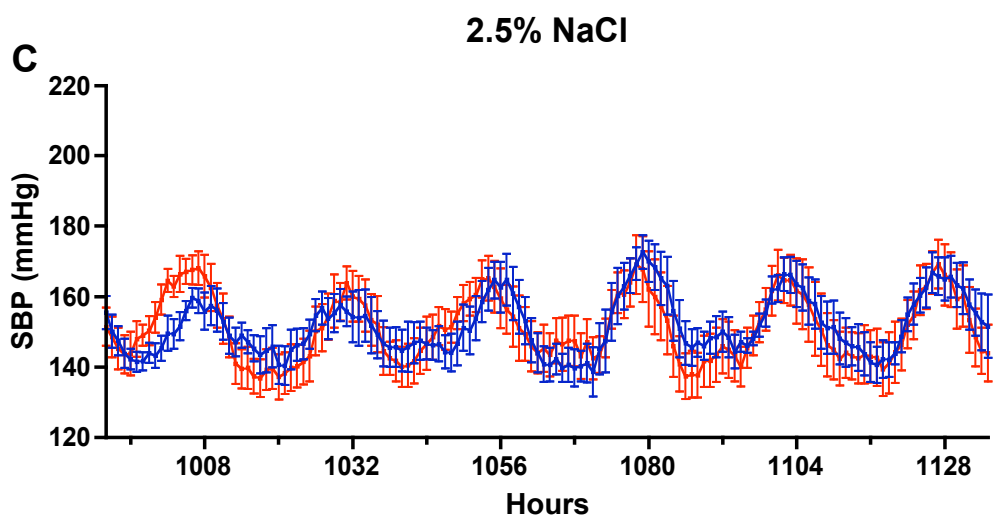
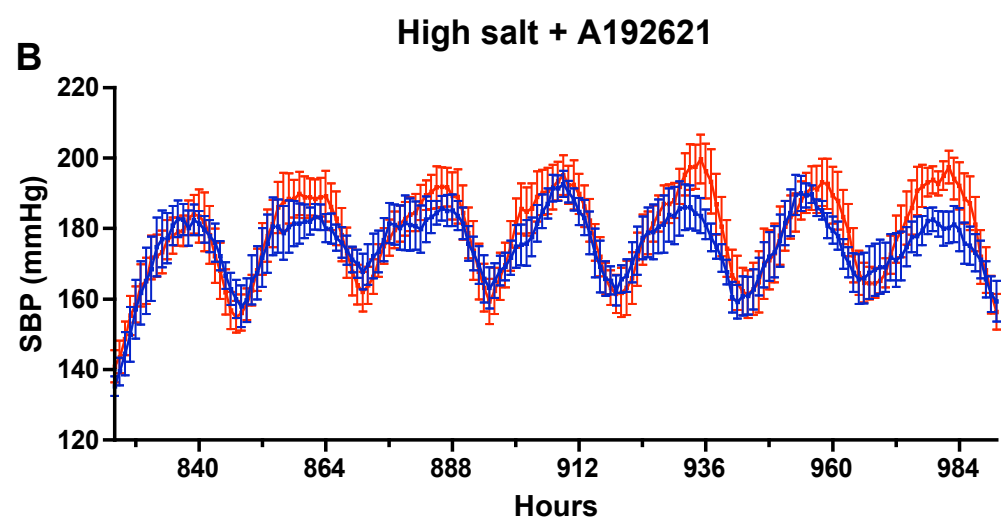
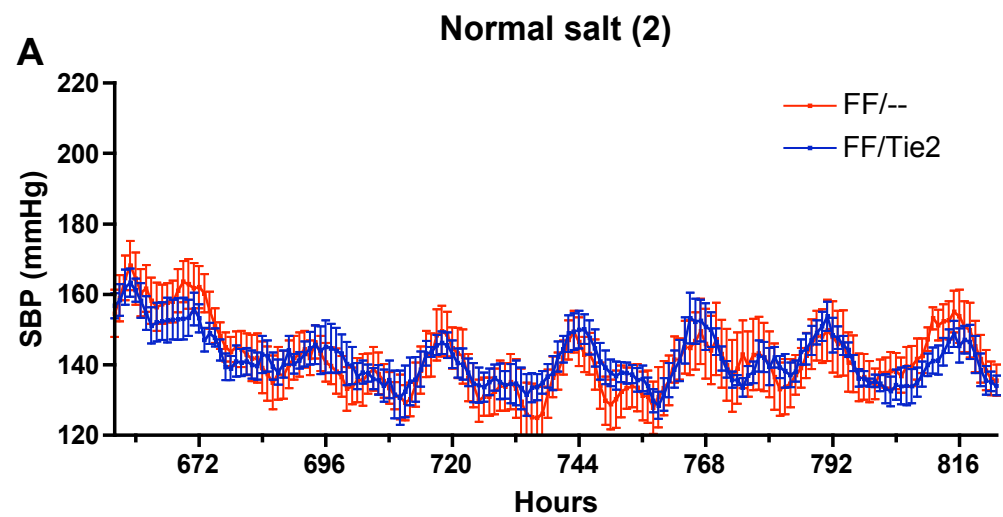


**Figure 4-30: SBP of telemetered mice during the second week of normal salt (0.76% NaCl) diet (week 5) [A], during the 7-days of high salt (7.6% NaCl) + A192621 (week 6) [B] and during the 7 days of 2.5% NaCl diet (week 7) [C].** Data shown are hourly rolling averages of the FF/-- (n=7) and FF/Tie2 (n=6) mice. (Note the data from the first 4 weeks of the second study is included in section 4.3.2.1)

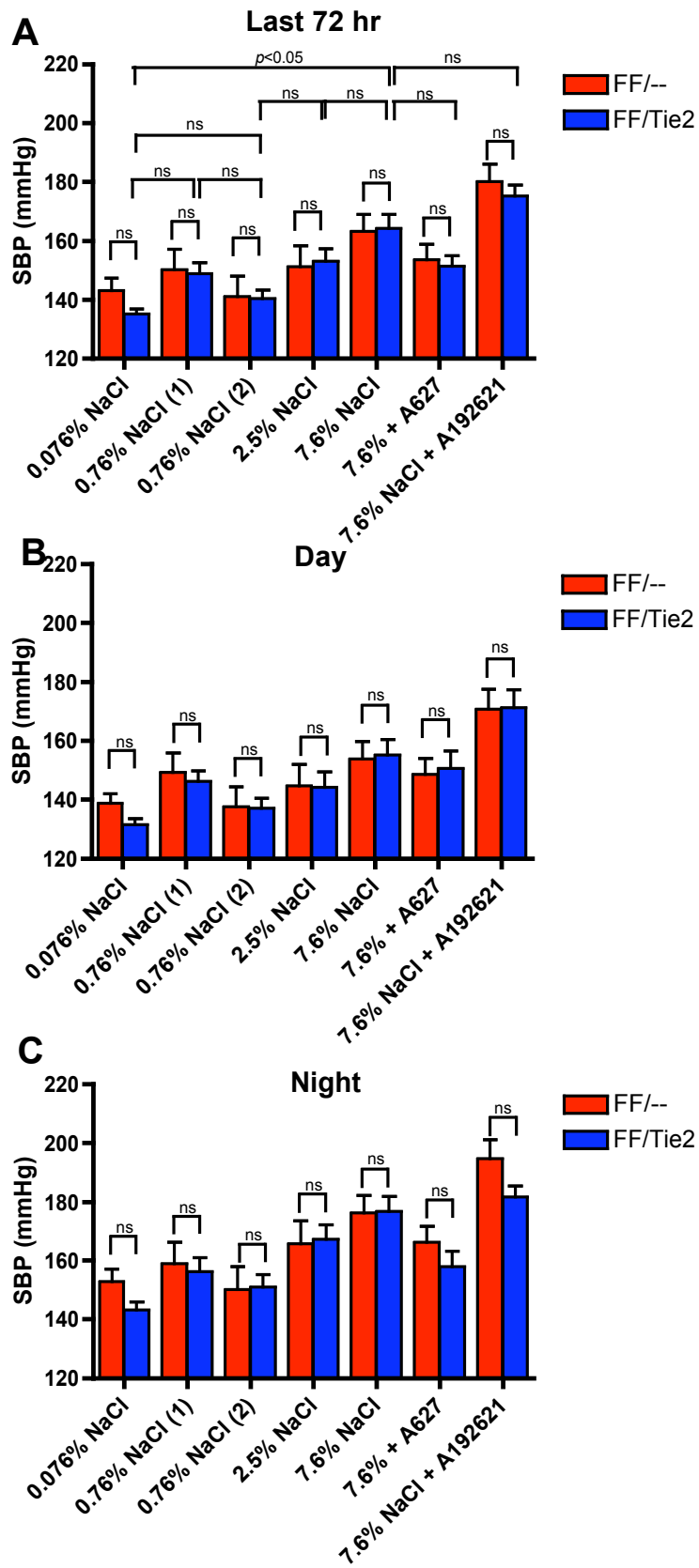


**Figure 4-31: Comparison of: the averaged SBP of FF/-- (n=7) and FF/Tie2 (n=6) mice during the last 72 hours of each week-long dietary period [A]; the averaged minimal SBP values during the day [B]; and the averaged maximal SBP values during the night [C].**

In the second extended study no significant difference in SBP during the last 72 hours of each treatment period was seen between genotypes on low salt diet (FF/Tie2:  $135.2 \pm 1.71$  mmHg; FF/--  $143.1 \pm 4.17$  mmHg), normal salt diet in week 1 (FF/Tie2:  $148.8 \pm 3.76$  mmHg; FF/--  $150.1 \pm 6.95$  mmHg) normal salt diet in week 5 (FF/Tie2:  $140.4 \pm 2.80$  mmHg; FF/--  $141.1 \pm 6.85$  mmHg), 2.5% salt diet (FF/Tie2:  $153.1 \pm 4.23$  mmHg; FF/--  $151.1 \pm 7.12$  mmHg), or high salt diet (FF/Tie2:  $164.2 \pm 4.72$  mmHg; FF/--  $163.1 \pm 5.89$  mmHg) (Figure 4-31A). In week 5 (second period of normal salt diet), after several weeks to recover from the stress of telemetry surgery, the SBP of both genotypes was marginally lower than during the first normal salt period (week 1). As seen with the combined data from both studies, increasing the proportion of salt in the diet raised SBP in both genotypes. ABT627 caused the SBP of both genotypes to fall, and A192621 exerted a hypertensive effect, but these changes both failed to reach statistical significance due to the limited numbers of animals in this second study.

No differences between genotypes were seen at the extremes of circadian rhythm – neither during the middle of the day nor the middle of the night (Figure 4-31B and C).

4.3.2.7 SECOND STUDY-DIASTOLIC BP

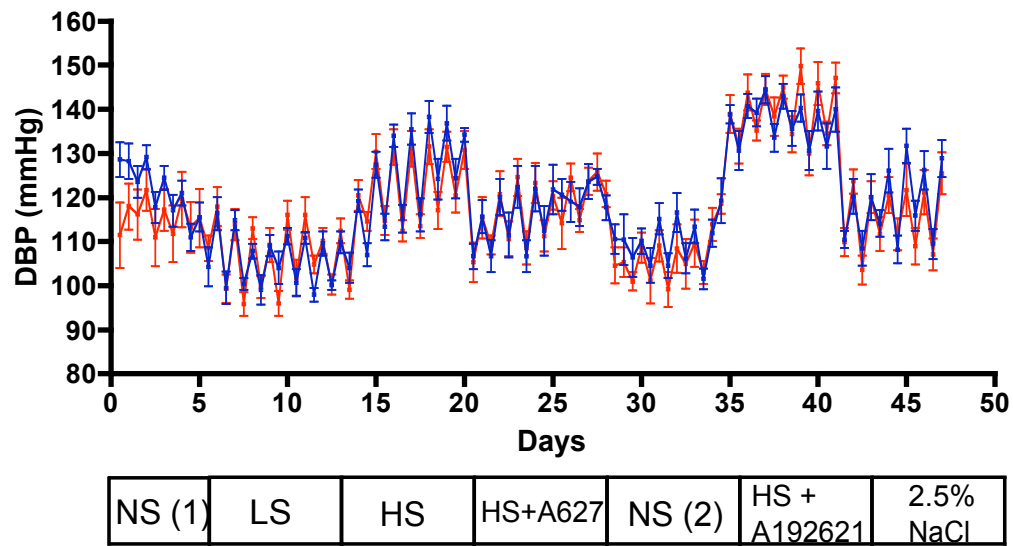


**Figure 4-32: 12 hourly DBP**

DBP of FF/-- (n=7) and FF/Tie2 (n=6) mice recorded 12 hourly over the 7-week of the second study (second study data only).



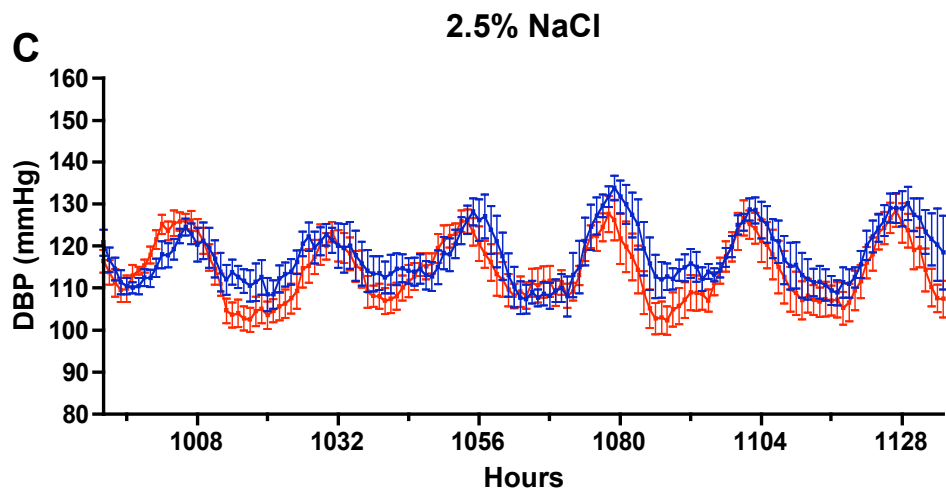
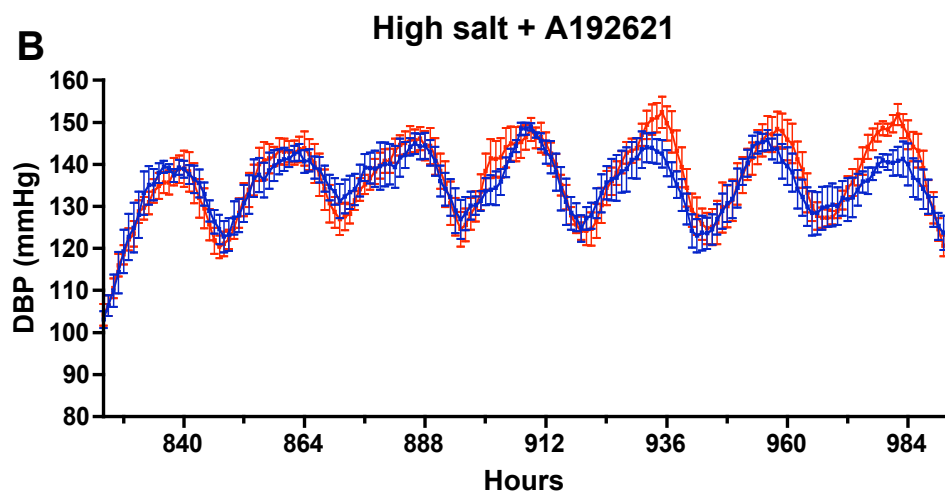
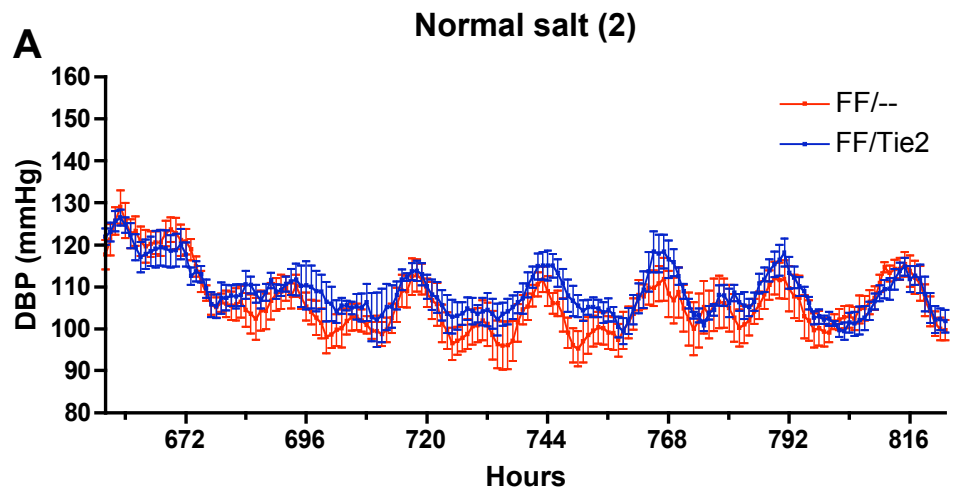


**Figure 4-33: DBP of telemetered mice during the second week of normal salt (0.76% NaCl) diet (week 5) [A], during the 7-days of high salt (7.6% NaCl) + A192621 (week 6) [B] and during the 7 days of 2.5% NaCl diet (week 7) [C].** Data shown are hourly rolling averages of the FF/-- (n=7) and FF/Tie2 (n=6) mice. (Note the data from the first 4 weeks of the second study is included in section 4.3.2.2).

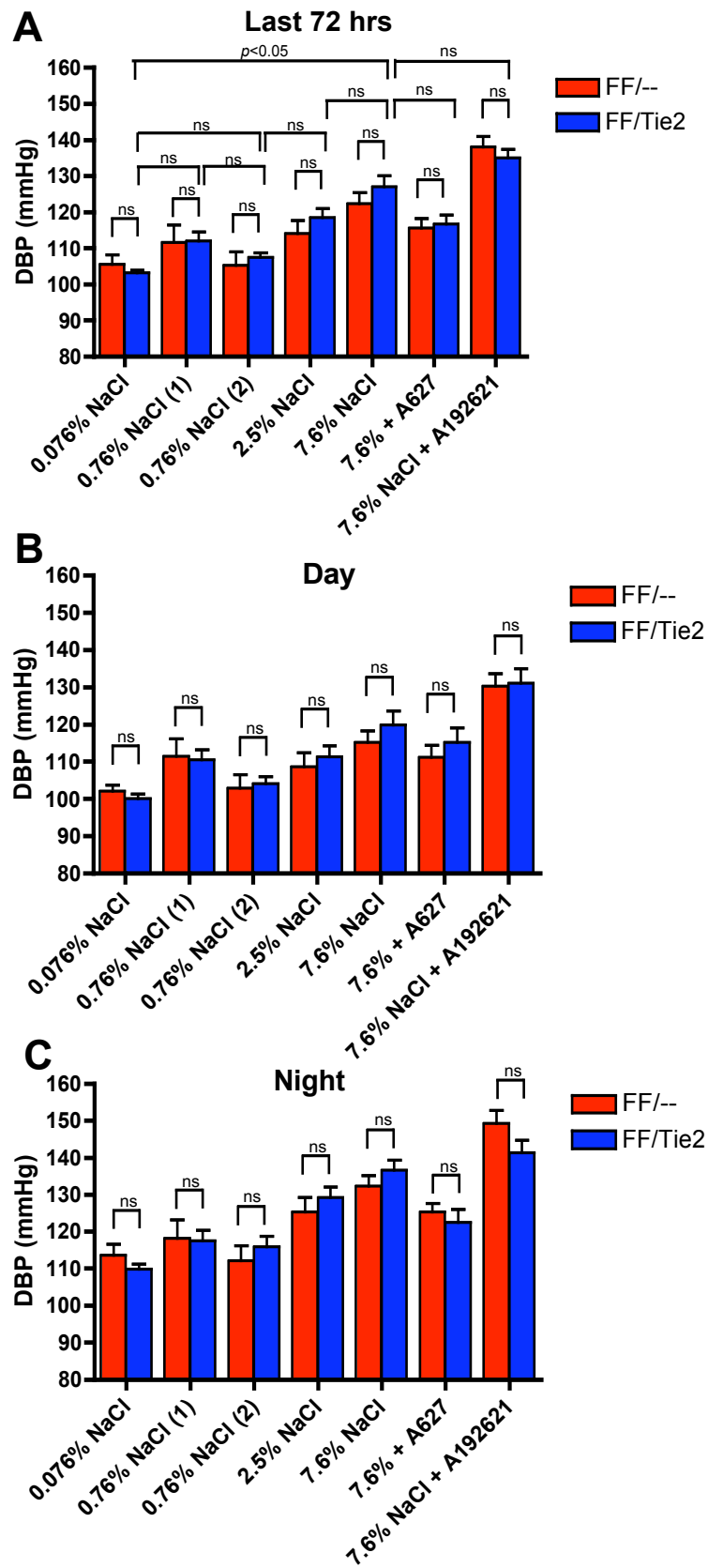


**Figure 4-34: Comparison of: the averaged DBP of FF/-- (n=7) and FF/Tie2 (n=6) mice during the last 72 hours of each week-long dietary period [A]; the averaged minimal DBP values during the day [B]; and the averaged maximal DBP values during the night [C].**

No significant difference in DBP was seen between genotypes, during the last 72 hours of each treatment period, on low salt diet (FF/Tie2:  $103.2 \pm 0.63$  mmHg; FF/--  $105.5 \pm 2.65$  mmHg), normal salt diet in week 1 (FF/Tie2:  $112.0 \pm 2.51$  mmHg; FF/--  $111.6 \pm 4.78$  mmHg) normal salt diet in week 5 (FF/Tie2:  $107.6 \pm 1.19$  mmHg; FF/--  $105.3 \pm 3.63$  mmHg), 2.5% salt diet (FF/Tie2:  $118.5 \pm 2.42$  mmHg; FF/--  $114 \pm 3.64$  mmHg), or high salt diet (FF/Tie2:  $127.0 \pm 3.02$  mmHg; FF/--  $122.3 \pm 3.05$  mmHg) (Figure 4-34A). Increased salt in the diet resulted in increased DBP in both genotypes. ABT627 lowered DBP and A192621 had the opposite effect, but again both of these failed to reach statistical significance.

No differences were seen between genotypes when comparing the maximum values at night, the minimum periods during the day and the average values during the last 3 days of each treatment period. Thus circadian rhythm appeared to exert little influence on the differences seen between the genotypes (Figure 4-34A, B and C).

#### 4.3.2.8 SECOND STUDY – MEAN BP

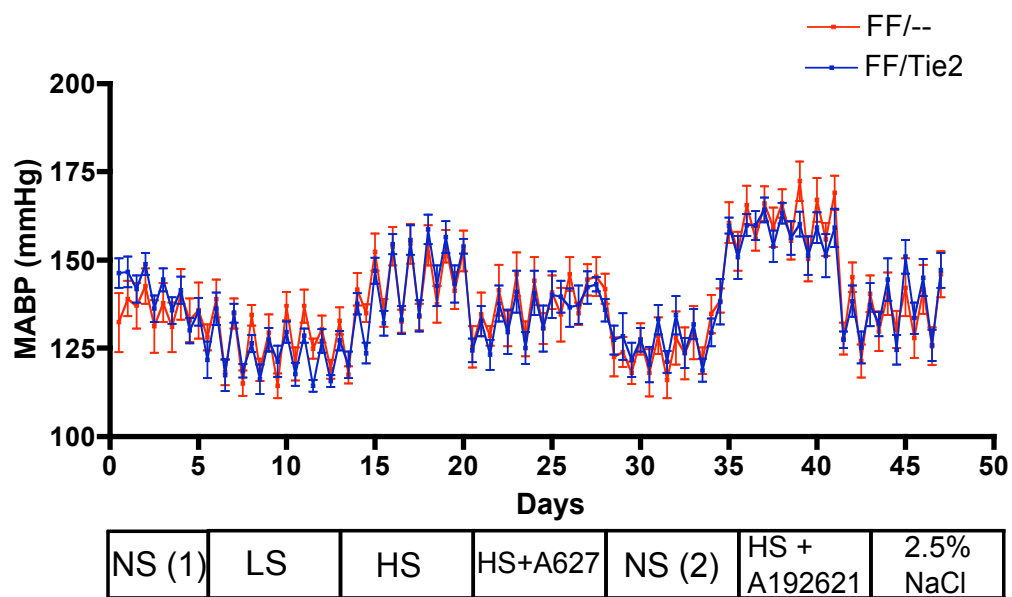


**Figure 4-35: 12 hourly MBP**

MBP of FF/-- (n=7) and FF/Tie2 (n=6) mice recorded 12 hourly over the 7-week of the second study (second study data only).

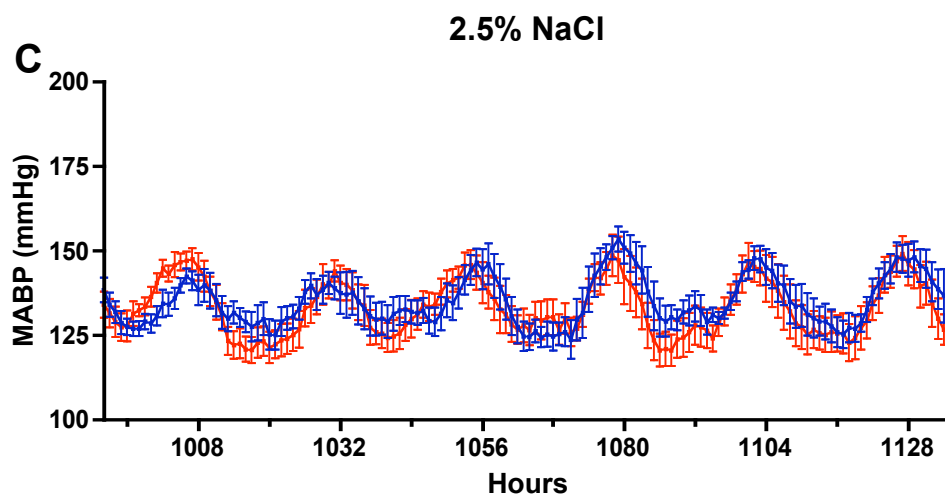
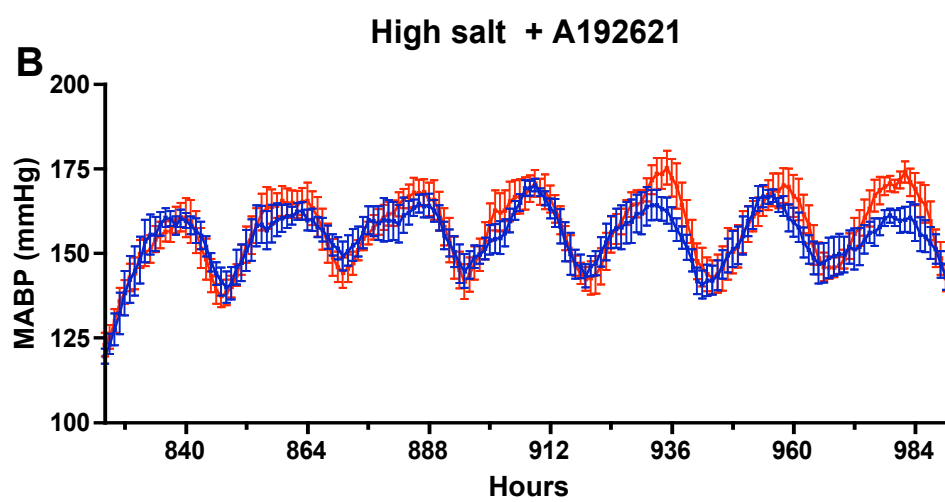
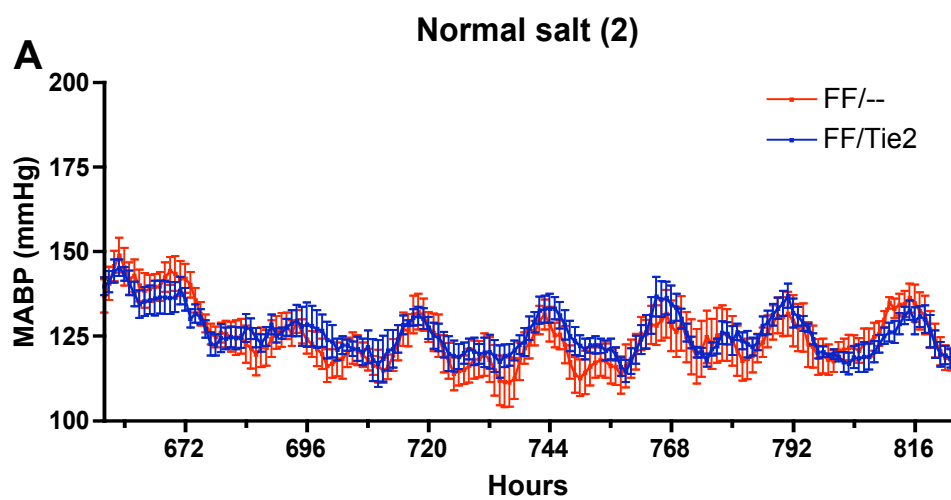


**Figure 4-36: MBP of telemetered mice during the second week of normal salt (0.76% NaCl) diet (week 5) [A], during the 7-days of high salt (7.6% NaCl) + A192621 (week 6) [B] and during the 7 days of 2.5% NaCl diet (week 7) [C].** Data shown are hourly rolling averages of the FF/-- (n=7) and FF/Tie2 (n=6) mice. (Note the data from the first 4 weeks of the second study is included in section 4.3.2.3).

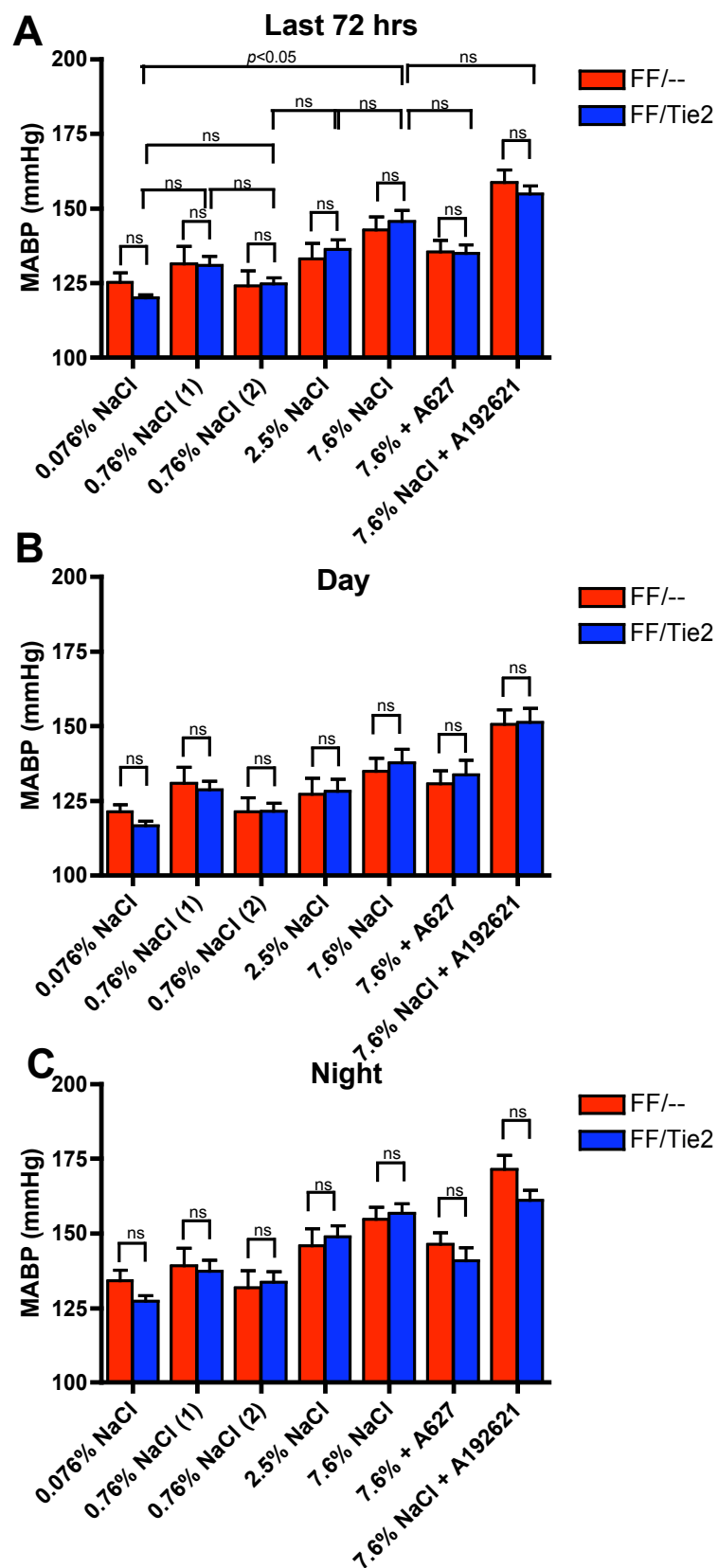




**Figure 4-37: Comparison of: the averaged MBP of FF/-- (n=7) and FF/Tie2 (n=6) mice during the last 72 hours of each week-long dietary period [A]; the averaged minimal MBP values during the day [B]; and the averaged maximal MBP values during the night [C].**

Over the last 3 days of each treatment period, no significant difference in MBP was observed between the genotypes on low salt diet (FF/Tie2:  $120.0 \pm 1.07$  mmHg; FF/--  $125.1 \pm 3.22$  mmHg), normal salt diet in week 1 (FF/Tie2:  $130.9 \pm 2.92$  mmHg; FF/--  $131.4 \pm 5.72$  mmHg) normal salt diet in week 5 (FF/Tie2:  $124.7 \pm 1.92$  mmHg; FF/--  $124.0 \pm 5.05$  mmHg), 2.5% salt diet (FF/Tie2:  $136.2 \pm 3.18$  mmHg; FF/--  $133.0 \pm 5.16$  mmHg), or high salt diet (FF/Tie2:  $145.6 \pm 3.67$  mmHg; FF/--  $142.9 \pm 4.33$  mmHg) (Figure 4-37A). MBP of both genotypes increased with increased salt in the diet. ABT627 lowered MBP and A192621 increased it, although this failed to reach statistical significance.

No differences between genotypes were seen during the middle of the night or the middle of the day (Figure 4-37B and C).

4.3.2.9 SECOND STUDY – HEART RATE

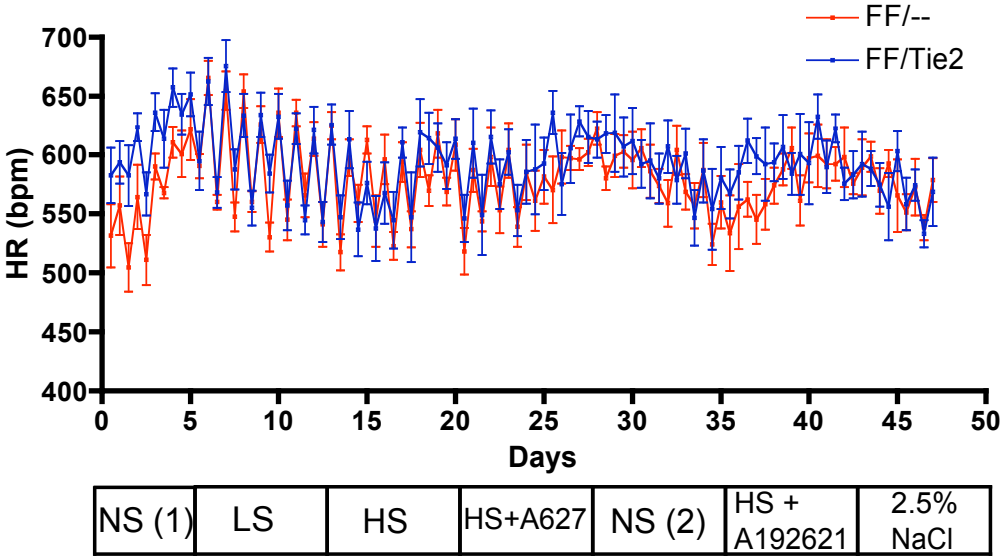


**Figure 4-38: 12 hourly HR**  
HR of FF/-- (n=7) and FF/Tie2 (n=6) mice recorded 12 hourly over the 7-week of the second study (second study data only).

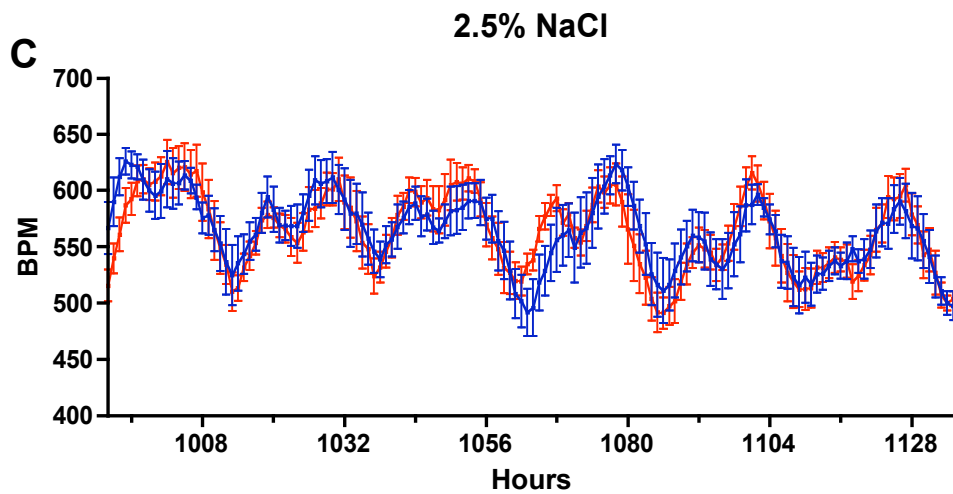
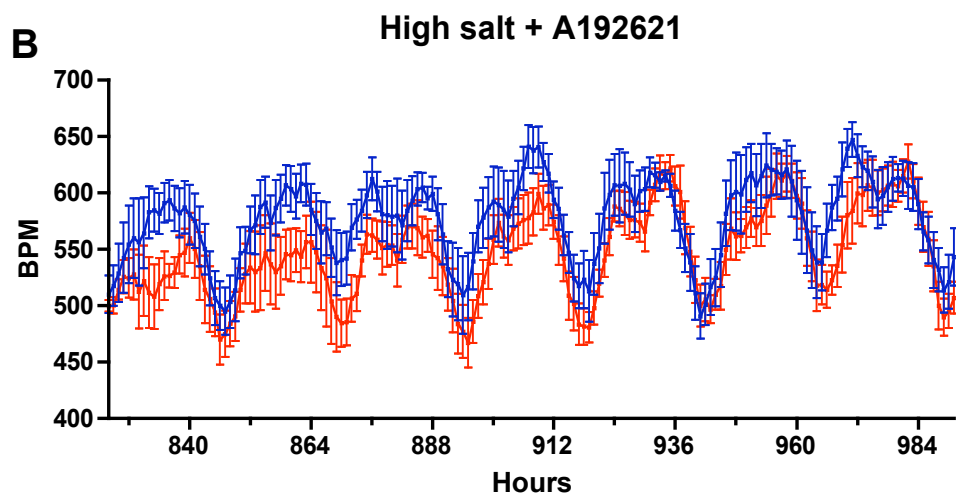
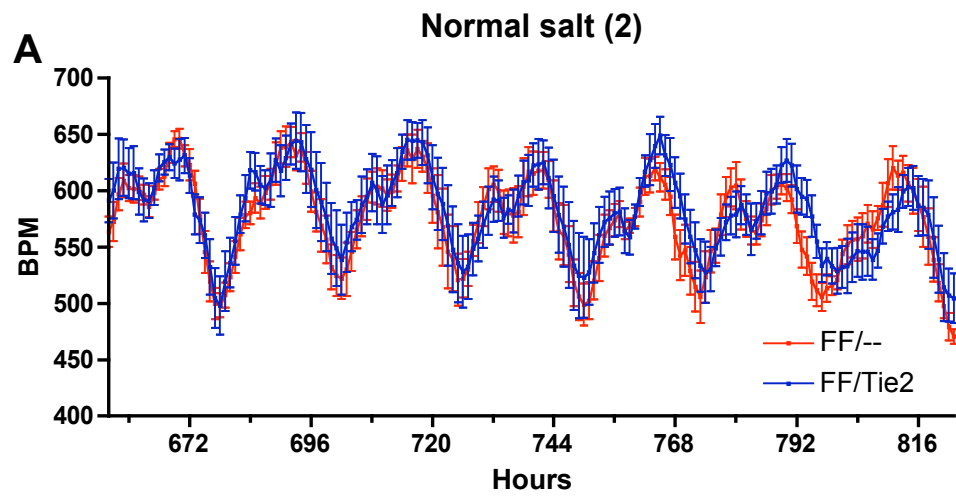


**Figure 4-39: HR of telemetered mice during the second week of normal salt (0.76% NaCl) diet (week 5) [A], during the 7-days of high salt (7.6% NaCl) + A192621 (week 6) [B] and during the 7 days of 2.5% NaCl diet (week 7) [C].** Data shown are hourly rolling averages of the FF/-- (n=7) and FF/Tie2 (n=6) mice. (Note the data from the first 4 weeks of the second study is included in section 4.3.2.4).

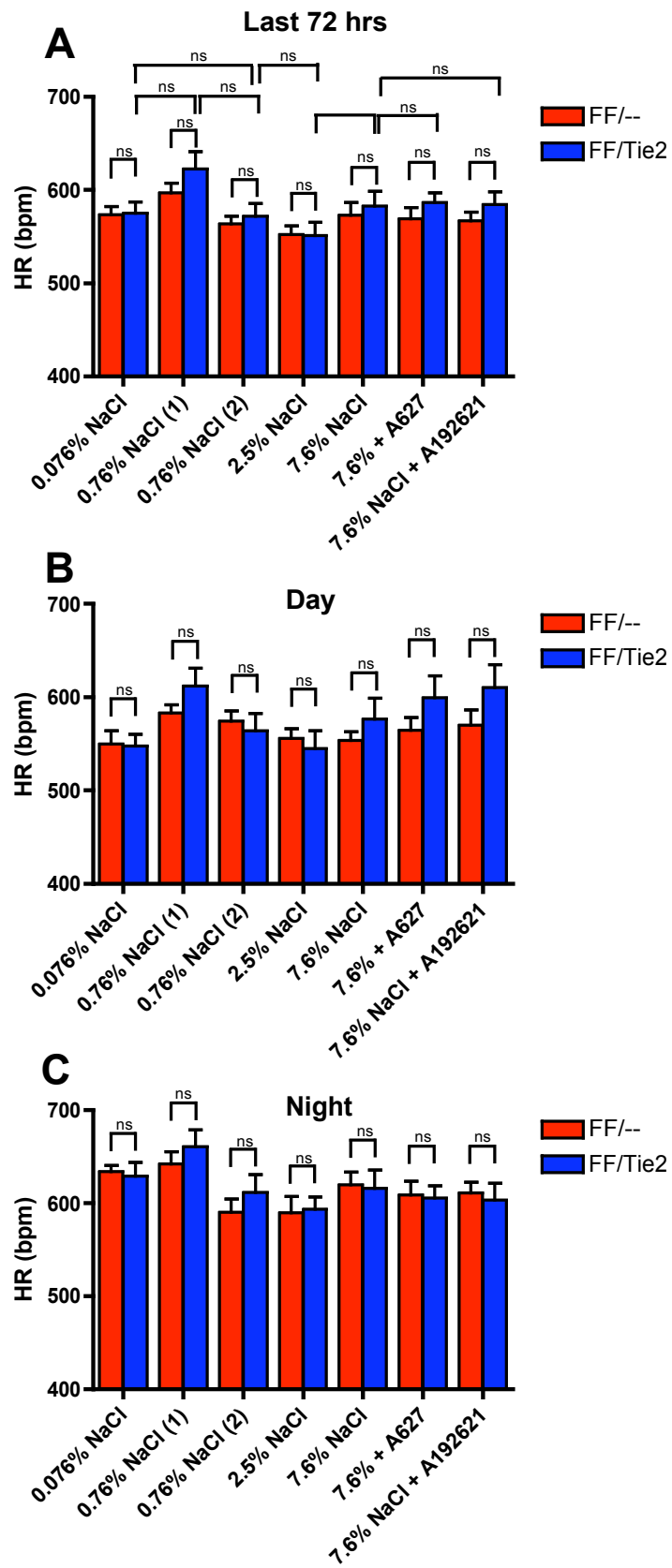


**Figure 4-40: Comparison of: the averaged HR of FF/-- (n=7) and FF/Tie2 (n=6) mice during the last 72 hours of each week-long dietary period [A]; the averaged minimal HR values during the day [B]; and the averaged maximal HR values during the night [C].**

No significant differences in HR were seen between genotypes (Figure 4-40A). Although ET<sub>A</sub> blockade lowered BP and ET<sub>B</sub> blockade had a hypertensive effect, these agents had no significant effect on HR.

HR was lower during the day than during the night, but even at these extremes of circadian rhythm no differences were seen between genotypes.

#### 4.3.2.10 SECOND STUDY – WATER, GEL CONSUMPTION AND BODY WEIGHT

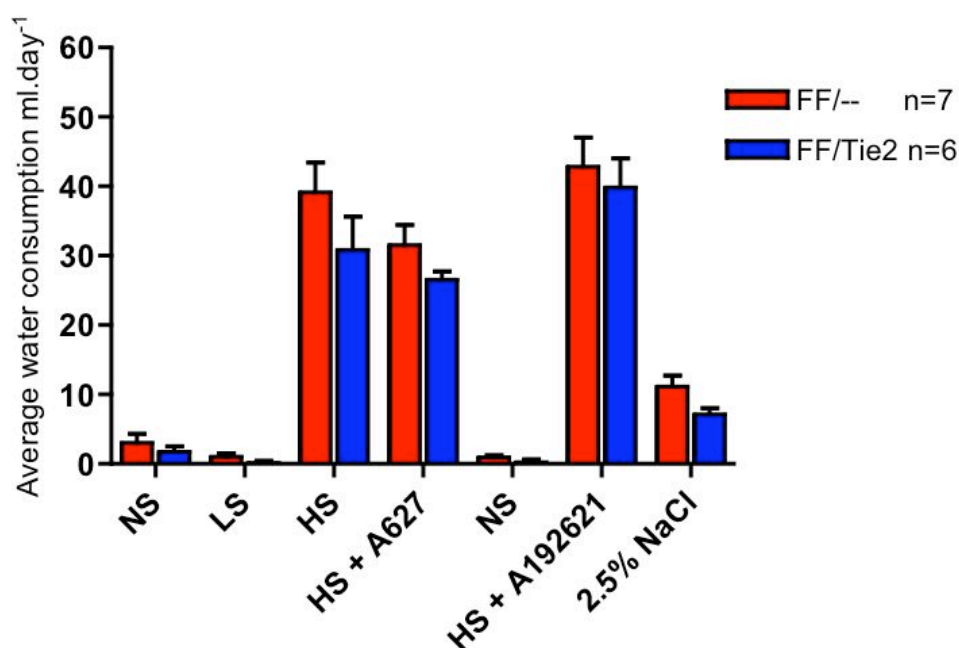


**Figure 4-41: Average daily water consumption (second extended study only).** Water consumed by FF/-- and FF/Tie2 mice during the second extended study. No significant differences between genotypes were seen.

In the second extended study, no significant differences in water consumption were seen between genotypes (Figure 4-41). Whilst the water intake of mice of both

genotypes fed the 2.5% NaCl diet was elevated compared to that seen on the normal salt, it was substantially less than that seen on the high salt diet. Although introduction of ET<sub>B</sub> blockade had a non-statistically significant hypertensive effect, it did not change this high water intake.

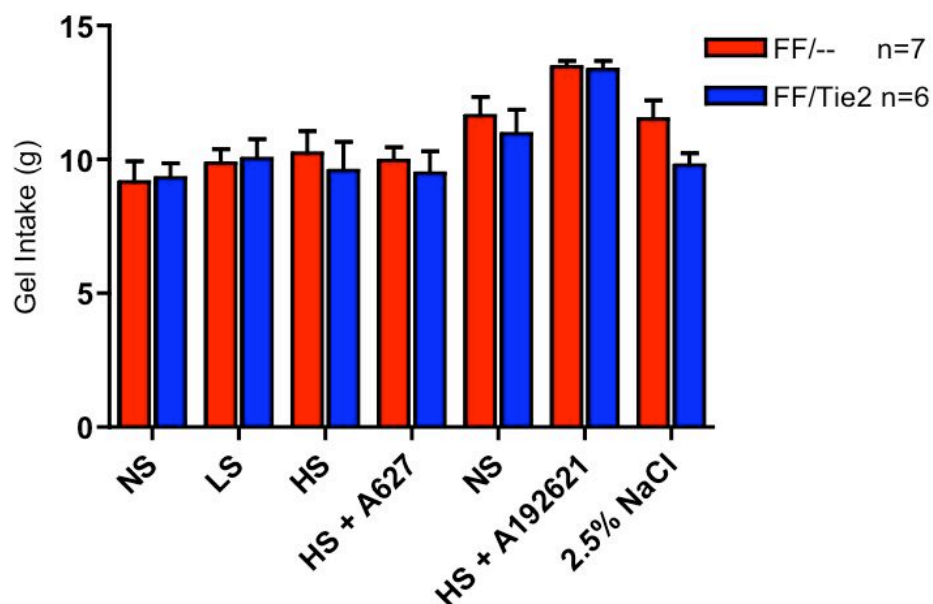


**Figure 4-42: Average daily gel intake (second extended study only).**

Gel diet consumption by FF/-- and FF/Tie2 mice during the second extended study. No significant differences between genotypes seen.

Gel intake was not different between genotypes, and unlike water intake did not vary with the different diets/ drug treatments (Figure 4-42).

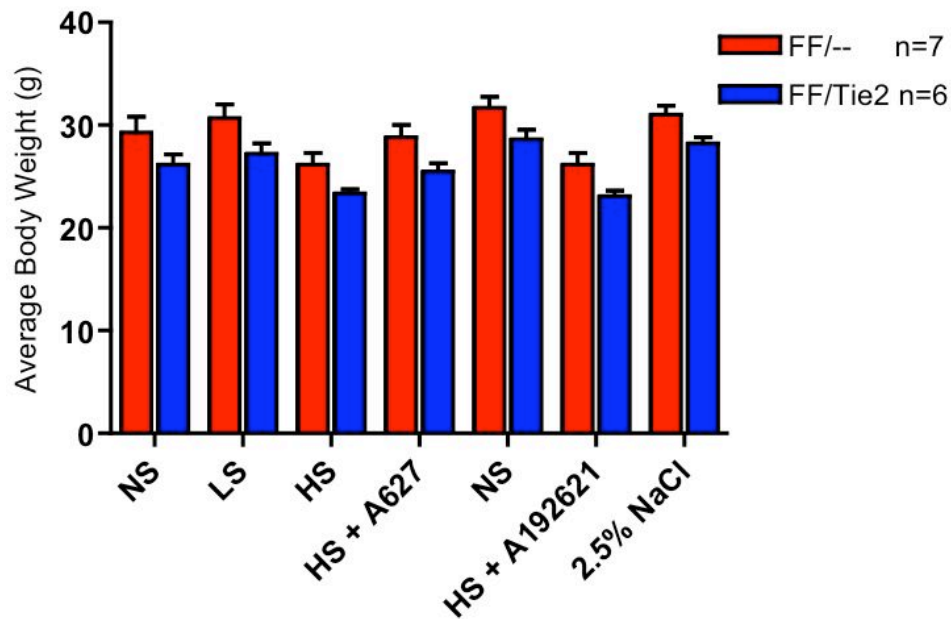


**Figure 4-43: Average daily body weight (second extended study only).**

Body weight of FF/-- and FF/Tie2 mice during the second extended study. No significant differences between genotypes seen.

Although there was a trend towards the FF/Tie2 mice being lighter than the FF/-- controls this failed to reach statistical significance (Figure 4-43).

#### 4.3.2.11 SECOND STUDY – HAEMATOCRIT

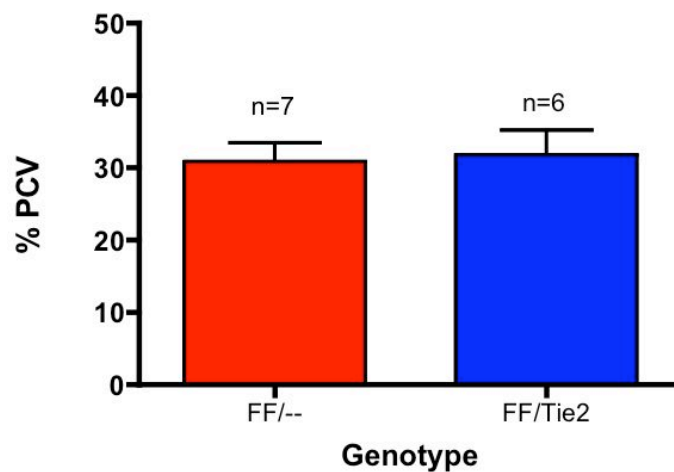


**Figure 4-44: Packed cell volume of mice in second study**

No significant difference in haematocrit (Packed Cell Volume [PCV]) was seen between the FF/-- and FF/Tie2 mice at the completion of the second telemetry study.



At the end of the second study, blood was taken and haematocrit was measured. The PCV of FF/-- mice ( $30.9 \pm 2.6\%$ ) was not different from that of the FF/Tie2 mice ( $31.8 \pm 3.5\%$ )(Figure 4-44).

#### 4.3.3 Influence of age on heart/ body weight ratio

Hearts were dissected from young mice (aged 8 –12 weeks old) and also from a smaller sample of older animals (13 - 15 months old). The free right ventricular wall (RV) was dissected free from the left ventricle plus septum (LV+S), as described in section 2.10.3. The heart to body weight ratio was calculated (Figure 4-45).

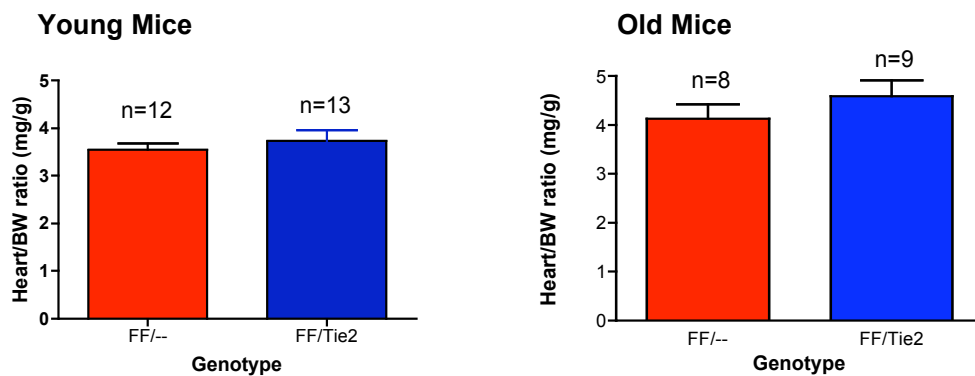


**Figure 4-45: Heart to body weight ratio for young and old mice**

Genotype did not affect the ratio of total heart to body weight (BW) for young (8-12 weeks) and old (52-60 weeks) male mice.

Although both genotypes showed a small increase in heart/ body weight ratio with age, no differences were observed between the 2 genotypes (Table 4-2). Old FF/-- mice were however significantly heavier than FF/Tie2 mice.

**Table 4-2: Heart and body weights for young (2 month old) and old (4 month) mice**

RV= Right ventricle; LV+S= Left ventricle + septum; TV= Total ventricles. For all data ( $\pm$  SEM) there is no difference between genotypes at either age, other than for body weight (\* $p=0.0496$ ).

|                      | <b>RV</b>      | <b>LV+S</b>    | <b>TV</b>      | <b>BW</b>       | <b>RV/TV</b>    | <b>RV/LV+S</b>  |
|----------------------|----------------|----------------|----------------|-----------------|-----------------|-----------------|
|                      | <b>(mg)</b>    | <b>(mg)</b>    | <b>(mg)</b>    | <b>(g)</b>      |                 |                 |
| <b>Young FF/--</b>   | 26.78          | 122.76         | 149.53         | 42.31           | 0.18            | 0.22            |
| <b>(n=12)</b>        | ( $\pm 1.20$ ) | ( $\pm 4.67$ ) | ( $\pm 5.3$ )  | ( $\pm 1.38$ )  | ( $\pm 0.006$ ) | ( $\pm 0.009$ ) |
| <b>Young FF/Tie2</b> | 29.36          | 125.24         | 154.6          | 42.12           | 0.19            | 0.24            |
| <b>(n=13)</b>        | ( $\pm 1.61$ ) | ( $\pm 6.44$ ) | ( $\pm 7.5$ )  | ( $\pm 1.79$ )  | ( $\pm 0.007$ ) | ( $\pm 0.011$ ) |
| <b>Old FF/--</b>     | 41.33          | 183.2          | 224.5          | 55.78           | 0.19            | 0.227           |
| <b>(n=8)</b>         | ( $\pm 1.21$ ) | ( $\pm 7.79$ ) | ( $\pm 8.63$ ) | ( $\pm 3.35$ )  | ( $\pm 0.005$ ) | ( $\pm 0.007$ ) |
| <b>Old FF/Tie2</b>   | 40.38          | 162.1          | 202.5          | 45.62           | 0.20            | 0.247           |
| <b>(n=9)</b>         | (2.81)         | ( $\pm 6.29$ ) | ( $\pm 8.76$ ) | ( $\pm 3.35$ )* | ( $\pm 0.007$ ) | ( $\pm 0.011$ ) |

## 4.4 DISCUSSION

BP measurement in experimental animals can be performed by several different techniques, each having their own particular advantages and disadvantages. When recorded by means of carotid artery cannulation, under both anaesthetised and conscious unrestrained conditions, we found EC ET<sub>B</sub> down-regulated mice to exhibit elevated MBP, unaffected by high salt diet. In contrast, when we went on to confirm our findings with continuous radiotelemetry measurements, the approach accepted as the ‘gold standard’ for detecting BP differences in genetically modified animals (Kurtz *et al.*, 2005; Lorenz, 2002), EC ET<sub>B</sub> down-regulated mice demonstrated no significant differences in either SBP, DBP or MBP compared to controls, even when fed high salt.

Therefore, on the basis of the telemetry results, it seems that down-regulation of the EC ET<sub>B</sub> does not result in hypertension or increased sensitivity to dietary salt. This contrasts with the elevated BP seen in ET<sub>B</sub> deficient rats (Garipey *et al.*, 2000), collecting duct specific ET-1 KO mice (Ahn *et al.*, 2004), and IMCD ET<sub>B</sub> down-regulated mice (Ge *et al.*, 2006), and suggests the target for collecting duct derived ET-1 in the kidney is likely to be ET<sub>B</sub> receptors situated on cells other than ECs.

### 4.4.1 Deletion of the EC ET<sub>B</sub> receptor does not alter the BP response to salt

In our detailed longitudinal telemetry studies, we have shown that down-regulation of the EC ET<sub>B</sub> receptor does not result in elevated BP, even in response to a high sodium diet. Our previous autoradiography studies demonstrated marked down-regulation of binding of the ET<sub>B</sub> receptor ligand BQ3020 within the renal medulla of EC ET<sub>B</sub> down-regulated mice (see section 3.2.6.3). This suggests that most ET<sub>B</sub> receptors within the medulla are expressed on vasa recta ECs (Yukimura *et al.*, 1996). The residual ET<sub>B</sub> receptor binding, observed in the renal medulla is likely to represent the functionally important non EC-ET<sub>B</sub> receptors, expressed on cells such as IMCDs or renal interstitial cells.

The two groups of mice in the radiotelemetry study - both the EC ET<sub>B</sub> receptor down-regulated mice and the control animals - demonstrate a clear relationship between salt intake and BP, complicating the interpretation of our results. Modest elevations in BP with salt loading have been seen with other mouse strains, particularly those featuring 2 copies of the renin gene (Wang *et al.*, 2002). The background of our mice is a mixture of 129/01a, known to harbour 2 copies of the renin gene (Sharp *et al.*, 1996) and C57BL/6, which have been shown to develop hypertension following salt loading (Carlson *et al.*, 2000; Gros *et al.*, 2002). Although we cannot discount the possibility that manipulation of the ET<sub>B</sub> gene during gene targeting may have disrupted previously unidentified loci determining salt sensitivity, this is unlikely as only ~ 1 kB of intron 2 was removed during floxing (see section 1.3.5). Further studies, following backcrossing of our mice onto a salt resistant strain, would not only allow more robust conclusions concerning the effect of EC ET<sub>B</sub> down-regulation on salt sensitivity to be made, but would also demonstrate whether floxing has any effect on the BP response to salt.

As previously described in the rat (Pollock *et al.*, 2001), we found that selective pharmacological antagonism of ET<sub>B</sub> during high-salt diet led to further increases in BP in both genotypes, although this failed to reach statistical significance most likely due to the smaller number of mice included in our second study and the influence of salt on our genetic background. In contrast, ET<sub>A</sub> blockade, introduced whilst the mice were on high salt diet, decreased BP in both genotypes to a similar extent. This further reinforces our autoradiography data showing that ET<sub>A</sub> expression is not altered in the EC ET<sub>B</sub> down-regulated mice.

As expected, BP and HR peaked during the night and were lowest during the day, the periods of fastest and slowest circadian rhythm respectively. However, during these periods of maximum and minimum activity, similar differences in BP were observed between genotypes, indicating that down-regulation of the EC ET<sub>B</sub> receptor does not have a significant influence on the response to circadian rhythm.

Other transgenic models, such as the collecting-duct specific ET-1 KO mouse, exhibit salt sensitive hypertension, thought largely to be due to volume expansion, as evidenced by elevated daily weight gain (Ahn *et al.*, 2004). Not only were our EC ET<sub>B</sub> down-regulated mice not hypertensive on a high salt diet, they displayed no difference in water intake, daily weight gain or haematocrit compared to controls, indicating that their intravascular volume was not increased.

There are 2 possible hypotheses explaining the lack of severe hypertension observed in the EC ET<sub>B</sub> receptor down-regulated mice.

Firstly, the ET-1/ ET<sub>B</sub> receptor signalling pathway, regulating tubular reabsorption of sodium and water, could be entirely dependent on ET<sub>B</sub> receptors located on cells other than vasa recta ECs. The importance of ET<sub>B</sub> receptors on IMCD cells has previously been demonstrated by the finding that IMCD ET<sub>B</sub> down-regulated mice exhibit salt sensitive hypertension (Ge *et al.*, 2006). However, this hypertension was more modest than that seen in either collecting duct specific ET-1 KO mice (Ahn *et al.*, 2004) or rescued ET<sub>B</sub> deficient mice (Quaschnig *et al.*, 2005). Thus it is likely that IMCD derived ET-1 not only acts in an autocrine manner at IMCDs, but also may act in a paracrine manner at ET<sub>B</sub> receptors located on other neighbouring cell types - such as renal interstitial cells. These are present in abundance in the inner medulla and are adjacent to the collecting duct. Renal interstitial cells not only express ET<sub>A</sub> and ET<sub>B</sub> receptors but they also produce NO and PGE<sub>2</sub> in response to ET-1 (Zhuo, 2000).

Second, the effect of loss of any paracrine IMCD ET-1/ EC ET<sub>B</sub> signalling pathway (Kotelevtsev *et al.*, 2001) that might normally regulate natriuresis by alteration of medullary blood flow (Vassileva *et al.*, 2003) may have been masked by changes in the glomerular filtration rate. Both ET<sub>A</sub> and ET<sub>B</sub> regulate afferent arteriolar vasoconstriction, whereas EC ET<sub>B</sub> produces vasodilatation of efferent arterioles (Inscho *et al.*, 2005). The balance between ET-1 mediated vasoconstriction and vasodilatation in the glomerulus may be important in determining tubular sodium delivery.

Key targets for future studies will thus be to examine the effects of selective IMCD or renal interstitial cell ET<sub>B</sub> receptor KO on sodium and water handling and to determine the influence of vascular (EC and VSMC) ET<sub>B</sub> receptors on glomerular function.

#### **4.4.2 BP measurement in mice**

The most straightforward way of measuring the BP of a laboratory animal is by means of a catheter inserted into a central conduit artery, under terminal general anaesthesia. This has the advantages of not causing pain to the animal studied (thereby reducing suffering and also limiting the effect of emotional stress on BP), not requiring the operating skills necessary for recovery surgery, and, some suggest, dampening any central BP modulation mechanisms (Ohuchi *et al.*, 1999). However, general anaesthesia has direct inhibitory effects on the cardiovascular system, resulting in major differences, often opposite, in the integrated responses of conscious and anaesthetised animals to changes in blood volume or after-load (Vatner, 1978). Thus, whilst in many situations anaesthetised preparations are the only way of studying a physiological parameter (such as pulmonary artery pressure – see chapter 6), BP is best studied in conscious animals (Kurtz *et al.*, 2005; Lorenz, 2002). For these reasons, whilst this approach is useful to hone surgical skills and to give preliminary data, other techniques were soon adopted.

The indirect measurement of systolic pressure, through tail sphygmomanometry, has been a standard technique for the long-term evaluation of BP in the conscious rat and has been applied to the mouse in a variety of studies (Cervenka *et al.*, 1999; Hefler *et al.*, 2001; Van Vliet *et al.*, 2000). The advantages of this approach are threefold. Firstly, it is non invasive and so can be used to get repeated BP measurements over an extended study period. Second, it requires relatively inexpensive equipment (particularly in comparison to radiotelemetry). Third, its ease of use means it can be used to screen large groups of animals for systolic hypertension. However, indirect methods, such as tail cuff syphygmomanometry, have several disadvantages. They

only measure BP over a very limited number of cardiac cycles, resulting in great variability between measurements. Furthermore, as these measurements are often only performed during a brief portion of the day, they provide no information whatsoever about BP during the night. Second, despite training, rodents remain significantly stressed by the restraint (Gross *et al.*, 2003; Popovic, 1988), warming (necessary to ensure adequate tail blood flow) (Bunag *et al.*, 1982) and sleep disruption (measurements are taken during the day, when mice are usually asleep) necessitated by tail cuff BP measurement. Heart rates of 650 – 700 beats per minute have been recorded, compared to rates of ~ 500 in undisturbed mice (Lorenz, 2002). Furthermore different experimental groups can respond differently to these stresses (Bidani *et al.*, 1993). Third, indirect methods are only able to determine systolic, not diastolic pressure and so are therefore unable to give a measure of mean arterial pressure or pulse pressure. Furthermore, a poor correlation of tail cuff measurements with direct methods has been demonstrated (Jamieson *et al.*, 1997; Whitesall *et al.*, 2004). For these reasons, the American Heart Association Council for High Blood Pressure Research recommends using indirect methods for screening large populations of animals for systolic hypertension, rather than for quantifying the relationship between BP and variables such as drug treatment or genotype (Kurtz *et al.*, 2005). The limitations of the tail-cuff approach require independent verification of a BP phenotype by an alternative method. For these reasons, we decided not to use this method.

Direct recording of BP in conscious unrestrained rodents, using a fluid filled catheter inserted into a major artery, such as the carotid, is well established. After recovery from the surgery, measurements are taken by connecting to a calibrated pressure transducer, connected in turn, to an amplifier - recorder set-up. This can be done for discrete periods or continuously with the use of swivel/ tether systems, which allow free movement of the animal (Ryan *et al.*, 2002). As well as being relatively inexpensive (compared to radiotelemetry), this system can be calibrated at any time during the study, avoiding problems with baseline drift or changes in pressure transducer sensitivity. However, there are a number of drawbacks to using direct catheterisation for BP measurement in conscious mice. The surgery can introduce

infection to the animal. The small size of the animals requires a high level of surgical skill and meticulous aseptic technique for both implantation and maintenance of the catheters. Furthermore, damping of pressure signals or complete loss of catheter function can occur because of clotting or growth of fibrous tissue around the catheter tip.

Implantation of carotid artery catheters into our mice was associated with a high rate of morbidity and mortality. Even following alterations and improvements to the surgical procedure, significant problems were encountered with catheter failure in the days following implantation. Frequently, flushing of the catheter was associated with the onset of hemiparesis in the animal, most likely due to an embolic stroke caused by a clot being dislodged from the tip of the carotid catheter. Such problems meant that BP could not be reliably recorded more than 48 hours following catheter implantation. Concerns that the mice might become entangled in the swivel/ tether system, when unsupervised overnight, meant that this had not been included on the Home Office Project Licence covering this work. Thus BP was measured only over a 30-minute period, always at the same time of day, as performed in many similar studies (Curzen *et al.*, 1995; Ohuchi *et al.*, 1999; Stec *et al.*, 2002). Like tail cuff measurements, this arrangement meant that we could not record BP during the majority of the 24 hour period. Although the mice were allowed a 30-minute acclimatisation period, before BP recording began, this may not have allowed full recovery from the stress associated with the restraint required to connect the mice to the recording equipment. Despite extensive consultation with others experienced in the technique (Dr I Sharif, Dr P Hadoke, Ms G Brooker [University of Edinburgh], Mr H van Wyk [Quintiles]) as well as with the University veterinary surgeons, the mortality and catheter failure rate remained high. Therefore, after discussions with the Home Office Inspector, the procedure was eventually removed from the Project Licence, with the intention for further studies to use radiotelemetry for BP recording. Ending the study prematurely imposed limits on the number of animals included and the choice of genotypes studied.



Wireless radiotelemetry, allows the direct continuous measurement of BP, by means of a sensing catheter in the carotid artery connected to a transmitter device placed subcutaneously on the flank of the mouse (Brockway *et al.*, 1991; Butz *et al.*, 2001; Kramer *et al.*, 2003). There is no need for restraint or tethering, and the length of recording is limited only by the battery life of the device. Measurements can be made 24-hours/day, including the more active night time hours, which is particularly important when assessing the BP of nocturnal animals such as mice. Continuous recording also reduces the variation in estimates of the average BP value (Van Vliet *et al.*, 2003) and allows the effect of different dietary or pharmacological treatments to be studied within the same group of animals. Thus the total number of mice needing to be studied can be reduced.

The major disadvantage of using radiotelemetry to measure the BP of mice is its great expense. The lack of competition in the market means that both the capital cost of the equipment, and the price of refurbishment of the devices after each use, have remained high despite the widening use of this technology. The system can only be calibrated at the start and finish of each study, requiring estimation of the rate of device sensitivity change. Furthermore, the size of the PA-C20 device (3.5g), which we used, could result in pain and distress when placed subcutaneously in the flank of small mice (20-25g). Recently a smaller model has been introduced.

#### **4.4.3 Why did the results from the radiotelemetry and direct catheter BP studies differ?**

The technical problems encountered with the carotid artery catheter BP measurements, combined with the recent statement from the American Heart Association (Kurtz *et al.*, 2005), led us to use radiotelemetry for our subsequent studies. Having demonstrated that EC ET<sub>B</sub> receptor down-regulated mice exhibit hypertension on both normal and high salt diet using carotid artery catheterisation, it was surprising to find no difference in MBP, and only mild salt sensitive diastolic hypertension, between EC ET<sub>B</sub> receptor down-regulated mice and control animals

using radiotelemetry. There are a number of possible reasons to explain these differing results using the two different approaches to measure BP.

Firstly, the different results from the 2 studies could be related to the use of different control groups: WW/-- were used as controls in the carotid artery catheterisation study and FF/-- in the radiotelemetry study. Initial intentions had been to include FF/--, WW/-- and FF/Tie2 mice in the carotid artery catheterisation study. However, too few of the FF/-- animals survived to allow any meaningful comparison with the FF/Tie2 mice. The main disadvantage of using the WW/-- mice as the sole control group related to their different genetic background. These mice were descended from intercross of WW/Tie2 mice [background 50% C57BL6; 50% SJF1(Kisanuki *et al.*, 2001)] and had been maintained as a separate strain within the colony. The high cost of the radiotelemetry study meant that only two groups of mice could be included in this later study. Here, FF/-- siblings were used as controls, as in many other studies involving mice generated using the Cre-Lox system (Ahn *et al.*, 2004; Kimura *et al.*, 2004; Shohet *et al.*, 2004). By using FF/-- sibling controls, which had the same background as the FF/Tie2 mice (25% 129/01a; 25% BKW; 25% C57BL6; 25% SJF1), differences in genetic background were minimised. Thus the difference in BP seen between WW/-- and FF/Tie2 mice, in the carotid catheter study, could have been due the differences in genetic background (Ryan *et al.*, 2002), rather than due to EC ET<sub>B</sub> down-regulation. Alternatively, the differences could have been caused by the floxing of the ET<sub>B</sub> gene. However, this seems less likely as we have found no difference between WW/-- and FF/-- mice in terms of ET<sub>B</sub> receptor binding in the autoradiography studies (see section 3.2.6), plasma ET-1 concentrations and clearance of ET-1 (see sections 5.3.1 and 5.3.3). As discussed above (see section 4.4.1), future studies will involve backcrossing of the FF/-- and FF/Tie2 mice onto a salt resistant background (duration ~ 20-24 months). Once this has been achieved, further telemetry studies, involving both WW/-- and FF/-- mice as control groups, can be performed, to clearly determine whether floxing the ET<sub>B</sub> gene results in an unexpected effect on BP control.

Second, the carotid catheter measurements are likely to have been taken too soon after surgery. Problems of catheter occlusion meant that measurements could not be made more than 48 hours after catheter implantation. Our own telemetry data (see Figure 4-9, Figure 4-13, Figure 4-17 and Figure 4-21), as well as that of other groups (Butz *et al.*, 2001; Leon *et al.*, 2004; Lorenz, 2002; Pollock *et al.*, 2001), has revealed that, following surgery, mice require at least 5-6 days to recover their physiological BP diurnal variation, and several more days to get back to their pre-operative weight. At 48 hours the mice had not fully recovered from the surgery. It is possible that the difference in BP observed in the first study was artefactual, due to not enough time being allowed for recovery.

Third, the high mortality and catheter failure rate limited the numbers of animals studied in the carotid artery catheterisation study. Whilst successful recordings were performed in 20 animals, many more were operated on. Perhaps previously unidentified factors (eg renin-angiotensin-aldosterone system polymorphisms; glucose tolerance; birth weight) may have influenced which mice survived the surgery required for carotid artery catheter insertion. If such factors also exerted different effects on the reflex control of the circulation in the EC ET<sub>B</sub> down-regulated mice, then this could explain why these mice were found to be hypertensive in the first study.

Fourth, radiotelemetry allows continuous recording of BP, over several weeks, whilst the carotid artery catheterisation measurements were only performed for 30 minutes following a 30-minute acclimatisation period. The extended recording period means that the radiotelemetry measurements are much less likely to have been affected by sampling or experimental errors.

Chronic hypertension frequently results in end organ damage, such as left ventricular hypertrophy (Fagher *et al.*, 1995; Messerli *et al.*, 1988). If the difference in BP between EC ET<sub>B</sub> down-regulated mice and controls was truly as large as that seen in the direct carotid catheter study, then old EC ET<sub>B</sub> down-regulated mice might have been expected to show evidence of such end organ damage. However, even when

aged more than 12 months, EC ET<sub>B</sub> down-regulated mice do not exhibit increased heart/ body weight ratios (see Figure 4-45), reinforcing the validity of the radiotelemetry data showing that these mice do not have elevated MBP and only mildly elevated DBP on a normal salt diet.

## 5 CHAPTER 5: ROLE OF THE EC-ET<sub>B</sub> RECEPTOR IN THE PLASMA CLEARANCE OF ET-1

### 5.1 INTRODUCTION

As detailed in chapter 1 (see section 1.1.6) it is generally accepted that ET<sub>B</sub> receptor mediated clearance is central to the elimination of extracellular ET-1. Studies, using ET<sub>B</sub> antagonists in rats, have demonstrated the important role of the lungs, kidney and liver in the clearance of ET-1 (Fukuroda *et al.*, 1994). However, such organs are composed of a range of different cell types, several of which express ET<sub>B</sub> receptors. Experiments using pharmacological blockade or general genetic down-regulation of ET<sub>B</sub> receptor expression are not able to identify the contribution of ET<sub>B</sub> receptors, located on individual cell types, to the clearance of ET-1.

Cultured ECs avidly internalise ET-1, a process that can be blocked with ET<sub>B</sub>, but not ET<sub>A</sub>, antagonists (Ozaki *et al.*, 1995). Chronic administration of high dose A192621 (a selective ET<sub>B</sub> antagonist) is thought to block both EC and VSMC ET<sub>B</sub>, whereas low dose A192621 is suggested to act predominantly at the endothelium (Honore *et al.*, 2005). Raised plasma ET-1 concentrations are only found following chronic high dose A192621, suggesting that VSMC ET<sub>B</sub> receptors play the more significant role in ET-1 clearance. However, supporting evidence that cell specific ET<sub>B</sub> receptor blockade has been achieved with certain doses of pharmacological antagonism is less easy to provide than evidence of cell specific ET<sub>B</sub> receptor down-regulation in a transgenic mouse (see sections 1.3.6 and 3.3.5).

Here I have combined both of these approaches, using both pharmacological ET<sub>B</sub> blockade and the EC ET<sub>B</sub> receptor down-regulated mouse model, to determine the contribution of EC ET<sub>B</sub> and non-EC ET<sub>B</sub> receptors to the clearance of ET-1.

## **5.2 METHODS/PROTOCOLS**

### **5.2.1 Plasma ET-1 and big ET-1 concentrations**

Following euthanasia with CO<sub>2</sub>, blood was collected by direct cardiac puncture from both FF/Tie2 mice and controls. After centrifugation at 4°C, the plasma was drawn off. Samples from 2 individual animals of the same genotype were pooled to resulting in a minimum sample volume of 500  $\mu$ l. ET-1 and big ET-1 extraction and radioimmunoassay performed as described in section 2.9.1.

### **5.2.2 Clearance studies**

As described in section 2.9.2, a bolus of [<sup>125</sup>I]-ET-1 (0.37 pmol/mouse; 28 kBq/mouse; 1200 000 cpm/mouse) was injected intravenously via a right internal jugular catheter and serial blood samples (10  $\mu$ l) were collected by means of a carotid artery catheter. The activity of these samples was determined to give a measure of their [<sup>125</sup>I]-ET-1 concentration. Measurements were compared for mice of different genotype and following treatment with ET<sub>B</sub> blockade.

## 5.3 RESULTS

### 5.3.1 Plasma ET-1 concentrations

Plasma concentrations of ET-1, measured by radioimmunoassay, were found to be approximately three fold higher in the FF/Tie2 mice ( $12.4 \pm 3.0 \text{ pg.ml}^{-1}$ ) compared to single transgenic controls (WW/--:  $2.9 \pm 0.8 \text{ pg.ml}^{-1}$ ; WW/Tie2:  $3.0 \pm 0.8 \text{ pg.ml}^{-1}$ ; FF/--:  $4.1 \pm 0.5 \text{ pg.ml}^{-1}$ ) (Figure 5-1).

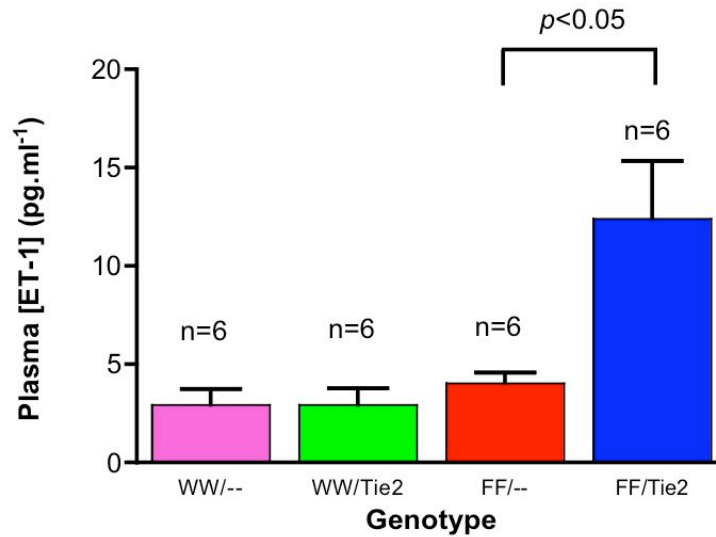


**Figure 5-1: Plasma concentrations of ET-1 were elevated in FF/Tie2 mice.**

Concentrations of ET-1 in plasma samples, each pooled from 2 individual mice of the same genotype, from FF/Tie2 and single transgenic control animals (where n = number of plasma samples).

### 5.3.2 Plasma big ET-1 concentrations

As ET-1 concentrations were similar between all single transgenic controls, big ET-1 analysis was only performed on FF/Tie2 and FF/-- controls. The plasma concentration of big ET-1 was increased in FF/Tie2 mice ( $199.8 \pm 8.0 \text{ pg.ml}^{-1}$ ) compared to FF/-- controls ( $137.1 \pm 12.6 \text{ pg.ml}^{-1}$ ), but to a lesser relative amount than seen with ET-1 (Figure 5-2).

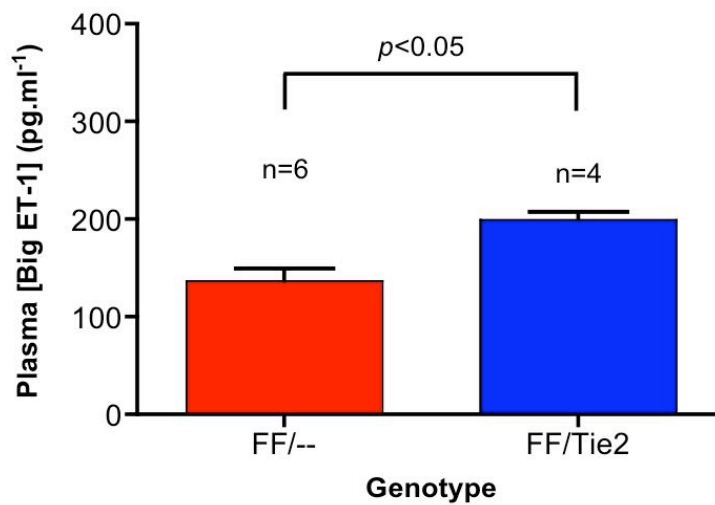


**Figure 5-2: Plasma concentration of big ET-1 was only marginally elevated in FF/Tie2 mice.**

Concentrations of big ET-1 in plasma samples, each pooled from 2 individual mice of the same genotype, from FF/Tie2 and FF/-- control animals (where n = number of plasma samples).



### 5.3.3 Effect of genotype on clearance of ET-1

The clearance of ET-1 was significantly impaired in the FF/Tie2 mice ( $0.053 \pm 0.006$  ml.sec<sup>-1</sup>) compared to WW/-- controls ( $0.175 \pm 0.032$  ml.sec<sup>-1</sup>;  $p < 0.01$ ) (Figure 5-3, Table 5-2 and Figure 5-8).

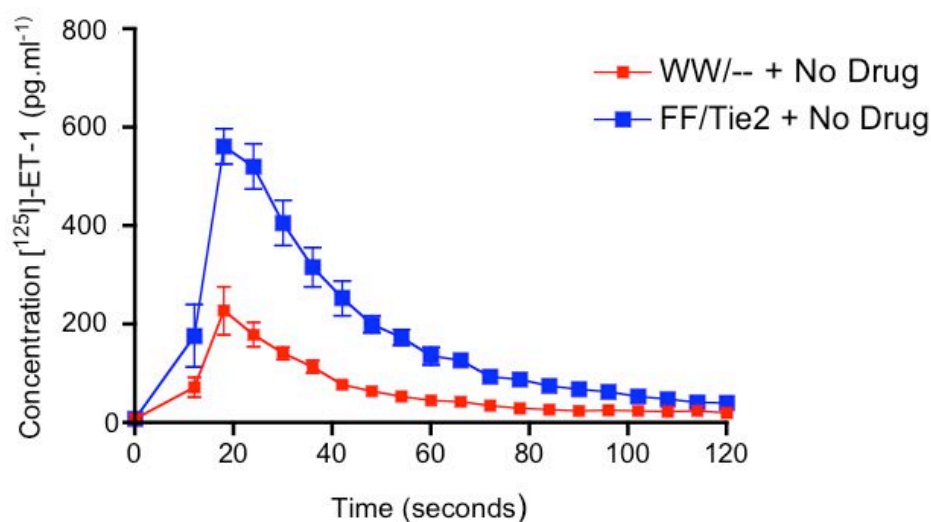


**Figure 5-3: Concentration – time graph showing that elimination of a bolus of radiolabelled ET-1 was impaired in FF/Tie2 compared to WW/-- mice.**

Concentration of [<sup>125</sup>I]-ET-1 in serial blood samples collected from the carotid artery of both FF/Tie2 (n=5) and WW/-- mice (n=6), following a bolus of 1080pg/mouse of radiolabelled ET-1 administered into the superior vena cavae.

Separate additional experiments showed no significant difference in the clearance of ET-1 between WW/-- ( $0.223 \pm 0.033 \text{ ml. sec}^{-1}$ ) and FF/-- animals ( $0.192 \pm 0.033 \text{ ml. sec}^{-1}$ ) (Figure 5-4).

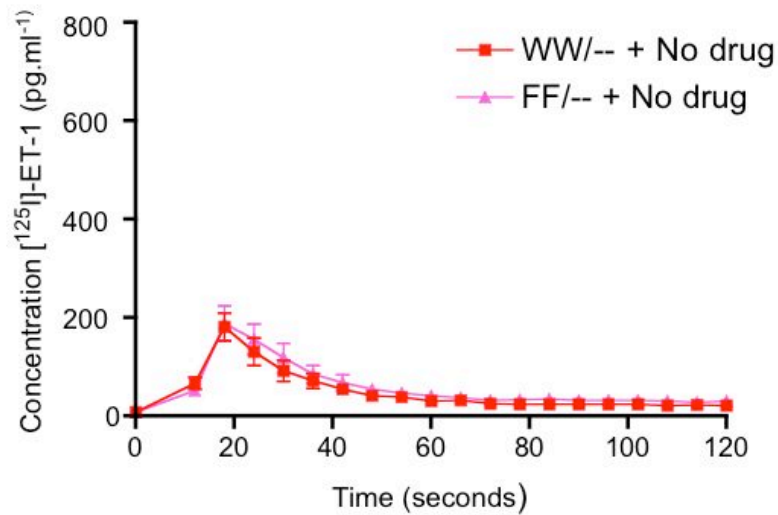


**Figure 5-4: Clearance of ET-1 was similar in WW/-- and FF/-- mice.**

Concentration of radiolabelled ET-1 in blood samples of both FF/-- (n=5) and WW/-- mice (n=4), following an i.v. bolus of 1080pg/mouse of  $[^{125}\text{I}]\text{-ET-1}$ .

### 5.3.4 Effect of pharmacological ET<sub>B</sub> blockade on clearance of ET-1

For the week preceding the study, mice were housed individually and fed either normal chow or chow containing A192621 (note: this method of administration was chosen as A192621 is highly insoluble in non-organic solvents, precluding its intravenous administration immediately before the clearance experiment). Neither genotype nor drug treatment had a significant effect on animal weight on the day of the study (Table 5-1).

**Table 5-1: Body weights on day of clearance study**

Body weights of mice on the day of study, following 7 days of pretreatment with either normal feed or chow containing the ET<sub>B</sub> antagonist A192621.

|                        | WW/--                 |   | FF/Tie2               |   |
|------------------------|-----------------------|---|-----------------------|---|
|                        | Mean weight (g) ± SEM | n | Mean weight (g) ± SEM | n |
| No drug                | 31.45 ± 1.99          | 6 | 32.45 ± 1.16          | 5 |
| A192621 (30mg/kg/day)  | 30.25 ± 1.44          | 5 | 32.23 ± 1.48          | 4 |
| A192621 (100mg/kg/day) | 26.78 ± 0.84          | 5 | 28.94 ± 1.52          | 5 |

Treatment of WW/-- mice with A192621 (100mg.kg<sup>-1</sup>.day<sup>-1</sup>) resulted in the clearance of ET-1 being impaired (0.052 ± 0.0052 ml.sec<sup>-1</sup>) to the same extent as untreated FF/Tie2 animals (0.053 ± 0.0055 ml.sec<sup>-1</sup>) (n=5; *p*>0.05) (Figure 5-5, Table 5-2 Figure 5-8). A192621 did not significantly alter the clearance of ET-1 in the FF/Tie-Cre mice (0.045 ± 0.0057 ml.sec<sup>-1</sup>) (Figure 5-5, Table 5-2 and Figure 5-8).

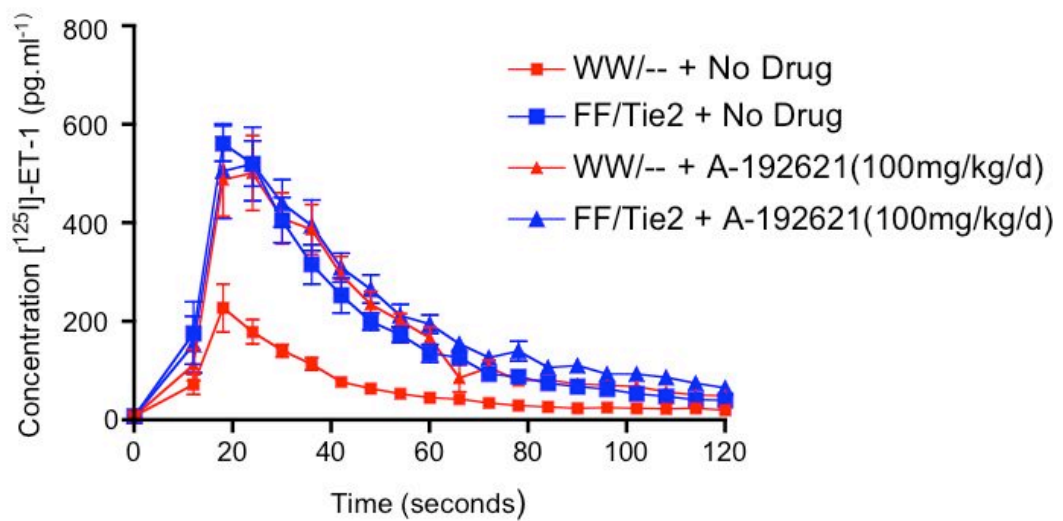


**Figure 5-5:  $ET_B$  blockade with A192621 impaired ET-1 clearance in WW/-- mice to a similar extent to that of untreated FF/Tie2 mice**

Concentration of radiolabelled ET-1 in blood samples of both FF/-- and WW/-- mice, following an i.v. bolus of 1080pg/mouse of [ $^{125}$ I]-ET-1, in the presence and absence of A192621 (100mg.kg<sup>-1</sup>.day<sup>-1</sup>). For numbers in group see Table 5-2.

Blockade with A192621 had a similar effect on clearance of ET-1 when administered to WW/-- mice at either 30mg.kg<sup>-1</sup>.day<sup>-1</sup> ( $0.064 \pm 0.0065$  ml.sec<sup>-1</sup>) or 100mg.kg<sup>-1</sup>.day<sup>-1</sup> ( $0.052 \pm 0.0052$  ml.sec<sup>-1</sup>) (Figure 5-6 and Table 5-2), implying that maximal  $ET_B$  antagonism was achieved at both doses.

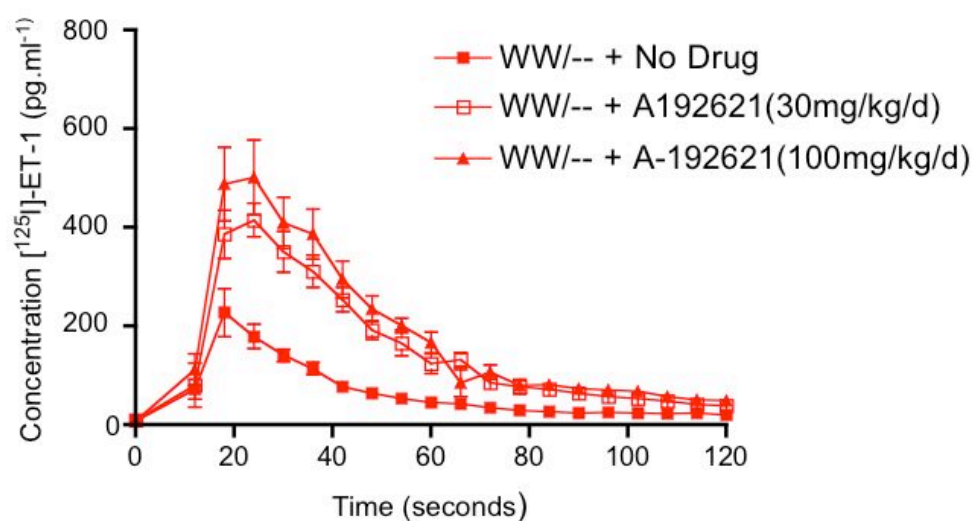


**Figure 5-6: Both low and high dose A192621 had similar effects on ET-1 clearance in WW/-- mice.**

Effect of dose of A192621 on clearance of ET-1 (n=5).

The slope of the  $\ln[\text{concentration}]$ -time graph gives the rate constant of ET-1 elimination ( $K_{el}$ ) from the plasma (Rang *et al.*, 2003). As shown in Figure 5-7, this is similar for both WW/-- ( $0.0390 \pm 0.0011 \text{ sec}^{-1}$ ) and FF/Tie2 ( $0.0331 \pm 0.0033 \text{ sec}^{-1}$ ) mice, and is not altered by ET<sub>B</sub> receptor blockade (Table 5-2). Thus the half-life of ET-1 ( $\ln 2 / K_{el}$ ) is also similar for both genotypes (Table 5-2).

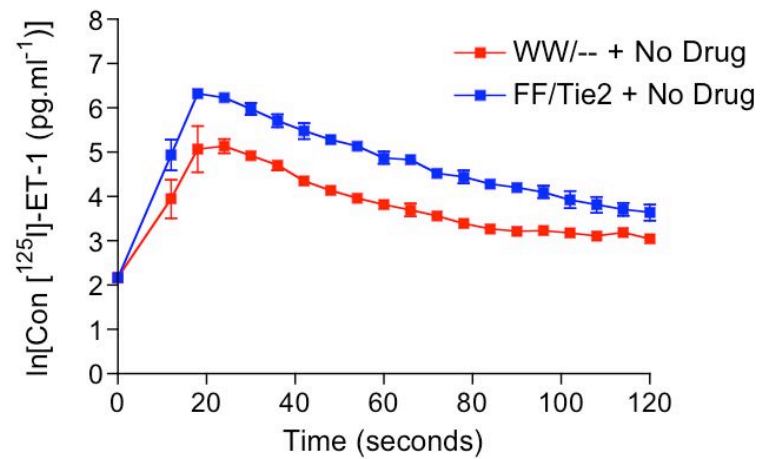


**Figure 5-7: Logarithmic plot of concentration against time was not different between genotypes**

By plotting the logarithm of the concentration of radiolabelled ET-1 against time, allows the  $K_{el}$  (equal to the inverse of the gradient) to be calculated. This was similar for both genotypes.

**Table 5-2: Pharmacokinetic data for elimination of a bolus of [<sup>125</sup>I]-ET-1**

Area under the curve (AUC), elimination constant ( $K_{el}$ ), half life ( $t_{1/2}$ ), clearance ( $C_L$ ) and volume of distribution ( $V_d$ ) for the elimination of radiolabelled ET-1 in both WW/-- and FF/Tie2 mice in the presence and absence of the ET<sub>B</sub> antagonist A192621. [\*  $p < 0.05$  WW/-- no drug versus FF/Tie2 no drug; †  $p < 0.005$  WW/-- no drug versus WW/-- plus A192621 (100mg/kg/day)].

|                       | WW/--                      |                      |           |                         |                     |   | FF/Tie2                    |                      |           |                         |                     |   |
|-----------------------|----------------------------|----------------------|-----------|-------------------------|---------------------|---|----------------------------|----------------------|-----------|-------------------------|---------------------|---|
|                       | AUC                        | $K_{el}$             | $t_{1/2}$ | $C_L$                   | $V_d$               | n | AUC                        | $K_{el}$             | $t_{1/2}$ | $C_L$                   | $V_d$               | n |
|                       | (pg.ml <sup>-1</sup> .sec) | (sec <sup>-1</sup> ) | (sec)     | (ml.sec <sup>-1</sup> ) | (ml <sup>-1</sup> ) |   | (pg.ml <sup>-1</sup> .sec) | (sec <sup>-1</sup> ) | (sec)     | (ml.sec <sup>-1</sup> ) | (ml <sup>-1</sup> ) |   |
| <b>No drug</b>        | 6640 ±                     | 0.0390 ±             | 17.84     | 0.175 ±                 | 4.42 ±              | 6 | 20000 ±                    | 0.0331 ±             | 21.96     | 0.053 ±                 | 1.74 ±              | 5 |
|                       | 867 *†                     | 0.00105              | ± 0.47    | 0.0319 *†               | 0.69 *†             |   | 1890                       | 0.00325              | ± 2.61    | 0.0055                  | 0.36                |   |
| <b>A192621</b>        | 16700 ±                    | 0.0330 ±             | 21.14     | 0.064 ±                 | 1.95 ±              | 5 | 23600 ±                    | 0.0299 ±             | 23.51     | 0.044 ±                 | 1.49 ±              | 4 |
| <b>(30mg/kg/day)</b>  | 1750                       | 0.00101              | ± 0.70    | 0.0065                  | 0.18                |   | 3200                       | 0.00186              | ± 1.58    | 0.0052                  | 0.18                |   |
| <b>A192621</b>        | 20500 ±                    | 0.0339 ±             | 20.50     | 0.052 ±                 | 1.54 ±              | 5 | 23700 ±                    | 0.0261 ±             | 26.85     | 0.045 ±                 | 1.76 ±              | 5 |
| <b>(100mg/kg/day)</b> | 2320                       | 0.00087              | ± 0.50    | 0.0052                  | 0.18                |   | 2820                       | 0.00110              | ± 1.14    | 0.0057                  | 0.26                |   |

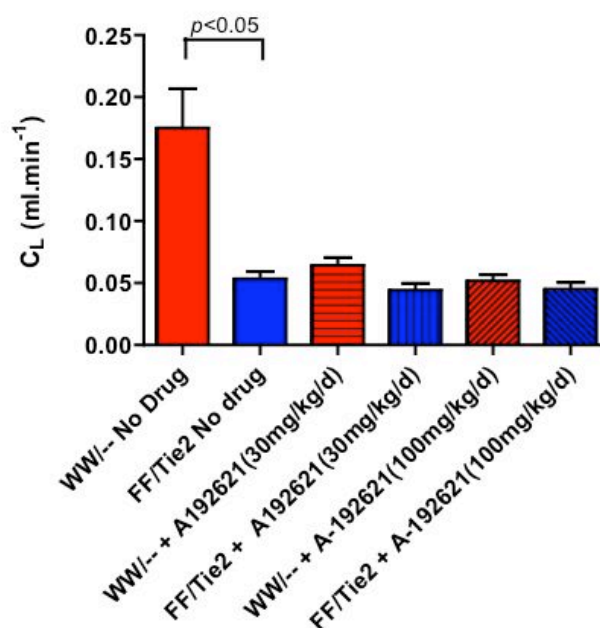


**Figure 5-8: Clearance of ET-1 was impaired in FF/Tie2 mice, and in mice of both genotypes treated with ET<sub>B</sub> blockade.**

Clearance of a bolus of radiolabelled ET-1 by both genotypes in the presence and absence of A192621.

## 5.4 DISCUSSION

We have demonstrated that plasma ET-1 concentrations are three to four fold higher in mice featuring EC ET<sub>B</sub> receptor down-regulation than in control animals. That the precursor of ET-1, big ET-1, is only mildly elevated in the EC ET<sub>B</sub> down-regulated mice, suggests that this receptor acts to eliminate ET-1 from the circulation, rather than inhibit the production of the peptide. Furthermore, we have found that the clearance of a bolus of radiolabelled exogenous ET-1 is impaired in untreated EC ET<sub>B</sub> down-regulated mice, as seen in control mice treated with a maximal dose of ET<sub>B</sub> antagonist. Thus we conclude that the EC ET<sub>B</sub> receptor makes a significant contribution towards the elimination of extracellular ET-1.

### 5.4.1 Plasma ET-1 and big ET-1 concentrations

The small size of mice restricts the volume of plasma that can be collected. The extraction prior to the RIA required a minimum of 500  $\mu$ l of plasma, and so samples



from more than one animal had to be pooled. Alternative techniques, such as Enzyme Linked Immunosorbent Assays (ELISA), are available (Amiri *et al.*, 2004; Gariepy *et al.*, 2000), which require smaller volumes of plasma for determination of ET-1 concentrations, but these are not currently established in our laboratory.

In common with other studies involving either genetic disruption (Gariepy *et al.*, 2000) or pharmacological blockade of the ET<sub>B</sub> (Brunner *et al.*, 1996; Goddard *et al.*, 2004a), down-regulation of the EC ET<sub>B</sub> receptor results in raised plasma concentrations of ET-1. This could be due to either increased production or impaired clearance of ET-1, mediated by EC ET<sub>B</sub>.

Higher production of ET-1 results from either increased expression of pre-proET-1 (causing higher plasma concentrations of big ET-1, the precursor to the mature peptide) or enhanced activity of ECE-1, the enzyme that converts big ET-1 into ET-1. We have shown that EC ET<sub>B</sub> receptor down-regulated mice demonstrate mildly elevated plasma concentrations of big ET-1. Nitric oxide (NO) is known to inhibit ET-1 production from the endothelium (Boulanger *et al.*, 1990), and so lack of tonic EC ET<sub>B</sub> mediated NO might be expected to contribute to the observed increased big ET-1 and ET-1 plasma concentrations in the EC ET<sub>B</sub> down-regulated mice. In cultured rat ECs, ET<sub>B</sub> activation has been shown to inhibit the expression of ECE-1 (Naomi *et al.*, 1998), suggesting that elevated enzyme concentrations would be seen in the EC ET<sub>B</sub> down-regulated mice, although this was not seen in our semi-quantitative RT-PCR studies (see Figure 3-21).

In contrast, other studies, involving both animals and humans, do not show ET<sub>B</sub> antagonists to alter the concentration of big ET-1 (Loffler *et al.*, 1993; Plumpton *et al.*, 1996). Furthermore, as ET<sub>B</sub> activation have been shown to mediate autoinduction of preproET-1 mRNA expression (Saito *et al.*, 1995), down-regulation of ET<sub>B</sub> would not be expected to result in elevated plasma ET-1 production.

To investigate the effect of EC ET<sub>B</sub> down-regulation on the elimination of ET-1 alone, studies investigating the elimination of a bolus of radiolabelled ET-1 were performed.

#### **5.4.2 Plasma clearance studies**

Previous studies, using exogenous radiolabelled [<sup>125</sup>I]-ET-1, have revealed the important role of ET<sub>B</sub> receptor in the removal of ET-1 from the circulation (Berthiaume *et al.*, 2000; Burkhardt *et al.*, 2000; Fukuroda *et al.*, 1994). By performing similar experiments, we have shown that down-regulation of the EC ET<sub>B</sub> receptor results in impaired ET-1 clearance that can be reproduced by treating control animals with pharmacological ET<sub>B</sub> blockade. That maximal ET<sub>B</sub> blockade was achieved with the doses of selective antagonist used in this study has been demonstrated by others (Pollock *et al.*, 2001) and also by the observation that both high and low doses of A192621 had the same effect on ET-1 clearance. Thus the contribution of ET<sub>B</sub> receptors located on cells other than ECs to the clearance of ET-1 would appear to be negligible. To identify the relative contribution of ET<sub>B</sub> receptors located on different cell types, others have used a novel pharmacological approach in the attempt to achieve tissue specific ET<sub>B</sub> receptor blockade (Honore *et al.*, 2005). Chronic low dose ET<sub>B</sub> blockade with A192621 (0.5mg/kg/day) blocked only the initial hypotensive response to a bolus of ET<sub>B</sub> agonist in anaesthetised hamsters, whereas high dose A192621 (30mg/kg/day) blocked both the initial hypotensive response as well as the later pressor response. From this they propose that low dose A192621 is predominantly blocking EC ET<sub>B</sub>, whereas the high dose is blocking both EC and VSMC ET<sub>B</sub>. Plasma ET-1 concentrations are increased only with the high dose of A192621. They therefore conclude that VSMC ET<sub>B</sub> contributes significantly to ET-1 clearance. However, the authors rely solely on the physiological assay of the pressor response to a bolus of ET<sub>B</sub> agonist (not ET-1 itself), to demonstrate tissue specific ET<sub>B</sub> blockade. This pressor response varies across species [depressor then pressor in rats (Garipey *et al.*, 2000), pressor only in mice (Giller *et al.*, 1997)] and so is not the most reliable evidence of cell specific ET<sub>B</sub> blockade. They do not provide evidence that, at the higher dose, A192621 is not

acting non-selectively at both ET<sub>A</sub> and ET<sub>B</sub> receptors. Furthermore, no clearance studies, using radiolabelled ET-1, were performed. Conclusions concerning ET-1 clearance were based merely on ET-1 plasma concentrations. By performing radiolabelled [<sup>125</sup>I]-ET-1 clearance studies, using a cell-specific ET<sub>B</sub> receptor down-regulated mouse (with both structural and functional evidence of EC specific knock-down – see sections 1.3.6 and 3.3.5) we have been able to robustly demonstrate the important contribution of the EC ET<sub>B</sub> receptor to ET-1 elimination. Although we have compared EC ET<sub>B</sub> down-regulated mice with control animals pretreated with supramaximal doses of ET<sub>B</sub> antagonists, to determine the overall contribution of the EC ET<sub>B</sub> to the clearance of ET-1, further control experiments would be valuable involving other tissue specific ET<sub>B</sub> knock-down animals, such as VSMC ET<sub>B</sub> down-regulated mice. It would be expected that such animals might have unimpaired clearance of ET-1 compared to controls.

#### **5.4.3 Non ET<sub>B</sub> receptor mediated ET-1 clearance**

As demonstrated previously (Berthiaume *et al.*, 2000; Burkhardt *et al.*, 2000), we have shown that even in the presence of maximal ET<sub>B</sub> receptor blockade, radiolabelled [<sup>125</sup>I]-ET-1 is still swiftly eliminated from the plasma (within 2 minutes). This is most likely due to enzymatic degradation (Deng *et al.*, 1992) by neutral endopeptidases (Abassi *et al.*, 1992). Studies comparing the uptake of radiolabelled ET-1 by different organs in the presence of ET<sub>B</sub> receptor blockade, indicate these enzymes are most likely to be located in the kidney and liver (Burkhardt *et al.*, 2000).

#### **5.4.4 Technical considerations in plasma clearance studies**

Serial blood sampling from an animal as small as a mouse can quickly result in depletion of the intravascular volume, and so the samples collected were kept as small as possible. The clearance studies involved the serial collection of 10µl arterial blood samples every 6 seconds over 2 minutes (200µl in total; less than 10% of the

circulating blood volume of a mouse). In preliminary experiments, the removal of such a volume in this way did not have a significant haemodynamic effect.

The small volumes of blood sampled (10 $\mu$ l) precluded the direct measurement of ET-1, using techniques such as radioimmunoassay (this requires ~500 – 700 $\mu$ l minimum sample volume). Therefore by injecting an exogenous bolus of [<sup>125</sup>I]-ET-1 of known activity and concentration, and by measuring the radioactivity of each blood sample collected, an estimate was made of the radiolabelled ET-1 concentration in each sample. However, using this technique, it is not possible to differentiate between radiolabelled ET-1 and any metabolised products of ET-1, which retain the radiolabel and remain in the plasma. We have had to assume therefore, that during the 2 minutes of each study, whilst ET-1 is internalised by ET<sub>B</sub> receptors, no metabolism occurs within the vascular compartment.

A further limitation of our study is that we have only considered plasma ET-1 concentrations, and have not measured tissue ET-1 concentrations. Given that ET-1 is considered by many to be an autocrine/paracrine agent, produced predominantly in the endothelium and acting at receptors situated on both EC and neighbouring vascular smooth muscle receptors (Battistini *et al.*, 1993; Kedzierski *et al.*, 2001; Kotelevtsev *et al.*, 2001), the effect of EC ET<sub>B</sub> down-regulation on tissue ET-1 availability may be more physiologically relevant than focusing on plasma ET-1 concentrations.

The clearance ( $C_L$ ) of a substance is defined as the volume of plasma from which that substance is removed per unit time (Guyton *et al.*, 2005). It can also be defined by the following equation:

$$C_L = V_d \cdot K_{el}$$

(where  $V_d$  is the volume of distribution and  $K_{el}$  is the elimination rate constant) (Rang *et al.*, 2003).

Plotting the concentration of radiolabelled ET-1 logarithmically against time, gives a straight line, where the inverse slope equals the elimination rate constant,  $K_{el}$  (Figure 5-7)(Rang *et al.*, 2003). This shows that  $K_{el}$  is similar in both strains of mice. Equivalent graphs, showing similar  $K_{el}$  for heterozygous  $ET_B$  +/- and wild type control mice, can be calculated using data from previous studies (Berthiaume *et al.*, 2000). However, we have shown that the plasma concentration of ET-1 is four fold greater in EC  $ET_B$  down-regulated mice, compared to control animals. This means, that even with a similar rate of elimination of ET-1, the volume cleared of ET-1 per unit time (i.e. the ET-1 clearance) is less in the EC  $ET_B$  down-regulated mice.

In our experiment, preliminary studies allowed for the optimum bolus dose of intravenous radiolabelled [ $^{125}I$ ]-ET-1 to be determined. Too high a dose causes a pressor effect (seen with a plasma concentration of  $\sim 45 \text{ ng.ml}^{-1}$  (Berthiaume *et al.*, 2000; Gariepy *et al.*, 2000; Giller *et al.*, 1997)). Too low a dose precludes detection of radiolabelled [ $^{125}I$ ]-ET-1 in the arterial blood samples above background in the gamma scintillation counter. As found previously (Berthiaume *et al.*, 2000; Burkhardt *et al.*, 2000), the dose required in our studies ( $0.37 \text{ pmol/mouse}$ ; equivalent to a mean plasma concentration of  $\sim 540 \text{ pg.ml}^{-1}$  [assuming a murine blood volume of  $\sim 2\text{ml}$ ]) whilst being well below the threshold to cause a pressure response, was  $\sim 100$  fold the physiological concentration of ET-1 ( $3\text{-}5 \text{ pg.ml}^{-1}$ ).

Therefore, in the control animals, it seems likely that the excess radiolabelled ET-1 swiftly saturates the EC  $ET_B$  within the initial seconds of the experiment. Following this the ET-1 is metabolised by non-EC  $ET_B$  mechanisms, such as neutral endopeptidases in the kidney and liver. In contrast, in the EC  $ET_B$  down-regulated mice, none of the labelled ET-1 binds to the EC  $ET_B$ , and so the measured labelled ET-1 concentration is higher, and is removed from the circulation solely by non-EC  $ET_B$  enzymatic degradation. Thus, the  $V_d$  (and therefore the clearance) of the radiolabelled ET-1 is much greater in the control animals, as the  $ET_B$  receptors on the endothelium allow it to pass freely into the ECs, whereas in the EC  $ET_B$  down-regulated mice the ET-1 remains in the plasma and so for these mice, the  $V_d$  is much reduced.

## **6 CHAPTER 6: ROLE OF THE EC-ET<sub>B</sub> RECEPTOR IN THE CONTROL OF PULMONARY VASCULAR TONE AND THE DEVELOPMENT OF PULMONARY ARTERIAL HYPERTENSION**

### **6.1 INTRODUCTION**

Pulmonary arterial hypertension (PAH) is a progressive and fatal condition of the cardiopulmonary circulation characterised by a sustained increase in pulmonary vascular resistance leading to right ventricular failure and premature death. This process is accompanied by an abnormal proliferation of VSMCs of small pulmonary arteries (PAs). As both a potent vasoconstrictor and mitogen, ET-1 has been implicated in the aetiology and progression of PAH. Plasma concentrations of ET-1 correlate with severity of PAH in both animal models (Frasch *et al.*, 1999; Nakanishi *et al.*, 1999; Stelzner *et al.*, 1992) and patients suffering from this debilitating condition (Cacoub *et al.*, 1997; Giaid *et al.*, 1993).

The lung is the most important site of ET-1 production with concentrations 5 times greater than those seen in other organs (Firth *et al.*, 1992). The highest concentration of ET<sub>B</sub> mRNA is also found in the lung (Li *et al.*, 1994b). ET<sub>A</sub> and ET<sub>B</sub> receptors are expressed throughout the lung in blood vessels, bronchioles and alveoli, with the greatest number of ET binding sites found in distal segments (Davie *et al.*, 2002). ET<sub>A</sub> receptors are localised to the media of the large proximal PAs and veins with relatively little expression in distal arterioles (Davie *et al.*, 2002; Soma *et al.*, 1999). ET<sub>B</sub> receptors, in contrast, are highly expressed in distal vascular segments (Davie *et al.*, 2002). Under normoxic conditions, ET<sub>B</sub> receptors of the distal pulmonary vasculature are mainly confined to the medial layer. However, hypoxia increases the expression of ET-1, ET<sub>A</sub> and ET<sub>B</sub> receptors throughout the lung (Li *et al.*, 1994a), with evidence to suggest a preferential increase in EC ET<sub>B</sub> receptor expression in distal segments in some (Soma *et al.*, 1999) but not all (Balyakina *et al.*, 2002; Black *et al.*, 2003) studies.

Non-selective antagonists of ET receptors have recently been granted approval for the treatment of primary pulmonary hypertension and have been shown to confer symptomatic and prognostic benefits (McLaughlin *et al.*, 2005; Rubin *et al.*, 2002). Both ET<sub>A</sub> and ET<sub>B</sub> receptors on VSMC mediate vasoconstriction and cellular hypertrophy (Davie *et al.*, 2002; MacLean *et al.*, 1994; Sato *et al.*, 1995) and hence may promote the progression of PAH. However, EC ET<sub>B</sub> receptors within the lung clear ET-1 from the plasma (Dupuis *et al.*, 1996a; Dupuis *et al.*, 1996b; Fukuroda *et al.*, 1994) (see chapter 5) and mediate vasodilatation and anti-mitogenic effects through the release of NO and PGI<sub>2</sub> (de Nucci *et al.*, 1988; Takayanagi *et al.*, 1991). Rescued ET<sub>B</sub> deficient rats demonstrate raised pulmonary arterial pressures when exposed to hypoxia (Ivy *et al.*, 2001; Ivy *et al.*, 2002), and develop plexiform lesions when treated with the endothelial toxin monocrotaline (Ivy *et al.*, 2005), suggesting that, at least in a rodent model of PAH, the net effect of ET<sub>B</sub> blockade is beneficial. Results from the STRIDE-2 trial show a modest increase in functional benefit with sitaxsentan treatment (ET<sub>A</sub> selective antagonist) compared to open label mixed ET blockade (Barst *et al.*, 2006). However, such studies are unable to reveal the contribution of the EC ET<sub>B</sub> receptor to the pathogenesis of PAH.

Several different animal models of PAH have been developed, including systemic to pulmonary shunts (Reddy *et al.*, 1995), bleomycin lung injury (Williams *et al.*, 1992), monocrotaline treatment (Todorovich-Hunter *et al.*, 1988) and chronic hypoxia exposure (Rabinovitch *et al.*, 1979). Using a toxin, such as monocrotaline, which damages all ECs, would obviate any advantage of studying an EC specific down-regulated mouse model. The surgery required for left to right shunting, particularly in small rodents, is formidable. Chronic hypoxia, induced by housing mice in hypobaric chambers, is well established in rodents, and offers a convenient and straightforward method of inducing PAH, using a well recognised secondary cause of the condition. Here I have investigated the effect of exposing EC ET<sub>B</sub> receptor down-regulated mice to hypobaric hypoxia to determine the contribution of this receptor to the pathogenesis of PAH.

## 6.2 METHODS/PROTOCOLS

Both FF/Tie2 and FF/-- mice were housed under hypobaric hypoxia for 14 days (see section 2.10.1). Normoxic controls of both genotypes were maintained in the same room under atmospheric pressure. Following haemodynamic assessment, as described in section 2.10.2, the mice were euthanased, hearts removed for weighing, the right lung taken for histology and the left lung put on ice for later dissection to isolate the left PA. This was used for wire myography as described in section 2.10.4.

### 6.2.1 Myography protocol

Following wake-up, as described in section 2.10.4.1, cumulative concentration-response curves (CRCs) were constructed to ET-1 for each pair of PA rings, one in the presence and the other in the absence of 100  $\mu$ M N-nitro-L-arginine methyl ester (L-NAME). These were performed by adding cumulative doses of ET-1 (Merck Biosciences Ltd., Nottingham, UK) in half-log increments ( $10^{-15}$ M -  $10^{-7}$ M), allowing the maximal response to each dose to plateau prior to subsequent additions. L-NAME (100  $\mu$ M) was added to the second of each pair of PA rings 30 minutes prior to ET-1. Previous studies using mice of a similar background to our FF/Tie2 animals (background: 129SV) have shown little dilatation to ACh, and so comparison of the responses in the presence and absence of L-NAME was used with the aim of assessing vascular endothelial function (Keegan et al., 2001).

All responses to ET-1 were expressed as a percentage of the second response to 50 mM KCl, during the wake-up period, to calculate the maximum contraction ( $E_{\max}$ ).  $pEC_{50}$  values were calculated from CRCs by graphical interpolation (Graphpad Prism 4.0). Statistical comparisons of the  $E_{\max}$  and  $pEC_{50}$  values were made by one-way analysis of variance, and the CRCs were compared by 2-way ANOVA. When significance was attained ( $p < 0.05$ ), differences were established using the Newman-Keuls multiple comparison test. Data are expressed as mean  $\pm$  SEM.



## 6.3 RESULTS

### 6.3.1 Weights

Genotype did not have a significant effect on animal weight by the time of euthanasia following the haemodynamic study, although hypoxia did cause the body weight of FF/Tie2 mice to fall ( $p<0.05$ ).

**Table 6-1: Weights of mice**

Mean weights of mice after 2 weeks under either hypoxic or normoxic conditions. (\*FF/Tie2 hypoxic vs FF/Tie2 normoxic:  $p<0.05$ ).

|          | FF/--                     |    | FF/Tie2                   |    |
|----------|---------------------------|----|---------------------------|----|
|          | Mean weight (g) $\pm$ SEM | n  | Mean weight (g) $\pm$ SEM | n  |
| Normoxia | 37.43 $\pm$ 1.42          | 9  | 34.85 $\pm$ 1.26          | 10 |
| Hypoxia  | 34.07 $\pm$ 1.74          | 10 | 31.44 $\pm$ 1.3*          | 10 |

### 6.3.2 Haemodynamic studies

Systemic mean arterial BP and heart rate, measured under halothane anaesthesia by means of an intra-arterial carotid catheter, were not significantly different in FF/Tie2 mice compared to FF/-- controls under both normoxic and hypoxic conditions.

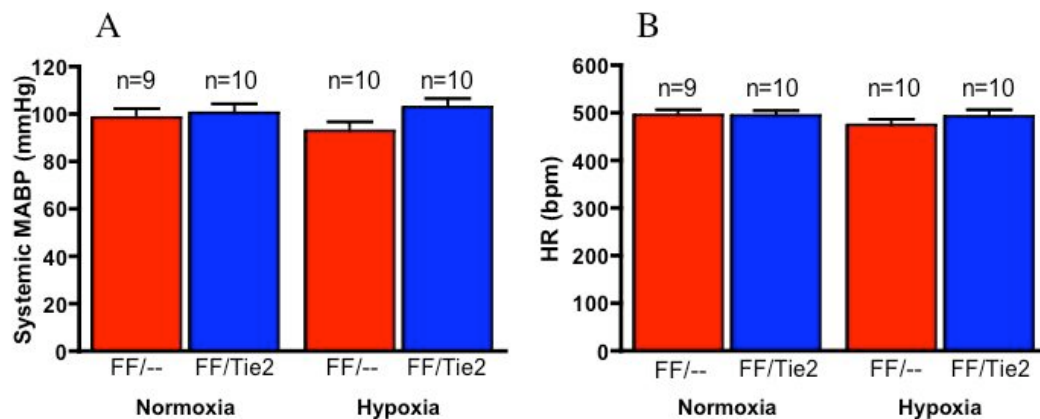


**Figure 6-1: Systemic haemodynamics did not differ between genotypes under both normoxic and hypoxic conditions.**

Systemic mean arterial BP (A) and heart rate (B) did not differ between anaesthetised FF/-- and FF/Tie2 mice housed under normoxic and hypoxic conditions.

Although systolic right ventricular pressure (RVP) was similar between genotypes under normoxic conditions, following 2 weeks of hypoxia, the systolic RVP of FF/Tie2 mice was significantly elevated in FF/Tie2 mice ( $34 \pm 1.2$  mmHg) compared to FF/-- controls ( $24 \pm 1.7$  mmHg;  $n=10$ ;  $p<0.001$ ).

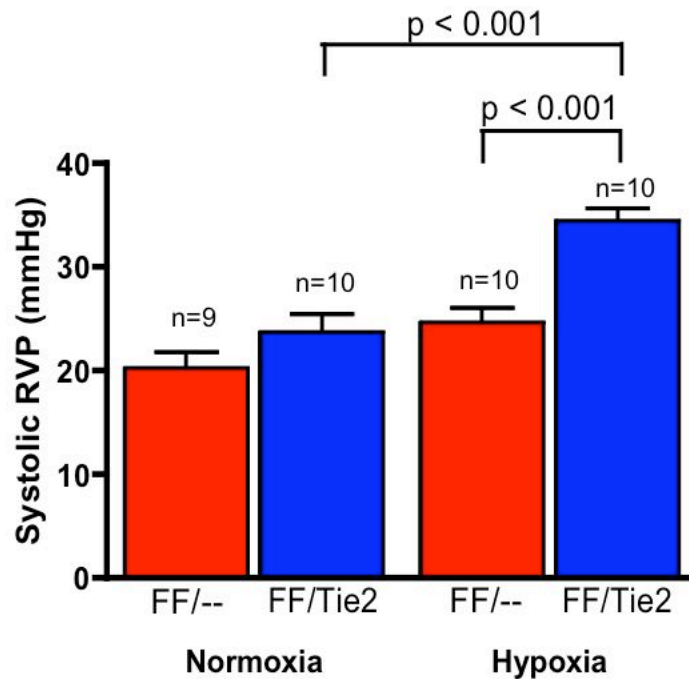


**Figure 6-2: The systolic RVP of FF/Tie2 mice was significantly elevated under hypoxic conditions**

Systolic right ventricular pressures of anaesthetised FF/-- and FF/Tie2 mice housed under normoxic were not significantly different. Exposure to hypoxia resulted in elevated systolic RVP in FF/Tie2 but not in FF/-- mice.

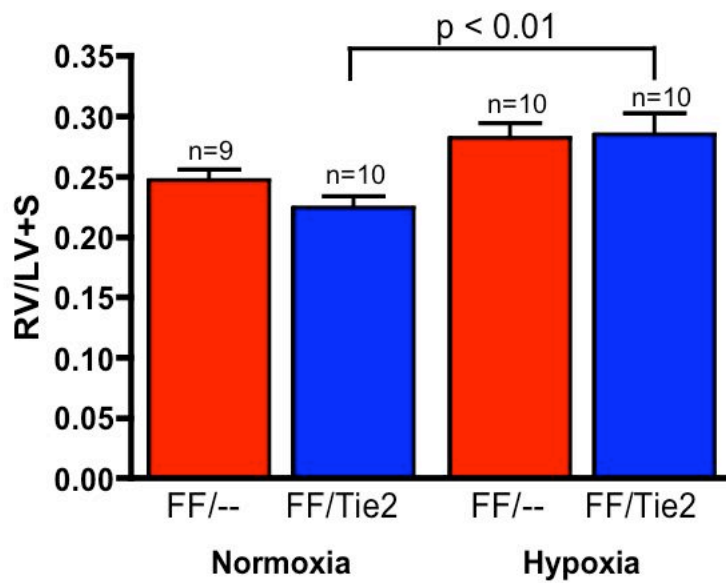
### 6.3.3 Right ventricular hypertrophy

**Table 6-2: Indices of right ventricular hypertrophy**

RV (right ventricular)(mg)/ LV+S (left ventricular plus septum weight) (mg); RV(mg)/ TV (total ventricle)(mg)/; and RV (mg)/ BW (body weight)(g) ratios  $\pm$  SEM of FF/Tie2 and FF/-- mice exposed to normoxic and hypoxic conditions. (\* compared to normoxic mice  $p < 0.05$ ; one way ANOVA).

|                 | FF/--      |            |            | FF/Tie2    |            |            |
|-----------------|------------|------------|------------|------------|------------|------------|
|                 | RV/LV+S    | RV/TV      | RV/BW      | RV/LV+S    | RV/TV      | RV/BW      |
| <b>Normoxic</b> | 0.25 $\pm$ | 0.20 $\pm$ | 0.80 $\pm$ | 0.22 $\pm$ | 0.18 $\pm$ | 0.75 $\pm$ |
|                 | 0.009      | 0.006      | 0.065      | 0.009      | 0.006      | 0.047      |
| <b>Hypoxic</b>  | 0.28 $\pm$ | 0.22 $\pm$ | 1.03 $\pm$ | 0.29 $\pm$ | 0.22 $\pm$ | 0.98 $\pm$ |
|                 | 0.012      | 0.007      | 0.083 *    | 0.017 *    | 0.010 *    | 0.045 *    |

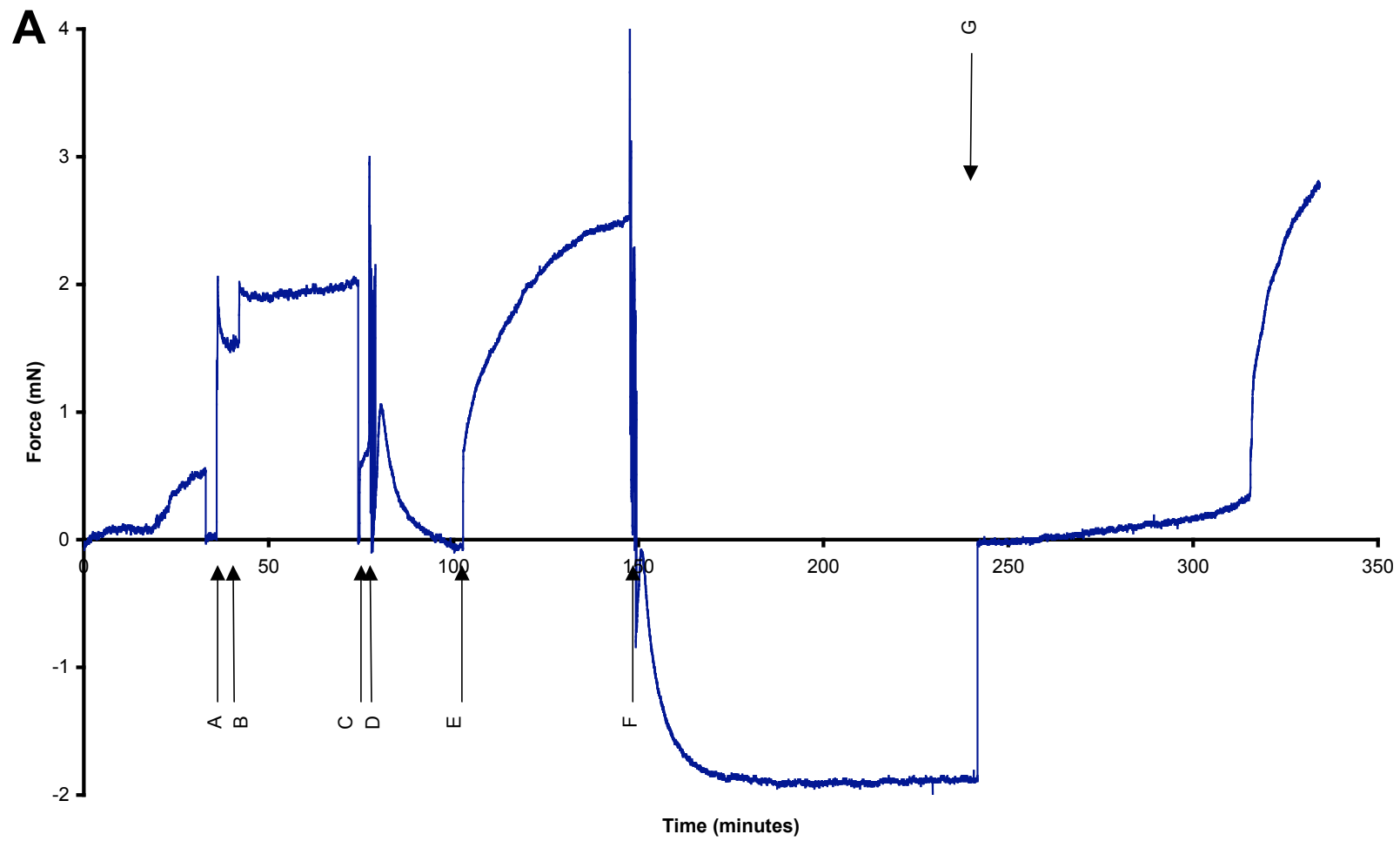
Both genotypes demonstrated a significant increase in RV/ BW ratio when exposed to hypoxia, although only FF/Tie2 mice demonstrated a significant increase in the ratio of RV/ LV+S mass (Table 6-2 and Figure 6-3).



**Figure 6-3: Hypoxia results in right ventricular hypertrophy in hypoxic mice FF/Tie2 mice**

Unlike FF/-- mice, FF/Tie2 mice housed under hypoxia showed significantly elevated RV/LV+S (right ventricular mass / left ventricle plus septum mass) compared to FF/Tie2 mice housed under normoxic conditions.

#### 6.3.4 Myography



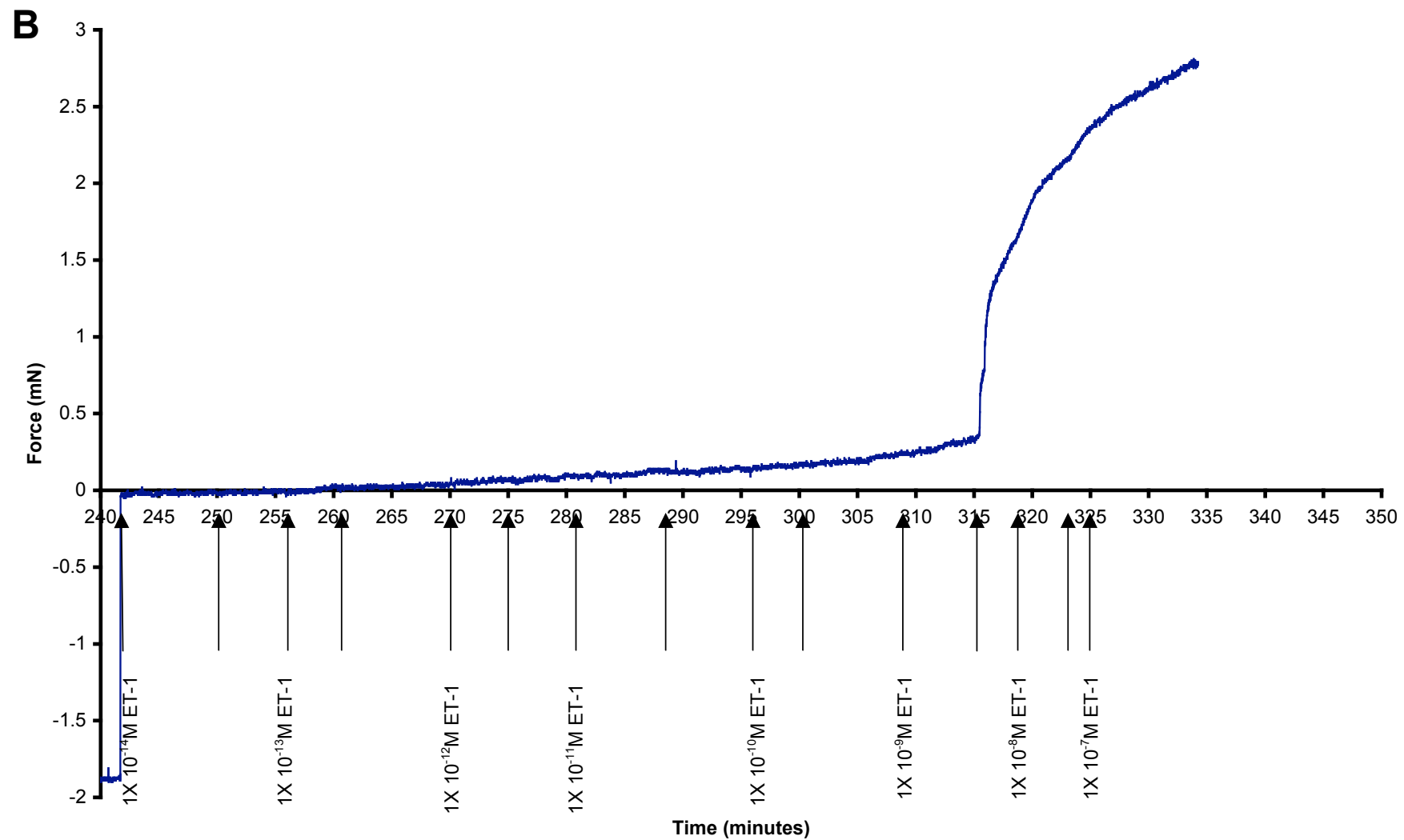


**Figure 6-4: (previous 2 pages). Representative tracing of a wire myography study of a 3<sup>rd</sup> order PA ring from FF/-- mouse, housed under normoxic conditions, not exposed to L-NAME.**

Figure 6-4A shows the PA ‘wake up’ protocol followed by the concentration response to increasing concentrations of ET-1. Tension was applied to give a transmural pressure equivalent to 12 - 14 mmHg (equivalent to normoxic conditions) (A, B). Following a 30 minute equilibration period, the PA ring were contracted to 50 mM KCl solution (C), which was then washed out with Krebs-buffer solution (D). The PA ring was contracted to 50 mM KCl for a second time (E) and then washed out 5 times with Krebs-buffer solution (F). Following this ‘wake up’ protocol, the cumulative-response to ET-1 was measured (G) – expanded time axis Figure 6-4B - ET-1 was added in half-log increments ( $10^{-14}$ M -  $10^{-7}$ M).

(These data were obtained from Dr Y Dempsey, University of Glasgow).

As detailed in the Methods chapter (see section 2.10.4), PA rings from mice housed under normoxic conditions were tensioned to give an equivalent transmural pressure between 12 –14 mmHg for tissue from normoxic mice and 30 – 33 mmHg for tissue from hypoxic mice. No difference was seen in the internal circumference/ tension relationship (a measure of stiffness) between PA rings from mice of different genotype.

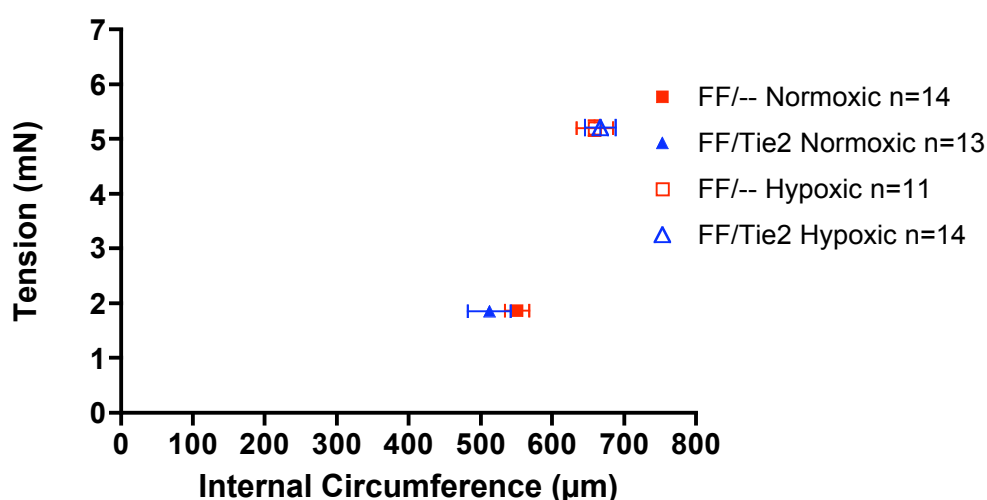


**Figure 6-5: Length (internal circumference) – tension relationship for all PA rings**

Mean internal circumference ( $\pm$ SEM) of PA rings in the wire myography study plotted against the tension ( $\pm$ SEM) required to result in a transmural pressure equivalent to 12-14 mmHg for mice under normoxic and 30-33 mmHg for mice under hypoxic conditions. Data is for all PA rings, before the addition of L-NAME. Overlapping error bars indicate no significant difference between genotypes. (These data were obtained from Dr Y Dempsey, University of Glasgow).

No significant difference in the maximum constriction ( $E_{\max}$ ) or tissue sensitivity ( $pEC_{50}$ ) of PA rings to ET-1 was observed under conditions of normoxia or hypoxia between FF/Tie2 mice and FF/-- controls (Table 6-3 and Figure 6-6). However, when all points on the CRC were analysed using 2-way ANOVA small differences in responses were demonstrated (Figure 6-6). Under normoxic conditions, the PA rings from FF/Tie2 mice are slightly less sensitive to ET-1 compared to FF/-- tissue (Figure 6-6A). However, under hypoxic conditions, no differences in the ET-1 CRCs were seen (Figure 6-6B).



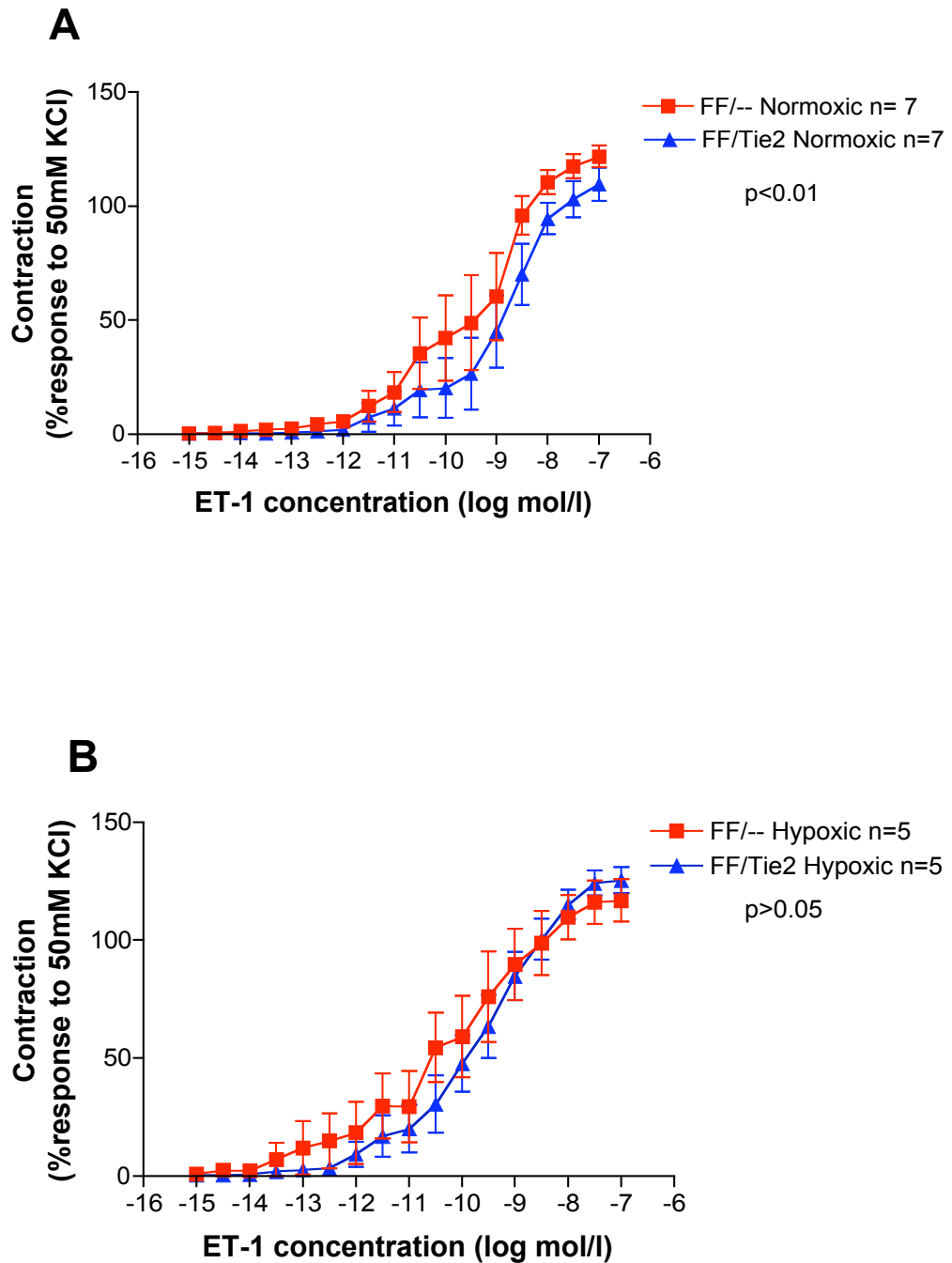


**Figure 6-6: CRC of PAs to ET-1 under normoxia and hypoxia**

ET-1 culminative concentration response curves for PA rings from FF/-- and FF/Tie2 mice housed under normoxic (A) and hypoxic (B) conditions. Two-way ANOVA showed a significant difference between the CRCs under normoxia ( $p < 0.01$ ), but no difference under hypoxic conditions ( $p > 0.05$ ).

(These data were obtained from Dr Y Dempsey, University of Glasgow).

Treatment with L-NAME did not have a significant effect on either the  $E_{\max}$  or  $pEC_{50}$  of the CRCs to ET-1 in either FF/Tie2 or FF/-- PA rings (Table 6-3, Figure 6-7 and Figure 6-8). However, slight differences were again demonstrated when 2-way ANOVA analysis was applied to the ET-1 CRCs. Under normoxic conditions, L-NAME caused PAs from FF/-- mice to constrict slightly more in response to ET-1 (Figure 6-7A), whereas no effect of L-NAME was seen with PA rings from FF/Tie2 mice (Figure 6-7B). In contrast, under hypoxic conditions, the opposite was seen: L-NAME caused no effect on PAs from FF/-- mice (Figure 6-8A), whereas it increased constriction of FF/Tie2 PA rings (Figure 6-8B).

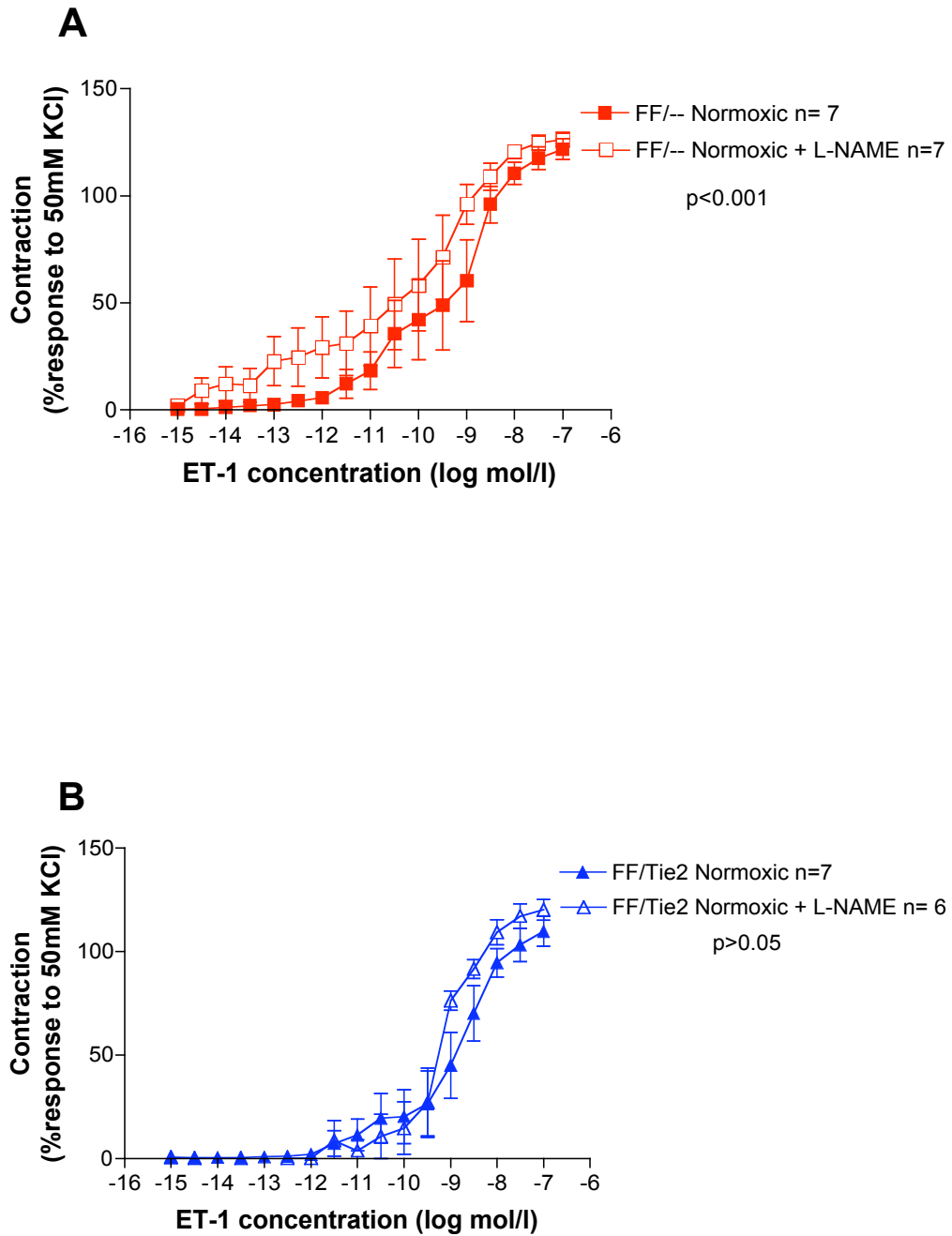


**Figure 6-7: CRC of normoxic PA rings to ET-1 in the presence and absence of L-NAME**

Two-way ANOVA showed that L-NAME caused a significant difference in the CRCs of normoxic FF/- mice ( $p < 0.001$ ) (A), but no such effect was seen between the CRCs of normoxic FF/Tie2 mice ( $p > 0.05$ ) (B).

(These data were obtained from Dr Y Dempsey, University of Glasgow).

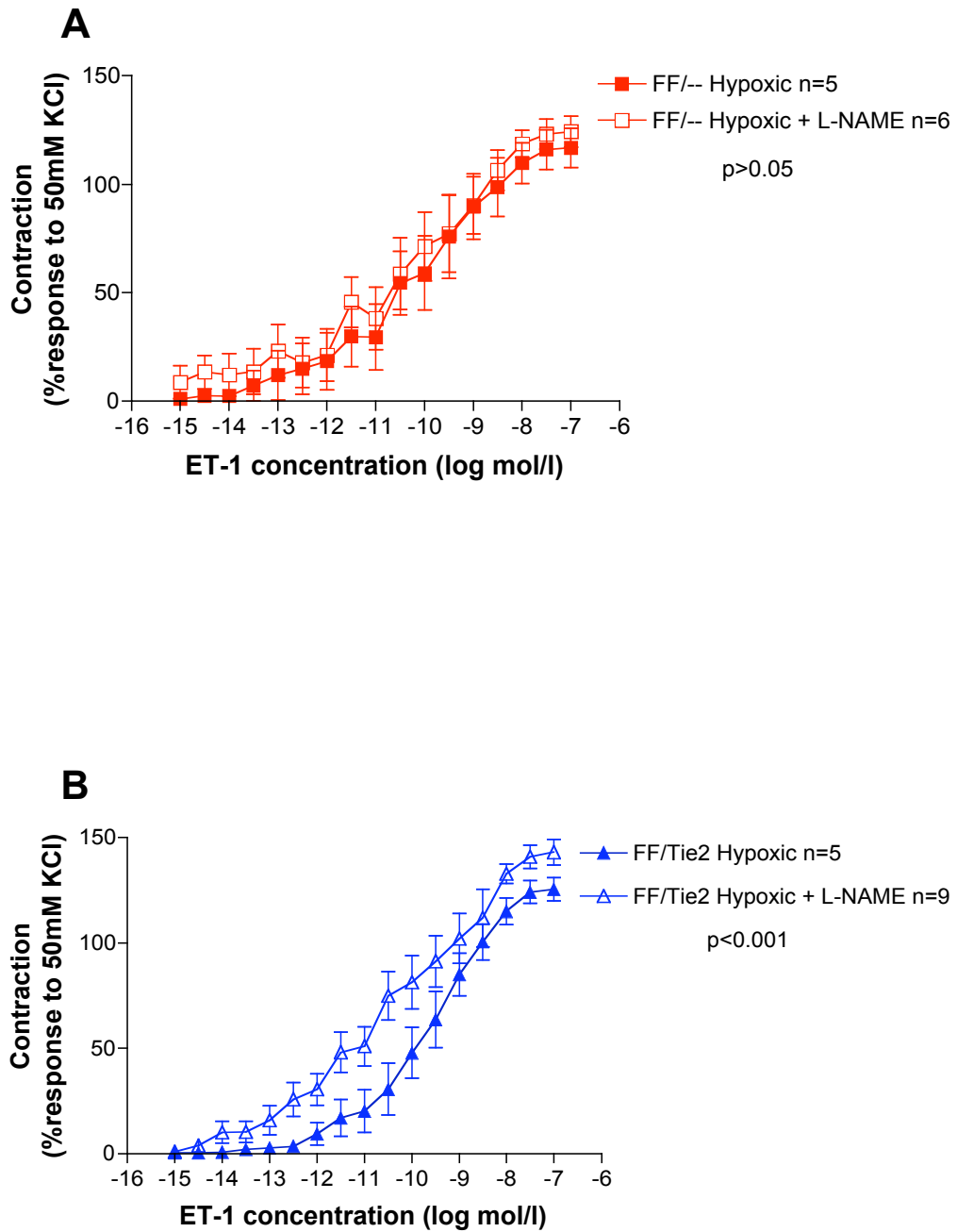


**Figure 6-8: CRC of hypoxic PA rings to ET-1 in the presence and absence of L-NAME**

Two-way ANOVA showed that L-NAME caused no significant difference in the CRCs of hypoxic FF/-- mice ( $p > 0.05$ ) (A), but it significantly shifted the ET-1 CRC of hypoxic FF/Tie2 mice to the left, indicating increased tissue sensitivity to ET-1 ( $p < 0.001$ ) (B).

(These data were obtained from Dr Y Dempsie, University of Glasgow).

**Table 6-3: Potency and maximum effect of ET-1 in PA rings from FF/Tie2 and FF/-- animals**

(These data were obtained from Dr Y Dempsie, University of Glasgow).

|                          | FF/--             |                  |   | FF/Tie2           |                  |   |
|--------------------------|-------------------|------------------|---|-------------------|------------------|---|
|                          | pEC <sub>50</sub> | E <sub>max</sub> | n | pEC <sub>50</sub> | E <sub>max</sub> | n |
| <b>Normoxic</b>          | 9.2 ± 0.13        | 121.9 ± 4.8      | 7 | 8.8 ± 0.12        | 109.7 ± 7.2      | 7 |
| <b>Hypoxic</b>           | 10.1 ± 0.17       | 116.8 ± 9.0      | 5 | 9.6 ± 0.10        | 125.4 ± 5.5      | 5 |
| <b>Normoxic + L-NAME</b> | 9.7 ± 0.18        | 126.3 ± 3.4      | 7 | 9.1 ± 0.90        | 120.2 ± 5.0      | 6 |
| <b>Hypoxic + L-NAME</b>  | 10.12 ± 0.17      | 124.3 ± 7.1      | 6 | 10.5 ± 0.12       | 143.0 ± 6.0      | 9 |

### 6.3.5 Vascular remodeling

Lung sections from 6 mice per group were stained as described (see section 2.10.5). All PAs (20 - 60  $\mu$ m O.D.) associated with an airway distal to the respiratory bronchiole were counted. The arteries were considered muscularised if they possessed a distinct double-elastic lamina visible for at least half the diameter in the vessel cross-section. The proportion of such remodeled muscularised vessels was calculated for each section (Keegan *et al.*, 2001) (Figure 6-9).

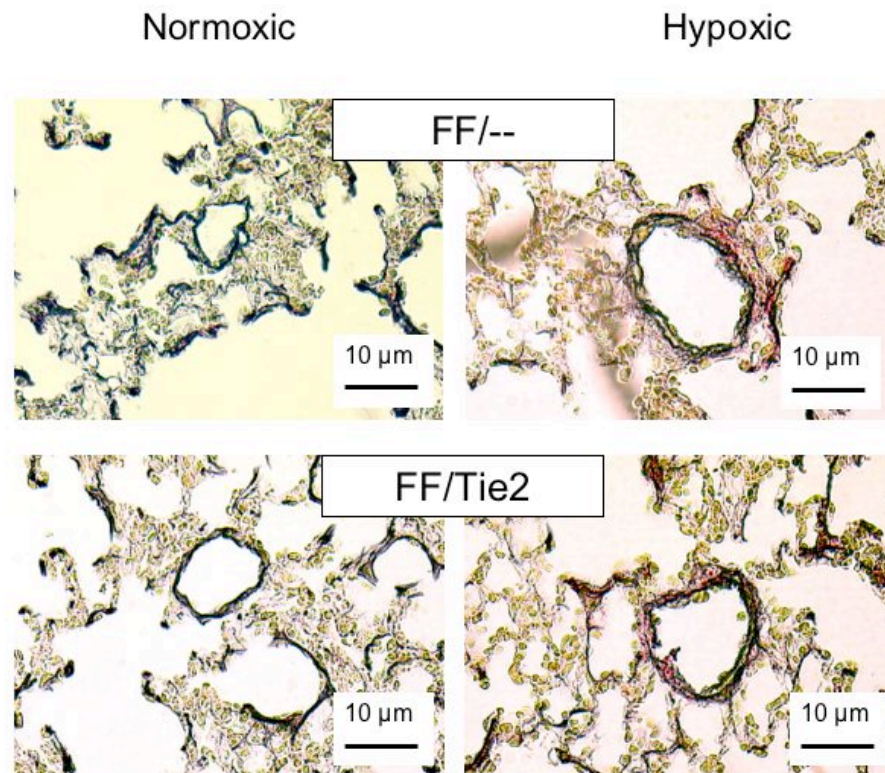


**Figure 6-9: Micrograph showing hypoxic remodeling**

Left: Normal small PAs in normoxic mice. Right: Muscularised remodeled small PAs in hypoxic mice. Sections stained with Miller's Elastin stain and Picro Sirius Red collagen stain. Scale bar = 10  $\mu$ m.

Under normoxia, the proportion of remodeled vessels in the lung sections studied was similar in FF/-- ( $5.57 \pm 0.57\%$ ) and FF/Tie2 ( $7.09 \pm 0.50\%$ ) mice. Following hypoxia, the proportion of remodeled vessels seen was significantly greater in FF/Tie2 mice ( $18.51 \pm 1.24\%$ ) compared to FF/-- controls ( $11.36 \pm 0.57\%$ ) (Figure 6-10).

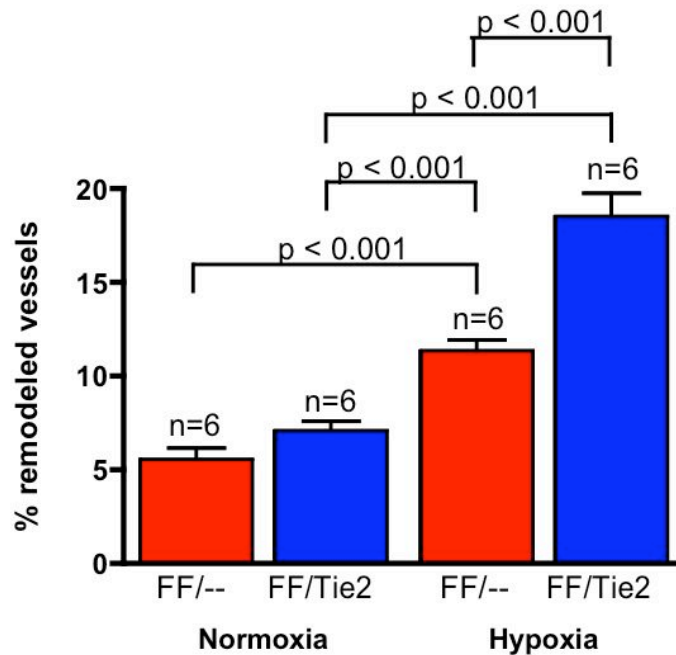


**Figure 6-10: The percentage of remodeled pulmonary vessels was increased in hypoxic FF/Tie2 mice**

No difference in the percentage of remodeled vessels was seen between genotypes in normoxic mice, but under hypoxic conditions FF/Tie2 mice were shown to have an increased proportion of remodeled vessels compared to FF/-- controls.

## 6.4 DISCUSSION

These results demonstrate that EC specific down-regulation of the  $ET_B$  receptor potentiates the development of PAH in response to chronic hypoxia. After 14 days of exposure to hypobaric hypoxia, EC  $ET_B$  down-regulated mice display elevated systolic RVP, increased right ventricular hypertrophy and greater pulmonary vascular remodeling. Preliminary myography studies suggest that this PAH is not caused by differences in the vasoconstrictive response of third order (first interlobar) order PAs to ET-1 between the EC  $ET_B$  receptor down-regulated mice and controls.

Interpretation of the myography data is not straightforward. In terms of maximum response and tissue sensitivity (comparison of  $E_{max}$  and  $pEC_{50}$ ) no difference was seen between the EC  $ET_B$  down-regulated mice and controls, under both normoxic and hypoxic conditions. Likewise L-NAME was not shown to have a significant

effect. However, more detailed comparison of the vasoconstrictive response to ET-1, using 2-way ANOVA analysis of the CRCs, revealed small but statistically significant differences. Constriction to ET-1, of PA rings from control mice housed under normoxic conditions, was enhanced by L-NAME, suggesting that their endothelial function was preserved. In contrast, this was not seen in PAs from normoxic EC ET<sub>B</sub> down-regulated mice, implying reduced endothelial dependent vasodilatation as seen in systemic vessels (Bagnall *et al.*, 2006). Unexpectedly however, hypoxia appeared to reverse this: L-NAME augmented the vasoconstriction to ET-1 of PAs from hypoxic EC ET<sub>B</sub> down-regulated mice, but had no effect on ET-1 vascular responsiveness in the hypoxic controls. The reason for this effect of hypoxia on PAs of this size is not clear. Furthermore, despite there being no difference in systolic RVP between normoxic EC ET<sub>B</sub> down-regulated mice and controls, somewhat surprisingly, control mice demonstrated enhanced vascular responsiveness to ET-1. Conversely, under hypoxic conditions, no difference in vasoconstriction to ET-1 was seen between genotypes, despite EC ET<sub>B</sub> down-regulated mice exhibiting significant PAH. Thus, it would seem that the mechanism causing hypoxia induced PAH in EC ET<sub>B</sub> down-regulated mice is not secondary to increased vascular responsiveness to ET-1, at least not in the size of PA studied.

#### **6.4.1 Mechanisms responsible for PAH**

There are several possible mechanisms that could be responsible for the development of PAH in EC ET<sub>B</sub> deficient mice. Firstly, studies involving transgenic mice featuring both loss and gain of function have revealed how reduced release of NO and PGI<sub>2</sub> from the endothelium, increases the vascular tone and muscularisation of PAs, exacerbating the development of PAH (Fagan *et al.*, 1999; Geraci *et al.*, 1999; Ozaki *et al.*, 2001; Steudel *et al.*, 1998). Isolated lung studies, using tissue from rescued ET<sub>B</sub> deficient rats, have shown exaggerated pressor responses to ET-1 (Ivy *et al.*, 2001), due in part to the observed reduced NO and PGI<sub>2</sub> production, not seen in wild type controls (Ivy *et al.*, 2002). Myography studies, using aortic rings performed by our group, have revealed that EC ET<sub>B</sub> down-regulated mice demonstrate endothelial dysfunction in the systemic circulation (Bagnall *et al.*,



2006). Similar behaviour in pulmonary vessels, distal to the interlobar arteries, might contribute to the development of PAH.

Second, elevated plasma concentrations of ET-1 may also have contributed to the PAH. As detailed in the previous chapter, EC ET<sub>B</sub> down-regulated mice exhibit raised plasma ET-1 concentrations due to impaired plasma clearance. However, the limited experimental evidence suggests that increased ET-1 concentration alone is not sufficient to cause PAH. Transgenic mice, featuring over-expression of preproET-1, develop pulmonary inflammation and fibrosis but fail to exhibit elevated pulmonary pressures compared with controls, when exposed to mild hypoxia (room air at 5280 feet = FiO<sub>2</sub> 16%) (Hoche *et al.*, 2000). Similarly rats, chronically infused with ET-1 by means of subcutaneous pumps, do not develop raised pulmonary pressures under normoxic conditions (no animals were exposed to hypoxia) (Migneault *et al.*, 2005). Although the influence of elevated ET-1 on pulmonary pressures under more profound hypoxia is not known, the results of the current study indicate that loss of vasodilator EC ET<sub>B</sub> receptors in combination with an increase in plasma ET-1 is required for PAH to develop.

ET<sub>B</sub> receptor-dependent NO/PGI<sub>2</sub>-mediated vasodilator/ antiproliferative pathways are therefore likely to be important protective mechanisms preventing the development of PAH when ET-1 production is increased.

#### **6.4.2 Influence of vascular remodeling and vasoconstriction in chronic hypoxic PAH**

It is thought that remodeling of PAs results in raised pulmonary vascular resistance (PVR) through 2 separate mechanisms: narrowing of the vascular lumen caused by increased muscularisation of the vessel wall, and loss of small PAs, known as pulmonary rarefaction, resulting in a fall in the total PA luminal cross sectional area (Stenmark *et al.*, 2005). That such structural changes are important determinants of increased resistance and pressure in chronic PAH is supported by observations that after prolonged exposure to hypoxia, acute re-exposure to normal or even high levels

of inspired oxygen becomes progressively less effective in reducing pulmonary arterial pressure. This lack of responsiveness to oxygen, or even to other pulmonary vasodilators such as calcium channel blockers, has led to the concept that chronic hypoxic PAH is associated with a 'fixed' structural component responsible for the increased PVR. However, recent work looking at hypoxic PAH in rats, has challenged this view (Hyvelin *et al.*, 2005). Using quantitative stereology (the study of three-dimensional properties of objects or matter usually observed two-dimensionally), it has been shown that pulmonary arterial remodeling does not reduce the vessel lumen (rather the thickening of the vessel wall causes outward not inward expansion) and there is no fall in luminal area of vessels of 30-200 $\mu$ m diameter. As vasodilatation with acute Rho kinase inhibition markedly decreased PVR, the authors conclude that hypoxic PAH is primarily due to increased vasoconstriction rather than structural changes. Others have emphasised the importance of correct preparation of histological specimens: maximal vasodilatation must be ensured (e.g. by perfusing the pulmonary vasculature with calcium free EGTA buffer) before lung sections are fixed and the lumen/ media ratio calculated (van Suylen *et al.*, 1998). It has been suggested that many studies describing decreased lumen/ media ratios in PAs from hypoxic PAH lungs, have not prepared their samples in this way and so report artefactual vessel narrowing (Stenmark *et al.*, 2005).

In our study an increased proportion of remodeled small PAs was observed in lungs from hypoxic EC ET<sub>B</sub> down-regulated mice. Although the pulmonary vasculature was not perfused before fixation to ensure maximal vasodilatation, we defined remodeling as the percentage of muscularised small PAs (double elastic lamina present for more than 50% of cross section) relative to the total number of vessels, a measure not affected by the size of vessel lumen calibre. Therefore, we can conclude that down-regulation of the EC ET<sub>B</sub> receptor causes increased vascular remodeling in response to hypoxia, irrespective of its effect on PA lumen cross sectional area. Our myography studies failed to demonstrate any difference in the maximum response ( $E_{max}$ ), tissue sensitivity ( $pEC_{50}$ ), or the CRC (by 2-way ANOVA analysis) to ET-1 between 3<sup>rd</sup> order interlobar arteries from hypoxic EC ET<sub>B</sub> down-regulated mice and

controls. Furthermore, genotype had no influence on the internal circumference-tension relationship (a measure of vessel stiffness) of the PA rings used in the myography study (increased stiffness would imply increased vascular remodeling). Thus in arteries of this size, we have not found evidence of raised vascular tone in vessels from the hypoxic EC ET<sub>B</sub> down-regulated mice, that would increase PVR sufficiently to result in the observed elevated systolic RVP. Smaller PAs are likely to behave differently, as the expression of ET<sub>B</sub> relative to ET<sub>A</sub> receptors is greater in distal segments of the pulmonary vascular tree (Davie *et al.*, 2002; Soma *et al.*, 1999). Myography with such small pulmonary vessels is not technically feasible, but their influence of vascular tone could be investigated using isolated lung preparations as performed previously (Hasegawa *et al.*, 2004; Ivy *et al.*, 2001).

#### **6.4.3 Study limitations**

Although normoxic mice did not demonstrate a significant difference in body weight at euthanasia between genotypes, the hypoxic EC ET<sub>B</sub> down-regulated mice were significantly lighter compared with controls. In several rodent studies of PAH, hypoxia did not have this effect (Ivy *et al.*, 2002; Keegan *et al.*, 2001; MacLean *et al.*, 2004), although it has been reported in eNOS KO mice with a similar genetic background (C57BL6/SV129) to our EC ET<sub>B</sub> down-regulated mice (Fagan *et al.*, 1999). Mice were not weighed at the start of the 14-day hypobaric hypoxia, and so this difference in weight may have occurred by chance. Whilst lower body weight could have been related to the severity of PAH displayed by the hypoxic EC ET<sub>B</sub> down-regulated mice, they all appeared healthy and behaved normally before sacrifice.

As discussed in chapter 4 (see section 4.4.2) physiological data collected from anaesthetised animal preparations must be interpreted with caution. My initial studies to determine the systemic BP of EC ET<sub>B</sub> down-regulated mice, performed under anaesthesia, found these mice to demonstrate hypertension (see section 4.3.1), in contrast to subsequent studies using radiotelemetry devices in conscious animals (see section 4.3.2). In the hamodynamic studies discussed in this chapter, using a different

control group (FF/-- not WW/--) and with a different anaesthetic (halothane not isoflurane), no difference in MBP was found between EC ET<sub>B</sub> down-regulated mice and controls (see section 6.3.2), further emphasising the potential problems of using non-recovery preparations. Whilst recording of pulmonary pressures in conscious animals is well established in rats (Ivy *et al.*, 2001; Ivy *et al.*, 2002), it represents a technical challenge in mice and is not currently possible. However, the validity of the haemodynamic data in this study is reinforced by the RVH demonstrated by the hypoxic EC ET<sub>B</sub> down-regulated mice (as the lack of systemic hypertension is reinforced by the lack of LVH seen in old EC ET<sub>B</sub> down-regulated mice – see section 4.3.3). It is likely that a longer period of exposure to hypoxia would have resulted in a more pronounced increase of pulmonary pressures, RVH and PA remodeling in the EC ET<sub>B</sub> down-regulated mice.

Endothelial-dependent vasodilatation to acetylcholine can be assessed following pre-treatment of vessels with a vasoconstrictor such as phenylephrine. Whilst this is helpful in rats, PA rings from mice, of a similar genetic background (129SV) to our EC ET<sub>B</sub> down-regulated mice, failed to display any acetylcholine mediated vasodilator responses (Keegan *et al.*, 2001). For this reason, we had intended to compare the vasoconstriction response to ET-1 in the presence and absence of NOS inhibition with L-NAME as an alternative way to assess endothelial function. However, L-NAME only marginally augmented the vasoconstrictive response to ET-1 in PAs from normoxic control mice, and had no influence on hypoxic control mice. Unexpectedly, L-NAME increased the constriction of PAs from hypoxic EC ET<sub>B</sub> down-regulated mice to ET-1. There are a number of possible explanations for these unexpected changes following NOS inhibition. Firstly, mounting of the PA rings onto the myograph may have damaged and denuded their endothelium to such an extent that little EC NO could be generated. Whilst this is possible, the dissection and mounting were performed by extremely experienced operators, who have previously demonstrated rat PAs, mounted in an identical manner, to have good endothelial function (Keegan *et al.*, 2001; Morecroft *et al.*, 2005). Damage during mounting is less likely to be the explanation as normoxic and hypoxic rat PA rings, which both demonstrated acetylcholine mediated vasodilatation, also exhibited

unchanged responses to ET-1 following treatment with L-NAME (MacLean *et al.*, 1998). Second, studies in rats have shown that eNOS expression in larger elastic conduit PAs differs from that seen in smaller more distal muscular resistance arteries (Shirai *et al.*, 2003). It is possible that in the mouse lung, the expression of eNOS, follows a similar pattern to that of ET<sub>B</sub> receptors: relatively low expression in the proximal pulmonary vascular tree but higher levels in distal vascular segments. Thus, NOS inhibition would be expected to have a minimal effect of ET-1 constriction in large proximal PAs, as seen here. Third, the use of L-NAME to potentiate a contraction to a vasoconstrictor such as ET-1 may result in much smaller relative changes than observed using NOS inhibition to block endothelial dependent vasodilatation. For example, vasoconstriction of PAs from wild type mice (C57BL/6; 129 background) to a TXA<sub>2</sub> agonist was little altered by pretreatment with L-NAME, whereas L-NAME significantly reduced the endothelial dependent vasodilatation to acetylcholine (Liu *et al.*, 2004).

Previous studies have shown that PA vasoconstriction to low concentrations of ET-1 is mediated by ET<sub>B</sub> receptors, whilst the responses seen to higher concentrations are ET<sub>A</sub> dependent (McCulloch *et al.*, 1996). By extending this work, to include VSMC ET<sub>B</sub> down-regulated mice, as well as using ET<sub>A</sub> and ET<sub>B</sub> selective ET antagonists, the exact role of these receptors on different cell types in the development of hypoxia induced PAH could be determined.

## **7 CHAPTER 7: CONCLUSIONS AND FUTURE WORK**

### **7.1 INTRODUCTION**

Full understanding of the cardiovascular effects of the ET system in both health and disease is complicated by the opposing action of ET<sub>B</sub> on VSMCs and neighbouring ECs. Neither pharmacological antagonism nor animal models featuring generalised down-regulation of the ET<sub>B</sub> receptor allow the contribution made by the EC ET<sub>B</sub> to be accurately determined. Using homologous recombination to insert lox P sites on either side of exons 3 and 4 of the ET<sub>B</sub> gene, others in our laboratory have generated a strain of ‘floxed’ ET<sub>B</sub> transgenic mice. By crossing these animals with Tie2-Cre mice, a strain in which expression of the bacteriophage enzyme Cre recombinase is restricted to ECs, mice featuring EC specific down-regulation of the ET<sub>B</sub> receptor were generated (see section 1.3). This thesis describes how I have investigated the phenotype of these EC ET<sub>B</sub> down-regulated mice. Having used autoradiography to confirm that EC specific down-regulation of ET<sub>B</sub> expression had been achieved, I went on to examine the effect of EC ET<sub>B</sub> down-regulation on systemic BP and the response to high salt diet; clearance of ET-1 from the plasma; and the role of this receptor in the development of hypoxia induced PAH.

### **7.2 LIMITATIONS OF THE PROJECT AS A WHOLE**

Whilst the use of a tissue specific down-regulated transgenic mouse offers many advantages to the investigation of the ET system, there are a number of limitations to the approach I have taken and to the use of murine models of cardiovascular disease in general.

#### **7.2.1 Genetic background**

It has long been established that genetic background can significantly affect gene expression, and in particular can have marked influences on cardiovascular phenotype (Ryan *et al.*, 2002). Indeed, because of this, experimental strains have

been developed, with identical genetic backgrounds, to allow the effect of individual gene knockout/ gain of function mutations to be studied in isolation (Moriwaki, 1999). However, the mice studied in this project were the result of crossing FF/-- mice (50% BKW; 50% 129) with Tie2-Cre animals (C57BL/6). Therefore the EC ET<sub>B</sub> down-regulated (FF/Tie2) mice had a variable genetic background, derived from each of 3 different inbred experimental strains, which could have influenced their cardiovascular phenotype. To limit this potential confounder, these studies involved the use of sibling single transgenic controls from the same litters as the FF/Tie2 mice studied. However, the possibility that segregation of key genes influencing cardiovascular phenotype may have differed between EC ET<sub>B</sub> down-regulated mice and control littermates cannot be excluded. Breeding of both EC ET<sub>B</sub> down-regulated mice and floxed controls onto a pure genetic background may be achieved by multiple backcrosses, which would essentially remove any differences in genetic background [99.8% C57BL/6 after 10 generations of backcrossing onto a C57BL/6 background (Jiang *et al.*)], but this would require a major breeding programme taking 25-30 months.

### **7.2.2 Possible compensatory mechanisms**

A further limitation to consider when interpreting loss of function/gain of function gene-targeting experiments is the potential effects of compensation from other genes throughout prenatal and postnatal development. As recombination of the ET<sub>B</sub> receptor gene in the ECs occurred during embryogenesis, it is not possible to exclude the possibility that any observed phenotypic changes in these mice are tempered by the action of other compensatory regulatory mechanisms. Such effects could be limited by using an inducible Cre, active only once development of the animal is complete (Sauer, 1998).

## **7.3 BODY WEIGHT OF EC ET<sub>B</sub> DOWN-REGULATED MICE**

The body weights of EC ET<sub>B</sub> down-regulated mice have been compared with controls as part of the studies presented in this thesis, as summarised in Figure 7-1

(this does not include studies where FF/Tie2 mice were compared with WW/-- controls).

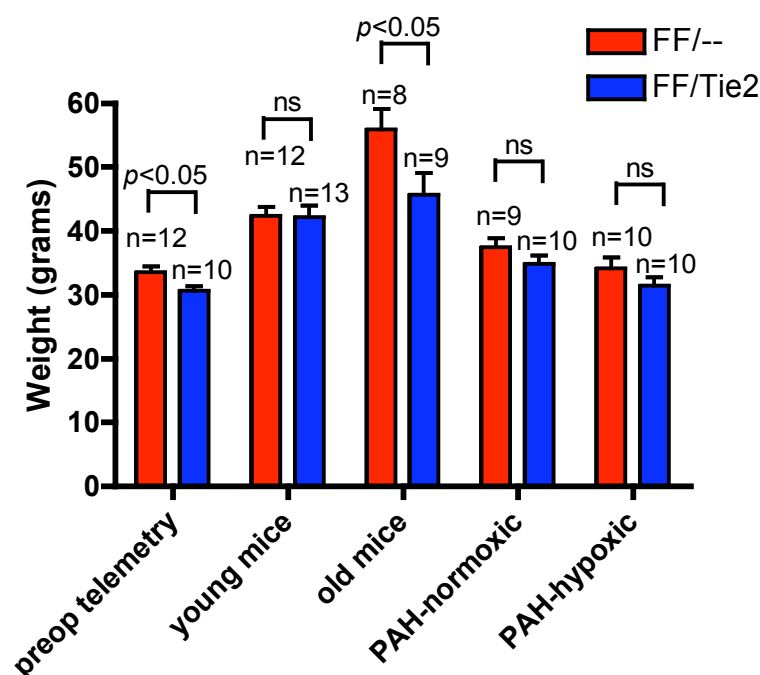


**Figure 7-1: Summary bar chart showing trend of EC ET<sub>B</sub> down-regulated mice to reduced body weights**

Comparison of body weight of FF/Tie2 mice and FF/-- controls in the different studies of this thesis: at the start of the BP telemetry study (mice aged 6-8 weeks) (see section 4.3.2.5); for young (2 month old) and old (4 month) mice (see section 4.3.3); and at the time of haemodynamic measurements in the PAH study for both normoxic and hypoxic mice (mice aged 6-8 weeks) (see section 6.3.1). Only pre-operative telemetry mice and 4-month old FF/Tie2 mice were found to be significantly lighter than controls.

In our studies, the weights of all mice, including FF/-- controls, were generally higher than those seen with other strains, which may have been an effect of their outbred genetic background. EC ET<sub>B</sub> down-regulated mice exhibited a trend toward lighter body weight that was statistically significant in the mice at the start of the telemetry study and in 4-month old mice. Other studies, phenotyping transgenic rodent models featuring genetic modification of the ET system, do not record the body weight of the animals studied (Gariépy *et al.*, 2000; Hocher *et al.*, 1997;



Quaschnig *et al.*, 2005). However, EC specific ET-1 overexpressing mice were found to be significantly lighter ( $21.4 \pm 0.5\text{g}$ ) than controls ( $22.9 \pm 0.7\text{g}$ ;  $n=6$ ;  $p<0.05$ ) (Amiri *et al.*, 2004). Similar to our EC ET<sub>B</sub> down-regulated mice, plasma ET-1 was found to be several fold higher in these EC specific ET-1 overexpressing mice compared to controls. In observational clinical studies, circulating ET-1 was significantly elevated in insulin resistant states, such as type 2 diabetes (Donatelli *et al.*, 1996; Mangiafico *et al.*, 1998), obesity (Ferri *et al.*, 1997) and impaired glucose tolerance (Caballero *et al.*, 1999). Selective ET<sub>A</sub> antagonists not only increased body weight when given to hypertensive rats (Opocensky *et al.*, 2006), but also improved glucose tolerance in a model of insulin resistance (Berthiaume *et al.*, 2005). Thus, the reduced body weight of our EC ET<sub>B</sub> down-regulated mice may have resulted from elevated plasma ET-1 activating ET<sub>A</sub> receptors to increase insulin resistance. Further metabolic studies, involving our EC ET<sub>B</sub> down-regulated mice, would help elucidate the role played by the ET<sub>B</sub> in insulin resistance and weight control.

#### **7.4 EXPRESSION OF ET RECEPTORS IN EC ET<sub>B</sub> DOWN-REGULATED MICE**

Before the FF/Tie2-Cre mouse could be used as a model of EC ET<sub>B</sub> deficiency, it was necessary to provide evidence that tissue specific down-regulation of the ET<sub>B</sub> had truly been achieved. Crossing of floxed ET<sub>B</sub> mice with mice that expressed Cre recombinase in all tissues, resulted in piebald ET<sub>B</sub> null animals that died at weaning due to aganglionic megacolon. Thus recombination of exons 3 and 4 of the gene was sufficient to prevent ET<sub>B</sub> expression. I next went on to breed Tie2-Cre mice with *lacZ* and GFP reporter strains, revealing that Tie2 restricts the expression of Cre recombinase to ECs. Autoradiography studies showed that ET<sub>B</sub> receptor binding was virtually abolished in EC rich tissues of FF/Tie2-Cre mice, but largely unaltered in other tissues, such as epithelium, providing convincing evidence of EC specific ET<sub>B</sub> down-regulation. Furthermore, using both autoradiography and semi-quantitative RT-PCR, the expression of ET<sub>A</sub> receptors was found not to be reduced in the FF/Tie2-Cre mice, despite elevated plasma ET-1 concentrations.

These studies show that the FF/Tie2-Cre mice have EC specific down-regulation of the ET<sub>B</sub> receptor, and support the use of this model to characterise the role of the EC ET<sub>B</sub> in the ensuing experimental studies.

Whilst the steps above provide convincing evidence of tissue specific down-regulation, an important component of any future studies would be to periodically check that EC ET<sub>B</sub> down-regulation is being maintained, as transgenic strains often lose expression of the transgene irreversibly through methylation of the insertion site (Jiang *et al.*). This could be done by repeating the autoradiography studies, looking for reduced binding of radiolabelled ET<sub>B</sub> ligands in EC rich tissue of FF/Tie2-Cre mice.

## **7.5 ROLE OF EC ET<sub>B</sub> IN CONTROL OF SYSTEMIC VASCULAR TONE AND RESPONSE TO SALT**

Initial experiments, using a range of techniques to measure the BP of the EC ET<sub>B</sub> down-regulated mice, indicated that these animals showed hypertension. However, in longitudinal studies in conscious unrestrained mice, where BP was measured using radiotelemetry [the ‘gold standard’ assessment method (Kurtz *et al.*, 2005)], the EC ET<sub>B</sub> down-regulated mice were not found to demonstrate elevated BP. The validity of this finding was reinforced by the lack of LVH seen in mice aged >12months. Furthermore, in contrast to models of total ET<sub>B</sub> ablation (Gariépy *et al.*, 2000) or pharmacological blockade (Pollock *et al.*, 2001), the BP response to salt was largely unchanged in EC ET<sub>B</sub> down-regulated mice.

From a methodology viewpoint, these studies emphasise the importance of using the appropriate technique to measure BP in laboratory animals. Furthermore, the lack of severe hypertension of the EC ET<sub>B</sub> down-regulated mouse and the absence of a significant BP response to salt indicate that ET<sub>B</sub> receptors situated on cells other than the ECs mediate natriuresis and diuresis.

To identify which cell type expresses the ET<sub>B</sub> receptor responsible for the salt sensitive hypertension observed in models of total ET<sub>B</sub> ablation, these studies should be repeated using other tissue specific ET<sub>B</sub> down-regulated mice, such as VSMC and renal interstitial cell ET<sub>B</sub> down-regulated mice. The generation of such mice is straightforward. Floxed ET<sub>B</sub> animals can be crossed with different strains of mice expressing Cre under the control of either a VSMC specific or renal interstitial cell specific promoter. Such an IMCD specific Cre has already been used to generate IMCD specific ET-1 KO mice (Ahn *et al.*, 2004), which exhibit marked salt sensitive hypertension, and IMCD specific ET<sub>B</sub> down-regulated mice (Ge *et al.*, 2006), which are only mildly hypertensive, suggesting a paracrine role for IMCD derived ET-1. As well as radiotelemetry, these experiments would include full metabolic studies to allow assessment of fluid and sodium balance.

## **7.6 CONTRIBUTION OF EC ET<sub>B</sub> RECEPTOR TO THE CLEARANCE OF PLASMA ET-1**

The elevation of the plasma concentration of ET-1 in EC ET<sub>B</sub> down-regulated mice is explained by their observed impaired clearance of a bolus of radiolabelled ET-1. As discussed in chapter 5, control mice behaved in a similar manner, once treated with a maximal dose of ET<sub>B</sub> antagonist, indicating that the EC receptor is responsible for a significant proportion of ET<sub>B</sub> mediated clearance. That EC ET<sub>B</sub> down-regulated mice do not demonstrate hypertension, despite elevated plasma ET-1 concentrations, reinforces the results of other studies featuring ET-1 overexpression (Amiri *et al.*, 2004; Hocher *et al.*, 1997), and indicates that the elevation of BP seen in situations of ET<sub>B</sub> down-regulation (Garipey *et al.*, 2000; Pollock *et al.*, 2001) is not merely due to impaired ET-1 clearance.

Extending the clearance studies to include other tissue specific ET<sub>B</sub> down-regulated strains, in particular VSMC ET<sub>B</sub> down-regulated mice, would allow the question of the role played in ET-1 clearance, by ET<sub>B</sub> receptors on these cells, to be definitively addressed. Tissue specific down-regulated mice are ideally suited to answering such questions, as opposed to pharmacological approaches where evidence of cell type

specific receptor blockade is not nearly as precise (Honore *et al.*, 2005). Furthermore, use of the indicator-dilution technique, where the injection of an inert tracer that remains in the vascular compartment (such as Evans blue dye which binds avidly to albumin) as well as the radiolabelled ET-1, allows the % extraction of ET-1 by the lungs to be calculated (Dupuis *et al.*, 1994). This would further clarify whether ET-1 clearance is impaired or production increased in the various tissue specific ET-1 KO/knockdown animals.

Positron emission tomography (PET) studies of the EC ET<sub>B</sub> down-regulated mice, following a bolus of [<sup>18</sup>F]-ET-1, as previously performed in rats (Johnstrom *et al.*, 2005), would allow *in vivo* imaging of sites of ET<sub>B</sub> mediated ET-1 sequestration, and also permit the localisation of the organs responsible for non ET<sub>B</sub> mediated ET-1 clearance.

## **7.7 THE EC ET<sub>B</sub> RECEPTOR IN THE CONTROL OF PULMONARY VASCULAR TONE**

In the final chapter of this thesis, I have shown how down-regulation of the EC ET<sub>B</sub> receptor exaggerates hypoxia-induced PAH, most likely secondary to the observed structural remodeling changes in the vessel walls of small PAs. This adds mechanistic support in favour ET<sub>A</sub> selective antagonists in comparison to mixed ET<sub>A/B</sub> blockade in the clinical management of PAH.

As in the areas of systemic vascular tone, natriuresis and clearance of ET-1, extending these studies by using other tissue specific ET<sub>B</sub> down-regulated mice, particularly VSMC ET<sub>B</sub> down-regulated animals, would complement the findings with the EC ET<sub>B</sub> down-regulated mouse, allowing a comprehensive overall understanding of the ET<sub>B</sub> receptor in the development of PAH. Furthermore, exposing both EC and VSMC ET<sub>B</sub> down-regulated mice to ET antagonists, in combination with other agents whose use is more established in the treatment of PAH (such as prostacyclin analogues, phosphodiesterase 5 inhibitors and NOS inhibitors) will provide valuable insights for clinical management.

## 7.8 SUMMARY

By characterising the phenotype of a line of transgenic mice in which the ET<sub>B</sub> receptor is selectively and specifically knocked-down in ECs, the role played by EC ET<sub>B</sub> in cardiovascular homeostasis has been determined, without the confounding effects of receptor down-regulation or blockade of the ET<sub>B</sub> receptor in all other tissues. Studies such as these, combined with experiments performed using other tissue specific down-regulated transgenic animals, permit ET-1 signalling to be more completely understood and will better inform clinical research in this area.

The principal findings of this project are summarised below:

- Crossing floxed ET<sub>B</sub> mice with Tie2-Cre animals resulted in a strain of mice featuring truly EC specific ET<sub>B</sub> receptor knock-down. Despite elevated plasma ET-1 concentrations, the density of ET<sub>A</sub> receptor binding was not found to be down-regulated in the EC ET<sub>B</sub> down-regulated mice.
- The EC ET<sub>B</sub> receptor does not appear to have a significant influence the control of BP though its influence on vascular tone.
- Non-EC ET<sub>B</sub> receptors, such as those on IMCD and other cell types, regulate natriuresis.
- The EC ET<sub>B</sub> receptor is responsible for clearing ET-1 from the plasma.
- The EC ET<sub>B</sub> receptor is protective against the development of hypoxia-induced pulmonary hypertension.

Thus, the ET<sub>B</sub> receptor on the endothelium exerts largely beneficial effects. Extension of these studies using other tissue specific down-regulated animal models will allow the overall contribution of ET<sub>B</sub> on all cell types to be accurately determined.

## CHAPTER 8: BIBLIOGRAPHY

- ABASSI, Z.A., TATE, J.E., GOLOMB, E. & KEISER, H.R. (1992). Role of neutral endopeptidase in the metabolism of endothelin. *Hypertension*, **20**, 89-95.
- ADAMICZA, A., PETAK, F., ASZTALOS, T. & HANTOS, Z. (1999). Effects of endothelin-1 on airway and parenchymal mechanics in guinea-pigs. *Eur Respir J*, **13**, 767-74.
- AHN, D., GE, Y., STRICKLETT, P.K., GILL, P., TAYLOR, D., HUGHES, A.K., YANAGISAWA, M., MILLER, L., NELSON, R.D. & KOHAN, D.E. (2004). Collecting duct-specific knockout of endothelin-1 causes hypertension and sodium retention. *J Clin Invest*, **114**, 504-11.
- AKIYAMA, Y., IWANAGA, R., SAITOH, K., SHIBA, K., USHIO, K., IKEDA, E., IWAMA, T., NOMIZU, T. & YUASA, Y. (1997). Transforming growth factor beta type II receptor gene mutations in adenomas from hereditary nonpolyposis colorectal cancer. *Gastroenterology*, **112**, 33-9.
- AMBUHL, P.M., AMEMIYA, M., DANCZKAY, M., LOTSCHER, M., KAISLING, B., MOE, O.W., PREISIG, P.A. & ALPERN, R.J. (1996). Chronic metabolic acidosis increases NHE3 protein abundance in rat kidney. *Am J Physiol*, **271**, F917-25.
- AMIRI, F., KO, E.A., TOUYZ, R.M., REUDELHUBER, T.L. & SCHIFFRIN, E.L. (2005). Combined effects of age and salt-loading on endothelial function, vascular remodeling and oxidative stress in a murine model of endothelial cell human endothelin-1 overexpression. *presented at the Ninth International Conference on Endothelin, Utah, USA*.
- AMIRI, F., VIRDIS, A., NEVES, M.F., IGLARZ, M., SEIDAH, N.G., TOUYZ, R.M., REUDELHUBER, T.L. & SCHIFFRIN, E.L. (2004). Endothelium-restricted overexpression of human endothelin-1 causes vascular remodeling and endothelial dysfunction. *Circulation*, **110**, 2233-40.
- ARAI, H., HORI, S., ARAMORI, I., OHKUBO, H. & NAKANISHI, S. (1990). Cloning and expression of a cDNA encoding an endothelin receptor. *Nature*, **348**, 730-2.

- ARCHER, S.L., TOLINS, J.P., RAIJ, L. & WEIR, E.K. (1989). Hypoxic pulmonary vasoconstriction is enhanced by inhibition of the synthesis of an endothelium derived relaxing factor. *Biochem Biophys Res Commun*, **164**, 1198-205.
- ATKINSON, C., STEWART, S., UPTON, P.D., MACHADO, R., THOMSON, J.R., TREMBATH, R.C. & MORRELL, N.W. (2002). Primary pulmonary hypertension is associated with reduced pulmonary vascular expression of type II bone morphogenetic protein receptor. *Circulation*, **105**, 1672-8.
- BABA, T., SHIMIZU, T., SUZUKI, Y., OGAWARA, M., ISONO, K., KOSEKI, H., KUROSAWA, H. & SHIRASAWA, T. (2005). Estrogen, insulin, and dietary signals cooperatively regulate longevity signals to enhance resistance to oxidative stress in mice. *J Biol Chem*, **280**, 16417-26.
- BAGNALL, A.J., KELLAND, N.F., GULLIVER-SLOAN, F., DAVENPORT, A.P., GRAY, G.A., YANAGISAWA, M., WEBB, D.J. & KOTELEVTSSEV, Y.V. (2006). Deletion of endothelial cell endothelin B receptors does not affect blood pressure or sensitivity to salt. *Hypertension*, **48**, 286-93.
- BALYAKINA, E.V., CHEN, D., LAWRENCE, M.L., MANNING, S., PARKER, R.E., SHAPPELL, S.B. & MEYRICK, B. (2002). ET-1 receptor gene expression and distribution in L1 and L2 cells from hypertensive sheep pulmonary artery. *Am J Physiol Lung Cell Mol Physiol*, **283**, L42-51.
- BARST, R.J., LANGLEBEN, D., BADESCH, D., FROST, A., LAWRENCE, E.C., SHAPIRO, S., NAEIJE, R. & GALIE, N. (2006). Treatment of pulmonary arterial hypertension with the selective endothelin-A receptor antagonist sitaxsentan. *J Am Coll Cardiol*, **47**, 2049-56.
- BARST, R.J., LANGLEBEN, D., FROST, A., HORN, E.M., OUDIZ, R., SHAPIRO, S., McLAUGHLIN, V., HILL, N., TAPSON, V.F., ROBBINS, I.M., ZWICKE, D., DUNCAN, B., DIXON, R.A. & FRUMKIN, L.R. (2004). Sitaxsentan therapy for pulmonary arterial hypertension. *Am J Respir Crit Care Med*, **169**, 441-7.
- BATRA, V.K., McNEILL, J.R., XU, Y., WILSON, T.W. & GOPALAKRISHNAN, V. (1993). ETB receptors on aortic smooth muscle cells of spontaneously hypertensive rats. *Am J Physiol*, **264**, C479-84.
- BATTISTINI, B., D'ORLEANS-JUSTE, P. & SIROIS, P. (1993). Endothelins: circulating plasma levels and presence in other biologic fluids. *Lab Invest*, **68**, 600-28.

- BAUER, M., WILKENS, H., LANGER, F., SCHNEIDER, S.O., LAUSBERG, H. & SCHAFERS, H.J. (2002). Selective upregulation of endothelin B receptor gene expression in severe pulmonary hypertension. *Circulation*, **105**, 1034-6.
- BAUMANS, V. (1999). The Laboratory Mouse. In *The UFAW Handbook on the Care and Management of Laboratory Animals*. ed Poole, T. pp. 284: Blackwell Science Ltd.
- BAYNASH, A.G., HOSODA, K., GIAID, A., RICHARDSON, J.A., EMOTO, N., HAMMER, R.E. & YANAGISAWA, M. (1994). Interaction of endothelin-3 with endothelin-B receptor is essential for development of epidermal melanocytes and enteric neurons. *Cell*, **79**, 1277-85.
- BELOHLAVKOVA, S., SIMAK, J., KOKESOVA, A., HNILICKOVA, O. & HAMPL, V. (2001). Fenfluramine-induced pulmonary vasoconstriction: role of serotonin receptors and potassium channels. *J Appl Physiol*, **91**, 755-61.
- BERTHIAUME, N., WESSALE, J.L., OPGENORTH, T.J. & ZINKER, B.A. (2005). Metabolic responses with endothelin antagonism in a model of insulin resistance. *Metabolism*, **54**, 735-40.
- BERTHIAUME, N., YANAGISAWA, M., LABONTE, J. & D'ORLEANS-JUSTE, P. (2000). Heterozygous knock-Out of ET(B) receptors induces BQ-123-sensitive hypertension in the mouse. *Hypertension*, **36**, 1002-7.
- BIDANI, A.K., GRIFFIN, K.A., PICKEN, M. & LANSKY, D.M. (1993). Continuous telemetric blood pressure monitoring and glomerular injury in the rat remnant kidney model. *Am J Physiol*, **265**, F391-8.
- BIRD, J.E., WALDRON, T.L., DORSO, C.R. & ASAAD, M.M. (1993). Effects of the endothelin (ET) receptor antagonist BQ 123 on initial and delayed vascular responses induced by ET-1 in conscious, normotensive rats. *J Cardiovasc Pharmacol*, **22**, 69-73.
- BJORNSSON, J. & EDWARDS, W.D. (1985). Primary pulmonary hypertension: a histopathologic study of 80 cases. *Mayo Clin Proc*, **60**, 16-25.
- BLACK, S.M., MATA-GREENWOOD, E., DETTMAN, R.W., OVADIA, B., FITZGERALD, R.K., REINHARTZ, O., THELITZ, S., STEINHORN, R.H., GERRETS, R., HENDRICKS-MUNOZ, K., ROSS, G.A., BEKKER, J.M., JOHENGEN, M.J. & FINEMAN, J.R. (2003). Emergence of smooth muscle cell endothelin B-



- mediated vasoconstriction in lambs with experimental congenital heart disease and increased pulmonary blood flow. *Circulation*, **108**, 1646-54.
- BLOBE, G.C., SCHIEMANN, W.P. & LODISH, H.F. (2000). Role of transforming growth factor beta in human disease. *N Engl J Med*, **342**, 1350-8.
- BORRAS, C., SASTRE, J., GARCIA-SALA, D., LLORET, A., PALLARDO, F.V. & VINA, J. (2003). Mitochondria from females exhibit higher antioxidant gene expression and lower oxidative damage than males. *Free Radic Biol Med*, **34**, 546-52.
- BOULANGER, C. & LUSCHER, T.F. (1990). Release of endothelin from the porcine aorta. Inhibition by endothelium-derived nitric oxide. *J Clin Invest*, **85**, 587-90.
- BRAUN-MOSCOVICI, Y., NAHIR, A.M. & BALBIR-GURMAN, A. (2004). Endothelin and pulmonary arterial hypertension. *Semin Arthritis Rheum*, **34**, 442-53.
- BROCKWAY, B.P., MILLS, P.A. & AZAR, S.H. (1991). A new method for continuous chronic measurement and recording of blood pressure, heart rate and activity in the rat via radio-telemetry. *Clin Exp Hypertens A*, **13**, 885-95.
- BRUNNER, F. & DOHERTY, A.M. (1996). Role of ET(B) receptors in local clearance of endothelin-1 in rat heart: studies with the antagonists PD 155080 and BQ-788. *FEBS Lett*, **396**, 238-42.
- BUNAG, R.D. & BUTTERFIELD, J. (1982). Tail-cuff blood pressure measurement without external preheating in awake rats. *Hypertension*, **4**, 898-903.
- BURKHARDT, M., BARTON, M. & SHAW, S.G. (2000). Receptor- and non-receptor-mediated clearance of big-endothelin and endothelin-1: differential effects of acute and chronic ETA receptor blockade. *J Hypertens*, **18**, 273-9.
- BUTZ, G.M. & DAVISSON, R.L. (2001). Long-term telemetric measurement of cardiovascular parameters in awake mice: a physiological genomics tool. *Physiol Genomics*, **5**, 89-97.
- CABALLERO, A.E., ARORA, S., SAOUAF, R., LIM, S.C., SMAKOWSKI, P., PARK, J.Y., KING, G.L., LOGERFO, F.W., HORTON, E.S. & VEVES, A. (1999). Microvascular and macrovascular reactivity is reduced in subjects at risk for type 2 diabetes. *Diabetes*, **48**, 1856-62.

- CACOUB, P., DORENT, R., NATAF, P., CARAYON, A., RIQUET, M., NOE, E., PIETTE, J.C., GODEAU, P. & GANDJBAKHCH, I. (1997). Endothelin-1 in the lungs of patients with pulmonary hypertension. *Cardiovasc Res*, **33**, 196-200.
- CARLSON, S.H. & WYSS, J.M. (2000). Long-term telemetric recording of arterial pressure and heart rate in mice fed basal and high NaCl diets. *Hypertension*, **35**, E1-5.
- CARRELL, T.W., BURNAND, K.G., WELLS, G.M., CLEMENTS, J.M. & SMITH, A. (2002). Stromelysin-1 (matrix metalloproteinase-3) and tissue inhibitor of metalloproteinase-3 are overexpressed in the wall of abdominal aortic aneurysms. *Circulation*, **105**, 477-82.
- CERVENKA, L., HARRISON-BERNARD, L.M., DIPP, S., PRIMROSE, G., IMIG, J.D. & EL-DAHR, S.S. (1999). Early onset salt-sensitive hypertension in bradykinin B(2) receptor null mice. *Hypertension*, **34**, 176-80.
- CHAKRAVARTI, A. (1996). Endothelin receptor-mediated signaling in hirschsprung disease. *Hum Mol Genet*, **5**, 303-7.
- CHALFIE, M., TU, Y., EUSKIRCHEN, G., WARD, W.W. & PRASHER, D.C. (1994). Green fluorescent protein as a marker for gene expression. *Science*, **263**, 802-5.
- CHALMERS, G.W., LITTLE, S.A., PATEL, K.R. & THOMSON, N.C. (1997). Endothelin-1-induced bronchoconstriction in asthma. *Am J Respir Crit Care Med*, **156**, 382-8.
- CHASSAGNE, C., EDDAHIBI, S., ADAMY, C., RIDEAU, D., MAROTTE, F., DUBOIS-RANDE, J.L., ADNOT, S., SAMUEL, J.L. & TEIGER, E. (2000). Modulation of angiotensin II receptor expression during development and regression of hypoxic pulmonary hypertension. *Am J Respir Cell Mol Biol*, **22**, 323-32.
- CHOMCZYNSKI, P. & QASBA, P.K. (1984). Alkaline transfer of DNA to plastic membrane. *Biochem Biophys Res Commun*, **122**, 340-4.
- CHOMCZYNSKI, P. & SACCHI, N. (1987). Single-step method of RNA isolation by acid guanidinium thiocyanate- phenol-chloroform extraction. *Anal Biochem*, **162**, 156-9.

- CHOW, L.H., SUBRAMANIAN, S., NUOVO, G.J., MILLER, F. & NORD, E.P. (1995). Endothelin receptor mRNA expression in renal medulla identified by in situ RT-PCR. *Am J Physiol*, **269**, F449-57.
- CHRISTMAN, B.W., MCPHERSON, C.D., NEWMAN, J.H., KING, G.A., BERNARD, G.R., GROVES, B.M. & LOYD, J.E. (1992). An imbalance between the excretion of thromboxane and prostacyclin metabolites in pulmonary hypertension. *N Engl J Med*, **327**, 70-5.
- CHU, T.S., PENG, Y., CANO, A., YANAGISAWA, M. & ALPERN, R.J. (1996). Endothelin(B) receptor activates NHE-3 by a Ca<sup>2+</sup>-dependent pathway in OKP cells. *J Clin Invest*, **97**, 1454-62.
- CHUN, M., LIN, H.Y., HENIS, Y.I. & LODISH, H.F. (1995). Endothelin-induced endocytosis of cell surface ETA receptors. Endothelin remains intact and bound to the ETA receptor. *J Biol Chem*, **270**, 10855-60.
- CLAVELL, A.L., STINGO, A.J., MARGULIES, K.B., BRANDT, R.R. & BURNETT, J.C., JR. (1995). Role of endothelin receptor subtypes in the in vivo regulation of renal function. *Am J Physiol*, **268**, F455-60.
- CLOUTHIER, D.E., HOSODA, K., RICHARDSON, J.A., WILLIAMS, S.C., YANAGISAWA, H., KUWAKI, T., KUMADA, M., HAMMER, R.E. & YANAGISAWA, M. (1998). Cranial and cardiac neural crest defects in endothelin-A receptor-deficient mice. *Development*, **125**, 813-24.
- CLOUTHIER, D.E. & SCHILLING, T.F. (2004). Understanding endothelin-1 function during craniofacial development in the mouse and zebrafish. *Birth Defects Res Part C Embryo Today*, **72**, 190-9.
- CLOUTHIER, D.E., WILLIAMS, S.C., YANAGISAWA, H., WIEDUWILT, M., RICHARDSON, J.A. & YANAGISAWA, M. (2000). Signaling pathways crucial for craniofacial development revealed by endothelin-A receptor-deficient mice. *Dev Biol*, **217**, 10-24.
- CLOZEL, J.P., SAUNIER, C., HARTEMANN, D. & FISCHLI, W. (1991). Effects of cilazapril, a novel angiotensin converting enzyme inhibitor, on the structure of pulmonary arteries of rats exposed to chronic hypoxia. *J Cardiovasc Pharmacol*, **17**, 36-40.

- CONSTIEN, R., FORDE, A., LILIENSIEK, B., GRONE, H.J., NAWROTH, P., HAMMERLING, G. & ARNOLD, B. (2001). Characterization of a novel EGFP reporter mouse to monitor Cre recombination as demonstrated by a Tie2 Cre mouse line. *Genesis*, **30**, 36-44.
- COOL, C.D., STEWART, J.S., WERAHERA, P., MILLER, G.J., WILLIAMS, R.L., VOELKEL, N.F. & TUDER, R.M. (1999). Three-dimensional reconstruction of pulmonary arteries in plexiform pulmonary hypertension using cell-specific markers. Evidence for a dynamic and heterogeneous process of pulmonary endothelial cell growth. *Am J Pathol*, **155**, 411-9.
- COWAN, K.N., HEILBUT, A., HUMPL, T., LAM, C., ITO, S. & RABINOVITCH, M. (2000a). Complete reversal of fatal pulmonary hypertension in rats by a serine elastase inhibitor. *Nat Med*, **6**, 698-702.
- COWAN, K.N., JONES, P.L. & RABINOVITCH, M. (2000b). Elastase and matrix metalloproteinase inhibitors induce regression, and tenascin-C antisense prevents progression, of vascular disease. *J Clin Invest*, **105**, 21-34.
- COWBURN, P.J., CLELAND, J.G., McDONAGH, T.A., MCARTHUR, J.D., DARGIE, H.J. & MORTON, J.J. (2005). Comparison of selective ET(A) and ET(B) receptor antagonists in patients with chronic heart failure. *Eur J Heart Fail*, **7**, 37-42.
- CURZEN, N.P., GRIFFITHS, M.J. & EVANS, T.W. (1995). Contraction to endothelin-1 in pulmonary arteries from endotoxin-treated rats is modulated by endothelium. *Am J Physiol*, **268**, H2260-6.
- D'ORLEANS-JUSTE, P., CLAING, A., TELEMAQUE, S., MAURICE, M.C., YANO, M. & GRATTON, J.P. (1994). Block of endothelin-1-induced release of thromboxane A2 from the guinea pig lung and nitric oxide from the rabbit kidney by a selective ETB receptor antagonist, BQ-788. *Br J Pharmacol*, **113**, 1257-62.
- D'ORLEANS-JUSTE, P., LABONTE, J., BKAILY, G., CHOUFANI, S., PLANTE, M. & HONORE, J. (2002). Function of the endothelin(B) receptor in cardiovascular physiology and pathophysiology. *Pharmacol Ther*, **95**, 221-38.
- DAVENPORT, A.P. & KUC, R.E. (2002). Radioligand binding assays and quantitative autoradiography of endothelin receptors. *Methods Mol Biol*, **206**, 45-70.
- DAVENPORT, A.P., KUC, R.E., ASHBY, M.J., PATT, W.C. & DOHERTY, A.M. (1998). Characterization of [125I]-PD164333, an ETA selective non-peptide

- radiolabelled antagonist, in normal and diseased human tissues. *Br J Pharmacol*, **123**, 223-30.
- DAVENPORT, A.P., KUC, R.E., FITZGERALD, F., MAGUIRE, J.J., BERRYMAN, K. & DOHERTY, A.M. (1994). [125I]-PD151242: a selective radioligand for human ETA receptors. *Br J Pharmacol*, **111**, 4-6.
- DAVIE, N., HALEEN, S.J., UPTON, P.D., POLAK, J.M., YACOUB, M.H., MORRELL, N.W. & WHARTON, J. (2002). ET(A) and ET(B) receptors modulate the proliferation of human pulmonary artery smooth muscle cells. *Am J Respir Crit Care Med*, **165**, 398-405.
- DAVISSON, R.L., YANG, G., BELTZ, T.G., CASSELL, M.D., JOHNSON, A.K. & SIGMUND, C.D. (1998). The brain renin-angiotensin system contributes to the hypertension in mice containing both the human renin and human angiotensinogen transgenes. *Circ Res*, **83**, 1047-58.
- DE NUCCI, G., THOMAS, R., D'ORLEANS-JUSTE, P., ANTUNES, E., WALDER, C., WARNER, T.D. & VANE, J.R. (1988). Pressor effects of circulating endothelin are limited by its removal in the pulmonary circulation and by the release of prostacyclin and endothelium-derived relaxing factor. *Proc Natl Acad Sci U S A*, **85**, 9797-800.
- DENG, Y., MARTIN, L.L., DELGRANDE, D. & JENG, A.Y. (1992). A soluble protease identified from rat kidney degrades endothelin-1 but not proendothelin-1. *J Biochem (Tokyo)*, **112**, 168-72.
- DENG, Z., MORSE, J.H., SLAGER, S.L., CUERVO, N., MOORE, K.J., VENETOS, G., KALACHIKOV, S., CAYANIS, E., FISCHER, S.G., BARST, R.J., HODGE, S.E. & KNOWLES, J.A. (2000). Familial primary pulmonary hypertension (gene PPH1) is caused by mutations in the bone morphogenetic protein receptor-II gene. *Am J Hum Genet*, **67**, 737-44.
- DINGEMANSE, J., CLOZEL, M. & VAN GIERBERGEN, P.L. (2002). Entry-into-humans study with tezosentan, an intravenous dual endothelin receptor antagonist. *J Cardiovasc Pharmacol*, **39**, 795-802.
- DONATELLI, M., HOFFMANN, E., COLLETTI, I., ANDOLINA, G., RUSSO, V., BUCALO, M.L., VALENTI, T.M., COMPAGNO, V., CATALDO, M.G. & MORICI, M.L.

- (1996). Circulating endothelin-1 levels in type 2 diabetic patients with ischaemic heart disease. *Acta Diabetol*, **33**, 246-8.
- DORAI, H., VUKICEVIC, S. & SAMPATH, T.K. (2000). Bone morphogenetic protein-7 (osteogenic protein-1) inhibits smooth muscle cell proliferation and stimulates the expression of markers that are characteristic of SMC phenotype in vitro. *J Cell Physiol*, **184**, 37-45.
- DOUGLAS, S.A., BECK, G.R., JR., ELLIOTT, J.D. & OHLSTEIN, E.H. (1995). Pharmacological evidence for the presence of three distinct functional endothelin receptor subtypes in the rabbit lateral saphenous vein. *Br J Pharmacol*, **114**, 1529-40.
- DOUGLAS, S.A. & OHLSTEIN, E.H. (1997). Signal transduction mechanisms mediating the vascular actions of endothelin. *J Vasc Res*, **34**, 152-64.
- DUPUIS, J., GORESKY, C.A. & FOURNIER, A. (1996a). Pulmonary clearance of circulating endothelin-1 in dogs in vivo: exclusive role of ETB receptors. *J Appl Physiol*, **81**, 1510-5.
- DUPUIS, J., GORESKY, C.A. & STEWART, D.J. (1994). Pulmonary removal and production of endothelin in the anesthetized dog. *J Appl Physiol*, **76**, 694-700.
- DUPUIS, J., ROULEAU, J.L. & CERNACEK, P. (1998). Reduced pulmonary clearance of endothelin-1 contributes to the increase of circulating levels in heart failure secondary to myocardial infarction. *Circulation*, **98**, 1684-7.
- DUPUIS, J., STEWART, D.J., CERNACEK, P. & GOSSELIN, G. (1996b). Human pulmonary circulation is an important site for both clearance and production of endothelin-1. *Circulation*, **94**, 1578-84.
- EDDAHIBI, S., HANOUN, N., LANFUMEY, L., LESCH, K.P., RAFFESTIN, B., HAMON, M. & ADNOT, S. (2000). Attenuated hypoxic pulmonary hypertension in mice lacking the 5-hydroxytryptamine transporter gene. *J Clin Invest*, **105**, 1555-62.
- EDERY, P., ATTIE, T., AMIEL, J., PELET, A., ENG, C., HOFSTRA, R.M., MARTELLI, H., BIDAUD, C., MUNNICH, A. & LYONNET, S. (1996). Mutation of the endothelin-3 gene in the Waardenburg-Hirschsprung disease (Shah-Waardenburg syndrome). *Nat Genet*, **12**, 442-4.

- EDWARDS, R.M., STACK, E.J., PULLEN, M. & NAMBI, P. (1993). Endothelin inhibits vasopressin action in rat inner medullary collecting duct via the ETB receptor. *J Pharmacol Exp Ther*, **267**, 1028-33.
- EHRENREICH, H., ANDERSON, R.W., FOX, C.H., RIECKMANN, P., HOFFMAN, G.S., TRAVIS, W.D., COLIGAN, J.E., KEHRL, J.H. & FAUCI, A.S. (1990). Endothelins, peptides with potent vasoactive properties, are produced by human macrophages. *J Exp Med*, **172**, 1741-8.
- EMORI, T., HIRATA, Y., IMAI, T., OHTA, K., KANNO, K., EGUCHI, S. & MARUMO, F. (1992). Cellular mechanism of thrombin on endothelin-1 biosynthesis and release in bovine endothelial cell. *Biochem Pharmacol*, **44**, 2409-11.
- ERGUL, A., GLASSBERG, M.K., WANNER, A. & PUETT, D. (1995). Characterization of endothelin receptor subtypes on airway smooth muscle cells. *Exp Lung Res*, **21**, 453-68.
- ERGUL, A., SHOEMAKER, K., PUETT, D. & TACKETT, R.L. (1998). Gender differences in the expression of endothelin receptors in human saphenous veins in vitro. *J Pharmacol Exp Ther*, **285**, 511-7.
- EVANS, R.G., BERGSTROM, G., COTTERILL, E. & ANDERSON, W.P. (1998). Renal haemodynamic effects of endothelin-1 and the ETA/ETB antagonist TAK-044 in anaesthetized rabbits. *J Hypertens*, **16**, 1897-905.
- FAGAN, K.A., FOUTY, B.W., TYLER, R.C., MORRIS, K.G., JR., HEPLER, L.K., SATO, K., LECRAS, T.D., ABMAN, S.H., WEINBERGER, H.D., HUANG, P.L., MCMURTRY, I.F. & RODMAN, D.M. (1999). The pulmonary circulation of homozygous or heterozygous eNOS-null mice is hyperresponsive to mild hypoxia. *J Clin Invest*, **103**, 291-9.
- FAGHER, B., VALIND, S. & THULIN, T. (1995). End-organ damage in treated severe hypertension: close relation to nocturnal blood pressure. *J Hum Hypertens*, **9**, 605-10.
- FEINBERG, A.P. & VOGELSTEIN, B. (1983). A technique for radiolabeling DNA restriction endonuclease fragments to high specific activity. *Anal Biochem*, **132**, 6-13.

- FERNANDES, L.B., HENRY, P.J., RIGBY, P.J. & GOLDIE, R.G. (1996). EndothelinB (ETB) receptor-activated potentiation of cholinergic nerve-mediated contraction in human bronchus. *Br J Pharmacol*, **118**, 1873-4.
- FERRI, C., BELLINI, C., DESIDERI, G., BALDONCINI, R., PROPERZI, G., SANTUCCI, A. & DE MATTIA, G. (1997). Circulating endothelin-1 levels in obese patients with the metabolic syndrome. *Exp Clin Endocrinol Diabetes*, **105 Suppl 2**, 38-40.
- FIRE, A. (1992). Histochemical techniques for locating Escherichia coli beta-galactosidase activity in transgenic organisms. *Genet Anal Tech Appl*, **9**, 151-8.
- FIRTH, J.D. & RATCLIFFE, P.J. (1992). Organ distribution of the three rat endothelin messenger RNAs and the effects of ischemia on renal gene expression. *J Clin Invest*, **90**, 1023-31.
- FRASCH, H.F., MARSHALL, C. & MARSHALL, B.E. (1999). Endothelin-1 is elevated in monocrotaline pulmonary hypertension. *Am J Physiol*, **276**, L304-10.
- FUKURODA, T., FUJIKAWA, T., OZAKI, S., ISHIKAWA, K., YANO, M. & NISHIKIBE, M. (1994). Clearance of circulating endothelin-1 by ETB receptors in rats. *Biochem Biophys Res Commun*, **199**, 1461-5.
- GALIE, N., MANES, A. & BRANZI, A. (2004). The endothelin system in pulmonary arterial hypertension. *Cardiovasc Res*, **61**, 227-37.
- GARIEPY, C.E. (2001). Intestinal motility disorders and development of the enteric nervous system. *Pediatr Res*, **49**, 605-13.
- GARIEPY, C.E., CASS, D.T. & YANAGISAWA, M. (1996). Null mutation of endothelin receptor type B gene in spotting lethal rats causes aganglionic megacolon and white coat color. *Proc Natl Acad Sci U S A*, **93**, 867-72.
- GARIEPY, C.E., OHUCHI, T., WILLIAMS, S.C., RICHARDSON, J.A. & YANAGISAWA, M. (2000). Salt-sensitive hypertension in endothelin-B receptor-deficient rats. *J Clin Invest*, **105**, 925-33.
- GARIEPY, C.E., WILLIAMS, S.C., RICHARDSON, J.A., HAMMER, R.E. & YANAGISAWA, M. (1998). Transgenic expression of the endothelin-B receptor prevents congenital intestinal aganglionosis in a rat model of Hirschsprung disease. *J Clin Invest*, **102**, 1092-101.



- GE, Y., AHN, D., STRICKLETT, P.K., HUGHES, A.K., YANAGISAWA, M., VERBALIS, J.G. & KOHAN, D.E. (2005). Collecting duct-specific knockout of endothelin-1 alters vasopressin regulation of urine osmolality. *Am J Physiol Renal Physiol*.
- GE, Y., BAGNALL, A., STRICKLETT, P.K., STRAIT, K., WEBB, D.J., KOTELEVTSSEV, Y. & KOHAN, D.E. (2006). Collecting duct-specific knockout of the endothelin B receptor causes hypertension and sodium retention. *Am J Physiol Renal Physiol*, **291**, F1274-80.
- GERACI, M.W., GAO, B., SHEPHERD, D.C., MOORE, M.D., WESTCOTT, J.Y., FAGAN, K.A., ALGER, L.A., TUDER, R.M. & VOELKEL, N.F. (1999). Pulmonary prostacyclin synthase overexpression in transgenic mice protects against development of hypoxic pulmonary hypertension. *J Clin Invest*, **103**, 1509-15.
- GIAID, A., GIBSON, S.J., HERRERO, M.T., GENTLEMAN, S., LEGON, S., YANAGISAWA, M., MASAKI, T., IBRAHIM, N.B., ROBERTS, G.W., ROSSI, M.L. & ET AL. (1991). Topographical localisation of endothelin mRNA and peptide immunoreactivity in neurones of the human brain. *Histochemistry*, **95**, 303-14.
- GIAID, A. & SALEH, D. (1995). Reduced expression of endothelial nitric oxide synthase in the lungs of patients with pulmonary hypertension. *N Engl J Med*, **333**, 214-21.
- GIAID, A., YANAGISAWA, M., LANGLEBEN, D., MICHEL, R.P., LEVY, R., SHENNIB, H., KIMURA, S., MASAKI, T., DUGUID, W.P. & STEWART, D.J. (1993). Expression of endothelin-1 in the lungs of patients with pulmonary hypertension. *N Engl J Med*, **328**, 1732-9.
- GIARDINA, J.B., GREEN, G.M., RINEWALT, A.N., GRANGER, J.P. & KHALIL, R.A. (2001). Role of endothelin B receptors in enhancing endothelium-dependent nitric oxide-mediated vascular relaxation during high salt diet. *Hypertension*, **37**, 516-23.
- GILCHRIST, D.S., URE, J., HOOK, L. & MEDVINSKY, A. (2003). Labeling of hematopoietic stem and progenitor cells in novel activatable EGFP reporter mice. *Genesis*, **36**, 168-76.

- GILLER, T., BREU, V., VALDENAIRE, O. & CLOZEL, M. (1997). Absence of ET(B)-mediated contraction in Piebald-lethal mice. *Life Sci*, **61**, 255-63.
- GODDARD, J., ECKHART, C., JOHNSTON, N.R., CUMMING, A.D., RANKIN, A.J. & WEBB, D.J. (2004a). Endothelin A receptor antagonism and angiotensin-converting enzyme inhibition are synergistic via an endothelin B receptor-mediated and nitric oxide-dependent mechanism. *J Am Soc Nephrol*, **15**, 2601-10.
- GODDARD, J., JOHNSTON, N.R., HAND, M.F., CUMMING, A.D., RABELINK, T.J., RANKIN, A.J. & WEBB, D.J. (2004b). Endothelin-A receptor antagonism reduces blood pressure and increases renal blood flow in hypertensive patients with chronic renal failure: a comparison of selective and combined endothelin receptor blockade. *Circulation*, **109**, 1186-93.
- GOLDIE, R.G., GRAYSON, P.S., KNOTT, P.G., SELF, G.J. & HENRY, P.J. (1994). Predominance of endothelinA (ETA) receptors in ovine airway smooth muscle and their mediation of ET-1-induced contraction. *Br J Pharmacol*, **112**, 749-56.
- GOLDIE, R.G., HENRY, P.J., KNOTT, P.G., SELF, G.J., LUTTMANN, M.A. & HAY, D.W. (1995). Endothelin-1 receptor density, distribution, and function in human isolated asthmatic airways. *Am J Respir Crit Care Med*, **152**, 1653-8.
- GOLDIE, R.G., KNOTT, P.G., CARR, M.J., HAY, D.W. & HENRY, P.J. (1996). The endothelins in the pulmonary system. *Pulm Pharmacol*, **9**, 69-93.
- GRAY, G.A. & WEBB, D.J. (1996). The endothelin system and its potential as a therapeutic target in cardiovascular disease. *Pharmacol Ther*, **72**, 109-48.
- GROS, R., VAN WERT, R., YOU, X., THORIN, E. & HUSAIN, M. (2002). Effects of age, gender, and blood pressure on myogenic responses of mesenteric arteries from C57BL/6 mice. *Am J Physiol Heart Circ Physiol*, **282**, H380-8.
- GROSS, V. & LUFT, F.C. (2003). Exercising restraint in measuring blood pressure in conscious mice. *Hypertension*, **41**, 879-81.
- GU, H., MARTH, J.D., ORBAN, P.C., MOSSMANN, H. & RAJEWSKY, K. (1994). Deletion of a DNA polymerase beta gene segment in T cells using cell type-specific gene targeting. *Science*, **265**, 103-6.

- GUYTON, A.C. & HALL, J.E. (2005). *Textbook of Medical Physiology, 11th edition*: Elsevier.
- GYGI, S.P., ROCHON, Y., FRANZA, B.R. & AEBERSOLD, R. (1999). Correlation between protein and mRNA abundance in yeast. *Mol Cell Biol*, **19**, 1720-30.
- HAASE, D., LEHMANN, M.H., KORNER, M.M., KORFER, R., SIGUSCH, H.H. & FIGULLA, H.R. (2002). Identification and validation of selective upregulation of ventricular myosin light chain type 2 mRNA in idiopathic dilated cardiomyopathy. *Eur J Heart Fail*, **4**, 23-31.
- HASEGAWA, J., WAGNER, K.F., KARP, D., LI, D., SHIBATA, J., HERINGLAKE, M., BAHLMANN, L., DEPPING, R., FANDREY, J., SCHMUCKER, P. & UHLIG, S. (2004). Altered pulmonary vascular reactivity in mice with excessive erythrocytosis. *Am J Respir Crit Care Med*, **169**, 829-35.
- HASUNUMA, K., RODMAN, D.M., O'BRIEN, R.F. & MCMURTRY, I.F. (1990). Endothelin 1 causes pulmonary vasodilation in rats. *Am J Physiol*, **259**, H48-54.
- HAYNES, W.G., FERRO, C.J., O'KANE, K.P., SOMERVILLE, D., LOMAX, C.C. & WEBB, D.J. (1996). Systemic endothelin receptor blockade decreases peripheral vascular resistance and blood pressure in humans. *Circulation*, **93**, 1860-70.
- HAYNES, W.G. & WEBB, D.J. (1994). Contribution of endogenous generation of endothelin-1 to basal vascular tone. *Lancet*, **344**, 852-4.
- HEFLER, L.A., TEMPFER, C.B., MORENO, R.M., O'BRIEN, W.E. & GREGG, A.R. (2001). Endothelial-derived nitric oxide and angiotensinogen: blood pressure and metabolism during mouse pregnancy. *Am J Physiol Regul Integr Comp Physiol*, **280**, R174-82.
- HELDIN, C.H., MIYAZONO, K. & TEN DIJKE, P. (1997). TGF-beta signalling from cell membrane to nucleus through SMAD proteins. *Nature*, **390**, 465-71.
- HENRY, P.J. (1993). Endothelin-1 (ET-1)-induced contraction in rat isolated trachea: involvement of ETA and ETB receptors and multiple signal transduction systems. *Br J Pharmacol*, **110**, 435-41.

- HENRY, P.J. & GOLDIE, R.G. (1995). Potentiation by endothelin-1 of cholinergic nerve-mediated contractions in mouse trachea via activation of ETB receptors. *Br J Pharmacol*, **114**, 563-9.
- HERGET, J., SUGGETT, A.J., LEACH, E. & BARER, G.R. (1978). Resolution of pulmonary hypertension and other features induced by chronic hypoxia in rats during complete and intermittent normoxia. *Thorax*, **33**, 468-73.
- HERVE, P., DROUET, L., DOSQUET, C., LAUNAY, J.M., RAIN, B., SIMONNEAU, G., CAEN, J. & DUROUX, P. (1990). Primary pulmonary hypertension in a patient with a familial platelet storage pool disease: role of serotonin. *Am J Med*, **89**, 117-20.
- HERVE, P., LAUNAY, J.M., SCROBOHACI, M.L., BRENOT, F., SIMONNEAU, G., PETITPRETZ, P., POUBEAU, P., CERRINA, J., DUROUX, P. & DROUET, L. (1995). Increased plasma serotonin in primary pulmonary hypertension. *Am J Med*, **99**, 249-54.
- HIRATA, Y., EMORI, T., EGUCHI, S., KANNO, K., IMAI, T., OHTA, K. & MARUMO, F. (1993). Endothelin receptor subtype B mediates synthesis of nitric oxide by cultured bovine endothelial cells. *J Clin Invest*, **91**, 1367-73.
- HIROTA, H., CHEN, J., BETZ, U.A., RAJEWSKY, K., GU, Y., ROSS, J., JR., MULLER, W. & CHIEN, K.R. (1999). Loss of a gp130 cardiac muscle cell survival pathway is a critical event in the onset of heart failure during biomechanical stress. *Cell*, **97**, 189-98.
- HOCHER, B., ROHMEISS, P., DIEKMANN, F., ZART, R., VOGT, V., SCHILLER, S., BAUER, C., KOPPENHAGEN, K., DISTLER, A. & GRETZ, N. (1995). Distribution of endothelin receptor subtypes in the rat kidney. Renal and haemodynamic effects of the mixed (A/B) endothelin receptor antagonist bosentan. *Eur J Clin Chem Clin Biochem*, **33**, 463-72.
- HOCHER, B., SCHWARZ, A., FAGAN, K.A., THONE-REINEKE, C., EL-HAG, K., KUSSEROW, H., ELITOK, S., BAUER, C., NEUMAYER, H.H., RODMAN, D.M. & THEURING, F. (2000). Pulmonary fibrosis and chronic lung inflammation in ET-1 transgenic mice. *Am J Respir Cell Mol Biol*, **23**, 19-26.
- HOCHER, B., THONE-REINEKE, C., ROHMEISS, P.L., NEUMAYER, H.H., SCHLEUNING, W.D. & THEURING, F. (1997). Endothelin-1 transgenic mice develop

- glomerulosclerosis, interstitial fibrosis, and renal cysts but not hypertension. *J Clin Invest*, **99**, 1380-9.
- HOESS, R.H., ZIESE, M. & STERNBERG, N. (1982). P1 site-specific recombination: nucleotide sequence of the recombining sites. *Proc Natl Acad Sci U S A*, **79**, 3398-402.
- HOFFMAN, A., ABASSI, Z.A., BRODSKY, S., RAMADAN, R. & WINAVER, J. (2000). Mechanisms of big endothelin-1-induced diuresis and natriuresis : role of ET(B) receptors. *Hypertension*, **35**, 732-9.
- HONORE, J.C., FECTEAU, M.H., BROCHU, I., LABONTE, J., BKAILY, G. & D'ORLEANS-JUSTE, P. (2005). Concomitant antagonism of endothelial and vascular smooth muscle cell ETB receptors for endothelin induces hypertension in the hamster. *Am J Physiol Heart Circ Physiol*, **289**, H1258-64.
- HORGAN, M.J., PINHEIRO, J.M. & MALIK, A.B. (1991). Mechanism of endothelin-1-induced pulmonary vasoconstriction. *Circ Res*, **69**, 157-64.
- HOSODA, K., HAMMER, R.E., RICHARDSON, J.A., BAYNASH, A.G., CHEUNG, J.C., GIAID, A. & YANAGISAWA, M. (1994). Targeted and natural (piebald-lethal) mutations of endothelin-B receptor gene produce megacolon associated with spotted coat color in mice. *Cell*, **79**, 1267-76.
- HUBER, K., BECKMANN, R., FRANK, H., KNEUSSL, M., MLCZUCH, J. & BINDER, B.R. (1994). Fibrinogen, t-PA, and PAI-1 plasma levels in patients with pulmonary hypertension. *Am J Respir Crit Care Med*, **150**, 929-33.
- HUGHES, A.K., BARRY, W.H. & KOHAN, D.E. (1995). Identification of a contractile function for renal medullary interstitial cells. *J Clin Invest*, **96**, 411-6.
- HUMBERT, M., SITBON, O. & SIMONNEAU, G. (2004). Treatment of pulmonary arterial hypertension. *N Engl J Med*, **351**, 1425-36.
- HYVELIN, J.M., HOWELL, K., NICHOL, A., COSTELLO, C.M., PRESTON, R.J. & McLOUGHLIN, P. (2005). Inhibition of Rho-kinase attenuates hypoxia-induced angiogenesis in the pulmonary circulation. *Circ Res*, **97**, 185-91.
- INOUE, A., YANAGISAWA, M., KIMURA, S., KASUYA, Y., MIYAUCHI, T., GOTO, K. & MASAKI, T. (1989). The human endothelin family: three structurally and pharmacologically distinct isopeptides predicted by three separate genes. *Proc Natl Acad Sci U S A*, **86**, 2863-7.

- INSCHO, E.W., IMIG, J.D., COOK, A.K. & POLLOCK, D.M. (2005). ETA and ETB receptors differentially modulate afferent and efferent arteriolar responses to endothelin. *Br J Pharmacol*, **146**, 1019-26.
- IVY, D., MCMURTRY, I.F., YANAGISAWA, M., GARIEPY, C.E., LE CRAS, T.D., GEBB, S.A., MORRIS, K.G., WISEMAN, R.C. & ABMAN, S.H. (2001). Endothelin B receptor deficiency potentiates ET-1 and hypoxic pulmonary vasoconstriction. *Am J Physiol Lung Cell Mol Physiol*, **280**, L1040-8.
- IVY, D.D., MCMURTRY, I.F., COLVIN, K., IMAMURA, M., OKA, M., LEE, D.S., GEBB, S. & JONES, P.L. (2005). Development of occlusive neointimal lesions in distal pulmonary arteries of endothelin B receptor-deficient rats: a new model of severe pulmonary arterial hypertension. *Circulation*, **111**, 2988-96.
- IVY, D.D., YANAGISAWA, M., GARIEPY, C.E., GEBB, S.A., COLVIN, K.L. & MCMURTRY, I.F. (2002). Exaggerated hypoxic pulmonary hypertension in endothelin B receptor-deficient rats. *Am J Physiol Lung Cell Mol Physiol*, **282**, L703-12.
- JAMIESON, M.J., GONZALES, G.M., JACKSON, T.I., KOERTH, S.M., ROMANO, W.F., TAN, D.X., CASTILLON, F., 3RD, SKINNER, M.H., GROSSMANN, M. & SHEPHERD, A.M. (1997). Evaluation of the IITC tail cuff blood pressure recorder in the rat against intraarterial pressure according to criteria for human devices. *Am J Hypertens*, **10**, 209-16.
- JASMIN, J.F., LUCAS, M., CERNACEK, P. & DUPUIS, J. (2001). Effectiveness of a nonselective ET(A/B) and a selective ET(A) antagonist in rats with monocrotaline-induced pulmonary hypertension. *Circulation*, **103**, 314-8.
- JIANG, W., LEPAGE, D., HE, Y., MANN, R. & CONLON, R. Case transgenic and targetting facility (<http://ko.cwru.edu/services/musfrming.html#bkgd>).
- JOHNSTROM, P., FRYER, T.D., RICHARDS, H.K., HARRIS, N.G., BARRET, O., CLARK, J.C., PICKARD, J.D. & DAVENPORT, A.P. (2005). Positron emission tomography using 18F-labelled endothelin-1 reveals prevention of binding to cardiac receptors owing to tissue-specific clearance by ET B receptors in vivo. *Br J Pharmacol*, **144**, 115-22.

- JUNQUEIRA, L.C., BIGNOLAS, G. & BRENTANI, R.R. (1979). Picrosirius staining plus polarization microscopy, a specific method for collagen detection in tissue sections. *Histochem J*, **11**, 447-55.
- KAM, K.W., QI, J.S., CHEN, M. & WONG, T.M. (2004). Estrogen reduces cardiac injury and expression of beta1-adrenoceptor upon ischemic insult in the rat heart. *J Pharmacol Exp Ther*, **309**, 8-15.
- KANNO, S., WU, Y.J., LEE, P.C., BILLIAR, T.R. & HO, C. (2001). Angiotensin-converting enzyme inhibitor preserves p21 and endothelial nitric oxide synthase expression in monocrotaline-induced pulmonary arterial hypertension in rats. *Circulation*, **104**, 945-50.
- KARET, F.E. & DAVENPORT, A.P. (1996). Localization of endothelin peptides in human kidney. *Kidney Int*, **49**, 382-7.
- KEDZIERSKI, R.M., GRAYBURN, P.A., KISANUKI, Y.Y., WILLIAMS, C.S., HAMMER, R.E., RICHARDSON, J.A., SCHNEIDER, M.D. & YANAGISAWA, M. (2003). Cardiomyocyte-specific endothelin A receptor knockout mice have normal cardiac function and an unaltered hypertrophic response to angiotensin II and isoproterenol. *Mol Cell Biol*, **23**, 8226-32.
- KEDZIERSKI, R.M. & YANAGISAWA, M. (2001). Endothelin system: the double-edged sword in health and disease. *Annu Rev Pharmacol Toxicol*, **41**, 851-76.
- KEEGAN, A., MORECROFT, I., SMILLIE, D., HICKS, M.N. & MACLEAN, M.R. (2001). Contribution of the 5-HT(1B) receptor to hypoxia-induced pulmonary hypertension: converging evidence using 5-HT(1B)-receptor knockout mice and the 5-HT(1B/1D)-receptor antagonist GR127935. *Circ Res*, **89**, 1231-9.
- KELLOGG, D.L., JR., LIU, Y. & PERGOLA, P.E. (2001). Selected contribution: Gender differences in the endothelin-B receptor contribution to basal cutaneous vascular tone in humans. *J Appl Physiol*, **91**, 2407-11; discussion 2389-90.
- KIMURA, A., KINJO, I., MATSUMURA, Y., MORI, H., MASHIMA, R., HARADA, M., CHIEN, K.R., YASUKAWA, H. & YOSHIMURA, A. (2004). SOCS3 is a physiological negative regulator for granulopoiesis and granulocyte colony-stimulating factor receptor signaling. *J Biol Chem*, **279**, 6905-10.

- KISANUKI, Y.Y., HAMMER, R.E., MIYAZAKI, J., WILLIAMS, S.C., RICHARDSON, J.A. & YANAGISAWA, M. (2001). Tie2-Cre transgenic mice: a new model for endothelial cell-lineage analysis in vivo. *Dev Biol*, **230**, 230-42.
- KISANUKI, Y.Y., OHUCHI, Y., TAKAHASHI, H., HAMMER, R.E., WILLIAMS, S.C. & YANAGISAWA, M. (1999). Endothelial cell-specific knock-out of the endothelin-1 gene in mice. Presented at the 6th International Conference on Endothelin, Montreal, Canada.
- KITAMURA, K., TANAKA, T., KATO, J., ETO, T. & TANAKA, K. (1989). Regional distribution of immunoreactive endothelin in porcine tissue: abundance in inner medulla of kidney. *Biochem Biophys Res Commun*, **161**, 348-52.
- KOHAN, D.E. (1991). Endothelin synthesis by rabbit renal tubule cells. *Am J Physiol*, **261**, F221-6.
- KOHAN, D.E. (1997). Endothelins in the normal and diseased kidney. *Am J Kidney Dis*, **29**, 2-26.
- KOHAN, D.E., HUGHES, A.K. & PERKINS, S.L. (1992). Characterization of endothelin receptors in the inner medullary collecting duct of the rat. *J Biol Chem*, **267**, 12336-40.
- KOHNO, M., HORIO, T., YOKOKAWA, K., KURIHARA, N. & TAKEDA, T. (1992). C-type natriuretic peptide inhibits thrombin- and angiotensin II-stimulated endothelin release via cyclic guanosine 3',5'-monophosphate. *Hypertension*, **19**, 320-5.
- KOLLER, B.H. & SMITHIES, O. (1992). Altering genes in animals by gene targeting. *Annu Rev Immunol*, **10**, 705-30.
- KONI, P.A., JOSHI, S.K., TEMANN, U.A., OLSON, D., BURKLY, L. & FLAVELL, R.A. (2001). Conditional vascular cell adhesion molecule 1 deletion in mice: impaired lymphocyte migration to bone marrow. *J Exp Med*, **193**, 741-54.
- KOTELEVTSOV, Y. & WEBB, D.J. (2001). Endothelin as a natriuretic hormone: the case for a paracrine action mediated by nitric oxide. *Cardiovasc Res*, **51**, 481-8.
- KRAMER, K. & KINTER, L.B. (2003). Evaluation and applications of radiotelemetry in small laboratory animals. *Physiol Genomics*, **13**, 197-205.



- KURIHARA, H., YOSHIKUMI, M., SUGIYAMA, T., TAKAKU, F., YANAGISAWA, M., MASAKI, T., HAMAOKI, M., KATO, H. & YAZAKI, Y. (1989). Transforming growth factor-beta stimulates the expression of endothelin mRNA by vascular endothelial cells. *Biochem Biophys Res Commun*, **159**, 1435-40.
- KURIHARA, Y., KURIHARA, H., ODA, H., MAEMURA, K., NAGAI, R., ISHIKAWA, T. & YAZAKI, Y. (1995). Aortic arch malformations and ventricular septal defect in mice deficient in endothelin-1. *J Clin Invest*, **96**, 293-300.
- KURIHARA, Y., KURIHARA, H., SUZUKI, H., KODAMA, T., MAEMURA, K., NAGAI, R., ODA, H., KUWAKI, T., CAO, W.H., KAMADA, N. & ET AL. (1994). Elevated blood pressure and craniofacial abnormalities in mice deficient in endothelin-1. *Nature*, **368**, 703-10.
- KURTZ, T.W., GRIFFIN, K.A., BIDANI, A.K., DAVISSON, R.L. & HALL, J.E. (2005). Recommendations for blood pressure measurement in humans and experimental animals: part 2: blood pressure measurement in experimental animals: a statement for professionals from the subcommittee of professional and public education of the american heart association council on high blood pressure research. *Hypertension*, **45**, 299-310.
- KUWAKI, T., ISHII, T., JU, K., YANAGISAWA, M. & FUKUDA, Y. (2002). Blood pressure of endothelin-3 null (-/-) knockout mice and endothelin A receptor null (-/-) knockout mice under anaesthesia. *Clin Sci (Lond)*, **103 Suppl 48**, 48S-52S.
- KUWAKI, T., LING, G.Y., ONODERA, M., ISHII, T., NAKAMURA, A., JU, K.H., CAO, W.H., KUMADA, M., KURIHARA, H., KURIHARA, Y., YAZAKI, Y., OHUCHI, T., YANAGISAWA, M. & FUKUDA, Y. (1999). Endothelin in the central control of cardiovascular and respiratory functions. *Clin Exp Pharmacol Physiol*, **26**, 989-94.
- LAGHMANI, K., PREISIG, P.A., MOE, O.W., YANAGISAWA, M. & ALPERN, R.J. (2001). Endothelin-1/endothelin-B receptor-mediated increases in NHE3 activity in chronic metabolic acidosis. *J Clin Invest*, **107**, 1563-9.
- LAGHMANI, K., SAKAMOTO, A., YANAGISAWA, M., PREISIG, P.A. & ALPERN, R.J. (2005). A consensus sequence in the endothelin-B receptor second

- intracellular loop is required for NHE3 activation by endothelin-1. *Am J Physiol Renal Physiol*, **288**, F732-9.
- LAL, H., WOODWARD, B. & WILLIAMS, K.I. (1996). Investigation of the contributions of nitric oxide and prostaglandins to the actions of endothelins and sarafotoxin 6c in rat isolated perfused lungs. *Br J Pharmacol*, **118**, 1931-8.
- LANE, K.B., MACHADO, R.D., PAUCIULO, M.W., THOMSON, J.R., PHILLIPS, J.A., 3RD, LOYD, J.E., NICHOLS, W.C. & TREMBATH, R.C. (2000). Heterozygous germline mutations in BMPR2, encoding a TGF-beta receptor, cause familial primary pulmonary hypertension. The International PPH Consortium. *Nat Genet*, **26**, 81-4.
- LE MONNIER DE GOUVILLE, A.C., LIPPTON, H., COHEN, G., CAVERO, I. & HYMAN, A. (1990). Vasodilator activity of endothelin-1 and endothelin-3: rapid development of cross-tachyphylaxis and dependence on the rate of endothelin administration. *J Pharmacol Exp Ther*, **254**, 1024-8.
- LEE, M.E., DE LA MONTE, S.M., NG, S.C., BLOCH, K.D. & QUERTERMOUS, T. (1990). Expression of the potent vasoconstrictor endothelin in the human central nervous system. *J Clin Invest*, **86**, 141-7.
- LEE, S.D., SHROYER, K.R., MARKHAM, N.E., COOL, C.D., VOELKEL, N.F. & TUDER, R.M. (1998). Monoclonal endothelial cell proliferation is present in primary but not secondary pulmonary hypertension. *J Clin Invest*, **101**, 927-34.
- LEE, S.L., WANG, W.W., MOORE, B.J. & FANBURG, B.L. (1991). Dual effect of serotonin on growth of bovine pulmonary artery smooth muscle cells in culture. *Circ Res*, **68**, 1362-8.
- LEON, L.R., WALKER, L.D., DUBOSE, D.A. & STEPHENSON, L.A. (2004). Biotelemetry transmitter implantation in rodents: impact on growth and circadian rhythms. *Am J Physiol Regul Integr Comp Physiol*, **286**, R967-74.
- LEVIN, E.R. (1995). Endothelins. *N Engl J Med*, **333**, 356-63.
- LI, H., CHEN, S.J., CHEN, Y.F., MENG, Q.C., DURAND, J., OPARIL, S. & ELTON, T.S. (1994a). Enhanced endothelin-1 and endothelin receptor gene expression in chronic hypoxia. *J Appl Physiol*, **77**, 1451-9.

- LI, H., ELTON, T.S., CHEN, Y.F. & OPARIL, S. (1994b). Increased endothelin receptor gene expression in hypoxic rat lung. *Am J Physiol*, **266**, L553-60.
- LIAO, Y., DAY, K.H., DAMON, D.N. & DULING, B.R. (2001). Endothelial cell-specific knockout of connexin 43 causes hypotension and bradycardia in mice. *Proc Natl Acad Sci U S A*, **98**, 9989-94.
- LIU, J.Q. & FOLZ, R.J. (2004). Extracellular superoxide enhances 5-HT-induced murine pulmonary artery vasoconstriction. *Am J Physiol Lung Cell Mol Physiol*, **287**, L111-8.
- LOFFLER, B.M., BREU, V. & CLOZEL, M. (1993). Effect of different endothelin receptor antagonists and of the novel non-peptide antagonist Ro 46-2005 on endothelin levels in rat plasma. *FEBS Lett*, **333**, 108-10.
- LORENZ, J.N. (2002). A practical guide to evaluating cardiovascular, renal, and pulmonary function in mice. *Am J Physiol Regul Integr Comp Physiol*, **282**, R1565-82.
- LOUGHNA, S. & SATO, T.N. (2001). Angiopoietin and Tie signaling pathways in vascular development. *Matrix Biol*, **20**, 319-25.
- LOYD, J.E., PRIMM, R.K. & NEWMAN, J.H. (1984). Familial primary pulmonary hypertension: clinical patterns. *Am Rev Respir Dis*, **129**, 194-7.
- LYSKO, P.G., WEBB, C.L. & FEUERSTEIN, G. (1995). Binding of the nonpeptide antagonist, SB 209670, to endothelin receptors on cultured neurons. *Peptides*, **16**, 1279-82.
- MACCUMBER, M.W., ROSS, C.A., GLASER, B.M. & SNYDER, S.H. (1989). Endothelin: visualization of mRNAs by in situ hybridization provides evidence for local action. *Proc Natl Acad Sci U S A*, **86**, 7285-9.
- MACHADO, R.D., JAMES, V., SOUTHWOOD, M., HARRISON, R.E., ATKINSON, C., STEWART, S., MORRELL, N.W., TREMBATH, R.C. & ALDRED, M.A. (2005). Investigation of second genetic hits at the BMPR2 locus as a modulator of disease progression in familial pulmonary arterial hypertension. *Circulation*, **111**, 607-13.
- MACHADO, R.D., PAUCIULO, M.W., THOMSON, J.R., LANE, K.B., MORGAN, N.V., WHEELER, L., PHILLIPS, J.A., 3RD, NEWMAN, J., WILLIAMS, D., GALIE, N., MANES, A., MCNEIL, K., YACoub, M., MIKHAIL, G., ROGERS, P., CORRIS, P.,

- HUMBERT, M., DONNAI, D., MARTENSSON, G., TRANEBJAERG, L., LOYD, J.E., TREMBATH, R.C. & NICHOLS, W.C. (2001). BMPR2 haploinsufficiency as the inherited molecular mechanism for primary pulmonary hypertension. *Am J Hum Genet*, **68**, 92-102.
- MACLEAN, M.R., DEUCHAR, G.A., HICKS, M.N., MORECROFT, I., SHEN, S., SHEWARD, J., COLSTON, J., LOUGHLIN, L., NILSEN, M., DEMPSIE, Y. & HARMAR, A. (2004). Overexpression of the 5-hydroxytryptamine transporter gene: effect on pulmonary hemodynamics and hypoxia-induced pulmonary hypertension. *Circulation*, **109**, 2150-5.
- MACLEAN, M.R., HERVE, P., EDDAHIBI, S. & ADNOT, S. (2000). 5-hydroxytryptamine and the pulmonary circulation: receptors, transporters and relevance to pulmonary arterial hypertension. *Br J Pharmacol*, **131**, 161-8.
- MACLEAN, M.R. & MCCULLOCH, K.M. (1998). Influence of applied tension and nitric oxide on responses to endothelins in rat pulmonary resistance arteries: effect of chronic hypoxia. *Br J Pharmacol*, **123**, 991-9.
- MACLEAN, M.R., MCCULLOCH, K.M. & BAIRD, M. (1994). Endothelin ETA- and ETB-receptor-mediated vasoconstriction in rat pulmonary arteries and arterioles. *J Cardiovasc Pharmacol*, **23**, 838-45.
- MALEK, A.M., ZHANG, J., JIANG, J., ALPER, S.L. & IZUMO, S. (1999). Endothelin-1 gene suppression by shear stress: pharmacological evaluation of the role of tyrosine kinase, intracellular calcium, cytoskeleton, and mechanosensitive channels. *J Mol Cell Cardiol*, **31**, 387-99.
- MANGIAFICO, R.A., MALATINO, L.S., SANTONOCITO, M. & SPADA, R.S. (1998). Plasma endothelin-1 concentrations in non-insulin-dependent diabetes mellitus and nondiabetic patients with chronic arterial obstructive disease of the lower limbs. *Int Angiol*, **17**, 97-102.
- MAO, X., FUJIWARA, Y. & ORKIN, S.H. (1999). Improved reporter strain for monitoring Cre recombinase-mediated DNA excisions in mice. *Proc Natl Acad Sci U S A*, **96**, 5037-42.
- MARSAULT, R., FEOLDE, E. & FRELIN, C. (1993). Receptor externalization determines sustained contractile responses to endothelin-1 in the rat aorta. *Am J Physiol*, **264**, C687-93.

- MATSUSHIMA, Y., SHINKAI, Y., KOBAYASHI, Y., SAKAMOTO, M., KUNIEDA, T. & TACHIBANA, M. (2002). A mouse model of Waardenburg syndrome type 4 with a new spontaneous mutation of the endothelin-B receptor gene. *Mamm Genome*, **13**, 30-5.
- MCCAFFREY, T.A., DU, B., CONSIGLI, S., SZABO, P., BRAY, P.J., HARTNER, L., WEKSLER, B.B., SANBORN, T.A., BERGMAN, G. & BUSH, H.L., JR. (1997). Genomic instability in the type II TGF-beta1 receptor gene in atherosclerotic and restenotic vascular cells. *J Clin Invest*, **100**, 2182-8.
- MCCULLOCH, K.M., DOCHERTY, C.C., MORECROFT, I. & MACLEAN, M.R. (1996). EndothelinB receptor-mediated contraction in human pulmonary resistance arteries. *Br J Pharmacol*, **119**, 1125-30.
- MCGOON, M.D. & VANHOUTTE, P.M. (1984). Aggregating platelets contract isolated canine pulmonary arteries by releasing 5-hydroxytryptamine. *J Clin Invest*, **74**, 828-33.
- MCLAUGHLIN, V.V., SITBON, O., BADESCH, D.B., BARST, R.J., BLACK, C., GALIE, N., RAINISIO, M., SIMONNEAU, G. & RUBIN, L.J. (2005). Survival with first-line bosentan in patients with primary pulmonary hypertension. *Eur Respir J*, **25**, 244-9.
- MESSERLI, F.H., OREN, S. & GROSSMAN, E. (1988). Left ventricular hypertrophy and antihypertensive therapy. *Drugs*, **35 Suppl 5**, 27-33.
- MICKLEY, E.J., GRAY, G.A. & WEBB, D.J. (1997). Activation of endothelin ETA receptors masks the constrictor role of endothelin ETB receptors in rat isolated small mesenteric arteries. *Br J Pharmacol*, **120**, 1376-82.
- MIGNEAULT, A., SAUVAGEAU, S., VILLENEUVE, L., THORIN, E., FOURNIER, A., LEBLANC, N. & DUPUIS, J. (2005). Chronically elevated endothelin levels reduce pulmonary vascular reactivity to nitric oxide. *Am J Respir Crit Care Med*, **171**, 506-13.
- MILLER, P.J. (1971). An elastin stain. *Med Lab Technol*, **28**, 148-9.
- MITANI, Y., ZAIDI, S.H., DUFOURCQ, P., THOMPSON, K. & RABINOVITCH, M. (2000). Nitric oxide reduces vascular smooth muscle cell elastase activity through cGMP-mediated suppression of ERK phosphorylation and AML1B nuclear partitioning. *Faseb J*, **14**, 805-14.

- MIZUGUCHI, T., NISHIYAMA, M., MOROI, K., TANAKA, H., SAITO, T., MASUDA, Y., MASAKI, T., DE WIT, D., YANAGISAWA, M. & KIMURA, S. (1997). Analysis of two pharmacologically predicted endothelin B receptor subtypes by using the endothelin B receptor gene knockout mouse. *Br J Pharmacol*, **120**, 1427-30.
- MOLENAAR, P., KUC, R.E. & DAVENPORT, A.P. (1992). Characterization of two new ETB selective radioligands, [125I]-BQ3020 and [125I]-[Ala1,3,11,15]ET-1 in human heart. *Br J Pharmacol*, **107**, 637-9.
- MORECROFT, I., LOUGHLIN, L., NILSEN, M., COLSTON, J., DEMPSIE, Y., SHEWARD, J., HARMAR, A. & MACLEAN, M.R. (2005). Functional Interactions between 5-Hydroxytryptamine Receptors and the Serotonin Transporter in Pulmonary Arteries. *J Pharmacol Exp Ther*, **313**, 539-48.
- MORITA, H., KURIHARA, H., KURIHARA, Y., KUWAKI, T., SHINDO, T., OH-HASHI, Y., KUMADA, M. & YAZAKI, Y. (1999). Responses of blood pressure and catecholamine metabolism to high salt loading in endothelin-1 knockout mice. *Hypertens Res*, **22**, 11-6.
- MORIWAKI, K. (1999). Genetic Background and Phenotypes in Animal Models of Human Diseases. In *Microbial and Phenotypic Definition of Rats and Mice: Proceedings of the 1998 US/Japan Conference*. pp. 44-47: The National Academies Press.
- MORRELL, N.W., UPTON, P.D., KOTECHEA, S., HUNTLEY, A., YACCOUB, M.H., POLAK, J.M. & WHARTON, J. (1999). Angiotensin II activates MAPK and stimulates growth of human pulmonary artery smooth muscle via AT1 receptors. *Am J Physiol*, **277**, L440-8.
- MORRELL, N.W. & WILKINS, M.R. (2001a). Genetic and molecular mechanisms of pulmonary hypertension. *Clin Med*, **1**, 138-45.
- MORRELL, N.W., YANG, X., UPTON, P.D., JOURDAN, K.B., MORGAN, N., SHEARES, K.K. & TREMBATH, R.C. (2001b). Altered growth responses of pulmonary artery smooth muscle cells from patients with primary pulmonary hypertension to transforming growth factor-beta(1) and bone morphogenetic proteins. *Circulation*, **104**, 790-5.

- MORSE, J.H., JONES, A.C., BARST, R.J., HODGE, S.E., WILHELMSSEN, K.C. & NYGAARD, T.G. (1998). Familial primary pulmonary hypertension locus mapped to chromosome 2q31-q32. *Chest*, **114**, 57S-58S.
- MOTOIKE, T., LOUGHNA, S., PERENS, E., ROMAN, B.L., LIAO, W., CHAU, T.C., RICHARDSON, C.D., KAWATE, T., KUNO, J., WEINSTEIN, B.M., STAINIER, D.Y. & SATO, T.N. (2000). Universal GFP reporter for the study of vascular development. *Genesis*, **28**, 75-81.
- MULVANY, M.J. & HALPERN, W. (1977). Contractile properties of small arterial resistance vessels in spontaneously hypertensive and normotensive rats. *Circ Res*, **41**, 19-26.
- MURAKOSHI, N., MIYAUCHI, T., KAKINUMA, Y., OHUCHI, T., GOTO, K., YANAGISAWA, M. & YAMAGUCHI, I. (2002). Vascular endothelin-B receptor system in vivo plays a favorable inhibitory role in vascular remodeling after injury revealed by endothelin-B receptor-knockout mice. *Circulation*, **106**, 1991-8.
- NAKANISHI, K., TAJIMA, F., NAKATA, Y., OSADA, H., TACHIBANA, S., KAWAI, T., TORIKATA, C., SUGA, T., TAKISHIMA, K., AURUES, T. & IKEDA, T. (1999). Expression of endothelin-1 in rats developing hypobaric hypoxia-induced pulmonary hypertension. *Lab Invest*, **79**, 1347-57.
- NAOMI, S., IWAOKA, T., DISASHI, T., INOUE, J., KANESAKA, Y., TOKUNAGA, H. & TOMITA, K. (1998). Endothelin-1 inhibits endothelin-converting enzyme-1 expression in cultured rat pulmonary endothelial cells. *Circulation*, **97**, 234-6.
- NELSON, R.D., STRICKLETT, P., GUSTAFSON, C., STEVENS, A., AUSIELLO, D., BROWN, D. & KOHAN, D.E. (1998). Expression of an AQP2 Cre recombinase transgene in kidney and male reproductive system of transgenic mice. *Am J Physiol*, **275**, C216-26.
- NICHOLS, W.C., KOLLER, D.L., SLOVIS, B., FOROUD, T., TERRY, V.H., ARNOLD, N.D., SIEMIENIAK, D.R., WHEELER, L., PHILLIPS, J.A., 3RD, NEWMAN, J.H., CONNEALLY, P.M., GINSBURG, D. & LOYD, J.E. (1997). Localization of the gene for familial primary pulmonary hypertension to chromosome 2q31-32. *Nat Genet*, **15**, 277-80.

- NICKENIG, G., BAUMER, A.T., GROHE, C., KAHLERT, S., STREHLOW, K., ROSENKRANZ, S., STABLEIN, A., BECKERS, F., SMITS, J.F., DAEMEN, M.J., VETTER, H. & BOHM, M. (1998). Estrogen modulates AT1 receptor gene expression in vitro and in vivo. *Circulation*, **97**, 2197-201.
- NIRANJAN, V., TELEMAQUE, S., DEWIT, D., GERARD, R.D. & YANAGISAWA, M. (1996). Systemic hypertension induced by hepatic overexpression of human preproendothelin-1 in rats. *J Clin Invest*, **98**, 2364-72.
- NOGUCHI, S., KASHIHARA, Y. & BERTRAND, C. (1996). The induction of a biphasic bronchospasm by the ETB agonist, IRL 1620, due to thromboxane A2 generation and endothelin-1 release in guinea-pigs. *Br J Pharmacol*, **118**, 1397-402.
- NUEDLING, S., VAN EICKELS, M., ALLERA, A., DOEVENDANS, P., MEYER, R., VETTER, H. & GROHE, C. (2003). 17 Beta-estradiol regulates the expression of endothelin receptor type B in the heart. *Br J Pharmacol*, **140**, 195-201.
- OHUCHI, T., KUWAKI, T., LING, G.Y., DEWIT, D., JU, K.H., ONODERA, M., CAO, W.H., YANAGISAWA, M. & KUMADA, M. (1999). Elevation of blood pressure by genetic and pharmacological disruption of the ETB receptor in mice. *Am J Physiol*, **276**, R1071-7.
- OIKARINEN, A., MAKELA, J., VUORIO, T. & VUORIO, E. (1991). Comparison on collagen gene expression in the developing chick embryo tendon and heart. Tissue and development time-dependent action of dexamethasone. *Biochim Biophys Acta*, **1089**, 40-6.
- OKADA, M., YAMASHITA, C. & OKADA, K. (1995). Endothelin receptor antagonists in a beagle model of pulmonary hypertension: contribution to possible potential therapy? *J Am Coll Cardiol*, **25**, 1213-7.
- OKSCHE, A., BOESE, G., HORSTMAYER, A., FURKERT, J., BEYERMANN, M., BIENERT, M. & ROSENTHAL, W. (2000). Late endosomal/lysosomal targeting and lack of recycling of the ligand-occupied endothelin B receptor. *Mol Pharmacol*, **57**, 1104-13.
- OPARIL, S., CHEN, S.J., MENG, Q.C., ELTON, T.S., YANO, M. & CHEN, Y.F. (1995). Endothelin-A receptor antagonist prevents acute hypoxia-induced pulmonary hypertension in the rat. *Am J Physiol*, **268**, L95-100.



- OPOCENSKY, M., KRAMER, H.J., BACKER, A., VERNEROVA, Z., EIS, V., CERVENKA, L., CERTIKOVA CHABOVA, V., TESAR, V. & VANECKOVA, I. (2006). Late-onset endothelin-A receptor blockade reduces podocyte injury in homozygous Ren-2 rats despite severe hypertension. *Hypertension*, **48**, 965-71.
- ORTE, C., POLAK, J.M., HAWORTH, S.G., YACOUB, M.H. & MORRELL, N.W. (2000). Expression of pulmonary vascular angiotensin-converting enzyme in primary and secondary plexiform pulmonary hypertension. *J Pathol*, **192**, 379-84.
- OZAKI, M., KAWASHIMA, S., YAMASHITA, T., OHASHI, Y., RIKITAKE, Y., INOUE, N., HIRATA, K.I., HAYASHI, Y., ITOH, H. & YOKOYAMA, M. (2001). Reduced hypoxic pulmonary vascular remodeling by nitric oxide from the endothelium. *Hypertension*, **37**, 322-7.
- OZAKI, S., OHWAKI, K., IHARA, M., FUKURODA, T., ISHIKAWA, K. & YANO, M. (1995). ETB-mediated regulation of extracellular levels of endothelin-1 in cultured human endothelial cells. *Biochem Biophys Res Commun*, **209**, 483-9.
- PALEVSKY, H.I., SCHLOO, B.L., PIETRA, G.G., WEBER, K.T., JANICKI, J.S., RUBIN, E. & FISHMAN, A.P. (1989). Primary pulmonary hypertension. Vascular structure, morphometry, and responsiveness to vasodilator agents. *Circulation*, **80**, 1207-21.
- PARK, S.H., SALEH, D., GIAID, A. & MICHEL, R.P. (1997). Increased endothelin-1 in bleomycin-induced pulmonary fibrosis and the effect of an endothelin receptor antagonist. *Am J Respir Crit Care Med*, **156**, 600-8.
- PATERSON, J.M., MORTON, N.M., FIEVET, C., KENYON, C.J., HOLMES, M.C., STAELS, B., SECKL, J.R. & MULLINS, J.J. (2004). Metabolic syndrome without obesity: Hepatic overexpression of 11beta-hydroxysteroid dehydrogenase type 1 in transgenic mice. *Proc Natl Acad Sci U S A*, **101**, 7088-93.
- PEARSON, B., ANDREWS, M. & GROSE, F. (1961). Histochemical demonstration of mammalian glucosidase by means of 3-(5-bromoindolyl)-beta-D-glucopyranoside. *Proc Soc Exp Biol Med*, **108**, 619-23.

- PETER, M.G. & DAVENPORT, A.P. (1996). Characterization of the endothelin receptor selective agonist, BQ3020 and antagonists BQ123, FR139317, BQ788, 50235, Ro462005 and bosentan in the heart. *Br J Pharmacol*, **117**, 455-462.
- PICKERING, T.G., HALL, J.E., APPEL, L.J., FALKNER, B.E., GRAVES, J., HILL, M.N., JONES, D.W., KURTZ, T., SHEPS, S.G. & ROCCELLA, E.J. (2005). Recommendations for blood pressure measurement in humans and experimental animals: Part 1: blood pressure measurement in humans: a statement for professionals from the Subcommittee of Professional and Public Education of the American Heart Association Council on High Blood Pressure Research. *Hypertension*, **45**, 142-61.
- PIETRA, G.G., EDWARDS, W.D., KAY, J.M., RICH, S., KERNIS, J., SCHLOO, B., AYRES, S.M., BERGOFSKY, E.H., BRUNDAGE, B.H., DETRE, K.M. & ET AL. (1989). Histopathology of primary pulmonary hypertension. A qualitative and quantitative study of pulmonary blood vessels from 58 patients in the National Heart, Lung, and Blood Institute, Primary Pulmonary Hypertension Registry. *Circulation*, **80**, 1198-206.
- PLUMPTON, C., FERRO, C.J., HAYNES, W.G., WEBB, D.J. & DAVENPORT, A.P. (1996). The increase in human plasma immunoreactive endothelin but not big endothelin-1 or its C-terminal fragment induced by systemic administration of the endothelin antagonist TAK-044. *Br J Pharmacol*, **119**, 311-4.
- POLLOCK, D.M., KEITH, T.L. & HIGHSMITH, R.F. (1995). Endothelin receptors and calcium signaling. *Faseb J*, **9**, 1196-204.
- POLLOCK, D.M. & OPGENORTH, T.J. (1994). ETA receptor-mediated responses to endothelin-1 and big endothelin-1 in the rat kidney. *Br J Pharmacol*, **111**, 729-32.
- POLLOCK, D.M. & POLLOCK, J.S. (2001). Evidence for endothelin involvement in the response to high salt. *Am J Physiol Renal Physiol*, **281**, F144-50.
- POPOVIC, V. (1988). Adaptation to restraint in the rat. *Physiologist*, **31**, S65-6.
- PRIE, S., LEUNG, T.K., CERNACEK, P., RYAN, J.W. & DUPUIS, J. (1997). The orally active ET(A) receptor antagonist (+)-(S)-2-(4,6-dimethoxy-pyrimidin-2-ylloxy)-3-methoxy-3,3-diphenyl-propionic acid (LU 135252) prevents the development of pulmonary hypertension and endothelial metabolic

- dysfunction in monocrotaline-treated rats. *J Pharmacol Exp Ther*, **282**, 1312-8.
- PRIE, S., STEWART, D.J. & DUPUIS, J. (1998). EndothelinA receptor blockade improves nitric oxide-mediated vasodilation in monocrotaline-induced pulmonary hypertension. *Circulation*, **97**, 2169-74.
- PRINS, B.A., HU, R.M., NAZARIO, B., PEDRAM, A., FRANK, H.J., WEBER, M.A. & LEVIN, E.R. (1994). Prostaglandin E2 and prostacyclin inhibit the production and secretion of endothelin from cultured endothelial cells. *J Biol Chem*, **269**, 11938-44.
- PUFFENBERGER, E.G., HOSODA, K., WASHINGTON, S.S., NAKAO, K., DEWIT, D., YANAGISAWA, M. & CHAKRAVART, A. (1994). A missense mutation of the endothelin-B receptor gene in multigenic Hirschsprung's disease. *Cell*, **79**, 1257-66.
- QUASCHNING, T., REBHAN, B., WUNDERLICH, C., WANNER, C., RICHTER, C.M., PFAB, T., BAUER, C., KRAEMER-GUTH, A., GALLE, J., YANAGISAWA, M. & HOCHER, B. (2005). Endothelin B receptor-deficient mice develop endothelial dysfunction independently of salt loading. *J Hypertens*, **23**, 979-985.
- RABINOVITCH, M., GAMBLE, W., NADAS, A.S., MIETTINEN, O.S. & REID, L. (1979). Rat pulmonary circulation after chronic hypoxia: hemodynamic and structural features. *Am J Physiol*, **236**, H818-27.
- RAJEWSKY, K., GU, H., KUHN, R., BETZ, U.A., MULLER, W., ROES, J. & SCHWENK, F. (1996). Conditional gene targeting. *J Clin Invest*, **98**, 600-3.
- RANG, H.P., DALE, M.M., RITTER, J.M. & MOORE, P.K. (2003). *Pharmacology*: Churchill Livingstone.
- REDDY, V.M., MEYRICK, B., WONG, J., KHOOR, A., LIDDICOAT, J.R., HANLEY, F.L. & FINEMAN, J.R. (1995). In utero placement of aortopulmonary shunts. A model of postnatal pulmonary hypertension with increased pulmonary blood flow in lambs. *Circulation*, **92**, 606-13.
- REED, K.C. & MANN, D.A. (1985). Rapid transfer of DNA from agarose gels to nylon membranes. *Nucleic Acids Res*, **13**, 7207-21.
- ROCKEY, D.C. & CHUNG, J.J. (1996). Regulation of inducible nitric oxide synthase in hepatic sinusoidal endothelial cells. *Am J Physiol*, **271**, G260-7.

- ROLINSKI, B., SADRI, I., BOGNER, J. & GOEBEL, F.D. (1994). Determination of endothelin-1 immunoreactivity in plasma, cerebrospinal fluid and urine. *Res Exp Med (Berl)*, **194**, 9-24.
- RONDELET, B., KERBAUL, F., MOTTE, S., VAN BENEDEN, R., REMMELINK, M., BRIMIOULLE, S., MCENTEE, K., WAUTHY, P., SALMON, I., KETELSLEGERS, J.M. & NAEIJE, R. (2003). Bosentan for the prevention of overcirculation-induced experimental pulmonary arterial hypertension. *Circulation*, **107**, 1329-35.
- ROTHMAN, R.B., AYESTAS, M.A., DERSCH, C.M. & BAUMANN, M.H. (1999). Aminorex, fenfluramine, and chlorphentermine are serotonin transporter substrates. Implications for primary pulmonary hypertension. *Circulation*, **100**, 869-75.
- RUBANYI, G.M. & BOTELHO, L.H. (1991). Endothelins. *Faseb J*, **5**, 2713-20.
- RUBANYI, G.M. & POLOKOFF, M.A. (1994). Endothelins: molecular biology, biochemistry, pharmacology, physiology, and pathophysiology. *Pharmacol Rev*, **46**, 325-415.
- RUBIN, L.J. (2004). Diagnosis and management of pulmonary arterial hypertension: ACCP evidence-based clinical practice guidelines. *Chest*, **126**, 7S-10S.
- RUBIN, L.J. (1997). Primary pulmonary hypertension. *N Engl J Med*, **336**, 111-7.
- RUBIN, L.J., BADESCH, D.B., BARST, R.J., GALIE, N., BLACK, C.M., KEOGH, A., PULIDO, T., FROST, A., ROUX, S., LECONTE, I., LANDZBERG, M. & SIMONNEAU, G. (2002). Bosentan therapy for pulmonary arterial hypertension. *N Engl J Med*, **346**, 896-903.
- RUDARAKANCHANA, N., TREMBATH, R.C. & MORRELL, N.W. (2001). New insights into the pathogenesis and treatment of primary pulmonary hypertension. *Thorax*, **56**, 888-90.
- RUNO, J.R. & LOYD, J.E. (2003). Primary pulmonary hypertension. *Lancet*, **361**, 1533-44.
- RUSSELL, F.D. & DAVENPORT, A.P. (1996). Characterization of the binding of endothelin ETB selective ligands in human and rat heart. *Br J Pharmacol*, **119**, 631-6.

- RUSSELL, F.D. & DAVENPORT, A.P. (1999). Evidence for intracellular endothelin-converting enzyme-2 expression in cultured human vascular endothelial cells. *Circ Res*, **84**, 891-6.
- RUSSELL, F.D., SKEPPER, J.N. & DAVENPORT, A.P. (1998a). Evidence using immunoelectron microscopy for regulated and constitutive pathways in the transport and release of endothelin. *J Cardiovasc Pharmacol*, **31**, 424-30.
- RUSSELL, F.D., SKEPPER, J.N. & DAVENPORT, A.P. (1998b). Human endothelial cell storage granules: a novel intracellular site for isoforms of the endothelin-converting enzyme. *Circ Res*, **83**, 314-21.
- RYAN, M.J., DIDION, S.P., DAVIS, D.R., FARACI, F.M. & SIGMUND, C.D. (2002). Endothelial dysfunction and blood pressure variability in selected inbred mouse strains. *Arterioscler Thromb Vasc Biol*, **22**, 42-8.
- SAETRUM OPGAARD, O., CANTERA, L., ADNER, M. & EDVINSSON, L. (1996). Endothelin-A and -B receptors in human coronary arteries and veins. *Regul Pept*, **63**, 149-56.
- SAITO, S., HIRATA, Y., IMAI, T. & MARUMO, F. (1995). Autocrine regulation of the endothelin-1 gene in rat endothelial cells. *J Cardiovasc Pharmacol*, **26 Suppl 3**, S84-7.
- SAKAI, S., MIYAUCHI, T., KOBAYASHI, M., YAMAGUCHI, I., GOTO, K. & SUGISHITA, Y. (1996). Inhibition of myocardial endothelin pathway improves long-term survival in heart failure. *Nature*, **384**, 353-5.
- SAKURAI, T., YANAGISAWA, M., TAKUWA, Y., MIYAZAKI, H., KIMURA, S., GOTO, K. & MASAKI, T. (1990). Cloning of a cDNA encoding a non-isopeptide-selective subtype of the endothelin receptor. *Nature*, **348**, 732-5.
- SATO, K., OKA, M., HASUNUMA, K., OHNISHI, M. & KIRA, S. (1995). Effects of separate and combined ETA and ETB blockade on ET-1-induced constriction in perfused rat lungs. *Am J Physiol*, **269**, L668-72.
- SAUER, B. (1998). Inducible gene targeting in mice using the Cre/lox system. *Methods*, **14**, 381-92.
- SCHLAEGER, T.M., BARTUNKOVA, S., LAWITTS, J.A., TEICHMANN, G., RISAU, W., DEUTSCH, U. & SATO, T.N. (1997). Uniform vascular-endothelial-cell-

- specific gene expression in both embryonic and adult transgenic mice. *Proc Natl Acad Sci U S A*, **94**, 3058-63.
- SCHMITTECKERT, E.M., PROKOP, C.M. & HEDRICH, H.J. (1999). DNA detection in hair of transgenic mice--a simple technique minimizing the distress on the animals. *Lab Anim*, **33**, 385-9.
- SCHUSTER, D.P., CROUCH, E.C., PARKS, W.C., JOHNSON, T. & BOTNEY, M.D. (1996). Angiotensin converting enzyme expression in primary pulmonary hypertension. *Am J Respir Crit Care Med*, **154**, 1087-91.
- SHARP, M.G., FETTES, D., BROOKER, G., CLARK, A.F., PETERS, J., FLEMING, S. & MULLINS, J.J. (1996). Targeted inactivation of the Ren-2 gene in mice. *Hypertension*, **28**, 1126-31.
- SHERER, A. & KINTER, L. (1995). A Guide to Manufacture, Surgical Implantation, Maintenance and Use of Micro-Renathane® Vascular Catheters in Laboratory Animals. *Braintree Scientific, Incorporated, Braintree, MA , USA*.
- SHIMADA, K., TAKAHASHI, M., IKEDA, M. & TANZAWA, K. (1995). Identification and characterization of two isoforms of an endothelin-converting enzyme-1. *FEBS Lett*, **371**, 140-4.
- SHIN, M.K., LEVORSE, J.M., INGRAM, R.S. & TILGHMAN, S.M. (1999). The temporal requirement for endothelin receptor-B signalling during neural crest development. *Nature*, **402**, 496-501.
- SHINDO, T., KURIHARA, H., MAEMURA, K., KURIHARA, Y., UEDA, O., SUZUKI, H., KUWAKI, T., JU, K.H., WANG, Y., EBIHARA, A., NISHIMATSU, H., MORIYAMA, N., FUKUDA, M., AKIMOTO, Y., HIRANO, H., MORITA, H., KUMADA, M., YAZAKI, Y., NAGAI, R. & KIMURA, K. (2002). Renal damage and salt-dependent hypertension in aged transgenic mice overexpressing endothelin-1. *J Mol Med*, **80**, 105-16.
- SHIRAI, M., PEARSON, J.T., SHIMOUCHI, A., NAGAYA, N., TSUCHIMOCCHI, H., NINOMIYA, I. & MORI, H. (2003). Changes in functional and histological distributions of nitric oxide synthase caused by chronic hypoxia in rat small pulmonary arteries. *Br J Pharmacol*, **139**, 899-910.

- SHOHET, R.V., KISANUKI, Y.Y., ZHAO, X.S., SIDDIQUEE, Z., FRANCO, F. & YANAGISAWA, M. (2004). Mice with cardiomyocyte-specific disruption of the endothelin-1 gene are resistant to hyperthyroid cardiac hypertrophy. *Proc Natl Acad Sci U S A*, **101**, 2088-93.
- SOFIA, M., MORMILE, M., FARAONE, S., ALIFANO, M., ZOFRA, S., ROMANO, L. & CARRATU, L. (1993). Increased endothelin-like immunoreactive material on bronchoalveolar lavage fluid from patients with bronchial asthma and patients with interstitial lung disease. *Respiration*, **60**, 89-95.
- SOMA, S., TAKAHASHI, H., MURAMATSU, M., OKA, M. & FUKUCHI, Y. (1999). Localization and distribution of endothelin receptor subtypes in pulmonary vasculature of normal and hypoxia-exposed rats. *Am J Respir Cell Mol Biol*, **20**, 620-30.
- SORIANO, P. (1999). Generalized lacZ expression with the ROSA26 Cre reporter strain. *Nat Genet*, **21**, 70-1.
- SPRATT, J.C., GODDARD, J., PATEL, N., STRACHAN, F.E., RANKIN, A.J. & WEBB, D.J. (2001). Systemic ETA receptor antagonism with BQ-123 blocks ET-1 induced forearm vasoconstriction and decreases peripheral vascular resistance in healthy men. *Br J Pharmacol*, **134**, 648-54.
- STEC, D.E., KEEN, H.L. & SIGMUND, C.D. (2002). Lower blood pressure in floxed angiotensinogen mice after adenoviral delivery of Cre-recombinase. *Hypertension*, **39**, 629-33.
- STELZNER, T.J., O'BRIEN, R.F., YANAGISAWA, M., SAKURAI, T., SATO, K., WEBB, S., ZAMORA, M., MCMURTRY, I.F. & FISHER, J.H. (1992). Increased lung endothelin-1 production in rats with idiopathic pulmonary hypertension. *Am J Physiol*, **262**, L614-20.
- STENMARK, K.R. & MCMURTRY, I.F. (2005). Vascular remodeling versus vasoconstriction in chronic hypoxic pulmonary hypertension: a time for reappraisal? *Circ Res*, **97**, 95-8.
- STERNBERG, N. & HAMILTON, D. (1981). Bacteriophage P1 site-specific recombination. I. Recombination between loxP sites. *J Mol Biol*, **150**, 467-86.
- STEUDEL, W., SCHERRER-CROSBIE, M., BLOCH, K.D., WEIMANN, J., HUANG, P.L., JONES, R.C., PICARD, M.H. & ZAPOL, W.M. (1998). Sustained pulmonary

- hypertension and right ventricular hypertrophy after chronic hypoxia in mice with congenital deficiency of nitric oxide synthase 3. *J Clin Invest*, **101**, 2468-77.
- STEWART, D.J., LEVY, R.D., CERNACEK, P. & LANGLEBEN, D. (1991). Increased plasma endothelin-1 in pulmonary hypertension: marker or mediator of disease? *Ann Intern Med*, **114**, 464-9.
- STOOS, B.A., GARCIA, N.H. & GARVIN, J.L. (1995). Nitric oxide inhibits sodium reabsorption in the isolated perfused cortical collecting duct. *J Am Soc Nephrol*, **6**, 89-94.
- STRACHAN, F.E., SPRATT, J.C., WILKINSON, I.B., JOHNSTON, N.R., GRAY, G.A. & WEBB, D.J. (1999). Systemic blockade of the endothelin-B receptor increases peripheral vascular resistance in healthy men. *Hypertension*, **33**, 581-5.
- STRICKLETT, P.K., NELSON, R.D. & KOHAN, D.E. (1998). Site-specific recombination using an epitope tagged bacteriophage P1 Cre recombinase. *Gene*, **215**, 415-23.
- SUTSCH, G., KIOWSKI, W., YAN, X.W., HUNZIKER, P., CHRISTEN, S., STROBEL, W., KIM, J.H., RICKENBACHER, P. & BERTEL, O. (1998). Short-term oral endothelin-receptor antagonist therapy in conventionally treated patients with symptomatic severe chronic heart failure. *Circulation*, **98**, 2262-8.
- TAKAYANAGI, R., KITAZUMI, K., TAKASAKI, C., OHNAKA, K., AIMOTO, S., TASAKA, K., OHASHI, M. & NAWATA, H. (1991). Presence of non-selective type of endothelin receptor on vascular endothelium and its linkage to vasodilation. *FEBS Lett*, **282**, 103-6.
- TAKEDA, S., SAWA, Y., MINAMI, M., KANEDA, Y., FUJII, Y., SHIRAKURA, R., YANAGISAWA, M. & MATSUDA, H. (1997). Experimental bronchiolitis obliterans induced by in vivo HVJ-liposome-mediated endothelin-1 gene transfer. *Ann Thorac Surg*, **63**, 1562-7.
- TAKIMOTO, M., INUI, T., OKADA, T. & URADE, Y. (1993). Contraction of smooth muscle by activation of endothelin receptors on autonomic neurons. *FEBS Lett*, **324**, 277-82.
- TANAKA, H., MOROI, K., IWAI, J., TAKAHASHI, H., OHNUMA, N., HORI, S., TAKIMOTO, M., NISHIYAMA, M., MASAKI, T., YANAGISAWA, M., SEKIYA, S.



- & KIMURA, S. (1998). Novel mutations of the endothelin B receptor gene in patients with Hirschsprung's disease and their characterization. *J Biol Chem*, **273**, 11378-83.
- TATCHUM-TALOM, R., MARTEL, C., LABRIE, C., LABRIE, F. & MARETTE, A. (2000). Gender differences in hemodynamic responses to endothelin-1. *J Cardiovasc Pharmacol*, **36**, S102-4.
- TAYLOR, T.A., GARIEPY, C.E., POLLOCK, D.M. & POLLOCK, J.S. (2003a). Gender differences in ET and NOS systems in ETB receptor-deficient rats: effect of a high salt diet. *Hypertension*, **41**, 657-62.
- TAYLOR, T.A., GARIEPY, C.E., POLLOCK, D.M. & POLLOCK, J.S. (2003b). Unique endothelin receptor binding in kidneys of ETB receptor deficient rats. *Am J Physiol Regul Integr Comp Physiol*, **284**, R674-81.
- TELEMAQUE-POTTS, S., KUC, R.E., MAGUIRE, J.J., OHLSTEIN, E., YANAGISAWA, M. & DAVENPORT, A.P. (2002). Elevated systemic levels of endothelin-1 and blood pressure correlate with blunted constrictor responses and downregulation of endothelin(A), but not endothelin(B), receptors in an animal model of hypertension. *Clin Sci (Lond)*, **103 Suppl 48**, 357S-362S.
- TERADA, Y., TOMITA, K., NONOGUCHI, H. & MARUMO, F. (1992). Different localization of two types of endothelin receptor mRNA in microdissected rat nephron segments using reverse transcription and polymerase chain reaction assay. *J Clin Invest*, **90**, 107-12.
- THEIS, M., DE WIT, C., SCHLAEGER, T.M., ECKARDT, D., KRUGER, O., DORING, B., RISAU, W., DEUTSCH, U., POHL, U. & WILLECKE, K. (2001). Endothelium-specific replacement of the connexin43 coding region by a lacZ reporter gene. *Genesis*, **29**, 1-13.
- THOMAS, K.R. & CAPECCHI, M.R. (1987). Site-directed mutagenesis by gene targeting in mouse embryo-derived stem cells. *Cell*, **51**, 503-12.
- THOMSON, J.R., MACHADO, R.D., PAUCIULO, M.W., MORGAN, N.V., HUMBERT, M., ELLIOTT, G.C., WARD, K., YACoub, M., MIKHAIL, G., ROGERS, P., NEWMAN, J., WHEELER, L., HIGENBOTTAM, T., GIBBS, J.S., EGAN, J., CROZIER, A., PEACOCK, A., ALLCOCK, R., CORRIS, P., LOYD, J.E., TREMBATH, R.C. & NICHOLS, W.C. (2000). Sporadic primary pulmonary hypertension is

- associated with germline mutations of the gene encoding BMPR-II, a receptor member of the TGF-beta family. *J Med Genet*, **37**, 741-5.
- TODOROVICH-HUNTER, L., JOHNSON, D.J., RANGER, P., KEELEY, F.W. & RABINOVITCH, M. (1988). Altered elastin and collagen synthesis associated with progressive pulmonary hypertension induced by monocrotaline. A biochemical and ultrastructural study. *Lab Invest*, **58**, 184-95.
- TUDER, R.M., COOL, C.D., GERACI, M.W., WANG, J., ABMAN, S.H., WRIGHT, L., BADESCH, D. & VOELKEL, N.F. (1999). Prostacyclin synthase expression is decreased in lungs from patients with severe pulmonary hypertension. *Am J Respir Crit Care Med*, **159**, 1925-32.
- TURNER, A.J., BARNES, K., SCHWEIZER, A. & VALDENAIRE, O. (1998). Isoforms of endothelin-converting enzyme: why and where? *Trends Pharmacol Sci*, **19**, 483-6.
- UCHIDA, Y., JUN, T., NINOMIYA, H., OHSE, H., HASEGAWA, S., NOMURA, A., SAKAMOTO, T., SARDESSAI, M.S. & HIRATA, F. (1996). Involvement of endothelins in immediate and late asthmatic responses of guinea pigs. *J Pharmacol Exp Ther*, **277**, 1622-9.
- VALDENAIRE, O., BARRET, A., SCHWEIZER, A., ROHRBACHER, E., MONGIAT, F., PINET, F., CORVOL, P. & TOUGARD, C. (1999). Two di-leucine-based motifs account for the different subcellular localizations of the human endothelin-converting enzyme (ECE-1) isoforms. *J Cell Sci*, **112 Pt 18**, 3115-25.
- VAN SUYLEN, R.J., SMITS, J.F. & DAEMEN, M.J. (1998). Pulmonary artery remodeling differs in hypoxia- and monocrotaline-induced pulmonary hypertension. *Am J Respir Crit Care Med*, **157**, 1423-8.
- VAN VLIET, B., CHAFE, L.L. & MONTANI, J.P. (2003). Characteristics of 24 h telemetered blood pressure in eNOS-knockout and C57Bl/6J control mice. *J Physiol*.
- VAN VLIET, B.N., CHAFE, L.L., ANTIC, V., SCHNYDER-CANDRIAN, S. & MONTANI, J.P. (2000). Direct and indirect methods used to study arterial blood pressure. *J Pharmacol Toxicol Methods*, **44**, 361-73.
- VASSILEVA, I., MOUNTAIN, C. & POLLOCK, D.M. (2003). Functional role of ETB receptors in the renal medulla. *Hypertension*, **41**, 1359-63.

- VATNER, S.F. (1978). Effects of anesthesia on cardiovascular control mechanisms. *Environ Health Perspect*, **26**, 193-206.
- VERHAAR, M.C., STRACHAN, F.E., NEWBY, D.E., CRUDEN, N.L., KOOMANS, H.A., RABELINK, T.J. & WEBB, D.J. (1998). Endothelin-A receptor antagonist-mediated vasodilatation is attenuated by inhibition of nitric oxide synthesis and by endothelin-B receptor blockade. *Circulation*, **97**, 752-6.
- VON GELDERN, T.W., TASKER, A.S., SORENSEN, B.K., WINN, M., SZCZEPANKIEWICZ, B.G., DIXON, D.B., CHIOU, W.J., WANG, L., WESSALE, J.L., ADLER, A., MARSH, K.C., NGUYEN, B. & OPGENORTH, T.J. (1999). Pyrrolidine-3-carboxylic acids as endothelin antagonists. 4. Side chain conformational restriction leads to ET(B) selectivity. *J Med Chem*, **42**, 3668-78.
- WAGENVOORT, C.A. (1980). Lung biopsy specimens in the evaluation of pulmonary vascular disease. *Chest*, **77**, 614-25.
- WAGNER, O.F., CHRIST, G., WOJTA, J., VIERHAPPER, H., PARZER, S., NOWOTNY, P.J., SCHNEIDER, B., WALDHAUSL, W. & BINDER, B.R. (1992). Polar secretion of endothelin-1 by cultured endothelial cells. *J Biol Chem*, **267**, 16066-8.
- WALLACE, A. (2003). Endothelin system expression and function in failing and non-failing myocardium. PhD Thesis: University of Edinburgh, UK.
- WALLACE, A., DENVIR, M.A. & GRAY, G.A. (2002). Seasonal variation of myocardial endothelin receptor mRNA expression in rats. *British Journal Pharmacology*, **136**, 65P.
- WANG, Q., HUMMLER, E., NUSSBERGER, J., CLEMENT, S., GABBIANI, G., BRUNNER, H.R. & BURNIER, M. (2002). Blood pressure, cardiac, and renal responses to salt and deoxycorticosterone acetate in mice: role of Renin genes. *J Am Soc Nephrol*, **13**, 1509-16.
- WARNER, T.D., ALLCOCK, G.H., CORDER, R. & VANE, J.R. (1993). Use of the endothelin antagonists BQ-123 and PD 142893 to reveal three endothelin receptors mediating smooth muscle contraction and the release of EDRF. *Br J Pharmacol*, **110**, 777-82.
- WEBER, C., SCHMITT, R., BIRNBOECK, H., HOPFGARTNER, G., VAN MARLE, S.P., PEETERS, P.A., JONKMAN, J.H. & JONES, C.R. (1996). Pharmacokinetics and

- pharmacodynamics of the endothelin-receptor antagonist bosentan in healthy human subjects. *Clin Pharmacol Ther*, **60**, 124-37.
- WEIR, E.K., REEVE, H.L., HUANG, J.M., MICHELAKIS, E., NELSON, D.P., HAMPL, V. & ARCHER, S.L. (1996). Anorexic agents aminorex, fenfluramine, and dexfenfluramine inhibit potassium current in rat pulmonary vascular smooth muscle and cause pulmonary vasoconstriction. *Circulation*, **94**, 2216-20.
- WEST, J., FAGAN, K., STEUDEL, W., FOUTY, B., LANE, K., HARRAL, J., HOEDT-MILLER, M., TADA, Y., OZIMEK, J., TUDER, R. & RODMAN, D.M. (2004). Pulmonary hypertension in transgenic mice expressing a dominant-negative BMPRII gene in smooth muscle. *Circ Res*, **94**, 1109-14.
- WESTCOTT, J.Y., McDONNELL, T.J., BOSTWICK, P. & VOELKEL, N.F. (1988). Eicosanoid production in isolated perfused lungs stimulated by calcium ionophore A23187. *Am Rev Respir Dis*, **138**, 895-900.
- WHITESALL, S.E., HOFF, J.B., VOLLMER, A.P. & D'ALECY, L.G. (2004). Comparison of simultaneous measurement of mouse systolic arterial blood pressure by radiotelemetry and tail-cuff methods. *Am J Physiol Heart Circ Physiol*, **286**, H2408-15.
- WILCOX, S.C. (2000). Arginine-nitric oxide pathway. In *The Kidney*. eds Seldin, D.W. & Giebisch, G. pp. 849-871. Philadelphia: Lippincott Williams and Wilkins.
- WILKES, B.M., RUSTON, A.S., MENTO, P., GIRARDI, E., HART, D., VANDER MOLEN, M., BARNETT, R. & NORD, E.P. (1991). Characterization of endothelin 1 receptor and signal transduction mechanisms in rat medullary interstitial cells. *Am J Physiol*, **260**, F579-89.
- WILLIAMS, J.H., JR., BODELL, P., HOSSEINI, S., TRAN, H. & BALDWIN, K.M. (1992). Haemodynamic sequelae of pulmonary fibrosis following intratracheal bleomycin in rats. *Cardiovasc Res*, **26**, 401-8.
- WU, F., PARK, F., COWLEY, A.W., JR. & MATTSON, D.L. (1999). Quantification of nitric oxide synthase activity in microdissected segments of the rat kidney. *Am J Physiol*, **276**, F874-81.
- XIE, J., YAMADA, T., CLOUTHIER, D.E., WILLIAMS, S.C., RICHARDSON, J.A. & YANAGISAWA, M. (1997). ET-3 provides environmental signals for

development of two ETB expressing neural crest derivatives. *Presented at the 5th International Conference on Endothelin, Kyoto, Japan.*

- XU, D., EMOTO, N., GIAID, A., SLAUGHTER, C., KAW, S., DEWIT, D. & YANAGISAWA, M. (1994). ECE-1: a membrane-bound metalloprotease that catalyzes the proteolytic activation of big endothelin-1. *Cell*, **78**, 473-85.
- YALCINTEPE, L., FRANKEL, A.E. & HOGGE, D. (2006). Expression of Interleukin-3 receptor subunits on defined subpopulations of acute myeloid leukemia blasts predicts the cytotoxicity of diphtheria toxin Interleukin-3 fusion protein against malignant progenitors which engraft in immunodeficient mice. *Blood*.
- YANAGISAWA, H., HAMMER, R.E., RICHARDSON, J.A., EMOTO, N., WILLIAMS, S.C., TAKEDA, S., CLOUTHIER, D.E. & YANAGISAWA, M. (2000). Disruption of ECE-1 and ECE-2 reveals a role for endothelin-converting enzyme-2 in murine cardiac development. *J Clin Invest*, **105**, 1373-82.
- YANAGISAWA, H., YANAGISAWA, M., KAPUR, R.P., RICHARDSON, J.A., WILLIAMS, S.C., CLOUTHIER, D.E., DE WIT, D., EMOTO, N. & HAMMER, R.E. (1998). Dual genetic pathways of endothelin-mediated intercellular signaling revealed by targeted disruption of endothelin converting enzyme-1 gene. *Development*, **125**, 825-36.
- YANAGISAWA, M., KURIHARA, H., KIMURA, S., TOMOBE, Y., KOBAYASHI, M., MITSUI, Y., YAZAKI, Y., GOTO, K. & MASAKI, T. (1988). A novel potent vasoconstrictor peptide produced by vascular endothelial cells. *Nature*, **332**, 411-5.
- YUAN, J.X., ALDINGER, A.M., JUHASZOVA, M., WANG, J., CONTE, J.V., JR., GAINE, S.P., ORENS, J.B. & RUBIN, L.J. (1998a). Dysfunctional voltage-gated K<sup>+</sup> channels in pulmonary artery smooth muscle cells of patients with primary pulmonary hypertension. *Circulation*, **98**, 1400-6.
- YUAN, X.J., WANG, J., JUHASZOVA, M., GAINE, S.P. & RUBIN, L.J. (1998b). Attenuated K<sup>+</sup> channel gene transcription in primary pulmonary hypertension. *Lancet*, **351**, 726-7.
- YUKIMURA, T., NOTOYA, M., MIZOJIRI, K., MIZUHIRA, V., MATSUURA, T., EBARA, T., MIURA, K., KIM, S., IWAO, H. & SONG, K. (1996). High resolution

localization of endothelin receptors in rat renal medulla. *Kidney Int*, **50**, 135-47.

ZHAO, L., LONG, L., MORRELL, N.W. & WILKINS, M.R. (1999). NPR-A-Deficient mice show increased susceptibility to hypoxia-induced pulmonary hypertension. *Circulation*, **99**, 605-7.

ZHUO, J.L. (2000). Renomedullary interstitial cells: a target for endocrine and paracrine actions of vasoactive peptides in the renal medulla. *Clin Exp Pharmacol Physiol*, **27**, 465-73.